Gata6 haploinsufficiency leads to aortic valve, conduction system and limbs defects

Lara Gharibeh

A Thesis Submitted to
The Faculty of Graduate and Postdoctoral Studies
In Partial Fulfillment of the Requirements for the Degree of
Doctor of Philosophy

Department of Biochemistry, Microbiology and Immunology
Specialization: Human and Molecular Genetics
Faculty of Medicine
University of Ottawa

Table of Content

Abstract

Cardiovascular diseases are the leading cause of morbidity and mortality worldwide. Congenital heart disease (CHD) is a risk factor for premature cardiovascular complications. Great advances have occurred in the past years leading to the identification of several genes essential for proper cardiac formation such as *GATA4/5/6* mutated in some individuals with CHD. GATA6 is a zinc finger transcription factor whose presence is crucial for early embryonic development. GATA6 is expressed in many cell types of the heart including myocardial, endocardial, neural crest, and vascular smooth muscle. In human, mutations in *GATA6* result in variable cardiac phenotypes. The objective of this thesis was to determine the roles that GATA6 play in the different cell types of the heart and to elucidate the molecular basis of the cardiac defects associated with *Gata6* haploinsufficiency. For this, a combination of cell and molecular techniques were used *in vitro* and *in vivo*. First, we show that *Gata6* heterozygozity leads to RL-type bicuspid aortic valve (BAV)- the most common CHD affecting 2% of the population. GATA6-dependent BAV is the result of disruption of valve remodeling and extracellular matrix composition in *Gata6* haploinsufficient mice. Cell-specific inactivation of one *Gata6* allele from *Isl-1* positive cells, but not from endothelial or neural crest cells, recapitulates the phenotype of *Gata6* heterozygous mice revealing an essential role for GATA6 in secondary heart field myocytes during valvulogenesis. We further uncovered a role for GATA6 as an important regulator of the cardiac conduction system and revealed that GATA6 expression regulates the activity of the cardiac pacemaker. GATA6 exerts its role via regulation of the cross-talk among the different cell types of the SAN. Lastly, some CHDs are characterized by abnormalities of both the limbs and the heart such as the Holt Oram syndrome (caused by mutation in *TBX5*

transcription factor). The molecular basis for limb-heart defects remain poorly understood. In the course of this work, we discovered that *Gata6* haploinsufficiency resulted in a partially penetrant polysyndactyly (extra digits fused together) phenotype. Together, the data provide novel molecular and cellular insight into GATA6 role in normal and pathologic heat development. Our results also suggest that *GATA6* should be added to the list of genes whose mutations are potentially associated with heart and limb abnormalities. Better knowledge of the molecular basis of CHD is a prerequisite for the development of diagnostic and therapeutic strategies to improve care of individuals with congenital heart disease.

Acknowledgement

"Every great work, every big accomplishment, has been brought into manifestation through holding to the vision, and often just before the big achievement, comes apparent failure and discouragement"

Florence Scovel Shinn

It has been a tough journey full of ups and downs, but I wouldn't have made it without the tremendous love and support of many people in my life. To my family, friends, lab mates and supervisors, you should know that your support and encouragement during the period of my PhD was worth more than any words I can express on paper.

I would like to begin by expressing my deepest appreciation to my supervisor, Professor Mona Nemer. I am so grateful for having the opportunity to work and graduate from your lab; I have for sure learned from the best. Your passion to research and your adventurous spirit were always a great motivation to me. Thank you for setting the bar high and for showing me that nothing is impossible to accomplish; "where there's a will, there's a way". Also thank you for being a second mother and for caring for us as if your own. Without your guidance and persistent help, this work would not have been possible.

I would like to express my appreciation to my TAC members, Dr. Balwant Tuana and Dr. Erik Suuronen, for their constructive criticism and insights, as well as their continuous support during the course of this work. I would like to thank the Bicuspid Aortic foundation and the University of Ottawa for granting me the prestigious M.E. Abbott scholarship and the UOttawa differential and excellence scholarships, respectively.

Furthermore, the people who have made the lab my second "Home", away from home, deserve special thanks. Thank you for helping me keep things in perspective, for your scientific advice, for all the support when experiment went wrong, for all the laughs and happy moments, for the birthday cakes and fun activities, and all the rest. To my dear Dr. Hiba Komati; thank you for being an amazing friend and for being always there with a word of encouragement or with a listening ear. To Dr. Wael Maharsy; thank you for being the punching bag when things go wrong, and for all your help and support. To the soon Doctor-to-be Jamie Whitcomb; Thank you for sharing this bumpy road with me and for being there at every step of the way ☺. Thank you "super" Megan Fortier and Janie Beauregard for your friendship and all your assistance. Thank you: Abir el Mazloum for your friendship and happy spirit; Dr. Alice Lau for all your support and comments on the thesis; Massomeh Sheikh-Hassani, Laura Collins and Mathieu Joyal for all your support.

A special thank you to the former Nemer lab members with whom I crossed the way during my PhD; your presence was great in so many ways, thank you: Dr. Rami Darwich, Dr. Smail Messaoudi, Dr. Omar Mansour, Claudia Terran, Dr. Wenjuan Li, Dr. Alicia Jurado, Ariana Rostami, Romina Hassanzadeh, Mercy Akuma, and all the rest. To Dr. Abir Yamak, my

great friend, shopping and gossip buddy ☺; thank you for your friendship, help and support throughout my PhD. Thank you, Hélène Touchette, for your continuous assistance.

To my other mentor, Dr. Georges Nemer; thank you for encouraging me to pursue an advanced degree and for your continuous support and guidance.

To my "Lab Musketeers", my brothers, Elias Abou Samra and Georges Kanaan; Thank you for your marvelous friendship, for keeping me sane and for providing me with a much-needed form of escape during this period. Without you, it wouldn't have been the same! *"One for all and all for one"* ☺ *(Alexandre Dumas père)*

Special thanks to the amazing people in my life, friends near and far, for all their support and for tolerating my weird temper during that period. I won't be stating all the names, but you know who you are!

Last, but not least, the deepest appreciation goes to my wonderful family. Dad, Mom and Melissa, my dear sister, you knew it would be a long and bumpy road, but you always encouraged me and supported me along the way. Thank you for your continuous support and unconditional love which were empowering me along the way. I am blessed to have you in my life. Therefore, I dedicate this thesis to you ☺

Ottawa, February 2018

Lara Gharibeh

List of Figures

List of Tables

Abbreviations

A	Atria
ACVR1/2b	Activin A receptor type 1/2b
ADAM 8, 33	ADAM metallopeptidase domain containing
ADAMTs 1/5/9/20	A disintegrin and metalloproteinase with thrombospondin motifs
AER	Apical ectodermal ridge
AHF	Anterior heart field
ALDH1A2	Aldehyde Dehydrogenase 1 Family Member A2
ALS	Amyotrophic lateral sclerosis
ANF	Atrial natriuretic factor
AngII	Angiotensin II
Ao	Aorta
A-P	Antero-posterior
APOE	Apolipoprotein E
AROS	Acro-renal-ocular syndrome
AscAA	Ascending aortic aneurysm
AT1R	Angiotensin type I receptor
AT1α	Angiotensin receptor 1 alpha
AV	Atrioventricular
AVB	Atrioventricular bundle
AVC	Atrioventricular cushion
AVD	Aortic valve disease
AVN	Atrioventricular node
AVSD	Atrioventricular septal defect
BAV	Bicuspid aortic valve
BBs	Bundle branches
BBS	Bardet-Biedl syndrome
BHLH	Basic helix loop helix
BIRC5	Baculoviral inhibitor of apoptosis repeat-containing 5
BMP2/4/7/10	Bone morphogenetic protein 2/4/7/10
BMPR1A/2/21	Bone morphogenetic protein receptor 1A/2/21
BNP	Brain natriuretic peptide
CADM4	Cell adhesion molecule 4
CAV1	Calveolin 1
CAV3.1/CACNA1G	Calcium channel, voltage-dependent, T type, alpha 1G subunit
CCN1	Cysteine-rich, angiogenic inducer, 1
CCS	Cardiac conduction system
CDKN1c	Cyclin dependent kinase inhibitor 1c
CFC1	Cryptic protein 1
CHD	Congenital heart disease
CITED1/2	Cbp/P300 Interacting Transactivator With Glu/Asp Rich Carboxy-Terminal Domain 1/2
CLD	Congenital limb defets
CNCC	Cardiac neural crest cells
CNTF	Ciliary neurotrophic factor

COLI/II/III	Collagen I/II/III
CRELD1	Cysteine rich with EGF like domains 1
CRIM1	Cystein rich transmembrane BMP regulator 1
CRM1	Chromosomal maintenance 1
CSQ	Calsequestrin
CT	Conotruncus
C-term	C-terminal
CTGF	Connective tissue growth factor
CTNI/C	Cardiac troponin I/C
CX30.2/40/43/45	Connexin 30.2/40/43/45
CYP26A1	Cytochrome P450 family 26
DKK1	Dickkopf 1
DNMAML	Dominant negative mastermind like
DORV	Double Outlet right ventricle
DS	Down syndrome
D-V	Dorso-ventral
E	Embryonic day
ECM	Extracellular matrix
EDN1	Endothelin 1
EFNB2	Ephrin B2
EMT	Epithelial to mesenchymal transformation
ES	Embryonic stem
ETV2	Ets variant 2
EVC	Ellis Van Creveld
EWAS	Epigenome-wide association study
FBLN1	Fibulin 1
FBN1/2	Fibrillin 1/2
FGF1/2/4/5/8/9/10	Fibroblast growth factor 1/2/4/5/8/9/10
FGFR1/2/3	Fibroblast growth factor receptor R1/2/3
FHF	First heart field
FLK1	Vascular endothelial growth factor receptor 1
FOG2	Friend of GATA2
FS	Fractional shortening
GDP1/GAPDH	Glyceraldehyde-3-phosphate dehydrogenase 1
GLI1/3	Gli family zinc finger 1
GREM1	DAN Family BMP Antagonist 1
GSK3	Glycogen synthase kinase 3
GWAS	Genome wide association study
HA	Hyaluronin
HAND1/2	Heart- and neural crest derivatives-expressed protein 1/2
HAPLN1	Hyaluronan and proteoglycan link protein 1
HAS2	Hyaluronan synthase 2
HCN1/4	Potassium/Sodium channel 1/4
HEY2	Hairy/enhancer-of-split related with YRPW motif protein 2
HF/HC	High fat high cholesterol
HFD	High fat diet
HIF1α	Hypoxia-inducible factor-1

HOX 11/12/13/D13	Homeobox protein 11/12/13/D13
HSA21	Copy number variations to chromosome 21
HSPG2	Heparan sulfate proteoglycan 2
Hu	Human
ICD	Interdigital cell death
IP3	Inositol triphosphate
IRX3/4/5	Iroquois homeodomain 3/4/5
ISL1	Lim homeodomain transcription factor 1
ITGA3/6	Integrin A 3/6
IVS	Interventricular septum
JAG1	Jagged 1
LA	Left atria
LAMA5	Laminin 5
LCA	Left coronary artery
LDLR	Low density lipoprotein receptor
LEFTY2	Left-right determination factor 2
LH	Left hindlimb
LMBR1	Limb development membrane protein 1
L-R	Left-right
LV	Left ventricle
MATR3	Matrin 3
MC	Mesenchymal cap
MEF2c	Myocyte-specific enhancer factor 2c
MESP1/2	Mesoderm posterior protein ½
MKP3	Mitogen-activated protein kinase phosphatase 3
MMP3/9	Matrix metalloproteinase 3/9
MMPs	Matrix metalloproteinases
Ms	Mouse
MSX1/2	Msh homeobox 1/2
MYCN	N-myc proto-oncogene protein
MYHC3	Slow myosin heavy chain 3
MYOR	Myogenic repressor
NCAM	Neural cell adhesion molecule
NCC	Neural crest cell
NCID	Intracellular domain of the notch protein
NC-RNAs	Non-coding RNAs
NCX1	Sodium-calcium exchanger (SLC8a1)
NEK1	NIMA related kinase 1
NF1	Neurofibromin 1
NFATc	Nuclear factor of activated T-cell
NID1/2	Nidogen 1/2
NKX3.2	NK 3 homeodomain 2
NLS	Nuclear localization signal
NMDs	Inherited neuromuscular diseases
NODAL	Nodal growth differentiation factor
NOTCH	Neurogenic locus notch homolog protein
NPPA	Atrial natriuretic peptide

NRG1	Neuregulin 1
NRP1	Neuropilin 1
N-term	N-terminal
OA	Overriding aorta
OFT	Outflow tract
PA	Pulmonary artery
PAC	Premature atrial contraction
PAS	Periodic acid-Schiff
PAX3	Paired box 3
PBX1	Pre-B-cell leukemia transcription factor 1
P-D	Proximo-distal
PDGFRβ	Platelet-derived growth factor receptor β
PECAM	Platelet endothelial cell adhesion molecule 1
PEN1	Pentacyclic triterpene synthase 1
PEO	Proepicardial organ
PH3	Phosphohistone H 3
PIK3	Phosphoinositide 3-kinase
PITX1/2	Paired-like homeodomain 2
POSTN	Periostin
PRX1	Mitochondrial thioredoxin peroxidase
PS	Pulmonary stenosis
PTA	Persistent truncus arteriosus
PTCH1	Patched 1
PTK2	Protein tyrosine kinase 2
PTPN11	Tyrosine-protein phosphatase non-receptor type 11
PWS	Parkes Weber syndrome
QTL	Quantitative trait loci
RA	Right atria
RAB23	Ras-Related Protein Rab-23
RALDH2	Retinaldehyde 2
RARɣ	Retinoic acid receptor gamma
RASA1	RAS p21 protein activator 1
RBPJK	Recombination signal binding protein for immunoglobulin kappa J region
RCA	Right coronary artery
RH	Right hindlimb
RV	Right ventricle
RXRα	Retinoid receptor alpha
SALL4	Sal-like 4
SAN	Sinoatrial node
SC	Subcutaneous
SCN5a	Sodium channel protein type 5 subunit alpha
SD	Syndactyly
SEM	Standard error of the mean
SEMA3C	Semaphorin 3C
SERCA	Sarco/endoplasmic reticulum Ca^{2+}-ATPase
SFRP2	Secreted Frizzled 2

SHF	Second heart Field
SHH	Sonic hedgehog
SHOX2	Short homeobox transcription factor 2
SM	Smooth muscle
SMA	Spinal muscular atrophy
SMAD1/4	SMAD family member 1/4
SNAIL/SNAI1	Snail Family Transcriptional Repressor 1
SNPs	Single nucleotide polymorphisms
SOD1	Superoxide dismutase 1
SOSTDC1	Sclerostin domain-containing-1
SOX4/9	Sex determining region Y-box 4/9
SP6	Transcription factor SP6
SR	Sarcoplasmic reticulum
SRF	Serum response factor
SSS	Sick sinus syndrome
SV	Sinus venosus
TAD	Transactivation domain
TBX1/3/5/18/20	Tbox transcription factor 1/3/5/18/20
TEF1	Translation elongation factor 1alpha
TF	Transcription factor
TGA	Transposition of the great arteries
TGFβ2/3	Transforming growth factor beta 2/3
TIMP1/2	Tissue inhibitor of matrix metalloproteinase ½
TIMPS	Tissue inhibitor of matrix metalloproteinases
TNNI3K	Cardiac troponin I interacting kinase
TOF	Tetralogy of Fallot
TTL1	Tolloid- like 1
TUNEL	Terminal deoxynucleotidyl transferase-mediated dUTP end labeling
TWIST1	Twist related protein 1
VCAM1	Vascular adhesion molecule 1
VCAN	Versican
VCS	Ventricular conduction system
VEGFA/R1/R2	Vascular endothelial growth factor A/R1/R2
VIC	Valvular interstitial cells
VSMC	Vascular smooth muscle cells
WDPCP	WD repeat containing planar cell polarity effector
WDR35	WD repeat-containing protein 35
WNT1/2/3a/8	Wnt family member1/2/3a/8
WT1	Wilms tumor gene 1
ZFI/II	Zinc finger I/II
ZIC3	Zinc finger of the cerebellum 3
ZPA	Zone polarizing activity
ZRS	sonic hedgehog regulatory sequence
α/β MHC	Alpha/Beta myosin heavy chain

1. Introduction

1.1. Heart development

1.1.1. Stages of embryonic heart formation

The human four-chambered heart is a powerful muscular pump that ensures, via the establishment of rhythmic contractions, the unidirectional circulation of blood throughout the entire body. By the second week of gastrulation, in order to satisfy its increasing nutritional needs, the human embryo now requires an efficient cardiovascular system [1]. The formation of the cardiovascular system in mammals is controlled by a genetic program that is evolutionarily conserved across species. Heart development begins at an early stage of embryonic life: embryonic day 7 (E7) in mouse and gestation day 21 in human. During this process and in a short period of time, by E15 in mouse and gestation day 50 in human, mesodermal cells transform into a fully mature and functional four-chambered heart capable of autonomously pumping blood **(Figure 1.1 A-D)**.

During gastrulation, the main layers composing the embryo will be established: the ectoderm (giving rise to the nervous system and skin), the mesoderm (required for muscle formation) and the endoderm (predominantly giving rise to the gut) [2]. Two distinct mesodermal cell populations, deriving from the same origin, seem to contribute to the developing heart in a spatially- and temporally- specific manner. Cardiac progenitor cells derived from the lateral plate mesoderm, also termed the First Heart Field (FHF) cells, will migrate to the region of the forming heart in an anterior to lateral direction and extend across the midline of the embryo forming the cardiac crescent (E7.5 in mouse) (**Figure 1.1 A**). The second population of cells to migrate forms the Secondary Heart Field (SHF), which lies medial and anterior to the FHF. By E8 in mouse and gestation day 21 in human, cells of the

FHF fuse along the ventral midline forming a primitive heart tube capable of beating (**Figure 1.1 B**). This linear heart tube contains an exterior layer of myocardial cells – which grants the heart its contraction properties – separated from an interior layer of endocardial cells lining the lumen, by an extracellular matrix (ECM). This ECM facilitates the signaling between the endocardial and myocardial layers [2–6].

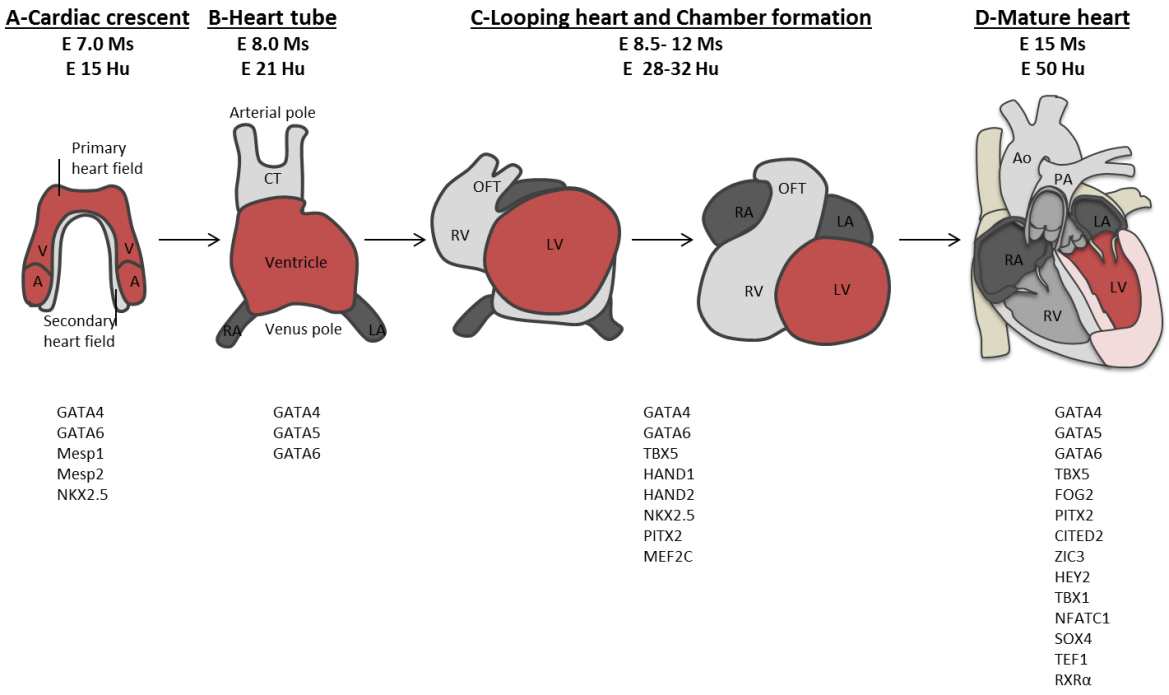

Figure 1.1: Schematic representation of stages of mammalian heart development and its transcriptional regulation. The embryonic days correspond to human (Hu) and mouse (Ms). FHF: primary/first heart field. SHF: secondary heart field. V: ventricle. A: atria. RA: right atria. LA: left atria. CT: conotruncus. OFT: outflowtract. RV: right ventricle. LV: left ventricle. Ao: aorta. PA: pulmonary artery (adapted from[4,7]).

As development progresses, the heart tube then elongates via division of myocardial cells and addition of SHF cells at the anterior and posterior regions of the heart tube. These cells will contribute later to the formation of the outflow tract (OFT), the right ventricle (RV)

and partially the right atria (RA). The proper alignment of the aortic and pulmonary trunks with the left and right ventricles, respectively, requires the lengthening of the OFT [8]. The first signs of cardiac remodeling occur when the heart tube breaks the symmetry of the embryo and loops to the right (E8.5 in mouse and gestation day 28 in human) initiating the formation of the future ventricles and atria [9] (**Figure 1.1 C**). Establishment of the right and left atria occurs early on and is controlled by right and left progenitor pools of undifferentiated cells from the lateral plate mesoderm. At the same time, ventricle specification starts along the antero-posterior (A-P) axis but switches, after cardiac looping, to the left-right (L-R) axis (**Figure 1.1 C**) [10]. The re-alignment and differential growth of the heart tube results in the formation of its inner and outer curvatures along the A-P and dorso-ventral (D-V) axes. This outer curvature will then balloon out to form the chambers (atria and ventricles) mainly composed of working myocardium that proliferate quickly and has a fast conduction potential. In the luminal surface of the ventricles, sponge-like structures called trabeculae will form from cells of the outer layer and compresses to give rise to the compacted myocardium. On the other hand, in the atria, pectinated muscles in a comb-like structure are present to ensure a great atrial contraction potential with minimum muscular mass [7,10–13].

Obtaining a fully functional four-chambered heart requires a series of septation and remodeling events. Valve formation (will be detailed in **section 1.3**) and proper heart septation are crucial steps to ensure correct blood flow between the systemic and pulmonary circuits. Following chamber formation, septation of the atria begins when a muscular structure grows from the atrial roof downward towards the atrioventricular cushion (AVC). This structure forms by active proliferation of myocardial cells with addition of

mesenchymal cells at its edge, to form the mesenchymal cap (MC). This muscular outgrowth septates the atrial chambers leaving a small opening between the MC and the AVC – the ostium primum. Closure of the ostium primum occurs when the MC along with the dorsal mesenchymal protrusion, a SHF derivative, merge with the AVC and form the mesenchymal complex. Simultaneously, a second opening – the ostium secundum – between the right and left atrium will result from the dissolution of the upper margin of the primary atrial septum. A secondary atrial septum will then form by folding of the atrial roof inward, resulting in closure of the ostium secundum. The fusion of both septums occurs shortly after birth, thereby completing the septation of the atrial chambers [14–16]. On the other hand, an interventricular muscular septum (IVS) will ensure septation of the ventricles, and this septum emerges upwards within the ventricular chamber towards the AVC. The IVS is found to have two components: 1) a muscular component emerging from proliferation of ventricular myocytes situated at the interventricular groove, and 2) a mesenchymal component resulting from fusion of the AVC with the conotruncal cushions [14,17].

The cardiac conduction system (CCS) starts developing around the same period as well. Its role is to ensure the proper propagation of the electrical impulse throughout the heart. Its major components as well as the stages of its formation will be detailed in **section 1.4**.

1.1.2. Transcription factor-mediated regulation of cardiogenesis

Heart development consists of a series of complex morphogenetic events that requires the functional presence of various proteins. The spatio-temporal expression of some genes, as well as the chamber-specific expression of others, is found to be highly regulated by the interactions of several TF with each other, and with their cofactors [18].

The heart is an asymmetric structure receiving signals along the three body axes – anterior-posterior (A-P), dorsal-ventral (D-V), and L-R – dictating its final structure [19]. The transformation of the linear heart tube into the C-shaped heart loop requires two major steps: 1) bending of the primitive ventricular region towards its ventral side while simultaneously rotating to the right, and 2) the proper positioning of the ventricle and the conotruncus (CT), in a caudal and ventral position respective to the atria [19]. This transformation controls the L-R asymmetry of the heart. NODAL (member of TGFβ family), LEFTY2 (Left right determination factor 2), and PITX2 (paired like homeodomain 2) are present in the splanchnic mesoderm of the arterial pole and have been shown to be involved in lateralization [19]. Fibroblast growth factor 8 (FGF8) in the mouse appears to be a left determinant factor whereas the homeodomain protein NKX3.2 is asymmetrically expressed on the right side [20]. Patterning along the A-P axis is mainly controlled by retinoic acid signaling. Deficiency of retinoic acid leads to expansion of the ventricular region, whereas its increase leads to expansion of the atrial region [21]. The homeobox protein IRX4 is shown to impose a ventricular phenotype over a default atrial phenotype whereas TBX5, a member of the T-box family of TF, is essential for atrial formation [22,23]. Finally, D-V patterning is governed by expression of atrial natriuretic peptide (NPPA), Heart- and neural crest derivatives-expressed protein 1 (HAND1), IRX3, IRX5 and CITED1 at the ventral side of the heart tube [21] (**Figure 1.1**).

Cells of the lateral plate mesoderm are first committed to a cardiac fate via inductive signals coming from the underlying endoderm; the migration of these cells requires mainly the function of the basic helix Loop helix (BHLH) TFs MESP1 and MESP2 [24]. Other signals include Bone Morphogenetic Protein 2 (BMP2), FGF8 and Wnt protein 11 (WNT11), all of

which act via positive signaling. However, inhibitory signals can be also induced, limiting the induction to a specific group of mesodermal cells, such as NOGGIN (anti-BMPs) and WNT3a and 8 (Wnt signaling) [10,25]. Induction of the SHF is controlled by expression of factors in the pharyngeal endoderm and splanchnic mesoderm, all important for OFT development: we mainly list FGF8, BMP2, sonic hedgehog (SHH) and Wnt/β-Catenin signaling [26]. These factors then induce expression of important cardiac TF such as GATA4, NKX2.5, and TBX5.

Studies have shown that GATA4, a TF that belongs to the GATA family of TF, plays a critical role as a regulator of the earliest stages of cardiogenesis. It has been reported that its presence allows cells to respond to primary inductive signals and it is able to mediate BMP signaling via its interaction with other factors such as NKX2.5 [27,28]. The *Nkx2.5* homologue in *Drosophila, Tinman*, is reported to be essential for heart formation [29]. In mouse, roles for NKX2.5 in cardiac regionalization and chamber specification have also been reported pointing to a specific role in left ventricle (LV) chamber development [30]. After specification of the cardiac mesoderm, the two heart fields fuse along the midline to form a single heart tube (**Figure 1.1 B**). Failure of fusion results in cardia bifida, which describes the formation of two tube-like structures. Mouse mutant for *Gata4* and the helix-loop-helix TF *Mesp1* display the cardia bifida phenotype [31,32]. Furthermore, right and left ventricular specification is controlled by HAND1 and HAND2, the basic helix-loop-helix TFs found to be expressed in the pre-cardiac mesoderm and non-cardiac precursor cells (**Figure 1.1 C**). HAND1 is specifically expressed in the anterior and posterior region of the heart tube, which will give rise to the LV and the CT, whereas HAND2 expression governs the whole heart tube but becomes restricted during the looping to the RV [33]. TFs NKX2.5, GATA5 and

TBX5 mark the myocardium of the developing chambers and regulate the expression of NPPA [4]. Finally, the process of epithelial to mesenchymal transformation (EMT) required for the septation of the OFT and the AVC, as well as valve formation, is controlled by BMP2 and BMP4 [21]. However, expression of endocardial-specific genes is induced by GATA5, another GATA family member, and Nuclear Factor of Activated T-cell c (NFATc) is shown to play a crucial role in septa and valve formation **(Figure 1.1)** [34].

1.1.3. GATA family of transcription factors

Complex morphological and tissue remodeling events orchestrate the complex process of heart development which is usually accompanied by gene expression changes regulated in a spatio-temporal manner. This combinatorial network of TF ensures the proper proliferation, differentiation and survival of cardiomyocytes; otherwise, developmental heart defects can result from disruption of these interactions.

The most intensively studied family of TF is the GATA family, which belongs to the zinc finger (ZF) superfamily of TFs harboring two ZFs DNA binding domains, Cys-X2-C-X17-Cys-X2-Cys (ZFI and ZFII), which recognize the sequences (A/T)GATA(A/G) [35]. In vertebrates, six members are present in this family (GATA 1-6) (**Figure 1.2**). Their ZF domains, which are the DNA binding regions, are more than 70% conserved, and are both involved in mediating protein-protein interactions. While the carboxyl (C-terminal, C-term) zinc finger, ZFII, is the major DNA binding domain, the amino (N-terminal, N-term) zinc finger, ZFI, is thought to play a role in the stabilization of DNA-protein interactions. The N-term and C-term regions of the proteins exhibit lower similarities and are more important for the transcriptional function of the protein [36]. The GATA protein family is further divided into two subgroups: 1) GATA1/2/3 are mainly expressed in the hematopoietic and central

nervous systems and are required for differentiation of mesoderm- and ectoderm-derived tissues, and 2) GATA4/5/6 are important for differentiation of embryonic stem cells and epithelial cells in the adult, in addition to their major role in the development of the cardiovascular system [37,38].

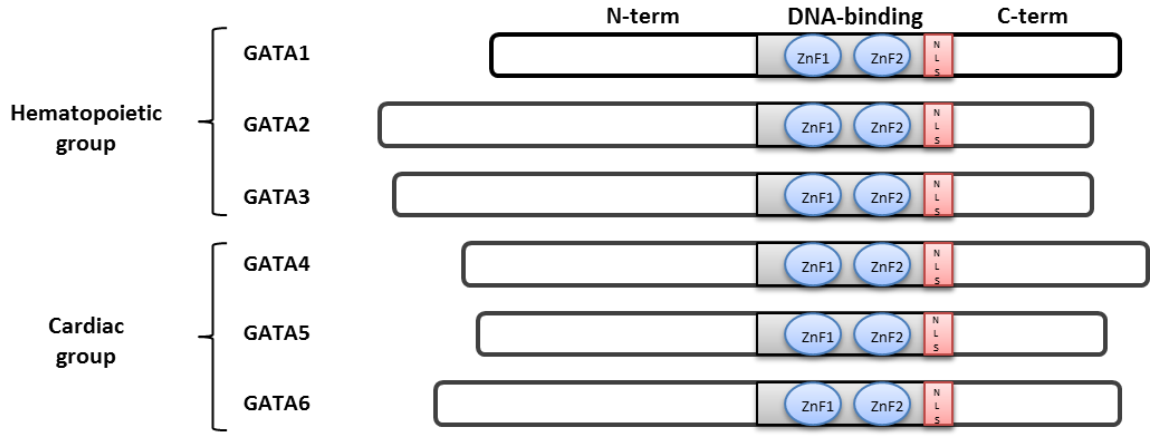

Figure 1.2: Schematic of the vertebrate family of GATA proteins: **GATA1-6.** All members share the same DNA-binding domain consisting of two zinc finger domains (one N-terminal and one C-terminal) and a nuclear localization signal (NLS). TAD: transactivation domain. N-term: N-terminal. C-term: C-terminal.

GATA1, the founding member of the family, is largely restricted to the hematopoietic lineage where its expression was found to mark differentiated structures such as erythroid cells and megakaryocytes. On the other hand, GATA2 is required for hematopoietic precursor cell proliferation. GATA3 expression is restricted to T lymphocytes and is crucial for T cell differentiation [39,40]. Targeted disruption of *Gata1*, *2* and *3* in mice leads to hematological abnormalities, further supporting the critical role of these factors in hematopoiesis. They are also required for the development of non-hematopoietic cells─ GATA1 participates in gonad development and GATA3 is crucial for brain and kidney development [38,41].

GATA4/5/6 proteins, the cardiac GATA members, are mainly expressed in the mesodermal precursors that develop into the heart [42]. They are found to be differentially regulated during development and show cellular and regional specificity, with GATA4 predominantly expressed at all stages in cardiac cells [43]. In addition to their role in cardiogenesis, GATA factors have been shown to play a role in development of the liver, pancreas, kidney, the gastrointestinal and urogenital tracts, and the central nervous system [37].

1.1.3.1. Role of cardiac GATA factors in embryonic development

GATA4 is one of the earliest TFs present in the precardiac splanchnic mesoderm and associated endoderm; its expression is detected as early as E7.0-7.5, preceding the expression of contractile protein and natriuretic peptide genes, which are the earliest markers of cardiac differentiation (**Figure 1.1**). At later stages, GATA4 transcripts are detected within the myocardium and endocardium , and continue to be well expressed in the postnatal heart [44]. *Gata4*$^{-/-}$ mice are embryonically lethal at E8.0 due to failure of heart tube development in addition to defects in ventral foregut closure [45]. Differentiated cardiomyocytes are observed in *Gata4*$^{-/-}$ mice suggesting a compensatory role of other proteins such as GATA6, whose expression level is increased in *Gata4*-null mice [46]. A role for GATA4 as a mediator of survival, proliferation, and differentiation signals has been also described after antisense-mediated knockdown of GATA4 from the pluripotent P19 embryonal carcinoma cells [47].

In the mouse embryonic heart, GATA5 is expressed within the myocardium as well as in the endocardial cushions and endocardium [48]. The requirement for GATA5 for endocardial differentiation has been demonstrated *in vitro*: terminal differentiation at a pre-endocardial stage was blocked when RA was added to drive cardiac mesoderm-derived cells

towards an endocardial fate [49]. Null mutations of *Gata5* in zebrafish lead to the formation of cardia bifida, whereas no obvious cardiac phenotype was observed in mice, suggesting different functions of this TF across species [50]. Partially penetrant (25% occurrence) bicuspid aortic valve (BAV) disease, which is the presence of two asymmetric aortic valve leaflets instead of three symmetrical ones, as well as hypoplastic hearts were found to result from deletion of both *Gata5* isoforms in mice [51].

On the other hand, GATA6 is expressed in the precardiac mesoderm at the late primitive streak stage and its expression governs myocardial and vascular smooth muscle cells at later stages [44,52]. GATA6 has been shown to play a crucial role during extra-embryonic endoderm development as *Gata6*$^{-/-}$ mice die at early embryonic stages (E4-4.5) due to extra-embryonic defects [53]. Forced expression of either GATA6 or GATA4 is able to drive differentiation of embryonic stem cells towards the extra-embryonic endoderm [54]. *In vitro* studies in heterozygous embryos revealed that *Gata6*$^{-/-}$ embryonic stem (ES) cells are able to contribute to the heart and to differentiate into myocardium, which indicates that the loss of GATA6 protein does not cause cell autonomous heart abnormalities [55]. Tissue specific deletion of *Gata6* from neural crest cells (NCC) and smooth muscle cells lead to persistent truncus arteriosus (PTA) and interrupted aortic arch revealing a crucial role for GATA6 in patterning of the aortic arch arteries [56].

1.1.3.2. Functional analysis and combinatorial interactions of GATA4/5/6

Structure function analysis of GATA4 has revealed the presence of two transcriptional activation domains located in its N- and C-term regions [36]. A role for GATA4 as a potent trans-activator of many cardiac promoters such as atrial natriuretic factor (*Anf*), brain natriuretic peptide (*Bnp*), cardiac troponin (*cTnC* and *cTnI*) and slow myosin heavy

chain (slow *MyHC3*) was reported through transfection studies in non-cardiac cells [57–59]. It has also been shown that following injury, and as a compensatory mechanism, GATA4 can regulate cardiac angiogenesis by inducing vascular endothelial growth factor (*Vegf*) [60]. As well, cardiogenic activity of GATA4 is enhanced by direct interaction with Cyclin D2 [61]. GATA4 was also shown to be a cofactor of NKX2.5 since their co-expression in heterologous cells resulted in a synergistic activation of the *Anf* promoter [62].

Gata5 is differentially regulated in chicken by two alternative non-coding exons; similarly, in mice, two distinct isoforms are produced [63]. This is a common feature in the GATA family since *Gata6* was also shown to possess distinct initiation sites in humans and mice [64]. *In vitro* studies revealed that GATA4 or 5 can interact, in combination with NKX2.5 and TBX20, to synergistically activate cardiac gene expression in fibroblasts (*Anf* and the endocardial channel Connexin40 (*Cx40*)). GATA5 has been shown to regulate endocardial differentiation and to activate *in vitro* cardiac promoter in cooperation with TBX20 [65]. Similarly, a cooperative role for NFATc and GATA5 in endocardial transcription has been highlighted, *in vitro*, using the GATA-dependent promoter of the endothelial gene ET-1 [34].

GATA6 have been shown to regulate several target genes in neuronal, cardiac and vascular cells such as the secreted glycoprotein Semaphorin 3C (*Sema3C*) and the Wnt family member 2 (*Wnt2*), which in its turn is able to regulate GATA6 expression in the posterior heart [56,66]. Studies have also demonstrated that GATA6 can interact with both serum response factor (SRF) and NKX3.2 (an Nkx2.5 homologue from smooth muscle cells) to synergistically activate the smooth muscle gene *α1-integrin* [67].

GATA factors are shown to regulate BMP signaling via two mechanisms: 1) by affecting the expression levels of BMP and 2) by interacting with downstream targets of the

pathway. Therefore, synergistic activation of the *Nkx2.5* promoter in P19 cells is caused by physical interaction of GATA4 with the N-term region of SMAD-1 and -4 (mediators of BMP signaling). This SMAD interaction is also possible with GATA5 and 6 with the latter shown to functionally substitute for GATA4 in this interaction [68]. Interestingly, GATA6 was shown to regulate BMP4 expression via binding to the functional GATA sites present on the promoter [43].

1.1.3.3. Role of cardiac GATA factors in postnatal heart development

Several studies point to the role of GATA4 and 6 in reprogramming gene expression in hypertrophic hearts and controlling adaptive responses in the postnatal myocardium. Since the knockout mice of either of these two cardiac GATA factors leads to embryonic lethality, it renders it difficult to use the murine model to assess the role of these factors in postnatal heart development. Therefore, adenovirus-mediated antisense strategies, designed specifically to inhibit GATA4 or GATA6 expression in cardiomyocytes, were used. Results revealed a downregulation of ANF, BNP, cTnI, alpha- and beta-myosin heavy chain (α- and β-MHC), and platelet-derived growth factor receptor β (PDGFRβ), in cardiomyocytes lacking GATA4 or GATA6, suggesting that these genes are targets of the latter two TFs [69,70]. GATA4 and 6 were shown to co-localize in postnatal cardiomyocytes and form a heterotypic complex that binds a single GATA binding site and therefore able to induce synergistically the transcriptional activation of target cardiac promoters (*Anf* and *Bnp*) [70].

A role for the GATA factors in regulating cardiac hypertrophy has also been extensively explored. Cardiac hypertrophy occurs when cardiomyocytes lose their ability to respond to growth stimuli and will increase in size instead of number. It has been shown that activation of angiotensin type 1 receptor (*At1r*) and *α–mhc* promoters, following pressure

overload, depends on GATA elements present in their promoter sequences [71,72]. Inhibition of GATA4 during hypertrophy can be achieved via regulation of nuclear localization, which is controlled by the serine/threonine protein kinase glycogen synthase kinase 3 (GSK3). By stimulating nuclear export through the nuclear exportin chromosomal maintenance 1 (CRM1) and via direct phosphorylation of GATA4, GSK3 is able to induce a decrease in GATA4 nuclear expression [73].

1.2. Cell lineages contribution to the heart

Several cell populations, some of which originating from outside the heart field, contribute to the formation of the embryonic heart. Regulated cellular proliferation, migration, differentiation, cell death and cell-cell interactions are critical events for proper cardiac formation and sculpturing. Knowledge of the different cell types composing the heart is important for diagnosis and treatment of heart diseases. Among the major cell lineages contributing to the heart are: myocardial cells, cells originating in the SHF, NCC, endocardial cells and epicardial cells **(Figure 1.3 and 1.4)**.

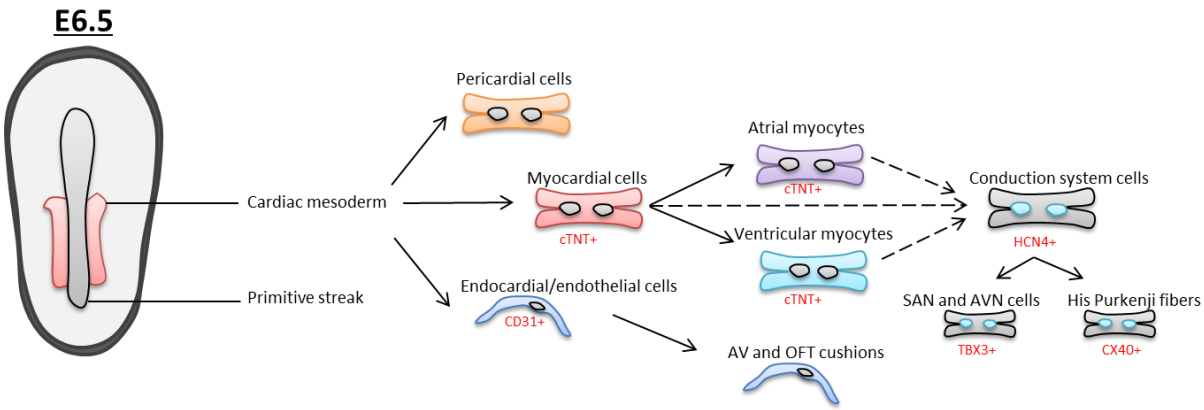

Figure 1.3: Schematic representation of the cell lineages contributing to the cells of the heart at E6.5. Highlighted in red are markers known to distinguish each of the cell types (adapted from [74]).

1.2.1. Myocardial cell lineage

Myocardial cells ensure the contractility of the mature heart, which also depends on other mesodermal cell types for its function. Myocardial lineages include atrial and ventricular myocytes as well as cardiac conduction cells (**Figure 1.3**). Differentiated myocardial cells are first detected around E7.5 in an epithelial crescent-shaped structure, where they are localized on either side of the midline under the head folds and subsequently fuse at the midline to form the early heart tube **(Figure 1.1)**. Two major lineages (first and second heart field) contribute to the heart myocardium: the first lineage is mainly the source for the left ventricular myocardium, whereas the second lineage gives rise to the OFT and most of the right ventricular myocardium; and both lineages contribute to the atria and other parts of the heart [75]. MESP1 and MESP2 are among the earliest cardiogenic markers and identify both myocardial lineages. Progenitor cells expressing both of these factors contribute to the entire myocardium [24]. MESP1 and 2 also play an important role in the delamination of the cardiac mesoderm since it was shown that no mesodermal cells can migrate out of the streak in the absence of either one of these factors [24]. *Mesp1* overexpression in ES cells has been shown to induce increased cardiomyocyte differentiation rendering MESP1 a crucial upstream regulator of myocardial cell fate [76,77]. Bone morphogenetic proteins (BMPs) and fibroblast growth factors (FGFs) are important for the early cardiogenic induction of a specific population of mesodermal cells and their proliferation and differentiation into cardiomyocytes [25].

Left and right atrial cardiomyocytes are formed by addition of progenitor cells derived from the left and right posterior regions of the SHF which is characterized by expression of ISL LIM Homeobox 1 (ISL1) and the lack of other SHF markers such as

TBX1 and FGF8/10 [78]. In the left side of the SHF, PITX2 expression is found to repress the RA identity [78]. The pulmonary trunk myocardium derives from both the anterior and the posterior SHF whereas the interventricular septum (IVS), which is a myocardium outgrowth, is marked by transgenes expressed in the left or right ventricular myocardium with a spatial distribution of labeled cells. There is an extensive contribution of cells from the LV to the dorsal part of the septum [17]. These results are suggestive of a contribution of both first and second lineages to the formation of the IVS. The T-box TF TBX5 is found to be selectively expressed in the LV and is thought to contribute to the positioning of the IVS and delineating the line separating between the right and left ventricles [79]. BMP10 is restricted to the working myocardium and is regulated by NKX2.5. It has been shown to play an important role in chamber formation via maintaining the proliferation and maturation of cardiomyocytes [80]. Within the ventricular chambers, the wall thickens in a process called trabeculation which is regulated by signals such as Notch and Neuregulin, as well as retinoic acid and FGF signaling from both the epicardium and endocardium [81–83]. At E12.5 in the mouse heart, the inner layer of myocardium, which expresses NPPA, the gap junction protein CX40, the Cyclin Dependent Kinase Inhibitor 1C (CDKN1c), and BMP10, forms the trabeculae; whereas the outer layer, expressing TBX20, hairy/enhancer-of-split related with YRPW motif protein 2 (HEY2), and MYCN (BHLH TF), constitutes only the compact layer within the chamber [77].

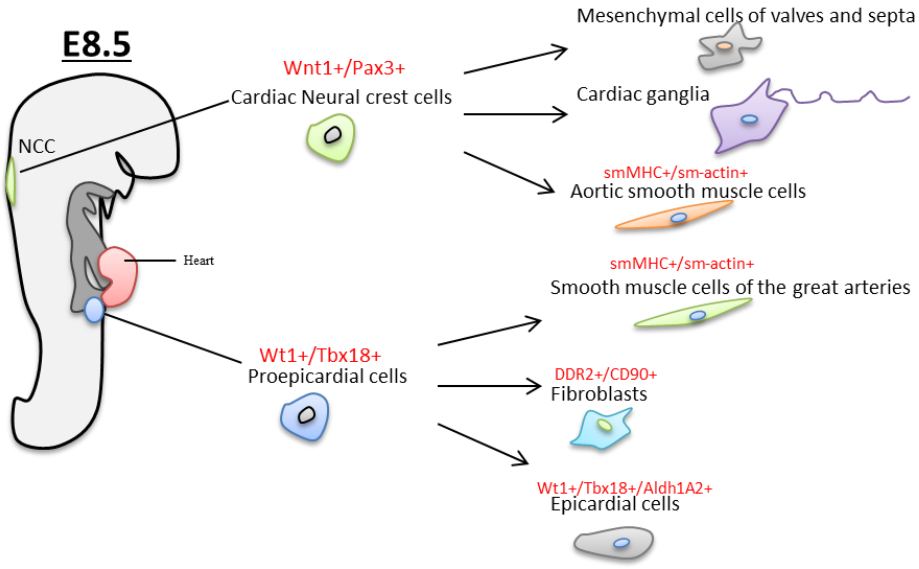

Figure 1.4: Schematic representation of the cell lineages contributing to the cells of the heart at E8.5. Highlighted in red are markers known to distinguish each of the cell types. NCC: neural crest cells (adapted from [74]).

1.2.2. Second heart field cells

The secondary heart field (SHF), also known as the anterior heart field, is a region of the pharyngeal mesoderm that contributes, within the heart, to the formation of the OFT and the RV. The SHF can be divided into many subdomains that contribute to the different regions of the arterial pole of the heart, as well as to facial muscles of the head [77]. SHF-progenitor cells are located medially to the cardiac crescent and do not immediately differentiate into the myocardial cells of the cardiac crescent (**Figure 1.1**). The contribution of progenitor cells of the anterior and posterior regions of the SHF to the RV, atria and OFT was revealed by genetic tracing and fluorescent dye labeling experiments [78,84]. A significant cell migration within the SHF occurs early on to contribute to the OFT myocardium. On the other hand, the posterior SHF contributes to the formation of the AV canal, as reported by clonal analysis [75,85]. The SHF also gives rise to endothelial cells forming the arterial tree at

the outflow region and to smooth muscle cells surrounding the great vessels at the arterial pole [86].

The SHF was first identified using an *Fgf10-LacZ* reporter transgene, which marks the cells forming the OFT and the RV, showing that they both originate from the pharyngeal mesoderm [87]. ISL1, the LIM homeodomain TF, is one of the main markers of the SHF that also marks the cardiac progenitors giving rise to a part of the inflow region and the LV as well as to both the OFT and RV. Morphogenesis abnormalities affecting the arterial and venous poles of the heart were observed after deletion of *Isl1* [88]. MEf2C enhancer sequence, FGF8, and TBX1 also mark the SHF [89,90]. TBX1, mostly found in the myocardial wall, has been suggested to regulate the expression of *Fgf8* and *Fgf10* therefore regulating SHF proliferation [91]. Together with NKX2.5, TBX1 regulates the expression of *Pitx2*, which is mainly found in the left region of the SHF [92]. An impaired elongation of the primary heart tube has been shown to result from the loss of *Fgf8* in the SHF during early cardiogenesis with altered expression of ISL1 and MEF2c [93]. Expression of the *Mef2C* enhancer in the anterior heart field (AHF) has been shown to be regulated by ISl1 and the GATA TFs, as well as by TBX20, which in its turn, is able to activate an *Nkx2.5* AHF enhancer [90,94]. In addition to that, a role for BMP signaling, Wnt-βcatenin and Wnt-TGFβ pathways, hedgehog and retinoic acid signaling in the regulation of the SHF elongation, proliferation, and survival has been suggested (reviewed in [74]). In the adult heart, a role for the SHF near the OFT is suggested to contribute to the cardiac regeneration process in zebrafish, where atrial cardiomyocytes were found to revert back to a cardiac progenitor state (expressing progenitor markers) before transforming into ventricular myocytes following injury [95].

1.2.3. Conduction cells

The contraction of the heart is initiated and regulated by different structures (nodes and working myocardium) composing what is known as the CCS. The CCS is composed of 1) the sinoatrial node (SAN), the pacemaker of the heart, 2) the atrioventricular node (AVN), situated at the proximity between the RA and RV, 3) the His bundle or the atrioventricular bundle (AVB), situated at the top of the IVS, and 4) the Purkinje fibers, which are conductive fibers delineating the IVS and propagating within the ventricular myocytes (**Figure 1.5**).

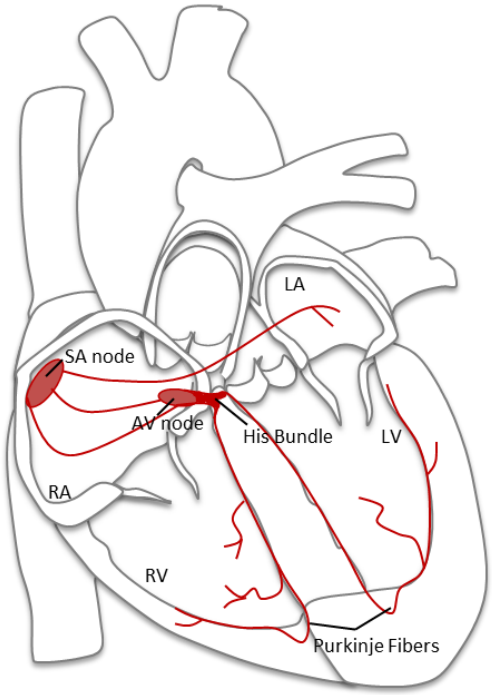

Figure 1.5: Schematic representation of the cardiac conduction. SA: sinoatrial. AV: atrioventricular. RA: right atria. RV: right ventricle. LA: left atria. LV: left ventricle.

Many controversial hypotheses exist concerning the cellular origin of the CCS. It has been initially suggested that the mammalian CCS derives from the NCC, but in fact approximately 80% of the ventricular conduction system (VCS) derives from the cardiac

mesoderm [96,97]. In the mouse, as early as E8, a primitive AV conduction system is formed, followed by formation of the AVN primordium around E11 at the dorsal canal and is usually marked by Periodic acid-Schiff (PAS) positive cells. Proliferation of these cells leads to the formation of the primitive AV bundle within the IVS and the proximal bundle branches (BBs) [98,99]. Finally, at E12, connective tissue forms around the conduction system and isolates it electrically [100]. The SAN is suggested to have a SHF origin and is derived from *Isl1*- and *Tbx18*-expressing cells [101]. It is found to be marked by expression of TBX3, which is important for its specification and formation via regulation of downstream targets.

SAN precursor cells expressing TBX3 are pre-specified early on (before E10) and become separated from the atrial myocytes that express NPPA that are unable to give rise to SAN cells [102]. A subset of *Tbx18* expressing cells also contribute to SAN formation [103]. The AVN and the bundle of His are thought to segregate from precursors of the working myocardium. In the chick embryo, two hypotheses regarding the origin of cells of the VCS have been proposed: one suggests that these cells arise from a population of cells at the top of the interventricular system, the other supports a recruitment of cardiomyocytes within the area to give rise to these cells [104–106]. The AVC and AVN derivatives are mainly derived from *Tbx2* expressing cells [107].

The peripheral conduction system, mainly composed of the Purkinje fibers, is thought to result from continuous recruitment of cardiomyocytes where the progenitor cells can give rise either to working cardiomyocytes or to conduction cells [108]. It is also thought that the left Purkinje fiber network and the LV originates from a different clonal cell population than that of the RV and right fiber branch [106]. Endothelin (EDN1) was shown to induce the differentiation of embryonic cardiomyocytes into Purkinje fibers by retroviral analysis in

chick embryo [109]. Similarly, in the mouse, Neuregulin 1 (NRG1) was able to induce the differentiation of cardiomyocytes into Purkinje fibers [110].

1.2.4. Cardiac neural crest cells

Cardiac neural crest cells (CNCC) generate initially from the neural plate and migrate to the third, fourth and sixth branchial arches, invading the heart through the venous and arterial poles (inflow and outflow tracts, respectively). CNCC contribute mainly to the formation of the OFT conotruncal cushions and the aorto-pulmonary septum as well as to the smooth muscle layer of the great vessels and the parasympathetic cardiac ganglia [111–113]. CNCC are crucial for the formation of the semilunar valves (aortic and pulmonary valves) and invade the proximal and distal OFT cushions [114]. CNCC are also important for the development of the tunica media of the aortic arch arteries and potentially play a role in the stabilization of the developing endothelial tube [115]. The septation of the OFT is controlled by two waves of CNCC: the first wave controls the cleavage of the single OFT into pulmonary and aortic trunks, whereas the second wave of migrating cells plays an important role in the remodeling of the great vessels and their branches. Abnormal remodeling process leads to interrupted or double aortic arch associated with ventricular septal defect (opening within the IVS) [116]. It has been shown that the ablation of the CNCC in avian embryos, prior to their migration, results in abnormal patterning of the OFT, the aortic arch arteries and the great vessels [117]. NCC constitute the nerve fibers of the sympathetic and parasympathetic networks of the heart, as well as the vagal nerve branches [118,119]. To track the migration of CNCC, several *cre* lines were generated for permanent lineage tracing in mice such as the *Wnt1-cre, Cx43-cre* and *Pax3-cre* transgenic lines allowing a better understanding of the role of CNCC within the heart [115,120,121]. The migration of the CNCC is found to be directed extrinsically by

the endoderm, mesoderm and ectoderm via complex signaling interactions rather than having an intrinsic control. As such, it has been shown that targeted inactivation of the mouse retinaldehyde dehydrogenase 2 (*Raldh2*), an enzyme whose role is to convert all trans-retinal into retinoic acid, leads to embryonic lethality due to the absence of OFT septation [122].

1.2.5. Endocardial/endothelial cells

As the cardiac crescent begins to form, myocardial cells begin to express contractile protein genes. At the same time, clusters of endocardial cells located more ventrally become detectable [123]. Under the control of angiogenic factors such as fibroblast growth factors and vascular endothelial growth factors, a small population of cells within the cardiac mesoderm, separate out and start to express marker genes for endothelial cell differentiation. The endothelial cells compose the inner surface of the heart which is also called the endocardium [124,125]. Within the heart, these cells contribute mainly to the septation of the chambers and OFT, and the formation of the valves and ventricular trabeculae, and they have been shown to play a role in the formation of the Purkinje fibers. It is thought that the endocardium may share mutual progenitors with the myocardium since myocardium (**Figure 1.3**) labeling has resulted in positive labeling of endocardial cells as well. Such is the case, for example, of cells in the cardiac crescent that express *Isl1* which can give rise to myocardial and endocardial cells, supporting the common progenitor theory [88]. In addition, deletion of *Nkx2.5*, one of the earliest myocardial marker, leads to defective endocardial cushion formation [126]. Another model suggests that cells are committed to the endocardial lineage even before gastrulation, prior to the mesoderm formation, with a separation of the myocardial and endocardial cell lineages at the blastula stage [127].

Endothelial cell proliferation and endocardium formation are found to be regulated by various TFs. Ets variant 2 (ETV2), is a TF required for endocardial cell specification: lack of *Etv2* results in cells failing to differentiate into endocardial cells [128,129]. A role for endocardial GATA5 TF has also been shown to regulate aortic valve formation and its absence there leads to BAV [51]. It was shown that cardiac progenitors isolated from mouse embryos, or those derived from ES cells, can result in cells expressing myocardial and endothelial/endocardial markers (e.g. the myocardial marker *Nppa* and the endocardial marker *Nfatc1*, crucial for valve and septa formation) [130,131]. This further highlights the crucial role of endocardial cells in providing the required mesenchymal cells for valves and septum formation.

1.2.6. Epicardial cells

The epicardium develops between E8.5 and E10.5 and is derived from a group of cells adjacent to the heart venous pole also called the proepicardial organ (PEO) (**Figure 1.4**). It is composed of a mesenchymal core and an external mesothelium [132]. During foregut closure, the PEO, initially located at the anterior region, acquires a more posterior position at the venous pole of the heart and cells deriving from it start covering the heart to form the epicardium [133]. Cells from the epicardium then delaminate, undergo EMT and invade the myocardium where they contribute to the formation of interstitial fibroblasts and the coronary vasculature or reside in the space between the myocardium and epicardium (**Figure 1.6**) [134].

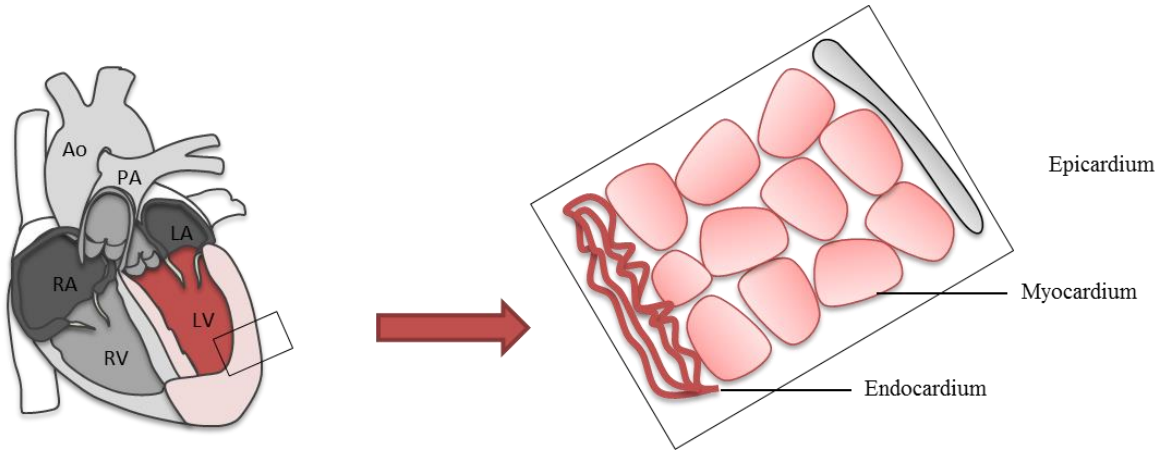

Figure 1.6: Layers of the heart wall. The wall of the heart consists of three layers: the epicardium (external layer), the myocardium (middle layer) and the endocardium (inner layer).

Lineage tracing experiments have shown that cells of the PEO as well its derivatives are marked positive for *Nkx2.5*, *Isl1*, *Tbx18* and Wilms tumor protein (*Wt1*) [135,136]. Wt1 is expressed in the epithelial cells of the proepicardium, in the subepicardial mesenchyme and in the migrating epicardial derived cells. Its loss in mice leads to abnormal epicardial formation, thin ventricles and pericardial bleeding [137]. GATA factors 4/5/6 are expressed in both the proepicardium and epicardium and GATA4 has been shown to be essential for the formation of the proepicardium, the septum transversum and the coronary vasculature [138,139]. A role for the Tbox TFs has been also suggested: TBX18 is thought to be an early marker of proepicardium formation, whereas TBX5 is found to be involved in proepicardial cell migration [140,141].

Signaling between the epicardium and myocardium is necessary for normal coronary vasculogenesis. It has been shown that loss of retinoic acid signaling from the epicardium results in myocardial hypoplasia due to the lack of either *Raldh2* or the retinoid receptor (*Rxr*). Retinoic acid is important for the induction of FGF9 in the epicardium, which plays a crucial role in myocardial development during heart formation [142,143]. Epicardial cells

expressing *Tbx18* have been shown to contribute to atrial and ventricular cardiomyocytes as well as to the IVS [144]. The epicardium has also been suggested to play an important role in adult heart regeneration. Interestingly, the addition of growth factors (*e.g.* BMP2) to PEO-derived cells in culture can give rise to myocardial cells highlighting the myocardial regenerative potential of epicardial cells [145].

1.3. Formation of the outflow tract and cardiac valves

The mature heart is composed of four chambers and four valves ensuring the unidirectional flow of blood from the heart into the systemic circulation. Complex morphogenetic processes as well as multiple cell lineages contribute to the septation of the heart chambers as well as the septation of the OFT and AV cushions. The AVC separates into left and right orifices connecting each atrium to its respective ventricle and gives rise to the AV (mitral and tricuspid) valves. On the other hand, the OFT divides into outlets connecting the left and right ventricles to the pulmonary and aortic trunks and gives rise to the semilunar (aortic and pulmonary) valves.

1.3.1. Outflow tract septation

NCC, delaminating from the neuroectodermal junction of rhombomeres 6-8 at the hindbrain, will migrate into the distal OFT where they play a major role in the septation of the cardiac OFT [112]. These NCCs then become the mesenchyme of the truncal cushions, structures that eventually fuse together to form the aortopulmonary septum that divides the distal OFT into aortic and pulmonary arteries [120]. On the other hand, the mesenchyme of the conal cushions is formed from the endocardium that undergoes epithelial-to-mesenchymal transformation (EMT) at the proximal OFT. These cushions then fuse together to give rise to the conal septum that separates the proximal OFT into the ventricular outlets. These right and

left ventricular outlets are aligned to the ventricles and the arteries by the fusion of the truncal and conal cushions with each other and the fusion of the latter cushion with the IVS **(Figure 1.7)** [146].

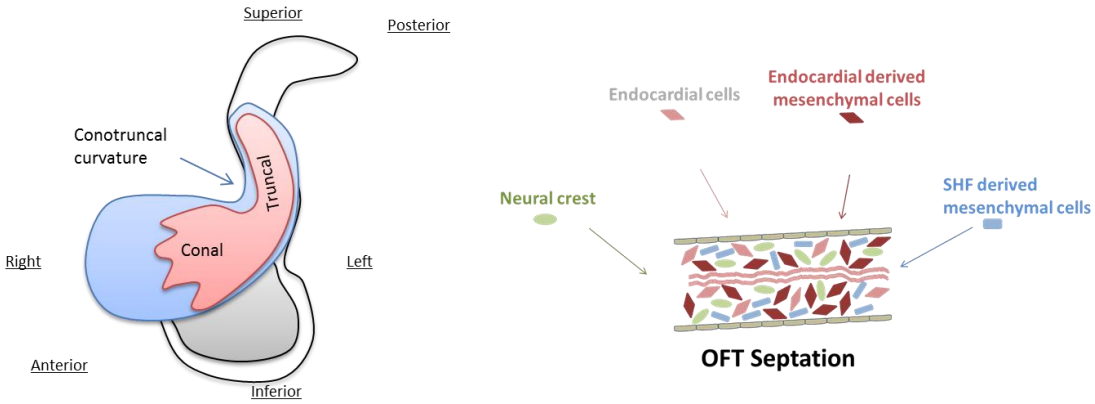

Figure 1.7: Schematic representation of the cardiac OFT and the different cell lineages contributing to the formation and septation of the OFT. The OFT contains two cushions: the conal also called proximal cushion and the truncal/distal cushion. The boundary between the conal and truncal cushions is marked by the conotruncal curvature, an outer curvature of the OFT (adapted from [15]). SHF: secondary heart field.

1.3.2. Cell lineages contribution to valvulogenesis

The OFT is composed of migratory progenitor cells that give rise to endocardial cells, myocardial cells as well as to cells derived from the EMT within the OFT itself. These progenitor cells of different origins interact with each other and with other cell types to direct this complex process of valve development and heart septation. Among these progenitor cells, we appoint the endocardium, the SHF, and the NCC as major contributors to this process **(Figure1.7)**.

1.3.2.1.Endocardial cells: Endocardial cells contribute to the formation of the cushions by undergoing epithelial-to-mesenchymal transformation (EMT; will be detailed in **section 1.3.3.**), a process that only occurs to the cushion endocardium and is induced by the signaling myocardium (BMP, TGFs, VEGFs) (**Figure 1.8**). The chamber

endocardium, on the other hand, does not express genes essential for valvular and septal development such as NFATc1 and VEGF receptors, and therefore, is not able to respond to myocardial signals and undergo EMT [147,148]. The cushion myocardium is programmed by genes in a way to suppress the chamber-specific genes, and is able to secrete ECM to support EMT and produce EMT-regulating molecules [149,150].

1.3.2.2. Cardiac neural crest cells: NCC migrate from their original location to the heart to form the aortopulmonary septum [112]. They exchange signals with their surrounding (OFT myocardium and pharyngeal arch) allowing their proper migration. The OFT myocardium secretes the ligand SEMA3C to attract the NCCs and promote them to migrate, since they express the SEMA3C receptor PLXNA2. Upon their arrival, they become the mesenchyme of the truncal cushions [151]. NCCs ablation has been shown to lead to the inhibition of OFT septation resulting in various OFT defects [152].

1.3.2.3.Secondary heart field cells: Studies have revealed that SHF progenitors contribute considerably to valve and septum formation. These cells, first of all, give rise to the OFT myocardium that plays two major roles during septo-valvulogenesis: 1) it secretes molecules to stimulate the conal endocardium to undergo EMT, and 2) it secretes chemotactic molecules to attract NCC to the OFT (*e.g.* SEMA3C) [146,151,153]. SHF-derived cells also give rise to vascular smooth muscle cells at the base of the aorta and pulmonary trunks [88]. Finally, these progenitors give rise to the dorsal mesenchymal protrusion (DMP) mesenchyme that will merge later on with the AVC and become part of the septum separating the right and left atria [154]. Disruption of different signaling pathways within the SHF using the *Mef2c-cre* and *Isl1-cre* mouse lines lead to a variety of phenotypes affecting the OFT or the semilunar valves [88,153].

1.3.3. Atrioventricular and semilunar valves formation

The complex process of valvulogenesis begins after heart looping, when the cardiac jelly, an extensive ECM separating the outer myocardium from the inner endothelium that forms the linear heart tube, extends to the AV junction and the OFT [155]. Myocardial cells present in this region start secreting molecules such as TGF-β1, BMP2, and BMP4, leading to the activation of adjacent endocardial cells (**Figure 1.8**).

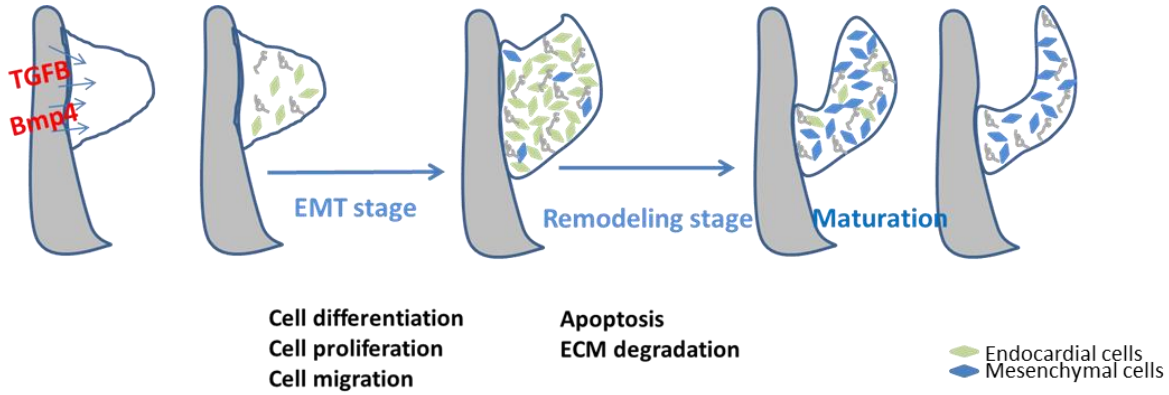

Figure 1.8: Different stages of semilunar valve formation. EMT: epithelial-to-mesenchymal transformation.

These cells lose cell-cell contact and the baso-apical polarity of epithelial cells, acquire a polarized golgi and extended filopodia, and transform into spindle shaped migratory cells that will invade the hyaluronin rich cardiac jelly [156,157]. At this stage, the endothelial markers are downregulated (PECAM1, NCAM1 and VE-cadherin), while mesenchymal markers, such as smooth muscle alpha-actin (SM-α actin) are upregulated; the resulting mesenchymal cells continue to proliferate and dilate to form swellings termed cushions [156]. The cells also digest the hyaluronen within the matrix and replace it with a denser matrix composed of collagens (COL I, II, and III), versican (VCAN) and other

proteoglycans [158]. These cushions expand from the myocardium to form the thin leaflets composed of one layer of endothelial cells rich in glycosaminoglycans, collagen and elastin at their central matrix. Afterwards, these structures undergo extensive remodeling to give rise to the semilunar and the AV valves [155]. The maturation process of the AV and semilunar valves is different, given that semilunar valves have free edges whereas the AV valves have tendinous chords attaching them to the chambers (**Figure 1.9**) [156]. These valves will only be functional at later stages of gestation and would not mature until after birth [159].

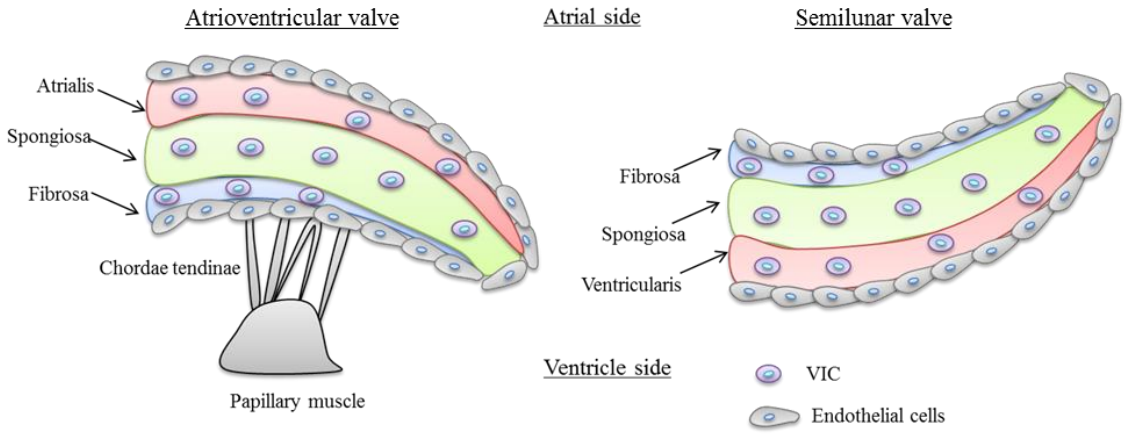

Figure 1.9: Schematic representation of the valve leaflets. An endothelial layer of cells surrounds the three layers composing the cardiac valves: the atrialis/ventricularis, the spongiosa and the fibrosa. VIC: valvular interstitial cells (adapted from [160]).

After birth, strengthening of the aorta and the aortic valve cusps occurs due to the increase of collagen-elastin lamellae number. This increase in the collagen-elastin content is the result of an increase in the aortic blood pressure accompanied by a decrease in the pulmonary artery (PA) pressure [161]. The mature valves are composed of three symmetrical leaflets referred to as “tricuspid valves” that regroup the aortic, pulmonary, and tricuspid valves (at the junction between the RA and ventricle). The mitral valve (at the junction between the LA and ventricle) is the only normal bicuspid (two leaflets) valve present in the

heart (**Figure 1.10**). The mature and remodeled valve is composed of three distinctive layers: 1) the atrialis (AV valve) or ventricularis (semilunar valve) layer rich in elastin, 2) the fibrosa layer rich in fibrillar collagen (middle layer) and 3) the spongiosa rich in proteoglycans (**Figure 1.9**) [162].

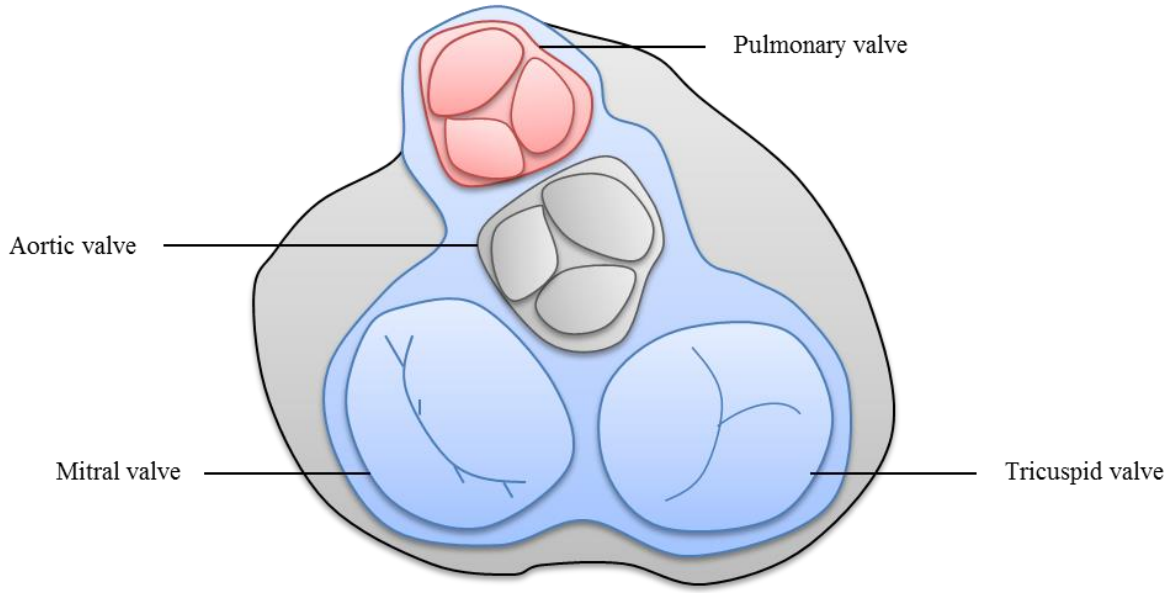

Figure 1.10: Transverse view of the valves composing the heart. Aortic valve: valve situated between the left ventricle and the aorta. Pulmonary valve: valve situated between the right ventricle and the pulmonary artery. Tricuspid valve: valve situated between the right atria and ventricle. Mitral valve: valve situated between the left atria and ventricle.

1.3.4. Molecular regulation of valve development

Coordinated signaling between several growth factors, TFs and cell adhesion/migration molecules, secreted from the endocardium and the myocardium, is crucial for the proper septation of the OFT and the development of the cardiac valves. Among the most well characterized pathways regulating these processes are the TGF/BMP/SMAD pathway, the NOTCH pathway, the VEGF/NFATc1/Calcineurin pathway, the WNT/β-catenin signaling, as well as pathways involving the ECM.

1.3.4.1. TGFβ/BMP/SMAD pathway: TGFβs are among the first regulators of EMT initiation. While TGFβ2 is expressed in the myocardium and endocardium of the cushions, TGFβ1 is only expressed in the endocardium. Endocardial TGFβ2 is mainly required for cell separation during EMT whereas TGFβ3, expressed in the endocardium and mesenchymal cells after EMT, is required for mesenchymal migration and transformation [163]. TGFβ2 is also known to promote EMT since it functions downstream of NOTCH1, BMP2 and TBX2, activating the WNT/β-catenin pathway [150,164]. BMPs are important mediators of valvulogenesis, with BMP2 and 4 being the most abundantly expressed within the cushions: BMP2 is expressed in the myocardium of the AV canal whereas BMP4 is expressed in the myocardial OFT [165]. Absence of myocardial BMP4 or defects in BMP receptors leads to either lethality or to absence of proper OFT septation [166,167]. SMADs are also known to modulate the TGF/BMP signaling and to be involved in septation and valve formation. Loss of *Smad4* in NCCs lead to PTA, OFT cushion hypoplasia and pharyngeal arch artery defects, while loss of *Smad6* leads to cushions and valve hyperplasia [168,169].

1.3.4.2. NOTCH pathway: NOTCH1, expressed in the cushion endocardium during valvulogenesis, is crucial for the induction of EMT, which is regulated by TGFβ/SNAIL signaling, inducing repression of endocardial markers and upregulation of the mesenchymal ones [170]. Constitutive activation of NOTCH1, mutation of NOTCH1 or its nuclear effector RBPJK, or activation/repression of its receptor Jagged1 (JAG1) lead to the absence of EMT [170,171]. Inhibition of *Notch* from the SHF downregulates expression of FGF8, causing impairment of NCCs migration to the OFT and reduction of EMT, therefore leading to thickened and unequal sized semilunar valves as well as septation defects (ASD, VSD, PTA) [164,172].

1.3.4.3. WNT/β-catenin: In Zebrafish, the WNT/β-catenin pathway plays an important role in valvulogenesis: overexpression of the secreted glycoprotein Dickkopf (DKK1), which inhibits Wnt signaling, leads to interruption of EMT. On the other hand, activation of the WNT pathway leads to excessive cushion development [173]. Other than its role in EMT, WNT signaling has been shown to be crucial for the recruitment of SHF-derived mesenchymal cells into the dorso-mesenchymal protrusion (DMP) and for the development of normal pharyngeal arteries. Therefore, mice lacking *Wnt2* or *β-catenin* from the SHF show a reduced DMP which result in chamber septation defects [174]. On the other hand, β-CATENIN is found to be crucial in NCCs to control OFT septation, functioning through PITX2. Lack of *β-catenin* from migrating NCCs leads to a downregulation of PITX2 expression, resulting in failure of proper NCC migration with appearance of PTA, double outlet right ventricle (DORV) and transposition of the great arteries (TGA) [175].

1.3.4.4. VEGF/NFATc1/Calcineurin: Regulation of valve development by VEGF signaling is complex, given the fact that VEGFs have differential functions and spatiotemporal expressions during this process. VEGFA, for example, is able to function as a growth factor for endocardial/endothelial cell proliferation, as an inhibitor of EMT, or as a promoter of valve elongation [148,176,177]. VEGF receptors have also been shown to have major roles during this process, with VEGFR1 being essential for EMT of the OFT cushion and VEGFR2 being important for the elongation of the AV valves after EMT [148]. VEGF regulates the endocardium via binding to its receptor FLK1 and providing calcium to calcineurin from the endoplasmic reticulum to the endocardium, through the inositoltriphosphate (IP3) second messenger pathway. Calcineurin then controls the expression of PECAM and phosphorylates NFATc1 to induce proliferation [178].

Myocardial NFAT first triggers EMT by repressing VEGFA, but a second wave of NFAT from the endocardium, signaling via calcineurin and Nfatc1, regulates valve remodeling and elongation. Deficiency of *Nfatc1*, whether in the endocardium or the myocardium, or blockage of *Calcineurin* leads to absence of EMT and hypoplasticity of the cushions [147]. In the OFT, NFATc1 delineates the boundary between EMT- and NCC-derived mesenchymal cells within the conal cushion to prevent excessive EMT and abnormal invasion of EMT-derived cells into the truncal cushion [179]. Absence of *Nfatc1-Calcineurin* from the SHF leads to enhanced apoptosis within the conal mesenchyme cushion and abnormal semilunar valve formation, highlighting an important role of SHF in this pathway for conal cushion development [180].

1.3.4.5. Extracellular matrix: EMT is mainly regulated by a well-organized ECM whose components are crucial for EMT progression and ECM remodeling. This matrix underlying the endocardium is primarily composed of proteoglycans, which are present throughout the valve but are predominantly expressed within the middle layer to provide tissue integrity and compressibility [181]. The glycosaminoglycan hyaluronan (HA), one of the most important components of the ECM, is secreted by the myocardium, and plays a role in valvulogenesis due to its ability to induce cell signaling [182]. Disruption of HA synthesis or digestion of HA, using hyaluronidase in cultured embryos, results in absence of cushion formation [183,184]. Many ECM remodeling enzymes are found to be expressed during valve maturation such as matrix metalloproteases (MMPs), tissue inhibitors of matrix metalloproteases (TIMPS), and Cathepsins. VCAN, a proteoglycan linking protein between hyaluronan and collagen, is also involved in ECM regulation since *Vcan* null mice fail to form valvular cushions [185].

1.4. Formation of the cardiac conduction system

Fusion of regions of the lateral plate mesoderm during embryogenesis results in the formation of a linear heart tube. SHF, located medially in the cardiac mesoderm, proliferate rapidly and serve as a progenitor pool for myocardial cells, which will eventually be added to both poles of the heart tube. These cells are then characterized at that stage by their reduced proliferation rate [3]. The myocardium of the initial embryonic tube has a phenotype resembling nodal tissues which display the following characteristics: poor contraction, atomicity, underdeveloped sarcomeres and sarcoplasmic reticulum (SR), and slow transmission of the impulse. The pacemaker activity in this tube is translated into peristaltic contractions showing a sinusoidal electrocardiogram (ECG). The electrical activity of the heart can be recorded, giving rise to the characteristic ECG tracing **(Figure 1.11)**. During elongation of the tube, the atria and ventricles acquire functioning myocytes and expand by accelerated proliferation rate including upregulation of gap junction and mitochondrial genes [21,186,187].

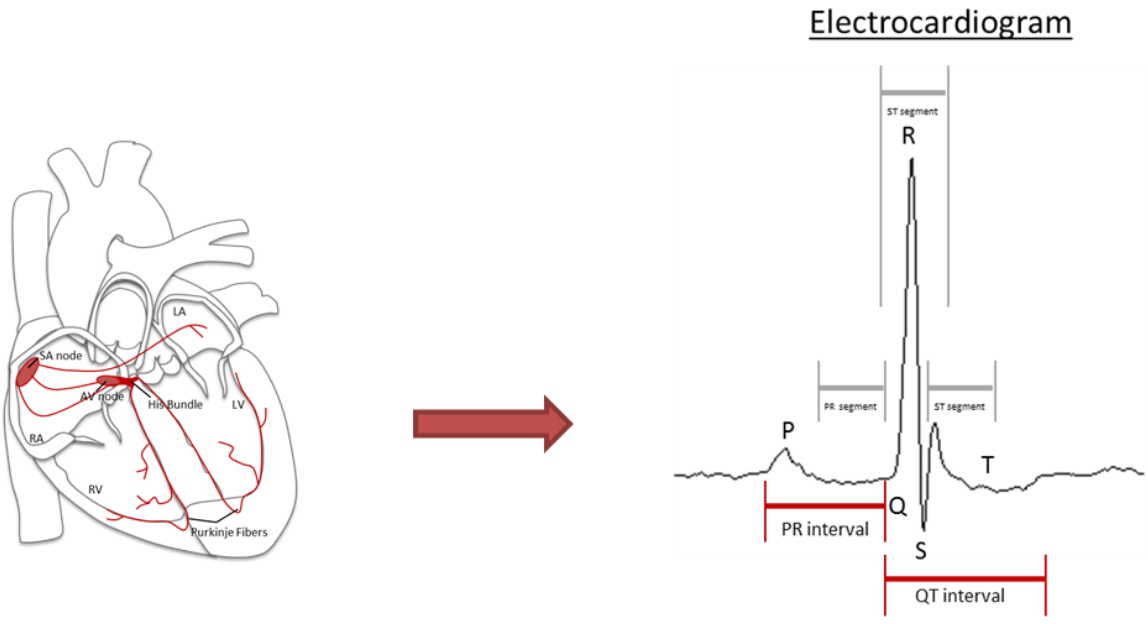

Figure 1.11: Schematic representation of the cardiac conduction system and the electrocardiogram tracing. SA: sinoatrial. AV: atrioventricular. RA: right atria. RV: right ventricle. LA: left atria. LV: left ventricle.

Not all the cardiac regions differentiate into chamber myocardium, some retain low proliferation rate such as the sinus venosus, the AVC, the OFT and inner curvatures. At this stage, the sinus venosus is the main pacemaker activity and the AVC retains a much slower mode of conductance than the surrounding chamber myocardium. The ECG starts to resemble that of a mature heart since serial and rapid contractions of the atrial and ventricular compartments start to occur. Early vertebrates show alternating configurations of slow (sinus venosus, AVC, OFT) conductance structures and fast conducting atrial and ventricular myocardium. Higher vertebrates develop distinctive conductance structures such as the SAN in the sinus venosus, the AVN within the AVC, the AV bundle (AVB), and the Purkinje fibers ensuring the ventricles' contraction [21,187,188].

To further understand the CCS, it is important to understand the arrangements of its components within the heart and how the electrical signal propagates within. The SAN, the pacemaker of the heart, is the first component of the CCS whose role is to initiate the electrical impulse. It is situated at the boundary between the superior caval vein and the right atrium. The impulse propagates then to the AVN, which is situated at the boundary between the atrium and the ventricle, forming the only myocardial connection between both chambers. The impulse arrives to the AVN through the atrial muscle, where its propagation is delayed, allowing the ventricles to be in diastole during the contraction of the atria. The slowing of the signal will also help protect from any ventricular arrhythmias which could be triggered by the atria. A switch to fast conducting structures allows the impulse to travel to the AVB and then to the Purkinje fibers, allowing the activation of the working ventricular

myocardium and therefore its contraction [189]. On the ECG, the atrial depolarization is represented as the P-wave, with the P-R interval showing the AV delay. The QRS complex represents the ventricular activation or depolarization, whereas the T wave indicates the repolarization of the ventricles **(Figure 1.11)**.

1.4.1. Sinoatrial node

The mature SAN is localized at the entrance of the right atrium at the intercaval region. Its core is composed of conduction cells surrounded by working myocardial cells (**Figure 1.11 and 1.12**). In between, transitional cells, with a phenotype resembling that of the SAN and working myocardium together, are found within the SAN. The outer border of the SAN is surrounded by a ring of connective tissue and arteries playing an important role in protecting it from the suppressing hyperpolarizing influence of the atrium [190]. Pacemaker activity requires the presence of gap-junctions with very low conductance (CX30.2, CX45) to protect it from the fast-conducting neighboring atrial myocardium (CX40/CX43/SCN5a). These gap junctions also serve as a good marker to distinguish the node cells [191]. The hyperpolarization-activated channel *HCN4* (Potassium/sodium channel 4) and the T-box TF TBX3 are both enriched in the SAN and serve as excellent nodal markers along with the atrial natriuretic peptide (NPPA or ANF). The latter is not expressed in these cells, but serves as an additional negative marker [192,193]. It is thought that SAN growth can be either mediated by recruitment of surrounding myocardial cells acquiring the SAN phenotype, or achieved by proliferation of specified SAN primordial cells. SAN progenitor cells were also shown to have features of progenitors of the secondary heart field (*Isl1*$^{+}$) and the sinus venosus (*Tbx18*$^{+}$) [194].

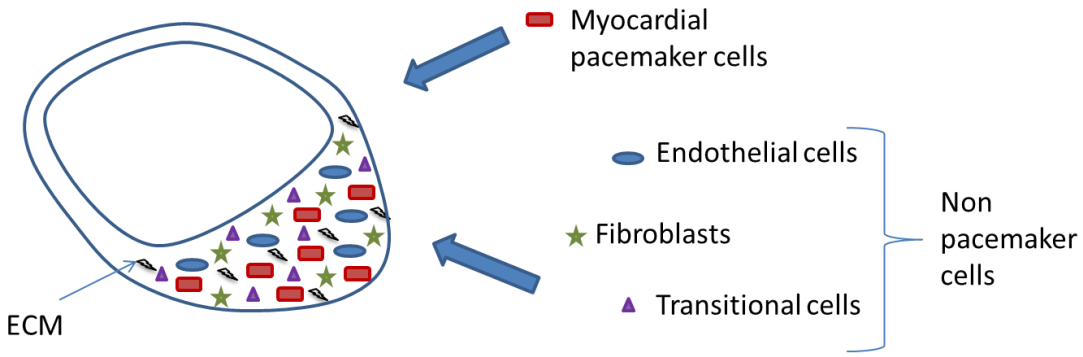

Figure 1.12: Schematic representation of the different type of cells composing the sinoatrial node. ECM: extracellular matrix.

Many TFs have been shown to regulate the development and function of the SAN (**Table 1.1.**). TBX5, expressed in the SV and atria, have been shown to regulate the expression of the short stature homeobox TF 2 (SHOX2), TBX3 and BMP4, all of which are important regulators of SAN formation, via interaction with its partner NKX2.5 [195,196]. Within the SAN, SHOX2 represses the expression of NKX2.5, inhibiting the working myocardium genetic program. Therefore, *Shox2* deletion in mice leads to conduction system defects manifested by a hypoplastic SV, an upregulation of NKX2.5, and a downregulation of the conduction cells markers HCN4 and TBX3 [197,198]. TBX3 prevents atrialization via inhibition of CX40, CX43, SCN5a and NPPA/B, markers of the myocardial program, with ectopic expression of TBX3 leading to the formation of new functional pacemaker cells within the atria [102]. The TF PITX2 has been shown to play a major role in SAN development as a mediator of the right-side development of the SAN which occurs via suppression of the SAN gene program in the left SV. For this reason, the SAN is formed at both sinoatrial junctions (left and right) in *Pitx2*-deficient embryos, [199]. TBX18 is expressed in the progenitor cells that give rise to the head and sinus horns of the SAN and its loss in mice

leads to an abnormal hypoplastic SV and SAN [194]. Finally, the LIM-homeobox TF ISL1has been extensively studied for its role as a regulator of SAN development, especially due to the fact that its expression is selectively maintained in the myocytes of the SAN during both embryogenesis and adulthood, yet its expression in regular myocytes is downregulated after their differentiation. ISL1 has been shown to be required for SAN proliferation and its deletion specifically from SAN cells leads to embryonic lethality in mice [200,201].

Table 1.1: Summary of the different genes important for the formation of the CCS structures. SAN: sinoatrial node. AVC: atrioventricular cushions. AVN: atrioventricular node. VCS: ventricular conduction system.

SAN	AVC/AVN	VCS
TBX5,TBX3, TBX18	TBX2, TBX3, TBX20, TBX5	TBX3, TBX5
BMP4	BMP2, BMPR1a	SCN5a
NKX2.5	NKX2.5	NKX2.5
HCN4, HCN1	MSX2	ID2
PITX2	GATA4, GATA6	IRX3
ISL1	MyoR	CX40
SHOX2	ID2	
CX30.2	SCLC8a1	
CAV3.1	CX30.2	

1.4.2. Atrioventricular node

The AVN is the structure situated at the interface between the right atrium and ventricle that ensure the slowing down of the propagated signal (**Figure 1.11**). Lineage tracing experiments revealed that *Tbx2*$^{+}$ cells of the inflowtract of the early tubular heart contribute to most of the AVC, which is first distinguished morphologically around E9 [107]. On the other hand, the left posterior SHF of E8-8.5 mouse embryos has been shown to contribute to the superior AVC, whereas the right posterior SHF contributes to the inferior AVC [85]. During AV valve formation, the deposition of the cardiac jelly and invasion of the

epicardial-mesenchyme physically separates the AVC myocardium from the endocardium resulting in the insulation of the atrial and ventricular working myocardium [202]. At this stage, and at the atrial side of the annulus fibrosus, the definitive AVN and AV bundles form from *Tbx3*$^{+}$ cells from within the cushion. Cells of the ventricular septum ridge then participate in the formation of the AVB, which is the only myocardial conducting structure between the atria and ventricles [203]. Many studies have investigated the different cell morphologies composing the AVN. Two of the cell types are regulated to be the most representative of this large heterogeneous population─ cells with ovoid shape and cells with rod shape. Both cell types are found to be autorhythmic but possess different action potential and ion pool profiles. Ovoid cells resemble the action potential of SAN cells and therefore have a high pacing rate, whereas a slower rate is found in the rod cells that resemble atrial cells [204,205].

Many studies have been conducted to further elucidate the molecular pathways regulating AVC/AVN development (**Table 1.1.**). TBX2 and TBX3 are crucial regulators of the development of this structure due to their role in maintaining the primitive phenotype of slow conduction by repression of the chamber myocardium genes (CX40, NPPA, SCN5a). They are known to interact with MSX2 and NKX2.5, as well as with TBX5, suppressing expression of downstream targets within the AVC cushion such as NPPA, CX43 and CX40 [203]. This explains the inactivation of *Tbx2*, whether from the myocardium or from the entire body, leads to abnormal formation of the annulus fibrosus and ectopic formation of conductive AV pathways [206,207]. BMP2 is required for AVC formation and controls the restricted expression of TBX2 and TBX3 within the AVC. On the other hand, TBX20 represses the activation of TBX2 by BMP/SMAD signaling, confining its expression to the AV canal and defining the AVC boundary [208,209]. NOTCH and canonical WNT signaling are both required for proper formation of the electrical programming within the AVN. Inhibition

of *Notch* in mice leads to hypoplastic AVN, whereas myocardial deletion of *Wnt* signaling leads to hypoplastic RV and loss of the AVC myocardium [210,211]. The GATA family members, GATA4 and GATA6, have also been shown to play a role in AVC/ANV development. GATA4 has been suggested to mediate the regulation of slow AV conduction genes (such as CX30.2) via its interaction with TBX5 and musculin (the basic helix-loop-helix (bHLH) TF MyoR) [212,213]. GATA6, on the other hand, has been shown to regulate expressions of ID2 and sodium-calcium exchanger NCX1 (SLC8a1), and that myocardial-specific deletion of *Gata6* leads to a prolongation of the PR interval in mice with the presence of fewer *Tbx3*$^{+}$ cells within the AVN [214].

1.4.3. Ventricular conduction system

The myocardium-derived VCS comprises the bundle of His or the AVB, the BBs─ running along the septum towards the apex, on both right and left sides below the endocardium─ and the Purkinje fibers (**Figure 1.11**) [215]. The VCS enables the fast conduction of the impulse from the AVN to the ventricles due to the presence of high levels of fast conducting genes such as SCN5a and CX40, which are the most specialized markers of the VCS. The cellular origin of the components of the VCS has been well studied. A domain within the AVC (*Tbx3*$^{+}$*)* extends into the ventricular compartment and through the crest of the ventricular septum to give rise to the interventricular ring, at the origin of the AV bundle. However the embryonic location of the AVB progenitors has not been uncovered to date [192]. The sub-endocardial myocytes of the septum trabeculae give rise to the BBs, whereas the Purkinje fibers are derived from the trabecular myocardium [203]. It is thought that the *Cx40*$^{-}$ ventricular myocardium and the *Cx40*$^{+}$ Purkinje fibers share the *Cx40*$^{+}$ Purkinje-like embryonic trabecular myocardium as a common precursor [216].

The molecular mechanisms underlying VCS formation have pointed out an important role for NOTCH signaling in promoting the transition of early embryonic myocardium into trabecular myocardium (**Table 1.1.**). This transformation has been shown to signal through Ephrin B2 (EFNB2) and neuregulin 1(NRG1), in addition to a role of BMP10 in maintaining the proliferation of trabecular cardiomyocytes. In this term, induction of a Purkinje-like gene program has been reported to be induced in neonatal ventricular cardiomyocytes following transient activation of NOTCH [217]. More specifically, AVB and BBs development have been shown to be controlled by TBX3, which inhibits genes of the working myocardium, and by TBX5, which stimulates the expression of fast conducting genes (CX40 and SCN5a) [218]. NKX2.5 have been shown to cooperate with TBX3 and TBX5 in VCS development with heterozygous mice for *Nkx2.5* displaying prolonged QRS interval, low amplitude of AVB depolarization, hypoplastic Purkinje fibers and upregulation of BMP10. In double *Tbx5/Nkx2.5* heterozygous mice, the AVB and BBs fail to develop with absence of ID2 activation, which have been thought to play an important role in the formation of these structures, given that its total knockout leads to an identical phenotype [219]. The Iroquois homeobox gene IRX3 has also been implicated in VCS development: mutant mice for *Irx3* display delayed and abnormal ventricular conduction as well as ventricular arrhythmias [220,221].

1.5. Congenital heart defects

A large number of TFs and complex molecular regulatory networks control heart and valve morphogenesis and any deviation or disruption, due to environmental or genetic factors, will result in congenital heart defects (CHD). The incidence of human CHD is over 1% of live births and represents a leading cause for death in infancy as well as a risk factor

for cardiovascular disease later in life [222]. These defects can be divided into two categories: 1) mild defects that initially do not affect the heart function but can later lead to cardiac complications if left untreated (*e.g.* ASD), and 2) life threatening defects that contributes to the majority of mortality cases. The spectrum of CHD is very wide and defects can result from OFT or chamber septation problems, cardiac valve formation problems, cardiac hypertrophy, or from defective conduction system morphogenesis. Despite remarkable progress in the past few years, the exact causes and pathways underlying the majority of CHD remain undefined, owing it to the multifactorial nature of CHDs─ mutations in one TF can lead to many phenotypes and one defect can be connected to several genes.

1.5.1. Outflow tract defects

Anomalies of the great arteries and cardiac OFT defects account for approximately 30% of all CHD cases [223]. Incomplete or mis-aligned OFT septation leads to a wide range of CHDs affecting either the great arteries or the cardiac valves. Abnormalities of the vessels include: 1) PTA, where the separation between pulmonary and aortic arteries fails resulting in one common trunk, 2) DORV, where the aorta and pulmonary trunks both exit from the RV, 3) TGA, where the pulmonary trunk arises from the LV and the aorta from the RV, and 4) overriding aorta (OA), which is an OFT alignment defect that is usually found associated with Tetralogy of Fallot (TOF) (a condition with multiple heart defects including pulmonary stenosis (PS), RV hypertrophy and ventricular septal defect) (**Table 1.2**) (reviewed in [224]).

Table 1.2: **Phenotypes resulting from abnormal septation of the OFT/great arteries and their associated genes.** PTA: persistent truncus arteriosus. TGA: transposition of the great arteries. DORV: double outlet right ventricle, OA: overriding aorta (reviewed in [224]).

Phenotype	Genes associated with the phenotype
PTA	SMAD4, SMAD7, NOGGIN, BMP4, ACVR1, BMPR2, BMPR1, TBX1, FGF15, FGF8, FGFR1/2, GATA6, SOX4, PTK2, SEMA3C, NRP1, PBX1, PAX3
TGA	NRP1,FGF8, ACVR2b, CFC1, GDF1, NODAL, ZIC3, HSPG2
DORV	NF1, TGFB2, BMP2/4, BMPR21, FGF15, FGF8, FGFR1/2, SMAD4, PSEN1, BIRC5, HIF1A
OA	NOTCH2, JAG1, HES1, DNMAML

Defects of the cardiac valves often results from abnormal valve formation or septation during embryogenesis. These defects involve abnormalities of 1) the tricuspid valve leading to tricuspid atresia (TA), where the valve is abnormally formed or missing, 2) the mitral valve leading to parachute mitral valve (PMV), which describes the presence of a single papillary muscle from which the tendinous cords of both valve leaflets divide, 3) the pulmonary valve, with pulmonary stenosis being the most common defect (narrowing of the pulmonary valve orifice causing a resistance to the blood flow), and 4) the aortic valve, resulting in aortic stenosis and BAV disease (to be detailed below).

1.5.1.1. Bicuspid aortic valve disease

BAV disease is the most common CHD, affecting 1-2% of the population with a higher male prevalence (3:1) [225]. It results from the failure of leaflet separation during valve formation and maturation, resulting in two asymmetrical leaflets instead of three symmetrical ones. BAV is an autosomal dominant heritable trait with a high prevalence among first-degree relatives and in families with multiple affected individuals (9% and 24% of total

prevalence) [226]. This incomplete penetrance in its inheritance suggests the presence of many gene-gene and gene-environment interactions. The leaflets position and orientation relative to the right and left coronary arteries varies among different BAV cases, resulting in the different BAV phenotypes. The right-left (RL) type BAV is the most frequently found, and results from the fusion of the right and left cusps, accounting for 59% of all cases[227]. The right-noncoronary (RN) type BAV, which accounts for 37%, results from fusion of the right and non-coronary cusps. The left-noncoronary (LN) type BAV, resulting from a failure of separation between the left and non-coronary leaflets, is the least common type [227] (**Figure 1.13**). It has been thought that RN-type BAV results from defective formation of the OFT cushion, while RL-type BAV is caused by a defective septation process during valve morphogenesis [228].

BAV can be isolated or occur in conjuction with other CHDs (*e.g.* VSD, interruption of the aortic arch), and can be asymptomatic or lead to life threatening events (*e.g.* aneurisms, stenosis, endocarditis). Therefore, it is considered a risk factor for many valvulo-vascular complications [229]. BAV patients often develop mid ascending aortic dilation that is found to correlate with older age. They can also develop aortic root dilation that is often more associated with younger males [230]. BAV can also lead to severe valve complications at later stage with changes in ECM composition, disruption of endothelial cells, and activation of valvular interstitial cells (VIC, which are fibroblast-like cells and quiescent in normal conditions), causing valve dysfunction and calcification [231,232]. Studies have shown that the presentation of valve dysfunction can vary among the different types of BAV: patients with RN-type BAV are found to have more severe regurgitation whereas RL-type BAV patients develop more severe stenosis and calcification [233].

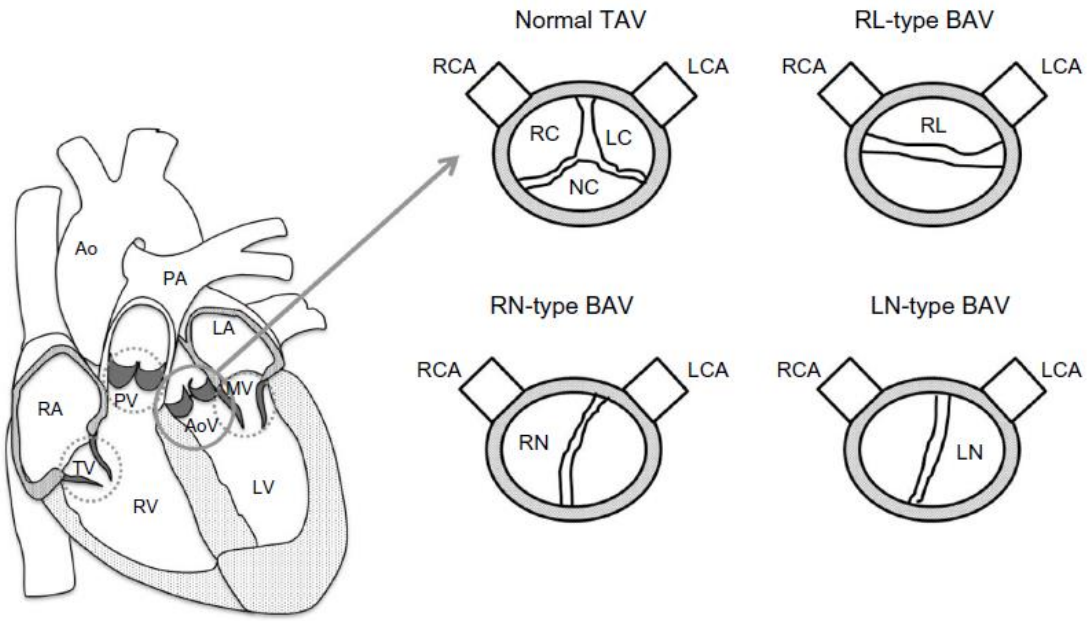

Figure 1.13: Schematic representation of a normal tricuspid valve and the different types of Bicuspid aortic valves. Ao: aorta. PA: pulmonary artery. RA: right atria. LA: left atria. RV: right ventricle. LV: left ventricle. PV: pulmonary valve. AoV: aortic valve. MV: mitral valve. TV: tricuspid valve. RC: right coronary. LC: left coronary. NC: non-coronary cusp. LCA: left coronary artery. RCA: right coronary artery. RN: right- non-coronary. LN: left-non-coronary. RL: right-left. TAV: tricuspid aortic valve. BAV: bicuspid aortic valve [234].

Great efforts have been devoted to determining the heritability and underlying pathways leading to BAV. However, in humans, only three genes have been reported to date to have BAV-causing mutations: 1) the transmembrane protein NOTCH1, 2) the GATA TF GATA5, and 3) the matrix nuclear gene matrin 3 (MATR3) [235–237,270]. With that in mind, animal models lacking other important regulators of valve development have been generated and examination of the aortic valve revealed the presence of BAV. The *Nos3*-null mouse model was one the first models of BAV to be reported where 41.6% of the mice display the RN type BAV [238,271]. The same study showed that NOS3 is able to regulate NOTCH1, with double *Nos3*$^{-/-}$ *Notch1*$^{+/-}$ displaying 100% BAV penetrance. Our group also reported that inactivation of *Gata5* in mice leads to 26% penetrant BAV [51]. Whether this deletion was

global or endocardial-specific, the partial RN-BAV penetrance was still observed. Deletion of the Activin type I receptor (*Alk2*), an important regulator of EMT, from the cushion mesenchyme also resultes in BAV [239]. A role for HOXA1 and NKX2.5 has been highlighted from animal studies in valvulogenesis since inactivation of *Hoxa1* or haploinsufficiency of *Nkx2.5* lead to partially penetrant RN-BAVs (24% for *Hoxa1* and 8.2% for *Nkx2.5* models) [240,241]. On the other hand, models to study RL-BAVs remain limited. The inbred Syrian hamster model was the first model of RL-BAV to be reported with almost half the animals displaying BAV[242]. In 2016, MacGrogan *et al.* reported that abrogation of NOTCH signaling from the endothelium leads to 34.6% mutants with BAV involving both the R-N and R-L types of BAV with a penetrance of 76.4% and 23.5%, respectively [243]. Genome wide association studies have also identified chromosomal regions 5q, 9q (*NOCTH1*), 13q, 17q (*KCJN2*) and 18q to contain genes associated with BAV (**Table 1.3**) [235,244,245].

BAV can occur in conjunction with other phenotypes in some human syndromes. For example, Marfan syndrome is shown to be caused by mutations in the fibrillin-1 (*FBN1*) gene, which is important for the formation of elastic fibers. Marfan syndrome is a connective tissue disorder with patients having cardiovascular, ocular and skeletal abnormalities [246]. As mentioned earlier, BAV can go undetected for a lifetime or can lead to cardiovascular complications that require surgery. It is therefore important to accelerate the discovery of new causative genes to allow genetic screening for early detection of affected individuals, to provide a better understanding of the basis of BAV formation and its degenerative nature, and to help in the development of genotype-phenotype correlations, allowing personalized treatment for patients.

Table 1.3: **Genes associated with human and animal (mouse) BAV phenotypes.** BAV: bicuspid aortic valve. CoA: coarctation of the aorta. PDA: patent ductus arteriosus. VSD: ventricular septal defect. (Adapted from [234]) [237,243].

Genes	Human valve phenotype	Animal model valve phenotype (mouse)
Trasncription factors		
NKX2.5	Not reported	Partial penetrance of BAV (8.2%) with aortic aneurism
HOXA1	Not reported	Partial penetrance of BAV (24%)
GATA5	BAV with aortic stenosis and regurgitation	Partial penetrance of BAV (30%)
MATR3	BAV with coarctation of the aorta	Partial penetrant BAV with PDA and CoA (15%)
Enzymes		
NOS3	Not reported	Partial penetrance of BAV (41.6%)
Channels		
KCNJ2	BAV with coarctation of aorta	Not reported
Ligands		
NOTCH1	BAV with aortic aneurism, calcification (5%)	Partial penetrance of BAV
JAG1	Not reported	Partial penetrant BAV with VSD (34.6%)
Receptors		
TGFBR2	BAV with aortic aneurism	Not reported
ALK2	Not reported	BAV with aortic insufficiency and/or stenosis
Chromosomal regions		
Loci 5q-gene unknown	Partial penetrance of BAV	
Loci 9q-gene unknown	Partial penetrance of BAV	
Loci 13q-gene unknown	Partial penetrance of BAV	
Loci 17q-gene unknown	Partial penetrance of BAV	
Loci 18q-gene unknown	Partial penetrance of BAV	
Xp gene	BAV	
Signal transducer		
SMAD6	BAV with mild aortic stenosis BAV with mild aortic stenosis and coarctation of the aorta	Not reported

1.5.2. Conduction system defects

The SAN and the AVN, together with the His-Purkinje fibers, form the functional CCS. Nodal cells of the CCS have a different organizational structure than cells of the working myocardium and are able to generate the cardiac action potential due to the presence of specific ion channels within them. Dysfunction of impulse generation and propagation can result from an imbalance of the ionic content and/or from structural disorganization of the cells. Abnormalities of the SAN and AVN can be either inherited or acquired at later stages of life due to the structural and physiological changes that these structures undergo. For example, the SAN, harboring a small number of nodal cells, is able to undergo extensive

remodeling (due to pathological conditions such as arrhythmia) leading to a decreased nodal area with increased fibrosis, therefore result in sinus dysfunction [204,247]. As well, sick sinus dysfunctions (SSD) are cardiac disorders affecting the ability of the SAN to generate a normal heart rate and leads to sinus arrest, sino-atrial exit block (where the depolarization cannot exit the node towards the atria), bradycardia (abnormally slow heart rate), tachycardia (abnormally fast heart rate), or alternating periods of the latter two [248,249]. Atrial arrhythmias are often associated with SSD with 40 to 70% of the patients displaying it at the time of diagnosis. Atrial fibrillation (AF) is the most common type of atrial arrhythmias, and is characterized by irregular and rapid atrial depolarisations showing abnormal/absent P waves by ECG [250,251].

The AVN is found to compensate in cases with abnormal SAN activity: it acts as a pacing unit of ventricular myocytes in cases of sinus arrest and bradycardia, and as a low-pass filter in cases of atrial tachyarrhythmia, protecting the ventricles from overwhelming excitations [204]. However, abnormalities of the AVN can also occur and cause a partial or a complete block of the action potential that passes through it (AV block). Gain and loss of function mutations in the sodium channel SCN5a have been shown to be associated with both sinus dysfunction (inducing bradycardia and sinus-exit block) as well as with AVN dysfunctions/AV block, which can be observed either alone or with Brugada and/or LQT3 syndromes (Brugada syndrome causes sudden death due to ventricular fibrillation). Long QT syndrome is caused by mutations in potassium or sodium ion channels [248,252]. As a result, a disturbance in their functionality leads to a prolonged QT interval and an abnormal T wave as shown on the ECG [253].

Studies using mouse models have helped bringing more insight into the pathological mechanisms of conduction diseases. Loss of function mutations in the hyperpolarized

channel HCN4 have been identified in patients with sinus bradycardia. Similar findings were shown when *Hcn4* was conditionally removed from the heart with mice showing sinus bradycardia and AV block that progressed from prolonged PQ interval to a complete heart block [254,255]. Given the important role that calcium plays within the nodal cells, especially during the excitation-contraction coupling process, human mutations in the sarcoplasmic Ca^{2+}-binding protein Calsequestrin (CASQ2) and the Ryanodine Receptor type 2 (RYR2), as well as mouse ablation of the Na^{+}/Ca^{2+} exchanger (*Ncx1*), have been shown to result in conduction abnormalities including ventricular tachycardia, sinus bradycardia, and elimination of the SAN pacemaker activity [256–258]. The identification of defective genes causing SAN and AVN dysfunctions, whether from animal models or from human screening, will further shed light on the functionality of important regulators of the conduction system and will help in the implementation of new and appropriate therapeutic treatments.

1.5.3. Heart and limb defects

As mentioned previously, CHDs can occur in isolation or in combination with other defects, as part of a more complex syndrome. Such is the case of skeletal/limb abnormalities, which form in addition to the heart phenotype, the Heart-Hand and Heart-Feet classes of syndromes. Before exploring the underlying mechanisms of heart-limb abnormalities, it is important to understand the origin/similarities shared by these two structures.

1.5.3.1. Heart and limb development

In humans, the anterior angioblastic chords, which give rise to the cardiac tubes, become visible at 19 days post-conception. The upper and lower limbs become visible later on at 26-27 days for the upper and at 27-28 days for the lower limbs. The embryonic head then folds shifting the heart tube closer to the upper limbs. Heart and limb primordia are

thought to derive from the same region located near the pre-chordal plate that will eventually give rise to the lateral plate mesoderm [259]. The proper differentiation of the regions of the heart tube (ventricles, atria, CT and sinus venosus) and of the limb (pre-axial: anterior/near the thumb, meso-axial: in the middle, and post-axial: posterior/digit 5 area), along the A-P axis, is required for the development of these structures [260,261]. Any chromosomal changes, gene mutations, or alterations affecting the A-P orientation, will perturb this early cardiomelic domain and will give rise to a wide range of heart, limb or heart and limb abnormalities together [259].

In **section 1.1.1**, we detailed the origin of the cardiac progenitor cells and indicated that they derive from the lateral plate mesoderm and migrate to the region of the forming heart to form the cardiac crescent (**Figure 1.1 A**). Studies on the limb were first performed in chicks where it was shown that the limb formation begins early, when mesenchymal cells from the somatic layer of the lateral plate mesoderm and somites, begin to proliferate and accumulate under the epidermal layer to form a bulging structure─ the limb bud. Cells deriving from the lateral plate mesoderm will contribute to the formation of the skeletal structures of the limb (skeletal precursors), whereas those from the somites will form the musculature of the limb (muscle precursors). The cells of the lateral plate mesoderm play a crucial role in limb bud initiation via secretion of the FGF10, a paracrine factor, which has an important role in initiating the different interactions between signals of the mesoderm and ectoderm [262,263]. At this stage, the limb buds have to be specified to either becoming forelimbs (upper extremities) or hindlimbs (lower extremities) via differential expression of TBX5 and TBX4 [262]. Following entrance of the mesenchymal cells into the limb forming region, they start secreting factors that induce formation of the apical ectodermal ridge (AER) from the overlying ectoderm. The role of the AER is 1) to maintain the proliferation

of the mesenchymal cells allowing the growth of the limb along the proximal distal (P-D) axis, 2) to express molecules required for the generation of the A-P axis and 3) to orchestrate the signals between the anterior-posterior and dorsal-ventral (D-V) axes ensuring proper cell differentiation [262]. Further details on the molecular mechanisms governing proper limb formation will be explained in **Chapter III**.

1.5.3.2. Examples of heart and limbs diseases

Human CHDs with heart and limb defects occur 1 in every 5000 live births [259]. It has been shown that there is an association between anterior or posterior cardiac problems and limb anomalies. The anterior anomalies generate heart conotruncal-limb pre-axial defects whereas posterior defects generates heart atrial-limb post-axial defects [259]. Many genes have been found to be crucial for heart and limb development; for example, TGF-β, BMP4, MSX-TFs, retinoic acid receptors and SHH. TGF-β and BMP4 are both expressed in the AV valve and in the early limb mesenchyme, MSX-TFs are expressed in the AV canal, the conduction system, and within the limb mesenchyme. The RA receptors are expressed in the conotruncal region and the limb bud, and SHH is expressed in the OFT region and within the limb bud [260,264]. Below are some examples of diseases displaying cardiac-limb anomalies and their underlying causes.

1.5.3.2.1. Holt Oram syndrome: HOS is the most common heart-hand disorder. 75% of patients with HOS also have CHD, most commonly being ASD, VSD, and conduction system defects [265]. The limb deformity phenotype affects only the upper extremities involving the radial (the bone extending from the lateral side of the elbow to the thumb side) or the carpal (small bones that make up the wrist) bones. These patients display polydactyly frequently (presence of more than 5

digits). HOS is inherited in an autosomal dominant manner with TBX5 being the disease causing gene [265].

1.5.3.2.2. ***Ellis-Van Creveld syndrome:*** EVC is a rare disease characterized by the presence of short ribs, short limbs, postaxial polydactyly, growth retardation, dysplastic fingernails and teeth, ectodermal defects and heart defects. Atrial septal defects are the most common CHD observed in EVC patients with a prevalence of ASD occurring in 60% of the patients [266]. It is an autosomal recessive skeletal dysplasia disease displaying variable expressivity. Mutations in the EVC1 and EVC2 genes have been shown to be associated with this syndrome [266].

1.5.3.2.3. ***Bardet-Biedl syndrome:*** BBS is characterized by primary features including cone-rod retinal dystrophy, polydactyly, renal defects, genital abnormalities, obesity, and learning difficulties. Secondary features of the disease also include developmental delay, brachydactyly or syndactyly (SD), dental defects, olfactory deficit, diabetes mellitus, and CHD (*e.g.* IVS hypertrophy and dilated cardiomyopathy). It is a rare autosomal recessive gene with a high prevalence in inbred populations. It has been shown that BBS can result from mutations affecting at least 14 genes (also called the BBS genes) that are known to play important roles in cilia formation. The most common mutations affecting BBS are BBS1 and BBS10 [267,268].

1.5.3.2.4. ***McKusick-Kaufman syndrome:*** MKS is a syndrome characterized by the combinatorial presence of post-axial polydactyly, heart disease and abnormalities in the formation of the genital organs. Cardiac malformations in MKS include ASD, VSD, small aorta and hypoplastic LV, TOF, and patent ductus arteriosus. It

is inherited in an autosomal recessive manner and have been shown to be caused by a mutation in the MKKS gene [269].

Finally, CHDs affect an estimated 1% of the population causing a variety of phenotypes, and are the main cause of morbidity and mortality. CHDs create a significant financial burden on the healthcare system as well as on the patients and their families. Nowadays, there are few, if any, curative therapies, despite our progress and good understanding of some of the genetic basis of many CHDs. New approaches are therefore needed to determine the altered pathways leading to disease. This may reveal potential biological targets which will be useful for prognosis and therapy development.

1.6. Objective and hypothesis

1.6.1. Objective: The objective of this PhD project is to investigate the role of transcription factor GATA6 in heart and limb formation and to identify the cellular and molecular pathways underlying its action (s).

1.6.2. Hypothesis: GATA6 is expressed in several cardiac cell types and mutations in *GATA6* are associated with variable cardiac phenotypes in human. Proper heart formation and function require well-orchestrated interaction between different cell types. I hypothesize that GATA6 plays a cell specific role in heart morphogenesis and homeostasis and that disruption of GATA6 from different cell types will lead to distinct cardiac phenotypes.

In the first and second chapters, we report a novel role for GATA6 in the formation of the aortic valve and the sinoatrial node. In the third chapter, a role for GATA6 as a potential heart and limb causing gene is revealed. The data presented in this thesis provide novel insights for understanding the different functions of GATA6 in heart and limb development.

1.7. References

1. Srivastava D. Genetic regulation of cardiogenesis and congenital heart disease. *Annu Rev Pathol*. 2006;1:199–213.

2. Abu-Issa R, Kirby ML. Heart field: from mesoderm to heart tube. *Annu Rev Cell Dev Biol*. 2007;23:45–68.

3. Buckingham M, Meilhac S, Zaffran S. Building the mammalian heart from two sources of myocardial cells. *Nat Rev Genet*. 2005;6:826–835.

4. Nemer M. Genetic insights into normal and abnormal heart development. *Cardiovasc Pathol Off J Soc Cardiovasc Pathol*. 2008;17:48–54.

5. Srivastava D. Making or breaking the heart: from lineage determination to morphogenesis. *Cell*. 2006;126:1037–1048.

6. Wu SM, Chien KR, Mummery C. Origins and fates of cardiovascular progenitor cells. *Cell*. 2008;132:537–543.

7. Christoffels VM, Habets PE, Franco D, Campione M, de Jong F, Lamers WH, Bao ZZ, Palmer S, Biben C, Harvey RP, Moorman AF. Chamber formation and morphogenesis in the developing mammalian heart. *Dev Biol*. 2000;223:266–278.

8. Dyer LA, Kirby ML. The role of secondary heart field in cardiac development. *Dev Biol*. 2009;336:137–144.

9. Packham EA, David Brook J. Interaction makes the heart grow stronger. *Trends Mol Med*. 2003;9:407–409.

10. Wagner M, Siddiqui M a. Q. Signal transduction in early heart development (II): ventricular chamber specification, trabeculation, and heart valve formation. *Exp Biol Med Maywood NJ*. 2007;232:866–880.

11. Christoffels VM, Burch JBE, Moorman AFM. Architectural plan for the heart: early patterning and delineation of the chambers and the nodes. *Trends Cardiovasc Med*. 2004;14:301–307.

12. Ho SY, Sánchez-Quintana D. The importance of atrial structure and fibers. *Clin Anat N Y N*. 2009;22:52–63.

13. Srivastava D, Olson EN. A genetic blueprint for cardiac development. *Nature*. 2000;407:221–226.

14. Anderson RH, Webb S, Brown NA, Lamers W, Moorman A. Development of the heart: (2) Septation of the atriums and ventricles. *Heart Br Card Soc*. 2003;89:949–958.

15. Lin C-J, Lin C-Y, Chen C-H, Zhou B, Chang C-P. Partitioning the heart: mechanisms of cardiac septation and valve development. *Dev Camb Engl*. 2012;139:3277–3299.

16. Wessels A, Markman MW, Vermeulen JL, Anderson RH, Moorman AF, Lamers WH. The development of the atrioventricular junction in the human heart. *Circ Res*. 1996;78:110–117.

17. Franco D, Meilhac SM, Christoffels VM, Kispert A, Buckingham M, Kelly RG. Left and right ventricular contributions to the formation of the interventricular septum in the mouse heart. *Dev Biol*. 2006;294:366–375.

18. Nemer G, Nemer M. Regulation of heart development and function through combinatorial interactions of transcription factors. *Ann Med*. 2001;33:604–610.

19. Brand T. Heart development: molecular insights into cardiac specification and early morphogenesis. *Dev Biol*. 2003;258:1–19.

20. Meyers EN, Martin GR. Differences in left-right axis pathways in mouse and chick: functions of FGF8 and SHH. *Science*. 1999;285:403–406.

21. Moorman AFM, Christoffels VM. Cardiac chamber formation: development, genes, and evolution. *Physiol Rev*. 2003;83:1223–1267.

22. Bruneau BG, Nemer G, Schmitt JP, Charron F, Robitaille L, Caron S, Conner DA, Gessler M, Nemer M, Seidman CE, Seidman JG. A murine model of Holt-Oram syndrome defines roles of the T-box transcription factor Tbx5 in cardiogenesis and disease. *Cell*. 2001;106:709–721.

23. Bruneau BG, Bao ZZ, Fatkin D, Xavier-Neto J, Georgakopoulos D, Maguire CT, Berul CI, Kass DA, Kuroski-de Bold ML, de Bold AJ, Conner DA, Rosenthal N, Cepko CL, Seidman CE, Seidman JG. Cardiomyopathy in Irx4-deficient mice is preceded by abnormal ventricular gene expression. *Mol Cell Biol*. 2001;21:1730–1736.

24. Kitajima S, Takagi A, Inoue T, Saga Y. MesP1 and MesP2 are essential for the development of cardiac mesoderm. *Dev Camb Engl*. 2000;127:3215–3226.

25. Wagner M, Siddiqui M a. Q. Signal transduction in early heart development (I): cardiogenic induction and heart tube formation. *Exp Biol Med Maywood NJ*. 2007;232:852–865.

26. Rochais F, Mesbah K, Kelly RG. Signaling pathways controlling second heart field development. *Circ Res*. 2009;104:933–942.

27. Klinedinst SL, Bodmer R. Gata factor Pannier is required to establish competence for heart progenitor formation. *Dev Camb Engl*. 2003;130:3027–3038.

28. Monzen K, Shiojima I, Hiroi Y, Kudoh S, Oka T, Takimoto E, Hayashi D, Hosoda T, Habara-Ohkubo A, Nakaoka T, Fujita T, Yazaki Y, Komuro I. Bone morphogenetic proteins induce cardiomyocyte differentiation through the mitogen-activated protein kinase kinase kinase TAK1 and cardiac transcription factors Csx/Nkx-2.5 and GATA-4. *Mol Cell Biol*. 1999;19:7096–7105.

29. Bodmer R. The gene tinman is required for specification of the heart and visceral muscles in Drosophila. *Dev Camb Engl*. 1993;118:719–729.

30. Harvey RP. NK-2 homeobox genes and heart development. *Dev Biol*. 1996;178:203–216.

31. Molkentin JD. The zinc finger-containing transcription factors GATA-4, -5, and -6. Ubiquitously expressed regulators of tissue-specific gene expression. *J Biol Chem*. 2000;275:38949–38952.

32. Saga Y, Miyagawa-Tomita S, Takagi A, Kitajima S, Miyazaki J i, Inoue T. MesP1 is expressed in the heart precursor cells and required for the formation of a single heart tube. *Dev Camb Engl*. 1999;126:3437–3447.

33. Srivastava D, Thomas T, Lin Q, Kirby ML, Brown D, Olson EN. Regulation of cardiac mesodermal and neural crest development by the bHLH transcription factor, dHAND. *Nat Genet*. 1997;16:154–160.

34. Nemer G, Nemer M. Cooperative interaction between GATA5 and NF-ATc regulates endothelial-endocardial differentiation of cardiogenic cells. *Dev Camb Engl*. 2002;129:4045–4055.

35. Lowry JA, Atchley WR. Molecular evolution of the GATA family of transcription factors: conservation within the DNA-binding domain. *J Mol Evol*. 2000;50:103–115.

36. Morrisey EE, Ip HS, Tang Z, Parmacek MS. GATA-4 activates transcription via two novel domains that are conserved within the GATA-4/5/6 subfamily. *J Biol Chem*. 1997;272:8515–8524.

37. Lentjes MHFM, Niessen HEC, Akiyama Y, de Bruïne AP, Melotte V, van Engeland M. The emerging role of GATA transcription factors in development and disease. *Expert Rev Mol Med*. 2016;18:e3.

38. Simon MC. Gotta have GATA. *Nat Genet*. 1995;11:9–11.

39. Briegel K, Lim KC, Plank C, Beug H, Engel JD, Zenke M. Ectopic expression of a conditional GATA-2/estrogen receptor chimera arrests erythroid differentiation in a hormone-dependent manner. *Genes Dev*. 1993;7:1097–1109.

40. Ting CN, Olson MC, Barton KP, Leiden JM. Transcription factor GATA-3 is required for development of the T-cell lineage. *Nature*. 1996;384:474–478.

41. Lakshmanan G, Lieuw KH, Lim KC, Gu Y, Grosveld F, Engel JD, Karis A. Localization of distant urogenital system-, central nervous system-, and endocardium-specific transcriptional regulatory elements in the GATA-3 locus. *Mol Cell Biol*. 1999;19:1558–1568.

42. Brewer A, Pizzey J. GATA factors in vertebrate heart development and disease. *Expert Rev Mol Med*. 2006;8:1–20.

43. Nemer G, Nemer M. Transcriptional activation of BMP-4 and regulation of mammalian organogenesis by GATA-4 and -6. *Dev Biol*. 2003;254:131–148.

44. Laverriere AC, MacNeill C, Mueller C, Poelmann RE, Burch JB, Evans T. GATA-4/5/6, a subfamily of three transcription factors transcribed in developing heart and gut. *J Biol Chem*. 1994;269:23177–23184.

45. Kuo CT, Morrisey EE, Anandappa R, Sigrist K, Lu MM, Parmacek MS, Soudais C, Leiden JM. GATA4 transcription factor is required for ventral morphogenesis and heart tube formation. *Genes Dev*. 1997;11:1048–1060.

46. Molkentin JD, Lin Q, Duncan SA, Olson EN. Requirement of the transcription factor GATA4 for heart tube formation and ventral morphogenesis. *Genes Dev*. 1997;11:1061–1072.

47. Grépin C, Robitaille L, Antakly T, Nemer M. Inhibition of transcription factor GATA-4 expression blocks in vitro cardiac muscle differentiation. *Mol Cell Biol*. 1995;15:4095–4102.

48. Morrisey EE, Ip HS, Tang Z, Lu MM, Parmacek MS. GATA-5: a transcriptional activator expressed in a novel temporally and spatially-restricted pattern during embryonic development. *Dev Biol*. 1997;183:21–36.

49. Kelley C, Blumberg H, Zon LI, Evans T. GATA-4 is a novel transcription factor expressed in endocardium of the developing heart. *Dev Camb Engl*. 1993;118:817–827.

50. Reiter JF, Alexander J, Rodaway A, Yelon D, Patient R, Holder N, Stainier DY. Gata5 is required for the development of the heart and endoderm in zebrafish. *Genes Dev*. 1999;13:2983–2995.

51. Laforest B, Andelfinger G, Nemer M. Loss of Gata5 in mice leads to bicuspid aortic valve. *J Clin Invest*. 2011;121:2876–2887.

52. Morrisey EE, Ip HS, Lu MM, Parmacek MS. GATA-6: a zinc finger transcription factor that is expressed in multiple cell lineages derived from lateral mesoderm. *Dev Biol*. 1996;177:309–322.

53. Morrisey EE, Tang Z, Sigrist K, Lu MM, Jiang F, Ip HS, Parmacek MS. GATA6 regulates HNF4 and is required for differentiation of visceral endoderm in the mouse embryo. *Genes Dev*. 1998;12:3579–3590.

54. Fujikura J, Yamato E, Yonemura S, Hosoda K, Masui S, Nakao K, Miyazaki Ji J, Niwa H. Differentiation of embryonic stem cells is induced by GATA factors. *Genes Dev*. 2002;16:784–789.

55. Zhao R, Watt AJ, Li J, Luebke-Wheeler J, Morrisey EE, Duncan SA. GATA6 is essential for embryonic development of the liver but dispensable for early heart formation. *Mol Cell Biol*. 2005;25:2622–2631.

56. Lepore JJ, Mericko PA, Cheng L, Lu MM, Morrisey EE, Parmacek MS. GATA-6 regulates semaphorin 3C and is required in cardiac neural crest for cardiovascular morphogenesis. *J Clin Invest*. 2006;116:929–939.

57. Grépin C, Dagnino L, Robitaille L, Haberstroh L, Antakly T, Nemer M. A hormone-encoding gene identifies a pathway for cardiac but not skeletal muscle gene transcription. *Mol Cell Biol*. 1994;14:3115–3129.

58. Murphy AM, Thompson WR, Peng LF, Jones L. Regulation of the rat cardiac troponin I gene by the transcription factor GATA-4. *Biochem J*. 1997;322 (Pt 2):393–401.

59. Wang GF, Nikovits W, Schleinitz M, Stockdale FE. A positive GATA element and a negative vitamin D receptor-like element control atrial chamber-specific expression of a slow myosin heavy-chain gene during cardiac morphogenesis. *Mol Cell Biol*. 1998;18:6023–6034.

60. Heineke J, Auger-Messier M, Xu J, Oka T, Sargent MA, York A, Klevitsky R, Vaikunth S, Duncan SA, Aronow BJ, Robbins J, Crombleholme TM, Cromblehol TM, Molkentin JD. Cardiomyocyte GATA4 functions as a stress-responsive regulator of angiogenesis in the murine heart. *J Clin Invest*. 2007;117:3198–3210.

61. Yamak A, Latinkic BV, Dali R, Temsah R, Nemer M. Cyclin D2 is a GATA4 cofactor in cardiogenesis. *Proc Natl Acad Sci U S A*. 2014;111:1415–1420.

62. Durocher D, Charron F, Warren R, Schwartz RJ, Nemer M. The cardiac transcription factors Nkx2-5 and GATA-4 are mutual cofactors. *EMBO J*. 1997;16:5687–5696.

63. MacNeill C, Ayres B, Laverriere AC, Burch JB. Transcripts for functionally distinct isoforms of chicken GATA-5 are differentially expressed from alternative first exons. *J Biol Chem*. 1997;272:8396–8401.

64. Brewer A, Gove C, Davies A, McNulty C, Barrow D, Koutsourakis M, Farzaneh F, Pizzey J, Bomford A, Patient R. The human and mouse GATA-6 genes utilize two promoters and two initiation codons. *J Biol Chem*. 1999;274:38004–38016.

65. Stennard FA, Costa MW, Elliott DA, Rankin S, Haast SJP, Lai D, McDonald LPA, Niederreither K, Dolle P, Bruneau BG, Zorn AM, Harvey RP. Cardiac T-box factor Tbx20 directly interacts with Nkx2-5, GATA4, and GATA5 in regulation of gene expression in the developing heart. *Dev Biol*. 2003;262:206–224.

66. Tian Y, Yuan L, Goss AM, Wang T, Yang J, Lepore JJ, Zhou D, Schwartz RJ, Patel V, Cohen ED, Morrisey EE. Characterization and in vivo pharmacological rescue of a Wnt2-Gata6 pathway required for cardiac inflow tract development. *Dev Cell*. 2010;18:275–287.

67. Nishida W, Nakamura M, Mori S, Takahashi M, Ohkawa Y, Tadokoro S, Yoshida K, Hiwada K, Hayashi K, Sobue K. A triad of serum response factor and the GATA and NK families governs the transcription of smooth and cardiac muscle genes. *J Biol Chem*. 2002;277:7308–7317.

68. Brown CO, Chi X, Garcia-Gras E, Shirai M, Feng X-H, Schwartz RJ. The cardiac determination factor, Nkx2-5, is activated by mutual cofactors GATA-4 and Smad1/4 via a novel upstream enhancer. *J Biol Chem*. 2004;279:10659–10669.

69. Charron F, Nemer M. GATA transcription factors and cardiac development. *Semin Cell Dev Biol*. 1999;10:85–91.

70. Charron F, Paradis P, Bronchain O, Nemer G, Nemer M. Cooperative interaction between GATA-4 and GATA-6 regulates myocardial gene expression. *Mol Cell Biol*. 1999;19:4355–4365.

71. Hasegawa K, Lee SJ, Jobe SM, Markham BE, Kitsis RN. cis-Acting sequences that mediate induction of beta-myosin heavy chain gene expression during left ventricular hypertrophy due to aortic constriction. *Circulation*. 1997;96:3943–3953.

72. Herzig TC, Jobe SM, Aoki H, Molkentin JD, Cowley AW, Izumo S, Markham BE. Angiotensin II type1a receptor gene expression in the heart: AP-1 and GATA-4 participate in the response to pressure overload. *Proc Natl Acad Sci U S A*. 1997;94:7543–7548.

73. Morisco C, Seta K, Hardt SE, Lee Y, Vatner SF, Sadoshima J. Glycogen synthase kinase 3beta regulates GATA4 in cardiac myocytes. *J Biol Chem*. 2001;276:28586–28597.

74. Yamak A, Nemer M. Role of Embryonic and Differentiated Cells in Cardiac Development [Internet]. In: Biomaterials for Cardiac Regeneration. Springer, Cham; 2015. p. 37–70.Available from: https://link.springer.com/chapter/10.1007/978-3-319-10972-5_2

75. Meilhac SM, Esner M, Kelly RG, Nicolas J-F, Buckingham ME. The clonal origin of myocardial cells in different regions of the embryonic mouse heart. *Dev Cell*. 2004;6:685–698.

76. Bondue A, Lapouge G, Paulissen C, Semeraro C, Iacovino M, Kyba M, Blanpain C. Mesp1 acts as a master regulator of multipotent cardiovascular progenitor specification. *Cell Stem Cell*. 2008;3:69–84.

77. Meilhac SM, Lescroart F, Blanpain C, Buckingham ME. Cardiac cell lineages that form the heart. *Cold Spring Harb Perspect Med*. 2014;4:a013888.

78. Galli D, Domínguez JN, Zaffran S, Munk A, Brown NA, Buckingham ME. Atrial myocardium derives from the posterior region of the second heart field, which acquires left-right identity as Pitx2c is expressed. *Dev Camb Engl*. 2008;135:1157–1167.

79. Takeuchi JK, Ohgi M, Koshiba-Takeuchi K, Shiratori H, Sakaki I, Ogura K, Saijoh Y, Ogura T. Tbx5 specifies the left/right ventricles and ventricular septum position during cardiogenesis. *Dev Camb Engl*. 2003;130:5953–5964.

80. Pashmforoush M, Lu JT, Chen H, Amand TS, Kondo R, Pradervand S, Evans SM, Clark B, Feramisco JR, Giles W, Ho SY, Benson DW, Silberbach M, Shou W, Chien KR. Nkx2-5 pathways and congenital heart disease; loss of ventricular myocyte lineage specification leads to progressive cardiomyopathy and complete heart block. *Cell*. 2004;117:373–386.

81. Grego-Bessa J, Luna-Zurita L, del Monte G, Bolós V, Melgar P, Arandilla A, Garratt AN, Zang H, Mukouyama Y-S, Chen H, Shou W, Ballestar E, Esteller M, Rojas A, Pérez-Pomares JM, de la Pompa JL. Notch signaling is essential for ventricular chamber development. *Dev Cell*. 2007;12:415–429.

82. Merki E, Zamora M, Raya A, Kawakami Y, Wang J, Zhang X, Burch J, Kubalak SW, Kaliman P, Izpisua Belmonte JC, Chien KR, Ruiz-Lozano P. Epicardial retinoid X receptor alpha is required for myocardial growth and coronary artery formation. *Proc Natl Acad Sci U S A*. 2005;102:18455–18460.

83. Peshkovsky C, Totong R, Yelon D. Dependence of cardiac trabeculation on neuregulin signaling and blood flow in zebrafish. *Dev Dyn Off Publ Am Assoc Anat*. 2011;240:446–456.

84. Zaffran S, Kelly RG, Meilhac SM, Buckingham ME, Brown NA. Right ventricular myocardium derives from the anterior heart field. *Circ Res*. 2004;95:261–268.

85. Domínguez JN, Meilhac SM, Bland YS, Buckingham ME, Brown NA. Asymmetric fate of the posterior part of the second heart field results in unexpected left/right contributions to both poles of the heart. *Circ Res*. 2012;111:1323–1335.

86. Waldo KL, Hutson MR, Ward CC, Zdanowicz M, Stadt HA, Kumiski D, Abu-Issa R, Kirby ML. Secondary heart field contributes myocardium and smooth muscle to the arterial pole of the developing heart. *Dev Biol*. 2005;281:78–90.

87. Kelly RG, Brown NA, Buckingham ME. The arterial pole of the mouse heart forms from Fgf10-expressing cells in pharyngeal mesoderm. *Dev Cell*. 2001;1:435–440.

88. Cai C-L, Liang X, Shi Y, Chu P-H, Pfaff SL, Chen J, Evans S. Isl1 identifies a cardiac progenitor population that proliferates prior to differentiation and contributes a majority of cells to the heart. *Dev Cell*. 2003;5:877–889.

89. Brown CB, Wenning JM, Lu MM, Epstein DJ, Meyers EN, Epstein JA. Cre-mediated excision of Fgf8 in the Tbx1 expression domain reveals a critical role for Fgf8 in cardiovascular development in the mouse. *Dev Biol*. 2004;267:190–202.

90. Dodou E, Verzi MP, Anderson JP, Xu S-M, Black BL. Mef2c is a direct transcriptional target of ISL1 and GATA factors in the anterior heart field during mouse embryonic development. *Dev Camb Engl*. 2004;131:3931–3942.

91. Xu H, Morishima M, Wylie JN, Schwartz RJ, Bruneau BG, Lindsay EA, Baldini A. Tbx1 has a dual role in the morphogenesis of the cardiac outflow tract. *Dev Camb Engl*. 2004;131:3217–3227.

92. Nowotschin S, Liao J, Gage PJ, Epstein JA, Campione M, Morrow BE. Tbx1 affects asymmetric cardiac morphogenesis by regulating Pitx2 in the secondary heart field. *Dev Camb Engl*. 2006;133:1565–1573.

93. Park EJ, Ogden LA, Talbot A, Evans S, Cai C-L, Black BL, Frank DU, Moon AM. Required, tissue-specific roles for Fgf8 in outflow tract formation and remodeling. *Dev Camb Engl*. 2006;133:2419–2433.

94. Takeuchi JK, Mileikovskaia M, Koshiba-Takeuchi K, Heidt AB, Mori AD, Arruda EP, Gertsenstein M, Georges R, Davidson L, Mo R, Hui C-C, Henkelman RM, Nemer M, Black BL, Nagy A, Bruneau BG. Tbx20 dose-dependently regulates transcription factor networks required for mouse heart and motoneuron development. *Dev Camb Engl*. 2005;132:2463–2474.

95. Zhang R, Han P, Yang H, Ouyang K, Lee D, Lin Y-F, Ocorr K, Kang G, Chen J, Stainier DYR, Yelon D, Chi NC. In vivo cardiac reprogramming contributes to zebrafish heart regeneration. *Nature*. 2013;498:497–501.

96. Gorza L, Schiaffino S, Vitadello M. Heart conduction system: a neural crest derivative? *Brain Res*. 1988;457:360–366.

97. Kitajima S, Miyagawa-Tomita S, Inoue T, Kanno J, Saga Y. Mesp1-nonexpressing cells contribute to the ventricular cardiac conduction system. *Dev Dyn Off Publ Am Assoc Anat*. 2006;235:395–402.

98. Virágh S, Challice CE. The development of the conduction system in the mouse embryo heart. I. The first embryonic A-V conduction pathway. *Dev Biol*. 1977;56:382–396.

99. Virágh S, Challice CE. The development of the conduction system in the mouse embryo heart. II. Histogenesis of the atrioventricular node and bundle. *Dev Biol*. 1977;56:397–411.

100. Virágh S, Challice CE. The development of the conduction system in the mouse embryo heart. *Dev Biol*. 1980;80:28–45.

101. Liang X, Wang G, Lin L, Lowe J, Zhang Q, Bu L, Chen Y, Chen J, Sun Y, Evans SM. HCN4 dynamically marks the first heart field and conduction system precursors. *Circ Res*. 2013;113:399–407.

102. Hoogaars WMH, Engel A, Brons JF, Verkerk AO, de Lange FJ, Wong LYE, Bakker ML, Clout DE, Wakker V, Barnett P, Ravesloot JH, Moorman AFM, Verheijck EE, Christoffels VM. Tbx3 controls the sinoatrial node gene program and imposes pacemaker function on the atria. *Genes Dev*. 2007;21:1098–1112.

103. Aanhaanen WTJ, Mommersteeg MTM, Norden J, Wakker V, de Gier-de Vries C, Anderson RH, Kispert A, Moorman AFM, Christoffels VM. Developmental origin, growth, and three-dimensional architecture of the atrioventricular conduction axis of the mouse heart. *Circ Res*. 2010;107:728–736.

104. Gourdie RG, Wei Y, Kim D, Klatt SC, Mikawa T. Endothelin-induced conversion of embryonic heart muscle cells into impulse-conducting Purkinje fibers. *Proc Natl Acad Sci U S A*. 1998;95:6815–6818.

105. Lamers WH, De Jong F, De Groot IJ, Moorman AF. The development of the avian conduction system, a review. *Eur J Morphol*. 1991;29:233–253.

106. Miquerol L, Bellon A, Moreno N, Beyer S, Meilhac SM, Buckingham M, Franco D, Kelly RG. Resolving cell lineage contributions to the ventricular conduction system with a Cx40-GFP allele: a dual contribution of the first and second heart fields. *Dev Dyn Off Publ Am Assoc Anat*. 2013;242:665–677.

107. Aanhaanen WTJ, Brons JF, Domínguez JN, Rana MS, Norden J, Airik R, Wakker V, de Gier-de Vries C, Brown NA, Kispert A, Moorman AFM, Christoffels VM. The Tbx2+ primary myocardium of the atrioventricular canal forms the atrioventricular node and the base of the left ventricle. *Circ Res*. 2009;104:1267–1274.

108. Cheng G, Litchenberg WH, Cole GJ, Mikawa T, Thompson RP, Gourdie RG. Development of the cardiac conduction system involves recruitment within a multipotent cardiomyogenic lineage. *Dev Camb Engl*. 1999;126:5041–5049.

109. Kanzawa N, Poma CP, Takebayashi-Suzuki K, Diaz KG, Layliev J, Mikawa T. Competency of embryonic cardiomyocytes to undergo Purkinje fiber differentiation is regulated by endothelin receptor expression. *Dev Camb Engl*. 2002;129:3185–3194.

110. Rentschler S, Zander J, Meyers K, France D, Levine R, Porter G, Rivkees SA, Morley GE, Fishman GI. Neuregulin-1 promotes formation of the murine cardiac conduction system. *Proc Natl Acad Sci U S A*. 2002;99:10464–10469.

111. Bockman DE, Redmond ME, Waldo K, Davis H, Kirby ML. Effect of neural crest ablation on development of the heart and arch arteries in the chick. *Am J Anat*. 1987;180:332–341.

112. Kirby ML, Gale TF, Stewart DE. Neural crest cells contribute to normal aorticopulmonary septation. *Science*. 1983;220:1059–1061.

113. Noden DM. The role of the neural crest in patterning of avian cranial skeletal, connective, and muscle tissues. *Dev Biol*. 1983;96:144–165.

114. de Lange FJ, Moorman AFM, Anderson RH, Männer J, Soufan AT, de Gier-de Vries C, Schneider MD, Webb S, van den Hoff MJB, Christoffels VM. Lineage and morphogenetic analysis of the cardiac valves. *Circ Res*. 2004;95:645–654.

115. Waldo KL, Lo CW, Kirby ML. Connexin 43 expression reflects neural crest patterns during cardiovascular development. *Dev Biol*. 1999;208:307–323.

116. Boot MJ, Gittenberger-De Groot AC, Van Iperen L, Hierck BP, Poelmann RE. Spatiotemporally separated cardiac neural crest subpopulations that target the outflow tract septum and pharyngeal arch arteries. *Anat Rec A Discov Mol Cell Evol Biol*. 2003;275:1009–1018.

117. Kirby ML, Turnage KL, Hays BM. Characterization of conotruncal malformations following ablation of "cardiac" neural crest. *Anat Rec*. 1985;213:87–93.

118. Kirby M, Stewart D. Adrenergic innervation of the developing chick heart: neural crest ablations to produce sympathetically aneural hearts. *Am J Anat*. 1984;171:295–305.

119. Verberne ME, Gittenberger-de Groot AC, Poelmann RE. Lineage and development of the parasympathetic nervous system of the embryonic chick heart. *Anat Embryol (Berl)*. 1998;198:171–184.

120. Jiang X, Rowitch DH, Soriano P, McMahon AP, Sucov HM. Fate of the mammalian cardiac neural crest. *Dev Camb Engl*. 2000;127:1607–1616.

121. Li J, Chen F, Epstein JA. Neural crest expression of Cre recombinase directed by the proximal Pax3 promoter in transgenic mice. *Genes N Y N 2000*. 2000;26:162–164.

122. Niederreither K, Vermot J, Messaddeq N, Schuhbaur B, Chambon P, Dollé P. Embryonic retinoic acid synthesis is essential for heart morphogenesis in the mouse. *Dev Camb Engl*. 2001;128:1019–1031.

123. Kaufman MH, Navaratnam V. Early differentiation of the heart in mouse embryos. *J Anat*. 1981;133:235–246.

124. Flamme I, Risau W. Induction of vasculogenesis and hematopoiesis in vitro. *Dev Camb Engl*. 1992;116:435–439.

125. Stalsberg H, DeHaan RL. The precardiac areas and formation of the tubular heart in the chick embryo. *Dev Biol*. 1969;19:128–159.

126. Lyons I, Parsons LM, Hartley L, Li R, Andrews JE, Robb L, Harvey RP. Myogenic and morphogenetic defects in the heart tubes of murine embryos lacking the homeo box gene Nkx2-5. *Genes Dev*. 1995;9:1654–1666.

127. Cohen-Gould L, Mikawa T. The fate diversity of mesodermal cells within the heart field during chicken early embryogenesis. *Dev Biol*. 1996;177:265–273.

128. De Val S, Chi NC, Meadows SM, Minovitsky S, Anderson JP, Harris IS, Ehlers ML, Agarwal P, Visel A, Xu S-M, Pennacchio LA, Dubchak I, Krieg PA, Stainier DYR, Black BL. Combinatorial regulation of endothelial gene expression by ets and forkhead transcription factors. *Cell*. 2008;135:1053–1064.

129. Rasmussen TL, Kweon J, Diekmann MA, Belema-Bedada F, Song Q, Bowlin K, Shi X, Ferdous A, Li T, Kyba M, Metzger JM, Koyano-Nakagawa N, Garry DJ. ER71 directs mesodermal fate decisions during embryogenesis. *Dev Camb Engl*. 2011;138:4801–4812.

130. Kattman SJ, Huber TL, Keller GM. Multipotent flk-1+ cardiovascular progenitor cells give rise to the cardiomyocyte, endothelial, and vascular smooth muscle lineages. *Dev Cell*. 2006;11:723–732.

131. Moretti A, Caron L, Nakano A, Lam JT, Bernshausen A, Chen Y, Qyang Y, Bu L, Sasaki M, Martin-Puig S, Sun Y, Evans SM, Laugwitz K-L, Chien KR. Multipotent embryonic isl1+ progenitor cells lead to cardiac, smooth muscle, and endothelial cell diversification. *Cell*. 2006;127:1151–1165.

132. Schulte I, Schlueter J, Abu-Issa R, Brand T, Männer J. Morphological and molecular left-right asymmetries in the development of the proepicardium: a comparative analysis on mouse and chick embryos. *Dev Dyn Off Publ Am Assoc Anat*. 2007;236:684–695.

133. van Wijk B, van den Berg G, Abu-Issa R, Barnett P, van der Velden S, Schmidt M, Ruijter JM, Kirby ML, Moorman AFM, van den Hoff MJB. Epicardium and myocardium separate from a common precursor pool by crosstalk between bone morphogenetic protein- and fibroblast growth factor-signaling pathways. *Circ Res*. 2009;105:431–441.

134. Martínez-Estrada OM, Lettice LA, Essafi A, Guadix JA, Slight J, Velecela V, Hall E, Reichmann J, Devenney PS, Hohenstein P, Hosen N, Hill RE, Muñoz-Chapuli R,

Hastie ND. Wt1 is required for cardiovascular progenitor cell formation through transcriptional control of Snail and E-cadherin. *Nat Genet*. 2010;42:89–93.

135. Kraus F, Haenig B, Kispert A. Cloning and expression analysis of the mouse T-box gene Tbx18. *Mech Dev*. 2001;100:83–86.

136. Zhou B, von Gise A, Ma Q, Rivera-Feliciano J, Pu WT. Nkx2-5- and Isl1-expressing cardiac progenitors contribute to proepicardium. *Biochem Biophys Res Commun*. 2008;375:450–453.

137. Moore AW, McInnes L, Kreidberg J, Hastie ND, Schedl A. YAC complementation shows a requirement for Wt1 in the development of epicardium, adrenal gland and throughout nephrogenesis. *Dev Camb Engl*. 1999;126:1845–1857.

138. Crispino JD, Lodish MB, Thurberg BL, Litovsky SH, Collins T, Molkentin JD, Orkin SH. Proper coronary vascular development and heart morphogenesis depend on interaction of GATA-4 with FOG cofactors. *Genes Dev*. 2001;15:839–844.

139. Watt AJ, Battle MA, Li J, Duncan SA. GATA4 is essential for formation of the proepicardium and regulates cardiogenesis. *Proc Natl Acad Sci U S A*. 2004;101:12573–12578.

140. Hatcher CJ, Diman NYS-G, Kim M-S, Pennisi D, Song Y, Goldstein MM, Mikawa T, Basson CT. A role for Tbx5 in proepicardial cell migration during cardiogenesis. *Physiol Genomics*. 2004;18:129–140.

141. Schlueter J, Männer J, Brand T. BMP is an important regulator of proepicardial identity in the chick embryo. *Dev Biol*. 2006;295:546–558.

142. Mic FA, Haselbeck RJ, Cuenca AE, Duester G. Novel retinoic acid generating activities in the neural tube and heart identified by conditional rescue of Raldh2 null mutant mice. *Dev Camb Engl*. 2002;129:2271–2282.

143. Sucov HM, Dyson E, Gumeringer CL, Price J, Chien KR, Evans RM. RXR alpha mutant mice establish a genetic basis for vitamin A signaling in heart morphogenesis. *Genes Dev*. 1994;8:1007–1018.

144. Cai C-L, Martin JC, Sun Y, Cui L, Wang L, Ouyang K, Yang L, Bu L, Liang X, Zhang X, Stallcup WB, Denton CP, McCulloch A, Chen J, Evans SM. A myocardial lineage derives from Tbx18 epicardial cells. *Nature*. 2008;454:104–108.

145. Kruithof BPT, van Wijk B, Somi S, Kruithof-de Julio M, Pérez Pomares JM, Weesie F, Wessels A, Moorman AFM, van den Hoff MJB. BMP and FGF regulate the differentiation of multipotential pericardial mesoderm into the myocardial or epicardial lineage. *Dev Biol*. 2006;295:507–522.

146. Anderson RH, Webb S, Brown NA, Lamers W, Moorman A. Development of the heart: (3) formation of the ventricular outflow tracts, arterial valves, and intrapericardial arterial trunks. *Heart Br Card Soc*. 2003;89:1110–1118.

147. Chang C-P, Neilson JR, Bayle JH, Gestwicki JE, Kuo A, Stankunas K, Graef IA, Crabtree GR. A field of myocardial-endocardial NFAT signaling underlies heart valve morphogenesis. *Cell*. 2004;118:649–663.

148. Stankunas K, Ma GK, Kuhnert FJ, Kuo CJ, Chang C-P. VEGF signaling has distinct spatiotemporal roles during heart valve development. *Dev Biol*. 2010;347:325–336.

149. Rivera-Feliciano J, Tabin CJ. Bmp2 instructs cardiac progenitors to form the heart-valve-inducing field. *Dev Biol*. 2006;295:580–588.

150. Shirai M, Imanaka-Yoshida K, Schneider MD, Schwartz RJ, Morisaki T. T-box 2, a mediator of Bmp-Smad signaling, induced hyaluronan synthase 2 and Tgfbeta2 expression and endocardial cushion formation. *Proc Natl Acad Sci U S A*. 2009;106:18604–18609.

151. Toyofuku T, Yoshida J, Sugimoto T, Yamamoto M, Makino N, Takamatsu H, Takegahara N, Suto F, Hori M, Fujisawa H, Kumanogoh A, Kikutani H. Repulsive and attractive semaphorins cooperate to direct the navigation of cardiac neural crest cells. *Dev Biol*. 2008;321:251–262.

152. Kirby ML. Role of extracardiac factors in heart development. *Experientia*. 1988;44:944–951.

153. Verzi MP, McCulley DJ, De Val S, Dodou E, Black BL. The right ventricle, outflow tract, and ventricular septum comprise a restricted expression domain within the secondary/anterior heart field. *Dev Biol*. 2005;287:134–145.

154. Snarr BS, Wirrig EE, Phelps AL, Trusk TC, Wessels A. A spatiotemporal evaluation of the contribution of the dorsal mesenchymal protrusion to cardiac development. *Dev Dyn Off Publ Am Assoc Anat*. 2007;236:1287–1294.

155. Armstrong EJ, Bischoff J. Heart valve development: endothelial cell signaling and differentiation. *Circ Res*. 2004;95:459–470.

156. Butcher JT, Markwald RR. Valvulogenesis: the moving target. *Philos Trans R Soc Lond B Biol Sci*. 2007;362:1489–1503.

157. Hay ED. The mesenchymal cell, its role in the embryo, and the remarkable signaling mechanisms that create it. *Dev Dyn Off Publ Am Assoc Anat*. 2005;233:706–720.

158. Person AD, Klewer SE, Runyan RB. Cell biology of cardiac cushion development. *Int Rev Cytol*. 2005;243:287–335.

159. Kruithof BPT, Krawitz SA, Gaussin V. Atrioventricular valve development during late embryonic and postnatal stages involves condensation and extracellular matrix remodeling. *Dev Biol*. 2007;302:208–217.

160. Delling FN, Vasan RS. Epidemiology and Pathophysiology of Mitral Valve Prolapse: New Insights Into Disease Progression, Genetics, and Molecular Basis. *Circulation*. 2014;129:2158–2170.

161. Colvée E, Hurle JM. Maturation of the extracellular material of the semilunar heart values in the mouse. A histochemical analysis of collagen and mucopolysaccharides. *Anat Embryol (Berl)*. 1981;162:343–352.

162. Combs MD, Yutzey KE. Heart valve development: regulatory networks in development and disease. *Circ Res*. 2009;105:408–421.

163. Boyer AS, Ayerinskas II, Vincent EB, McKinney LA, Weeks DL, Runyan RB. TGFbeta2 and TGFbeta3 have separate and sequential activities during epithelial-mesenchymal cell transformation in the embryonic heart. *Dev Biol*. 1999;208:530–545.

164. Luna-Zurita L, Prados B, Grego-Bessa J, Luxán G, del Monte G, Benguría A, Adams RH, Pérez-Pomares JM, de la Pompa JL. Integration of a Notch-dependent mesenchymal gene program and Bmp2-driven cell invasiveness regulates murine cardiac valve formation. *J Clin Invest*. 2010;120:3493–3507.

165. Abdelwahid E, Rice D, Pelliniemi LJ, Jokinen E. Overlapping and differential localization of Bmp-2, Bmp-4, Msx-2 and apoptosis in the endocardial cushion and adjacent tissues of the developing mouse heart. *Cell Tissue Res*. 2001;305:67–78.

166. Délot EC, Bahamonde ME, Zhao M, Lyons KM. BMP signaling is required for septation of the outflow tract of the mammalian heart. *Dev Camb Engl*. 2003;130:209–220.

167. Jiao K, Kulessa H, Tompkins K, Zhou Y, Batts L, Baldwin HS, Hogan BLM. An essential role of Bmp4 in the atrioventricular septation of the mouse heart. *Genes Dev*. 2003;17:2362–2367.

168. Galvin KM, Donovan MJ, Lynch CA, Meyer RI, Paul RJ, Lorenz JN, Fairchild-Huntress V, Dixon KL, Dunmore JH, Gimbrone MA, Falb D, Huszar D. A role for smad6 in development and homeostasis of the cardiovascular system. *Nat Genet*. 2000;24:171–174.

169. Jia Q, McDill BW, Li S-Z, Deng C, Chang C-P, Chen F. Smad signaling in the neural crest regulates cardiac outflow tract remodeling through cell autonomous and non-cell autonomous effects. *Dev Biol*. 2007;311:172–184.

170. Timmerman LA, Grego-Bessa J, Raya A, Bertrán E, Pérez-Pomares JM, Díez J, Aranda S, Palomo S, McCormick F, Izpisúa-Belmonte JC, de la Pompa JL. Notch

promotes epithelial-mesenchymal transition during cardiac development and oncogenic transformation. *Genes Dev*. 2004;18:99–115.

171. Noseda M, McLean G, Niessen K, Chang L, Pollet I, Montpetit R, Shahidi R, Dorovini-Zis K, Li L, Beckstead B, Durand RE, Hoodless PA, Karsan A. Notch activation results in phenotypic and functional changes consistent with endothelial-to-mesenchymal transformation. *Circ Res*. 2004;94:910–917.

172. Jain R, Engleka KA, Rentschler SL, Manderfield LJ, Li L, Yuan L, Epstein JA. Cardiac neural crest orchestrates remodeling and functional maturation of mouse semilunar valves. *J Clin Invest*. 2011;121:422–430.

173. Hurlstone AFL, Haramis A-PG, Wienholds E, Begthel H, Korving J, Van Eeden F, Cuppen E, Zivkovic D, Plasterk RHA, Clevers H. The Wnt/beta-catenin pathway regulates cardiac valve formation. *Nature*. 2003;425:633–637.

174. Lin L, Cui L, Zhou W, Dufort D, Zhang X, Cai C-L, Bu L, Yang L, Martin J, Kemler R, Rosenfeld MG, Chen J, Evans SM. Beta-catenin directly regulates Islet1 expression in cardiovascular progenitors and is required for multiple aspects of cardiogenesis. *Proc Natl Acad Sci U S A*. 2007;104:9313–9318.

175. Kioussi C, Briata P, Baek SH, Rose DW, Hamblet NS, Herman T, Ohgi KA, Lin C, Gleiberman A, Wang J, Brault V, Ruiz-Lozano P, Nguyen HD, Kemler R, Glass CK, Wynshaw-Boris A, Rosenfeld MG. Identification of a Wnt/Dvl/beta-Catenin --> Pitx2 pathway mediating cell-type-specific proliferation during development. *Cell*. 2002;111:673–685.

176. Dor Y, Klewer SE, McDonald JA, Keshet E, Camenisch TD. VEGF modulates early heart valve formation. *Anat Rec A Discov Mol Cell Evol Biol*. 2003;271:202–208.

177. Olsson A-K, Dimberg A, Kreuger J, Claesson-Welsh L. VEGF receptor signalling - in control of vascular function. *Nat Rev Mol Cell Biol*. 2006;7:359–371.

178. Johnson EN, Lee YM, Sander TL, Rabkin E, Schoen FJ, Kaushal S, Bischoff J. NFATc1 mediates vascular endothelial growth factor-induced proliferation of human pulmonary valve endothelial cells. *J Biol Chem*. 2003;278:1686–1692.

179. Wu B, Wang Y, Lui W, Langworthy M, Tompkins KL, Hatzopoulos AK, Baldwin HS, Zhou B. Nfatc1 coordinates valve endocardial cell lineage development required for heart valve formation. *Circ Res*. 2011;109:183–192.

180. Lin C-Y, Lin C-J, Chen C-H, Chen RM, Zhou B, Chang C-P. The secondary heart field is a new site of calcineurin/Nfatc1 signaling for semilunar valve development. *J Mol Cell Cardiol*. 2012;52:1096–1102.

181. Hinton RB, Yutzey KE. Heart Valve Structure and Function in Development and Disease. *Annu Rev Physiol*. 2011;73:29–46.

182. Toole BP. Hyaluronan in morphogenesis. *Semin Cell Dev Biol*. 2001;12:79–87.

183. Baldwin HS, Lloyd TR, Solursh M. Hyaluronate degradation affects ventricular function of the early postlooped embryonic rat heart in situ. *Circ Res*. 1994;74:244–252.

184. Camenisch TD, Spicer AP, Brehm-Gibson T, Biesterfeldt J, Augustine ML, Calabro A, Kubalak S, Klewer SE, McDonald JA. Disruption of hyaluronan synthase-2 abrogates normal cardiac morphogenesis and hyaluronan-mediated transformation of epithelium to mesenchyme. *J Clin Invest*. 2000;106:349–360.

185. Mjaatvedt CH, Yamamura H, Capehart AA, Turner D, Markwald RR. The Cspg2 gene, disrupted in the hdf mutant, is required for right cardiac chamber and endocardial cushion formation. *Dev Biol*. 1998;202:56–66.

186. Dehaan RL. Differentiation of the atrioventricular conducting system of the heart. *Circulation*. 1961;24:458–470.

187. de Jong F, Opthof T, Wilde AA, Janse MJ, Charles R, Lamers WH, Moorman AF. Persisting zones of slow impulse conduction in developing chicken hearts. *Circ Res*. 1992;71:240–250.

188. Paff GH, Boucek RJ, Harrell TC. Observations on the development of the electrocardiogram. *Anat Rec*. 1968;160:575–582.

189. Stolte M. The Conduction System of the Heart. Edited by M. J. Davies, R. H. Anderson, and A. E. Becker. Butterworths, London (1983) 336 pages, illustrations, $53.75 (approx.) ISBN: 0-407-00133-6. *Clin Cardiol*. 1983;6:A43–A43.

190. Opthof T. The mammalian sinoatrial node. *Cardiovasc Drugs Ther*. 1988;1:573–597.

191. Christoffels VM, Smits GJ, Kispert A, Moorman AFM. Development of the pacemaker tissues of the heart. *Circ Res*. 2010;106:240–254.

192. Hoogaars WMH, Tessari A, Moorman AFM, de Boer PAJ, Hagoort J, Soufan AT, Campione M, Christoffels VM. The transcriptional repressor Tbx3 delineates the developing central conduction system of the heart. *Cardiovasc Res*. 2004;62:489–499.

193. Stieber J, Herrmann S, Feil S, Löster J, Feil R, Biel M, Hofmann F, Ludwig A. The hyperpolarization-activated channel HCN4 is required for the generation of pacemaker action potentials in the embryonic heart. *Proc Natl Acad Sci U S A*. 2003;100:15235–15240.

194. Wiese C, Grieskamp T, Airik R, Mommersteeg MTM, Gardiwal A, de Gier-de Vries C, Schuster-Gossler K, Moorman AFM, Kispert A, Christoffels VM. Formation of the sinus node head and differentiation of sinus node myocardium are independently regulated by Tbx18 and Tbx3. *Circ Res*. 2009;104:388–397.

195. Mori AD, Zhu Y, Vahora I, Nieman B, Koshiba-Takeuchi K, Davidson L, Pizard A, Seidman JG, Seidman CE, Chen XJ, Henkelman RM, Bruneau BG. Tbx5-dependent rheostatic control of cardiac gene expression and morphogenesis. *Dev Biol*. 2006;297:566–586.

196. Puskaric S, Schmitteckert S, Mori AD, Glaser A, Schneider KU, Bruneau BG, Blaschke RJ, Steinbeisser H, Rappold G. Shox2 mediates Tbx5 activity by regulating Bmp4 in the pacemaker region of the developing heart. *Hum Mol Genet*. 2010;19:4625–4633.

197. Blaschke RJ, Hahurij ND, Kuijper S, Just S, Wisse LJ, Deissler K, Maxelon T, Anastassiadis K, Spitzer J, Hardt SE, Schöler H, Feitsma H, Rottbauer W, Blum M, Meijlink F, Rappold G, Gittenberger-de Groot AC. Targeted mutation reveals essential functions of the homeodomain transcription factor Shox2 in sinoatrial and pacemaking development. *Circulation*. 2007;115:1830–1838.

198. Espinoza-Lewis RA, Yu L, He F, Liu H, Tang R, Shi J, Sun X, Martin JF, Wang D, Yang J, Chen Y. Shox2 is essential for the differentiation of cardiac pacemaker cells by repressing Nkx2-5. *Dev Biol*. 2009;327:376–385.

199. Mommersteeg MTM, Hoogaars WMH, Prall OWJ, de Gier-de Vries C, Wiese C, Clout DEW, Papaioannou VE, Brown NA, Harvey RP, Moorman AFM, Christoffels VM. Molecular pathway for the localized formation of the sinoatrial node. *Circ Res*. 2007;100:354–362.

200. Liang X, Zhang Q, Cattaneo P, Zhuang S, Gong X, Spann NJ, Jiang C, Cao X, Zhao X, Zhang X, Bu L, Wang G, Chen HSV, Zhuang T, Yan J, Geng P, Luo L, Banerjee I, Chen Y, Glass CK, Zambon AC, Chen J, Sun Y, Evans SM. Transcription factor ISL1 is essential for pacemaker development and function. *J Clin Invest*. 2015;125:3256–3268.

201. Mommersteeg MTM, Domínguez JN, Wiese C, Norden J, de Gier-de Vries C, Burch JBE, Kispert A, Brown NA, Moorman AFM, Christoffels VM. The sinus venosus progenitors separate and diversify from the first and second heart fields early in development. *Cardiovasc Res*. 2010;87:92–101.

202. Bressan M, Yang PB, Louie JD, Navetta AM, Garriock RJ, Mikawa T. Reciprocal myocardial-endocardial interactions pattern the delay in atrioventricular junction conduction. *Dev Camb Engl*. 2014;141:4149–4157.

203. van Weerd JH, Christoffels VM. The formation and function of the cardiac conduction system. *Dev Camb Engl*. 2016;143:197–210.

204. Milanesi R, Bucchi A, Baruscotti M. The genetic basis for inherited forms of sinoatrial dysfunction and atrioventricular node dysfunction. *J Interv Card Electrophysiol Int J Arrhythm Pacing*. 2015;43:121–134.

205. Munk AA, Adjemian RA, Zhao J, Ogbaghebriel A, Shrier A. Electrophysiological properties of morphologically distinct cells isolated from the rabbit atrioventricular node. *J Physiol*. 1996;493 (Pt 3):801–818.

206. Aanhaanen WTJ, Boukens BJD, Sizarov A, Wakker V, de Gier-de Vries C, van Ginneken AC, Moorman AFM, Coronel R, Christoffels VM. Defective Tbx2-dependent patterning of the atrioventricular canal myocardium causes accessory pathway formation in mice. *J Clin Invest*. 2011;121:534–544.

207. Christoffels VM, Hoogaars WMH, Tessari A, Clout DEW, Moorman AFM, Campione M. T-box transcription factor Tbx2 represses differentiation and formation of the cardiac chambers. *Dev Dyn Off Publ Am Assoc Anat*. 2004;229:763–770.

208. Singh R, Horsthuis T, Farin HF, Grieskamp T, Norden J, Petry M, Wakker V, Moorman AFM, Christoffels VM, Kispert A. Tbx20 interacts with smads to confine tbx2 expression to the atrioventricular canal. *Circ Res*. 2009;105:442–452.

209. Singh R, Hoogaars WM, Barnett P, Grieskamp T, Rana MS, Buermans H, Farin HF, Petry M, Heallen T, Martin JF, Moorman AFM, 't Hoen PAC, Kispert A, Christoffels VM. Tbx2 and Tbx3 induce atrioventricular myocardial development and endocardial cushion formation. *Cell Mol Life Sci CMLS*. 2012;69:1377–1389.

210. Gillers BS, Chiplunkar A, Aly H, Valenta T, Basler K, Christoffels VM, Efimov IR, Boukens BJ, Rentschler S. Canonical wnt signaling regulates atrioventricular junction programming and electrophysiological properties. *Circ Res*. 2015;116:398–406.

211. Rentschler S, Harris BS, Kuznekoff L, Jain R, Manderfield L, Lu MM, Morley GE, Patel VV, Epstein JA. Notch signaling regulates murine atrioventricular conduction and the formation of accessory pathways. *J Clin Invest*. 2011;121:525–533.

212. Harris JP, Bhakta M, Bezprozvannaya S, Wang L, Lubczyk C, Olson EN, Munshi NV. MyoR modulates cardiac conduction by repressing Gata4. *Mol Cell Biol*. 2015;35:649–661.

213. Munshi NV, McAnally J, Bezprozvannaya S, Berry JM, Richardson JA, Hill JA, Olson EN. Cx30.2 enhancer analysis identifies Gata4 as a novel regulator of atrioventricular delay. *Dev Camb Engl*. 2009;136:2665–2674.

214. Liu F, Lu MM, Patel NN, Schillinger KJ, Wang T, Patel VV. GATA-Binding Factor 6 Contributes to Atrioventricular Node Development and Function. *Circ Cardiovasc Genet*. 2015;8:284–293.

215. Gourdie RG, Mima T, Thompson RP, Mikawa T. Terminal diversification of the myocyte lineage generates Purkinje fibers of the cardiac conduction system. *Dev Camb Engl*. 1995;121:1423–1431.

216. Christoffels VM, Moorman AFM. Development of the cardiac conduction system: why are some regions of the heart more arrhythmogenic than others? *Circ Arrhythm Electrophysiol*. 2009;2:195–207.

217. de la Pompa JL, Epstein JA. Coordinating tissue interactions: Notch signaling in cardiac development and disease. *Dev Cell*. 2012;22:244–254.

218. Moskowitz IPG, Pizard A, Patel VV, Bruneau BG, Kim JB, Kupershmidt S, Roden D, Berul CI, Seidman CE, Seidman JG. The T-Box transcription factor Tbx5 is required for the patterning and maturation of the murine cardiac conduction system. *Dev Camb Engl*. 2004;131:4107–4116.

219. Moskowitz IPG, Kim JB, Moore ML, Wolf CM, Peterson MA, Shendure J, Nobrega MA, Yokota Y, Berul C, Izumo S, Seidman JG, Seidman CE. A molecular pathway including Id2, Tbx5, and Nkx2-5 required for cardiac conduction system development. *Cell*. 2007;129:1365–1376.

220. Koizumi A, Sasano T, Kimura W, Miyamoto Y, Aiba T, Ishikawa T, Nogami A, Fukamizu S, Sakurada H, Takahashi Y, Nakamura H, Ishikura T, Koseki H, Arimura T, Kimura A, Hirao K, Isobe M, Shimizu W, Miura N, Furukawa T. Genetic defects in a His-Purkinje system transcription factor, IRX3, cause lethal cardiac arrhythmias. *Eur Heart J*. 2016;37:1469–1475.

221. Zhang S-S, Kim K-H, Rosen A, Smyth JW, Sakuma R, Delgado-Olguín P, Davis M, Chi NC, Puviindran V, Gaborit N, Sukonnik T, Wylie JN, Brand-Arzamendi K, Farman GP, Kim J, Rose RA, Marsden PA, Zhu Y, Zhou Y-Q, Miquerol L, Henkelman RM, Stainier DYR, Shaw RM, Hui C, Bruneau BG, Backx PH. Iroquois homeobox gene 3 establishes fast conduction in the cardiac His-Purkinje network. *Proc Natl Acad Sci U S A*. 2011;108:13576–13581.

222. van der Linde D, Konings EEM, Slager MA, Witsenburg M, Helbing WA, Takkenberg JJM, Roos-Hesselink JW. Birth prevalence of congenital heart disease worldwide: a systematic review and meta-analysis. *J Am Coll Cardiol*. 2011;58:2241–2247.

223. Thom T, Haase N, Rosamond W, Howard VJ, Rumsfeld J, Manolio T, Zheng Z-J, Flegal K, O'Donnell C, Kittner S, Lloyd-Jones D, Goff DC, Hong Y, Adams R, Friday G, Furie K, Gorelick P, Kissela B, Marler J, Meigs J, Roger V, Sidney S, Sorlie P, Steinberger J, Wasserthiel-Smoller S, Wilson M, Wolf P, American Heart Association Statistics Committee and Stroke Statistics Subcommittee. Heart disease and stroke statistics--2006 update: a report from the American Heart Association Statistics Committee and Stroke Statistics Subcommittee. *Circulation*. 2006;113:e85-151.

224. Neeb Z, Lajiness JD, Bolanis E, Conway SJ. Cardiac outflow tract anomalies. *Wiley Interdiscip Rev Dev Biol*. 2013;2:499–530.

225. Ward C. Clinical significance of the bicuspid aortic valve. *Heart Br Card Soc*. 2000;83:81–5.

226. Cripe L, Andelfinger G, Martin LJ, Shooner K, Benson DW. Bicuspid aortic valve is heritable. *J Am Coll Cardiol*. 2004;44:138–143.

227. Friedman T, Mani A, Elefteriades JA. Bicuspid aortic valve: clinical approach and scientific review of a common clinical entity. *Expert Rev Cardiovasc Ther*. 2008;6:235–248.

228. Fernández B, Durán AC, Fernández-Gallego T, Fernández MC, Such M, Arqué JM, Sans-Coma V. Bicuspid aortic valves with different spatial orientations of the leaflets are distinct etiological entities. *J Am Coll Cardiol*. 2009;54:2312–2318.

229. Yuan S-M, Jing H. The bicuspid aortic valve and related disorders. *Sao Paulo Med J Rev Paul Med*. 2010;128:296–301.

230. Della Corte A, Bancone C, Quarto C, Dialetto G, Covino FE, Scardone M, Caianiello G, Cotrufo M. Predictors of ascending aortic dilatation with bicuspid aortic valve: a wide spectrum of disease expression. *Eur J Cardio-Thorac Surg Off J Eur Assoc Cardio-Thorac Surg*. 2007;31:397-404; discussion 404-405.

231. Hinton RB, Lincoln J, Deutsch GH, Osinska H, Manning PB, Benson DW, Yutzey KE. Extracellular matrix remodeling and organization in developing and diseased aortic valves. *Circ Res*. 2006;98:1431–1438.

232. Tao G, Kotick JD, Lincoln J. Heart valve development, maintenance, and disease: the role of endothelial cells. *Curr Top Dev Biol*. 2012;100:203–232.

233. Sonoda M, Takenaka K, Uno K, Ebihara A, Nagai R. A larger aortic annulus causes aortic regurgitation and a smaller aortic annulus causes aortic stenosis in bicuspid aortic valve. *Echocardiogr Mt Kisco N*. 2008;25:242–248.

234. Gharibeh L, Nemer M. The hereditary basis of bicuspid aortic valve disease: a role for screening? [Internet]. Adv. Genomics Genet. 2014;Available from: https://www.dovepress.com/the-hereditary-basis-of-bicuspid-aortic-valve-disease-a-role-for-scree-peer-reviewed-article-AGG

235. Mohamed SA, Aherrahrou Z, Liptau H, Erasmi AW, Hagemann C, Wrobel S, Borzym K, Schunkert H, Sievers HH, Erdmann J. Novel missense mutations (p.T596M and p.P1797H) in NOTCH1 in patients with bicuspid aortic valve. *Biochem Biophys Res Commun*. 2006;345:1460–1465.

236. Padang R, Bagnall RD, Richmond DR, Bannon PG, Semsarian C. Rare non-synonymous variations in the transcriptional activation domains of GATA5 in bicuspid aortic valve disease. *J Mol Cell Cardiol*. 2012;53:277–281.

237. Quintero-Rivera F, Xi QJ, Keppler-Noreuil KM, Lee JH, Higgins AW, Anchan RM, Roberts AE, Seong IS, Fan X, Lage K, Lu LY, Tao J, Hu X, Berezney R, Gelb BD, Kamp A, Moskowitz IP, Lacro RV, Lu W, Morton CC, Gusella JF, Maas RL. MATR3

disruption in human and mouse associated with bicuspid aortic valve, aortic coarctation and patent ductus arteriosus. *Hum Mol Genet*. 2015;24:2375–2389.

238. Bosse K, Hans CP, Zhao N, Koenig SN, Huang N, Guggilam A, LaHaye S, Tao G, Lucchesi PA, Lincoln J, Lilly B, Garg V. Endothelial nitric oxide signaling regulates Notch1 in aortic valve disease. *J Mol Cell Cardiol*. 2013;60:27–35.

239. Thomas PS, Sridurongrit S, Ruiz-Lozano P, Kaartinen V. Deficient signaling via Alk2 (Acvr1) leads to bicuspid aortic valve development. *PloS One*. 2012;7:e35539.

240. Biben C, Weber R, Kesteven S, Stanley E, McDonald L, Elliott DA, Barnett L, Köentgen F, Robb L, Feneley M, Harvey RP. Cardiac septal and valvular dysmorphogenesis in mice heterozygous for mutations in the homeobox gene Nkx2-5. *Circ Res*. 2000;87:888–895.

241. Makki N, Capecchi MR. Cardiovascular defects in a mouse model of HOXA1 syndrome. *Hum Mol Genet*. 2012;21:26–31.

242. Sans-Coma V, Fernández B, Durán AC, Thiene G, Arqué JM, Muñoz-Chápuli R, Cardo M. Fusion of valve cushions as a key factor in the formation of congenital bicuspid aortic valves in Syrian hamsters. *Anat Rec*. 1996;244:490–498.

243. MacGrogan D, D'Amato G, Travisano S, Martinez-Poveda B, Luxán G, Del Monte-Nieto G, Papoutsi T, Sbroggio M, Bou V, Gomez-Del Arco P, Gómez MJ, Zhou B, Redondo JM, Jiménez-Borreguero LJ, de la Pompa JL. Sequential Ligand-Dependent Notch Signaling Activation Regulates Valve Primordium Formation and Morphogenesis. *Circ Res*. 2016;118:1480–1497.

244. Andelfinger G, Tapper AR, Welch RC, Vanoye CG, George AL, Benson DW. KCNJ2 mutation results in Andersen syndrome with sex-specific cardiac and skeletal muscle phenotypes. *Am J Hum Genet*. 2002;71:663–668.

245. Martin LJ, Ramachandran V, Cripe LH, Hinton RB, Andelfinger G, Tabangin M, Shooner K, Keddache M, Benson DW. Evidence in favor of linkage to human chromosomal regions 18q, 5q and 13q for bicuspid aortic valve and associated cardiovascular malformations. *Hum Genet*. 2007;121:275–284.

246. Loeys BL, Chen J, Neptune ER, Judge DP, Podowski M, Holm T, Meyers J, Leitch CC, Katsanis N, Sharifi N, Xu FL, Myers LA, Spevak PJ, Cameron DE, De Backer J, Hellemans J, Chen Y, Davis EC, Webb CL, Kress W, Coucke P, Rifkin DB, De Paepe AM, Dietz HC. A syndrome of altered cardiovascular, craniofacial, neurocognitive and skeletal development caused by mutations in TGFBR1 or TGFBR2. *Nat Genet*. 2005;37:275–281.

247. Dobrzynski H, Anderson RH, Atkinson A, Borbas Z, D'Souza A, Fraser JF, Inada S, Logantha SJRJ, Monfredi O, Morris GM, Moorman AFM, Nikolaidou T, Schneider H, Szuts V, Temple IP, Yanni J, Boyett MR. Structure, function and clinical relevance of

the cardiac conduction system, including the atrioventricular ring and outflow tract tissues. *Pharmacol Ther*. 2013;139:260–288.

248. Benson DW, Wang DW, Dyment M, Knilans TK, Fish FA, Strieper MJ, Rhodes TH, George AL. Congenital sick sinus syndrome caused by recessive mutations in the cardiac sodium channel gene (SCN5A). *J Clin Invest*. 2003;112:1019–1028.

249. Mangrum JM, DiMarco JP. The evaluation and management of bradycardia. *N Engl J Med*. 2000;342:703–709.

250. John RM, Kumar S. Sinus Node and Atrial Arrhythmias. *Circulation*. 2016;133:1892–1900.

251. Lamas GA, Lee KL, Sweeney MO, Silverman R, Leon A, Yee R, Marinchak RA, Flaker G, Schron E, Orav EJ, Hellkamp AS, Greer S, McAnulty J, Ellenbogen K, Ehlert F, Freedman RA, Estes NAM, Greenspon A, Goldman L, Mode Selection Trial in Sinus-Node Dysfunction. Ventricular pacing or dual-chamber pacing for sinus-node dysfunction. *N Engl J Med*. 2002;346:1854–1862.

252. Wang DW, Viswanathan PC, Balser JR, George AL, Benson DW. Clinical, genetic, and biophysical characterization of SCN5A mutations associated with atrioventricular conduction block. *Circulation*. 2002;105:341–346.

253. Gilbert-Barness E. Conduction defects/cardiomyopathies. *Adv Pediatr*. 2014;61:127–148.

254. Baruscotti M, Bucchi A, Viscomi C, Mandelli G, Consalez G, Gnecchi-Rusconi T, Montano N, Casali KR, Micheloni S, Barbuti A, DiFrancesco D. Deep bradycardia and heart block caused by inducible cardiac-specific knockout of the pacemaker channel gene Hcn4. *Proc Natl Acad Sci U S A*. 2011;108:1705–1710.

255. Milanesi R, Baruscotti M, Gnecchi-Ruscone T, DiFrancesco D. Familial sinus bradycardia associated with a mutation in the cardiac pacemaker channel. *N Engl J Med*. 2006;354:151–157.

256. Groenke S, Larson ED, Alber S, Zhang R, Lamp ST, Ren X, Nakano H, Jordan MC, Karagueuzian HS, Roos KP, Nakano A, Proenza C, Philipson KD, Goldhaber JI. Complete atrial-specific knockout of sodium-calcium exchange eliminates sinoatrial node pacemaker activity. *PloS One*. 2013;8:e81633.

257. Lahat H, Eldar M, Levy-Nissenbaum E, Bahan T, Friedman E, Khoury A, Lorber A, Kastner DL, Goldman B, Pras E. Autosomal recessive catecholamine- or exercise-induced polymorphic ventricular tachycardia: clinical features and assignment of the disease gene to chromosome 1p13-21. *Circulation*. 2001;103:2822–2827.

258. Sumitomo N, Sakurada H, Taniguchi K, Matsumura M, Abe O, Miyashita M, Kanamaru H, Karasawa K, Ayusawa M, Fukamizu S, Nagaoka I, Horie M, Harada K, Hiraoka M. Association of atrial arrhythmia and sinus node dysfunction in patients

with catecholaminergic polymorphic ventricular tachycardia. *Circ J Off J Jpn Circ Soc*. 2007;71:1606–1609.

259. Wilson GN. Correlated heart/limb anomalies in Mendelian syndromes provide evidence for a cardiomelic developmental field. *Am J Med Genet*. 1998;76:297–305.

260. Olson EN, Srivastava D. Molecular pathways controlling heart development. *Science*. 1996;272:671–676.

261. Tabin C. The initiation of the limb bud: growth factors, Hox genes, and retinoids. *Cell*. 1995;80:671–674.

262. Gilbert SF. Formation of the Limb Bud. 2000;Available from: https://www.ncbi.nlm.nih.gov/books/NBK10003/

263. Ohuchi H, Nakagawa T, Yamamoto A, Araga A, Ohata T, Ishimaru Y, Yoshioka H, Kuwana T, Nohno T, Yamasaki M, Itoh N, Noji S. The mesenchymal factor, FGF10, initiates and maintains the outgrowth of the chick limb bud through interaction with FGF8, an apical ectodermal factor. *Dev Camb Engl*. 1997;124:2235–2244.

264. Roberts DJ, Tabin C. The genetics of human limb development. *Am J Hum Genet*. 1994;55:1–6.

265. McDermott DA, Fong JC, Basson CT. Holt-Oram Syndrome [Internet]. In: Pagon RA, Adam MP, Ardinger HH, Wallace SE, Amemiya A, Bean LJ, Bird TD, Ledbetter N, Mefford HC, Smith RJ, Stephens K, editors. GeneReviews(®). Seattle (WA): University of Washington, Seattle; 1993

266. Baujat G, Le Merrer M. Ellis-van Creveld syndrome. *Orphanet J Rare Dis*. 2007;2:27.

267. Suspitsin EN, Imyanitov EN. Bardet-Biedl Syndrome. *Mol Syndromol*. 2016;7:62–71.

268. Yadav DK, Beniwal MK, Jain A. Bardet-Biedl syndrome a rare cause of cardiomyopathy. *Indian Pediatr*. 2013;50:599–601.

269. Slavotinek AM. McKusick-Kaufman Syndrome [Internet]. In: Pagon RA, Adam MP, Ardinger HH, Wallace SE, Amemiya A, Bean LJ, Bird TD, Ledbetter N, Mefford HC, Smith RJ, Stephens K, editors. GeneReviews(®). Seattle (WA): University of Washington, Seattle; 1993

270. Garg V, Muth AN, Ransom JF, Schluterman MK, Barnes R, King IN, Grossfeld PD, Srivastava D. Mutations in NOTCH1 cause aortic valve disease. *Nature*. 2005;437:270–274.

271. Lee TC, Zhao YD, Courtman DW, Stewart DJ. Abnormal Aortic Valve Development in Mice Lacking Endothelial Nitric Oxide Synthase. *Circulation*. 2000;101:2345–2348.

2. Chapter I: GATA6 regulates aortic valve remodeling and its haploinsufficiency leads to RL-type Bicuspid Aortic Valve

Lara Gharibeh, Hiba Komati, Yohan Bossé, Munir Boodhwani, Mahyar Heydarpour, Megan Fortier, Romina Hassanzadeh, Janet Ngu, Patrick Mathieu, Simon Body, Bicuspid Aortic Valve Consortium, Mona Nemer*.

1- From the Molecular Genetics and Cardiac Regeneration Laboratory, Department of Biochemistry, Microbiology, and Immunology, University of Ottawa, Ottawa, Ontario, Canada (L.G., H.K., M.F., R.H., M.N.).
2- Institut Universitaire de Cardiologie et de Pneumologie de Québec, Department of Molecular Medicine, Laval University, Québec, Canada (Y.B., P.M.).
3- Division of Cardiac Surgery, University of Ottawa Heart Institute, Ottawa, ON, Canada (M.B., J.N.).
4- Department of Anesthesiology, Perioperative and Pain Medicine, Brigham and Women's Hospital, Harvard Medical School, Boston, Mass, USA (M.H., S.B.).

*Corresponding author:
Dr. Mona Nemer
University of Ottawa
550 Cumberland, Room 246
Ottawa, Ontario K1N 6N5
Tel: 613 562 5270
Fax: 613 562 5271
Email: mona.nemer@uottawa.ca

2.1. Statement of the manuscript

The manuscript ***"GATA6 regulates aortic valve remodeling and its haploinsufficiency leads to RL-type Bicuspid Aortic Valve"*** has been submitted and is in final review in *Circulation* journal (January 24, 2018).

2.2. Contribution statement

In this chapter, I performed almost all the *in vivo* and *in vitro* work and contributed to their analysis. RH helped in cloning the mutants. MF performed mice echocardiography. The human data experiments were performed by our colleagues (YB, MB, MH, SB, PM, JN). LG, MN and HK interpreted and analyzed results. LG and MN wrote the manuscript. All authors have approved the final version.

2.3. Acknowledgement

The authors are grateful to Janie Beauregard for technical support, Hélène Touchette for secretarial help and members of the Nemer Lab for helpful discussions. The authors thank Prof. Wolfgang Eberhardt for sharing the MMP9-Luc reporter construct. The authors acknowledge the invaluable support of the uOttawa histology and animal physiology cores.

2.4. Sources of funding

This work was funded by grants from the Canadian Institutes of Health Research to MN and YB (MOP201009 and MOP137058). LG holds a graduate scholarship from the University of Ottawa and YB is recipient of a Canada Research Chair in Genomics of Heart and Lung Diseases. SCB was funded by a grant from the National Institutes of Health (R01HL114823).

2.5. Disclosure

None

2.6. Abstract

Background: Bicuspid aortic valve (BAV), the most common congenital heart defect affecting 1-2% of the population, is a major risk factor for premature aortic valve disease and accounts for the majority of valve replacement. The mechanisms of disease etiology and pathogenesis remain largely undefined.

Methods: Cardiac structure and function was analyzed in mice lacking a *Gata6* allele. Human *GATA6* gene variants were analyzed in 452 BAV cases from the BAV consortium and 1849 controls from the Framingham GWAS study. GATA6 expression was determined in mice and human tissues using qRT-PCR and immunohistochemistry. Mechanistic studies were done in cultured cells.

Results: *Gata6* heterozygous mice have highly penetrant RL type BAV, the most frequent type in human. GATA6 transcript levels are lower in human BAV as compared to normal tricuspid valves. Mechanistically, *Gata6* haploinsufficiency disrupts valve remodeling and extracellular matrix composition through dysregulation of important signaling molecules including matrix metalloproteinase 9. Cell-specific inactivation of *Gata6* reveals an essential role for GATA6 in secondary heart field myocytes as loss of one *Gata6* allele from *Isl-1* positive cells- but not from endothelial or neural crest cells-recapitulates the phenotype of *Gata6* heterozygous mice.

Conclusion: The data identify a new cellular and molecular mechanism underlying BAV. The availability of an animal model for the most frequent human BAV opens the way for the elucidation of BAV pathogenesis and the development of much needed therapies.

Keywords: Bicuspid Aortic Valve- GATA proteins- Extracellular Matrix- MMP9- GWAS

2.7. Introduction

Aortic valve disease (AVD) is a major cause of morbidity and mortality worldwide and represents a significant health and socio-economic burden. From 2000 to 2012, hospitalization for AVD increased by 59% and in 2015, the cost to the healthcare system was estimated at $3.207 billion in the USA alone[1]. Despite intense efforts, the etiology and pathophysiology of AVD remain incompletely elucidated which impedes to the development of effective preventive and therapeutic regimens. At present, surgical approaches including valve replacement, the second leading cardiac surgery in North America, are the only effective treatment options. Cardiovascular diseases such as atherosclerosis and hypertension as well as congenital malformations likebicuspid aortic valve (BAV) and Marfan Syndrome are risk factors for premature valve deterioration and aortopathy[2]. BAV is the most common heart defect affecting 1-2% of the population with a higher male prevalence. It featuresthe presence of two usually-asymmetric instead of the normal three symmetrical leaflets. Individuals with BAV are at increased risk of valve deterioration and account for the majority of valve replacements particularly in patients under 65 years of age. They are also at increased risk of aortic dilatation and dissection and many develop serious cardiovascular complications 10 years earlier than individuals with a tricuspid aortic valve (TAV)[2,3]. As such, BAV has the greatest health burden of all other congenital heart diseases. The molecular mechanisms underlying the etiology and pathophysiology of BAV and BAV related valvulo-aortopathy remain largely undefined.

BAV is an autosomal dominant trait with variable expressivity and incomplete penetrance suggestive of genetic and environmental modifiers. Human genetic studies have provided evidence for linkage of 3 loci, 18q, 5q and 13q[4] with BAV with *MATRIN3* as the

candidate 5q gene[5]. Mutations in *NOTCH1* and in *GATA5* –a regulator of the Notch pathway- have also been identified in some BAV patients[6,7]. Loss of function mutations in genetically engineered mice confirmed a causal relationship between the *Notch1* and *Gata5* genes and BAV [8]. However, mutations in these genes account for only a small percentage of human BAV and the genetic basis for the majority of BAVs remains undetermined.

Additionnally, we lack mechanistic understanding of BAVpathophysiology. For example, it is unclear why BAV is associated with accelerated valve calcification and deterioration, or with aorthopathy. Why different BAV subtypes are associated with different clinical outcomes supports the genetic hypothesis. In human, BAVs are classified according to which leaflets – right (R), left (L), and non-coronary (N)- are fused together. The RL type (right and left leaflet fusion), is the most frequent in human, accounting for 59% of BAV whereas the RN type accounts for 37% [9]. Retrospective analysis suggests that BAV morphology is of prognostic relevance with RN BAV being associated with a greater degree of valve dysfunction and a shorter time to valve intervention[10,11]. BAV morphology also results in different types of aortopathy and distinct hemodynamics across the ascending aorta[12]. Elucidating the molecular mechanisms underlying BAV associated aortopathy has been hampered by the paucity of BAV animal models. *Gata5* null mice provides a model for RN type BAV[8]. In the case of RL-BAV, an inbred line of Syrian hamsters for which the genetic basis remains unknown is available[13]. Both RL and RN type BAVs were reported in mice lacking *Jag1* in cardiac cells or *Notch1* in endothelial cells; these mice have additional cardiac defects and compromised postnatal survival[14]. We now report that mice heterozygous for a mutated *Gata6* allele have highly penetrant RL type BAV. Mechanistically, defective valve remodeling due to dysregulated extracellular matrix (ECM) degradation and decreased

cell death are the underlying cause of BAV formation. In human, we found that GATA6 transcripts and protein levels are lower in the valves and aorta of individuals with BAV as compared to those with TAV and that three *GATA6* gene variants associate with BAV in a cohort of European ancestry. Together, the data suggests that *GATA6* may be a novel BAV causing gene. The study also provides a well-defined animal model of the most frequent type of BAV in human, opening the way for molecular dissection of BAV associated aorthopathy.

2.8. Methods

The data, analytic methods, and study materials will be available to other researchers for purposes of reproducing the results or replicating the procedure.

Animals. Mouse handling and experimentation were performed in accordance with institutional guidelines. Protocols were approved by the institutional Animal Care committee. *Gata6* heterozygous (*Gata6*$^{+/-}$, C57/B6) mice were previously described[15]. Cell-specific knockouts were generated by crossing *Gata6* floxed mice with mice harboring Cre recombinase. The *Tie-cre* (C57/B6) expressing mouse line was previously described[8]. *Wnt1-cre* (129S4) and *Isl1-cre* lines (C57/B6) were obtained from Jackson laboratories (USA). Unless otherwise specified, mice were put on regular chow (Harlan 2018). For high fat diet experiment, mice were put on high fat/high carb chow for a period of 4 months (bioserv High Fat/High Carb Diet (F3282, 5kg box)).

Echocardiography. Transthoracic echocardiography was performed using a visual sonics Vevo 770 ultrasound system with a RMV 707 30-MHz transducer as previously described[16]. M-mode imaging was obtained from 150-220 day old mice (n=11–14 mice per group).

Histology. Mouse tissues were fixed with 4% paraformaldehyde in PBS, paraffin embedded, sectioned at 4-μm intervals, and processed. Masson trichrome, Alcian Blue and Movat Pentachrome stainings were performed by the histology facility at the University of Ottawa.

Immunohistochemistry and immunofluorescence. Immunohistochemical studies were performed as described previously[8,17]. The GATA6 antibody[18] was used at 1/1000 dilution. Goat polyclonal IgG GATA4 (C20) antibody was purchased from SANTA CRUZ (SC-1237X; dilution 1/600). The following antibodies were purchased from ABCAM:

Semaphorin3C (ab 135842; dilution 1/350), SOX9 (ab3697, dilution 1/100), periostin (POSTN) (ab14041, dilution 1/1000), alpha smooth muscle actin (ab5694, dilution 1/750), total and cleaved Versican (ab19345 and ab177480, dilution 1/250 each), and NCID (ab8925, dilution 1/500). The Anti-phospho-Histone H3 (Ser10) antibody was from MILLIPORE (06-570, dilution 1/750). The biotinylated anti-Goat IgG and anti-Rabbit antibodies were from Vector Laboratories (BA5000) and Jackson (Cederlane) (711-065-152) respectively. Streptavidin-HRP conjugate was from Perkin Elmer (NEL 750000 1EA). Immunofluorescence was carried out using Anti-HA (Santa Cruz, Santa Cruz, CA, USA, sc-805) and Alexa Fluor 546 Goat Anti-Rabbit IgG (Life Technologies, Carlsbad, CA, USA, A-11035) at a dilution of 1/500 respectively. Image acquisition was completed using the Zeiss AxioObserver D1 microscope (Oberkochen, Germany).

Cell count and TUNEL. Image J software was used to count the number of mesenchymal and endocardial cells in AV and OFT cushions in 3 different sections of 3-4 hearts per genotype. Terminal deoxynucleotidyl transferase-mediated dUTP end labeling (TUNEL) assays were carried out using Apoptag kit according to the manufacturer's instructions (Intergen, Purchase, NY, USA).

qRT-PCR. Total RNA was isolated from snap-frozen hearts with TRIzol reagent (Life technologies, 15596018) using FastPrep beads (MP-Bio, 6913-100); cDNAs were generated using the Omniscript RT kit (Qiagen, 205113). Oligonucleotide sequences are available on request.

Luciferase assay. Transfections were carried out as previously described[17]. Total amount of DNA was maintained constant by adding appropriate amounts of empty DNA vector. The

BMP4-Luc and GATA6 constructs were previously described[17]. Full length MMP9-Luc reporter construct[19] was a kind gift from Prof. Wolfgang Eberhardt. Site-directed mutagenesis was used to generate mutant constructs which were verified by sequencing.

Western blot and Electrophoretic mobility shift assays. Nuclear and cytoplasmic extracts from AD293 cell line overexpressing GATA6 WT and mutant proteins were used. Anti-HA (Santa Cruz, Santa Cruz, CA, USA, sc-805), anti-GAPDH (ABCAM, ab8245) and anti-nucleolin (Cell Signaling, D4C70, 14574) were used at a dilution of 1/2000. Secondary anti-mouse (Jackson, Cedarlane, 715-035-151) and anti-rabbit (Jackson, Cedarlane, 711-035-152) antibodies were used at 1/40000 dilution. DNA binding activity of GATA6 proteins was assessed using nuclear extracts and the proximal GATA site from the BMP4 and MMP9 promoters as described previously[18].

Human subjects. Written informed consent was received from participants prior to inclusion in all the studies. Microarray analysis: study was approved by the ethics committee of the "Institut Universitaire de Cardiologie et de Pneumologie de Québec" (IUCPQ). Human genetic study: The study was approved by the Partners HealthCare Human Research Committee. Human aorta staining: the study was approved by the University of Ottawa Heart Institute Research Ethics Board.

Microarray analysis. Gene expression was obtained from 12 aortic valves in each group and measured with the HumanHT-12 v4 Expression BeadChip. Bicuspid aortic valves (BAV) were obtained from male patients who underwent aortic valve replacement surgery. Normal tricuspid aortic valves (TAVn) were obtained from male patients who underwent heart

transplantation. Gene expression differences between groups of valves were tested using t-test.

Human aortas staining. Patients from the University of Ottawa Heart Institute undergoing surgical intervention for aortic valve and/or aortic disease were included in this study. Aortic wall tissue specimens were obtained and fixed for 24 hours in 10% buffered formalin. Six sections were taken horizontally across the excised aortic segment and paraffin embedded; 5µm sections were prepared.

Human genetic studies. 480 Caucasian BAV cases genotyped with the Omni2.5 chip were used yielding 2,379,855 genetic markers from BAV-Consortium database, and 2,477 Caucasian controls genotyped using the HumanOmni5.0 bead chip with 4,271,233 genetic markers from dbGaP (FHS*). Quality control (QC) of the genotype data from both cohorts was performed using Genome Studio and PLINK (**Supplementary Figure 2.2**). We considered markers with a MAF>1% and performed extensive principal components-based filtering for population stratification. After merging cases and controls and further QC, we used 452 BAV cases and 1,849 Caucasian controls with a common set of 1,355,128 single nucleotide polymorphisms (SNPs). An additive logistic regression model was performed for association analysis adjusted for gender and race using PLINK.

*http://www.ncbi.nlm.nih.gov/projects/gap/cgi-bin/study.cgi?study_id=phs000007.v22.p8

Statistics. For echocardiography and gene expression analysis, values are presented as means ± standard error of the mean (SEM). P values were generated using Student's 2-tailed t test. For statistical analysis of phenotype-genotype association, Fisher Exact Test (2×2 contingency table) was used. For luciferase assay, statistical analysis was done by one-way

ANOVA followed by Dunnett's multiple comparison post-hoc analysis. In all cases, P values < 0.05 were considered as an index of statistical significance.

2.9. Results

2.9.1. *Gata6* haploinsufficiency leads to RL-type BAV.

Previously, we reported that transcription factor *Gata5* is involved in valvulogenesis and that its loss leads to BAV[8]. Genetic studies aimed at determining modifiers of *Gata5* revealed a strong interaction with *Gata6*. Whereas *Gata5* heterozygous mice have no detectable cardiac phenotype, *Gata5*$^{+/-}$ *Gata6*$^{+/-}$ compound heterozygous embryos have disrupted valvulogenesis and die perinatally due to severe defects in outflow track (OFT) formation[15].Similarly, *Gata4*$^{+/-}$ *Gata6*$^{+/-}$ mice die embryonically at E13.5 due to vascular and OFT defects[20]. Functional cardiac analysis of adult *Gata6* heterozygous mice using echocardiography revealed a significant decrease in fractional shortening (FS) vs their control littermates (**Figure 2.1 A**). Additionally, large percentage of *Gata6*$^{+/-}$ mice had significantly elevated aortic valve gradient- with no changes in the aortic root diameter- suggestive of AVD (**Figure 2.1 B, C and D**). Consistent with the presence of cardiac stress, qRT-PCR performed on adult ventricular tissues revealed increased levels of stress markers (ANF, HIF1alpha) and cardiac remodeling genes (FGFR1/3, CTGF), and decreased levels of sarcoplasmic calcium-ATPase (SERCA). GATA4 levels were unchanged (**Figure 2.1 E**).

Analysis of cardiac structure revealed the presence of BAV in 56% of *Gata6*$^{+/-}$ males and in 27% of *Gata6*$^{+/-}$ females (32 out of 57 males and 7 out of 26 females) (**Figure 2.1 F**). BAV frequency was assessed by the Fisher exact test for both male ($p<0.0001$) and female ($p=0.0043$) groups. Interestingly, all BAVs were of the RL-type, the most frequently occurring type in human (**Figure 2.1 F and 2.1 G**). Thickening of aortic valve leaflets was also observed in *Gata6*$^{+/-}$ mice (**Figures 2.1 H and 2.2 A, left panels a-c**). This could be reflective of postnatal remodeling caused by vascular or myocardial disease. Defective

valvulogenesis could also be the underlying cause of the valve phenotype. Masson Trichrome staining of newborn *Gata6*$^{+/-}$ mouse heart sections (P0) showed significant aortic valve thickening in 7 out of 11 *Gata6*$^{+/-}$ mice but not in their *Gata6*$^{+/+}$ littermates (n=6) (**Figure 2.1 I, left panels a-c**). No thickening was observed in the mitral or tricuspid valves (data not shown) suggesting defective OFT but normal AV cushion formation. Movat pentachrome staining revealed thickened valves of unequal size with an increase in ECM deposition in *Gata6*$^{+/-}$ (blue color) when compared to controls. Increased collagen fiber content (yellow color) was also evident especially in the cushion-like aortic valves (**Figure 2.1 I, right panels d-f**). These results suggest the presence of abnormal ECM content in the aortic valves of *Gata6*$^{+/-}$ mice. Similarly, Alcian blue staining of adult *Gata6*$^{+/-}$ sections revealed greater glycosaminoglycan content in the valves of *Gata6*$^{+/-}$ mice, indicative of abnormal matrix composition (**Figure 2.2 A, right panels d-f**).

BAV is a risk factor for premature AVD including valve calcification and sclerosis (presence of accelerated fibrosis). To determine whether *Gata6*$^{+/-}$ are prone to AVD, we analyzed adult Ao valves using Masson trichrome staining which revealed increased total collagen content in some *Gata6*$^{+/-}$ BAV and TAV, indicative of valve sclerosis (**Figure 2.2 B**). We also analyzed the levels of several transcripts in dissected aortic valves. As shown in **Figure 2.2C**, significant gene expression changes were noted in *Gata6*$^{+/-}$ valves including decreased levels of TIMP1 (Tissue inhibitor of Metalloproteinase 1), FBN1 (Fibrillin 1), and VCAN (Versican). These changes are consistent with altered ECM integrity and valve elasticity. Reduced level of SOX9 transcripts in *Gata6*$^{+/-}$ valves is also noteworthy since decreased expression of SOX9 promotes heart valve calcification[21] (**Figure 2.2D, panels a-b**). Similarly, decreased levels of periostin (POSTN) causes de-repression of the osteogenic

potential of the mesenchymal cells within the OFT and calcium deposition within the aortic valve[22]. Immunohistochemistry showed that expression of POSTN is downregulated in *Gata6*$^{+/-}$ valves compared to wildtype littermates (**Figure 2.2 E, panels a-c**). Interestingly, levels of SOX9 and periostin were differentially regulated in mice fed a normal or a high fat diet (HFD). In *Gata6*$^{+/+}$ valves, SOX9 levels were increased in mice on the HFD whereas POSTN levels were decreased. In contrast, POSTN levels were upregulated in *Gata6*$^{+/-}$ mice on HFD and SOX9 levels remained unchanged (**Figure 2.2 D and 2.2 E, lower panels**). Thus, *Gata6* haploinsufficiency promotes a pro-osteogenic state in the aortic valves and disrupts genetic reprogramming in response to pro-osteogenic stimuli.

2.9.2. Abnormal ECM and valve remodeling underlie GATA6-dependent BAV.

Defects in Epithelial to Mesenchymal transformation (EMT)-a critical stage during valvulogenesis- can lead to BAV[23]. To determine whether cell number and composition of the OFT cushions are changed in *Gata6*$^{+/-}$, we performed Alcian blue staining and cell counts on E11-11.5 cushions. Cell number was similar in *Gata6*$^{+/-}$ and *Gata6*$^{+/+}$ mice (**Supplementary Figure 2.1 A and C**) and staining for Phosphohistone H3 (PHH3) revealed no changes in proliferation, neither in OFT nor in AV cushions (**Supplementary Figure 2.1 D**). Smooth muscle alpha actin staining was also similar in both groups suggesting normal differentiation (**Supplementary Figure 2.1 B**). Next, cardiac neural crest cell (CNCC) dysregulation was examined. qRT-PCR revealed that expressions of SEMA3C- a secreted class 3 semaphorin present in and adjacent to migrating CNCC- and PLXNA2 (Plexin A2)- a semaphorin receptor expressed on CNCC-[24] were similar in *Gata6*$^{+/-}$ and *Gata6*$^{+/+}$ littermates (**Supplementary Figure 2.1 E, right panel**). Immunohistochemistry revealed a similar SEMA3C expression pattern at the level of the cells surrounding the branchial arch

arteries and in the left lateral wall of the conus in E11-11.5 from both genotypes (**Supplementary Figure 2.1 E, left panels**). These results suggest that the defect observed in *Gata6*$^{+/-}$ is not due to defective CNCC migration to the OFT cushions. Thus, the formation of BAV in *Gata6*$^{+/-}$ does not appear to be caused by defective cell proliferation, migration or differentiation processes.

Abnormal septation and valve thickening could be the result of either excessive proliferation in the valves or defective remodeling which involves cell apoptosis. Valve remodeling was examined in transverse sections of E14.5 embryos using TUNEL or PHH3 staining. As shown in **Figure 2.3 A and B**, cell death was significantly lower in *Gata6*$^{+/-}$ valves whereas cell proliferation was modestly increased. This result suggests abnormal apoptosis and valve remodeling in *Gata6*$^{+/-}$ mice which could result from an abnormal synthesis and/or breakdown of the ECM, a regulator of cell survival, migration and proliferation[25]. Matrix metalloproteinases (MMPs) and their endogenous inhibitors, tissue inhibitors of MMPs (TIMPs), play an important role in the ECM degradation process. Expression of mRNA levels of MMP9, TIMP1, MMP2 and TIMP2 was assessed in *Gata6*$^{+/-}$ E11.5 hearts. At this stage, a significant decrease in MMP9 levels along with a trend of decrease in MMP2 was observed (**Figure 2.3 D**), which could lead to dysregulated ECM degradation. Consistent with this, immunohistochemistry revealed lower levels of cleaved versican in E14.5 *Gata6*$^{+/-}$ valves (**Figure 2.3 C**). Expression of genes known to be involved in OFT formation and valve remodeling was also examined. BMP4, a direct target for GATA6, whose deletion from the anterior heart field (AHF) alters OFT septation[18,26], was significantly decreased (48%) in *Gata6*$^{+/-}$ hearts (**Figure 2.3 D**).

We tested whether MMP9 is transcriptionally regulated by GATA6. In silico analysis of the MMP9 promoter revealed the presence of conserved GATA binding sites (**Figure 2.3 E**). Co-transfection in NIH3T3 cells of GATA6 expressing vector and MMP9 luciferase constructs showed significant GATA6 activation of the MMP9 promoter that is dependent on the presence of the proximal GATA site (**Figure 2.3 E and 2.4 B**). Mutations in human *GATA6* have been reported in congenital heart disease associated with OFT defects (**Figure 2.4 A and supplementary Table 2.1**)[27]. The 2nd zinc finger (ZnF) in GATA6 mediates most protein-protein interactions as well as binding to DNA and is the site of many human mutations. We examined the effect of several GATA6 mutant proteins on transcriptional activation. All mutants showed reduced transcriptional activation of MMP9 and BMP4 promoters (**Figure 2.4 B** and data not shown). Interestingly, most mutations (except for T452A) showed reduced nuclear accumulation and increased cytoplasmic localization (**Supplementary Figure 2.3 A and B**). Additionally, all GATA6 mutants tested were unable to bind GATA elements (**Supplementary Figure 2.3 C**). The results suggest that functional *GATA6* haploinsufficiency resulting from these mutations may cause human CHD.

2.9.3. Loss of one *Gata6* allele in *Isl1+* cells recapitulates the aortic valve phenotype of *Gata6* heterozygous mice.

Endothelial, neural crest and second heart field myocytes contribute to OFT formation. Endothelial cells within and lining the interior of the OFT vessels undergo EMT, giving rise to the endocardial cushions[28]. Cardiac neural crest cells (CNCC) that arise from the dorsal neural tube and migrate as mesenchymal cells to populate the OFT, are known to contribute to the formation of the endocardial cushion and the septum separating the aortic and pulmonary trunks[29]. Recent studies have suggested that secondary heart field (SHF)

precursors lying in the ventral pharynx are able to interact with CNCC migrating to the OFT cushion; together they control ECM development and apoptosis during valve remodeling[30]. Later on, invading CNCC merge with the endocardial cushions cells and SHF mesenchymal cells to ensure the elongation and proper septation of the OFT. Since GATA6 is present in all these lineages[18,31,32], we used mouse genetics to test which cell types are responsible for BAV formation. *Gata6* was deleted from endothelial, neural crest and SHF cells by crossing *Gata6*$^{Fl/Fl}$ mice with *Tie2cre*, *Wnt1cre* and *Isl1cre* mice respectively. No BAVs were found in mice with a deleted *Gata6* allele in endothelial (*Tie2cre+ G6*$^{Wt/Fl}$) or neural crest (*Wnt1cre+ G6*$^{Wt/Fl}$) cells. However, removal of one copy of *Gata6* from *Isl1+* cells resulted in BAV in 44% of *Isl1cre+ G6*$^{Wt/Fl}$ mice and recapitulated the valve phenotype of *Gata6*$^{+/-}$ mice (**Figure 2.5 A, B and C**). The BAV frequency in *Isl1cre+ G6*$^{Wt/Fl}$ mice was significant as assessed by the Fisher Exact Test (p=0.0021). Thus, GATA6 appears to be essential in SHF cells for proper aortic valve formation.

2.9.4. GATA6 expression and variants in Human BAV

We investigated whether variants within the *GATA6* gene associate with human BAV using 452 sporadic BAV cases and 1849 controls. After quality control (detailed in **supplementary Figure 2.2**), an additive logistic regression model revealed nominal association of several variants (**Figures 2.6 A and B** and **supplementary Table 2.2 a and b**). However, none reached the locus wide significance (0.00014). Since the genotyping platform would not detect rare missense variants, we analyzed GATA6 expression in human tissues of individuals with BAV and TAV. In human aortic valve tissues, GATA6 transcripts were significantly lower in the BAV vs TAV specimens (**Figure 2.6 C** and **supplementary Table 2.3**). Similarly, GATA6 immunoreactivity was lower in aortic tissue sections from BAV vs

TAV patients who underwent aortic repair surgery (**Figure 2.6 D** and **supplementary Table 2.4**)). Interestingly, this decrease was more pronounced in tissues from patients with RL vs RN type BAV. Immunostaining for activated Notch intracellular domain (NCID) and smooth muscle actin were used as controls. Together the data suggests a potential role for GATA6 in human aortic valve disease.

2.10. Discussion

Bicuspid aortic valve is the most common congenital heart defect in human and a risk factor for aortic valve disease. The genetic basis of BAV formation and aortopathy in the majority of individuals remains unknown. The data presented identify *GATA6* as a potential BAV causing gene and offers a unique animal model to study the pathogenesis of the most frequent type of human BAV.

2.10.1. GATA6 regulation of aortic valve formation

BAV is a genetically heterogeneous defect. Mutations in *GATA5* and *NOTCH1* have been reported in some BAV patients. In addition, 5 distinct loci on human chromosomes 5q, 9q, 13q, 17q and 18q, have been associated with BAV in families[4,33,34]. *MATR3*, the gene encoding MATRIN3, is located on 5q; it is reportedly linked to human BAV and its deletion in mice leads to partially penetrant BAV[5]. The identity of the causative genes within the other linked loci remains undetermined. The *GATA6* gene is located on 18q11.2 and mutations in *GATA6* as well as a microdeletion including *GATA6* have been reported in patients with congenital heart disease[35,36]. The present study shows that GATA6 expression is decreased in the valves and aortas of individuals with a BAV vs TAV. Whether this reflects the presence of missense mutations within the *GATA6* gene deserves to be determined using whole exome sequencing or targeted gene sequencing.

GATA6 belongs to the GATA family of zinc finger transcription factors and is predominantly expressed in the heart and gut[18]. Its role within the heart is not fully elucidated and often overlaps with that of another GATA protein, GATA4. *Gata6* null mice are embryonic lethal at implantation but cell-specific loss of *Gata6* from myocytes, smooth muscle, or neural crest cells affects cell proliferation and hypertrophic growth and is

associated with structural cardiac defects[37,38]. No gross defects were reported in *Gata6* heterozygote mice. The data presented unravels a new role for GATA6 in aortic valve formation and points to its essential function in second heart field (SHF)-derived cells therein. Loss of one *Gata6* allele from *Isl-1+* cells recapitulates the highly penetrant BAV and thickened valve phenotypes seen in *Gata6* heterozygote mice. Both phenotypes reflect remodeling defects caused, at least in part, by changes in ECM degradation and dysregulated cellular apoptosis. These can result from decreased levels of GATA6 regulated genes such as BMP4 and MMP9. BMP4 is a known GATA6 target[18] and this study identifies MMP9 as a new GATA6 downstream target.

Regulation of ECM plays an important role in normal and pathogenic development and is a key feature of many diseases such as congenital heart disease, cancer and inflammatory disorders. Interestingly, in colorectal cancers, GATA6 expression correlates with increased invasion and metastasis while in vitro gain and loss of function indicate that GATA6 levels regulate cell migration and invasion[39]. Human *GATA6* mutations have been reported in a wide spectrum of CHD (ASD, VSD, PDA, PTA, TOF) all of which implicate defective ECM due to alteration in expression of several metalloproteinases. For example, increased MMP2 and MMP9 activities were linked with the pathogenesis of VSD in 96 children with peri-membranous VSD[40]. Similarly, loss of metalloproteinase Tolloid –like (TTL-1) leads to incomplete formation of the interventricular septum in *Tll-1* knockout mice. An insertion mutation in the exon 10 of TLL-1 was found in patients with ASD, VSD and PDA[41]. Another matricellular protein, Cysteine-rich angiogenic inducer 1 (CCN1), plays a role in heart development as *Ccn1*-null mice have impaired cardiac valvulo-septal morphogenesis resulting in severe atrioventricular septal defect (AVSD); impaired gelatinase

activity and apoptosis may underlie the phenotype[42]. It is now well established that matrix metalloproteases regulate cell survival, proliferation and differentiation as well as cell adhesion and migration. More specifically, it is reported that MMP9 can lead to increased apoptosis during development. In fact *Mmp9* null mice display a delay in hypertrophic chondrocyte apoptosis in addition to delayed vascularization and ossification[43]. Together with our findings, this raises the intriguing possibility for a broader role for GATA6 as ECM regulator in development and disease.

2.10.2. Development of an animal model of RL-type BAV

BAV is a major risk for premature onset of potentially fatal aortic disease. The heterogeneity of BAV and associated aortopathy combined with the paucity of corresponding animal models constitute a formidable challenge for the development of predictive tools for patient management. Identifying patients who could benefit from prophylactic reparative surgery or other interventions is presently an unachieved goal. Evidence is mounting that BAV aortopathy is not similar to that of genetic connective tissue disorders, like Marfan Syndrome, yet the clinical guidelines for BAV are extrapolated from those of Marfan Syndrome in which the molecular mechanisms of disease are well delineated[44]. Recent reviews of knowledge gaps have emphasized the critical need of deciphering the molecular pathology of BAV in order to identify markers of complications and targets for therapies[2]. As mentioned earlier, very few mouse models of BAV have been reported and in most cases, the BAV orientation is exclusively RN (*Gata5*$^{-/-}$ and *Nos3*$^{-/-}$ mice)[8,45]. Loss of the Notch ligand *Jag1* from cardiac cells results in a polyvalvular phenotype with 47% BAV of both RN and RL orientations; these mice have VSD and significantly reduced late gestational/perinatal viability[14]. The development of an animal model of RL type BAV, the

most common type in human, represents a step forward towards understanding the etiology and pathophysiology of BAV including the role of genetics in BAV associated aortopathy. Among others, the presence of BAV in only 50% of *Gata6*$^{+/-}$ mice will make it possible to address the unanswered question of the contribution of genetics vs hemodynamics to BAV aortopathy and ultimately to developing much needed biomarkers. Indeed, the influence of cusp orientation on the 3D flow patterns across the ascending aorta remains controversial[12] and genetically controlled studies in human patients have proved to be challenging. Similarly, retrospective analyses have associated valve configuration with distinct aortopathy risks and long term outcome of BAV repair[46]. However, the lack of molecular knowledge prevents development of much needed predictive tools.

In human, BAV is twice as common in male as in female but the reason for this gender bias is unclear. Remarkably, the prevalence of BAV is greater in male *Gata6*$^{+/-}$ mice vs female. BAV presentation is also heterogeneous in human even within each subtype (RL, RN, LN). Variations include presence/ absence of raphe and leaflet thickness and size. This heterogeneity is also observed in the *Gata6*$^{+/-}$ mice, with variable valve thickness and functionality. The availability of a mouse model that faithfully recapitulates features of the human disease will help unravel the genetic and environmental modifiers of BAV and BAV aortopathy. For example, the work presented indicates profound gene expression changes in BAV as well as TAV from *Gata6*$^{+/-}$ mice (Figure 2). In both cases, we observed increased evidence of sclerosis as well as increased markers of the pro-osteogenic program. In addition, gene expression changes in response to a pro-inflammatory/pro-calcific stimulus (HFD) were disrupted in *Gata6*$^{+/-}$ mice irrespective of the valve orientation. Together, these observations suggest that genetics may play a critical role in progression of aortic valve

disease. The availability of mice with bicuspid or tricuspid aortic valves on the same genetic background opens the way for molecular dissection of the etiology and pathophysiology of aortic valve disease which will ultimately result in the identification of biomarkers and therapeutic targets.

2.11. References

1. Badheka AO, Singh V, Patel NJ, Arora S, Patel N, Thakkar B, Jhamnani S, Pant S, Chothani A, Macon C, Panaich SS, Patel J, Manvar S, Savani C, Bhatt P, Panchal V, Patel N, Patel A, Patel D, Lahewala S, Deshmukh A, Mohamad T, Mangi AA, Cleman M, Forrest JK. Trends of Hospitalizations in the United States from 2000 to 2012 of Patients >60 Years With Aortic Valve Disease. *Am J Cardiol*. 2015;116:132–141.

2. Michelena HI, Prakash SK, Corte AD, Bissell MM, Anavekar N, Mathieu P, Bossé Y, Limongelli G, Bossone E, Benson DW, Lancellotti P, Isselbacher EM, Enriquez-Sarano M, Sundt TM, Pibarot P, Evangelista A, Milewicz DM, Body SC. Bicuspid Aortic Valve: Identifying Knowledge Gaps and Rising to the Challenge From the International Bicuspid Aortic Valve Consortium (BAVCon). *Circulation*. 2014;129:2691–2704.

3. Mathieu P, Bossé Y, Huggins GS, Corte AD, Pibarot P, Michelena HI, Limongelli G, Boulanger M, Evangelista A, Bédard E, Citro R, Body SC, Nemer M, Schoen FJ. The pathology and pathobiology of bicuspid aortic valve: State of the art and novel research perspectives. *J Pathol Clin Res*. 2015;1:195–206.

4. Martin LJ, Ramachandran V, Cripe LH, Hinton RB, Andelfinger G, Tabangin M, Shooner K, Keddache M, Benson DW. Evidence in favor of linkage to human chromosomal regions 18q, 5q and 13q for bicuspid aortic valve and associated cardiovascular malformations. *Hum Genet*. 2007;121:275–284.

5. Quintero-Rivera F, Xi QJ, Keppler-Noreuil KM, Lee JH, Higgins AW, Anchan RM, Roberts AE, Seong IS, Fan X, Lage K, Lu LY, Tao J, Hu X, Berezney R, Gelb BD, Kamp A, Moskowitz IP, Lacro RV, Lu W, Morton CC, Gusella JF, Maas RL. MATR3 disruption in human and mouse associated with bicuspid aortic valve, aortic coarctation and patent ductus arteriosus. *Hum Mol Genet*. 2015;24:2375–2389.

6. Garg V, Muth AN, Ransom JF, Schluterman MK, Barnes R, King IN, Grossfeld PD, Srivastava D. Mutations in NOTCH1 cause aortic valve disease. *Nature*. 2005;437:270–274.

7. Bonachea EM, Chang S-W, Zender G, LaHaye S, Fitzgerald-Butt S, McBride KL, Garg V. Rare GATA5 sequence variants identified in individuals with bicuspid aortic valve. *Pediatr Res*. 2014;76:211–216.

8. Laforest B, Andelfinger G, Nemer M. Loss of Gata5 in mice leads to bicuspid aortic valve. *J Clin Invest*. 2011;121:2876–2887.

9. Friedman T, Mani A, Elefteriades JA. Bicuspid aortic valve: clinical approach and scientific review of a common clinical entity. *Expert Rev Cardiovasc Ther*. 2008;6:235–248.

10. Schaefer BM, Lewin MB, Stout KK, Gill E, Prueitt A, Byers PH, Otto CM. The bicuspid aortic valve: an integrated phenotypic classification of leaflet morphology and aortic root shape. *Heart Br Card Soc*. 2008;94:1634–1638.

11. Fernandes SM, Khairy P, Sanders SP, Colan SD. Bicuspid aortic valve morphology and interventions in the young. *J Am Coll Cardiol*. 2007;49:2211–2214.

12. Mahadevia R, Barker AJ, Schnell S, Entezari P, Kansal P, Fedak PWM, Malaisrie SC, McCarthy P, Collins J, Carr J, Markl M. Bicuspid aortic cusp fusion morphology alters aortic three-dimensional outflow patterns, wall shear stress, and expression of aortopathy. *Circulation*. 2014;129:673–682.

13. Fernández MC, Durán AC, Real R, López D, Fernández B, de Andrés AV, Arqué JM, Gallego A, Sans-Coma V. Coronary artery anomalies and aortic valve morphology in the Syrian hamster. *Lab Anim*. 2000;34:145–154.

14. MacGrogan D, D'Amato G, Travisano S, Martinez-Poveda B, Luxán G, Del Monte-Nieto G, Papoutsi T, Sbroggio M, Bou V, Gomez-Del Arco P, Gómez MJ, Zhou B, Redondo JM, Jiménez-Borreguero LJ, de la Pompa JL. Sequential Ligand-Dependent Notch Signaling Activation Regulates Valve Primordium Formation and Morphogenesis. *Circ Res*. 2016;118:1480–1497.

15. Laforest B, Nemer M. GATA5 interacts with GATA4 and GATA6 in outflow tract development. *Dev Biol*. 2011;358:368–378.

16. Messaoudi S, He Y, Gutsol A, Wight A, Hébert RL, Vilmundarson RO, Makrigiannis AP, Chalmers J, Hamet P, Tremblay J, McPherson R, Stewart AFR, Touyz RM, Nemer M. Endothelial Gata5 transcription factor regulates blood pressure. *Nat Commun*. 2015;6:8835.

17. Nemer G, Nemer M. Cooperative interaction between GATA5 and NF-ATc regulates endothelial-endocardial differentiation of cardiogenic cells. *Dev Camb Engl*. 2002;129:4045–4055.

18. Nemer G, Nemer M. Transcriptional activation of BMP-4 and regulation of mammalian organogenesis by GATA-4 and -6. *Dev Biol*. 2003;254:131–148.

19. Eberhardt W, Schulze M, Engels C, Klasmeier E, Pfeilschifter J. Glucocorticoid-mediated suppression of cytokine-induced matrix metalloproteinase-9 expression in rat mesangial cells: involvement of nuclear factor-kappaB and Ets transcription factors. *Mol Endocrinol Baltim Md*. 2002;16:1752–1766.

20. Xin M, Davis CA, Molkentin JD, Lien C-L, Duncan SA, Richardson JA, Olson EN. A threshold of GATA4 and GATA6 expression is required for cardiovascular development. *Proc Natl Acad Sci U S A*. 2006;103:11189–11194.

21. Peacock JD, Levay AK, Gillaspie DB, Tao G, Lincoln J. Reduced sox9 function promotes heart valve calcification phenotypes in vivo. *Circ Res*. 2010;106:712–719.

22. Tkatchenko TV, Moreno-Rodriguez RA, Conway SJ, Molkentin JD, Markwald RR, Tkatchenko AV. Lack of periostin leads to suppression of Notch1 signaling and calcific aortic valve disease. *Physiol Genomics*. 2009;39:160–168.

23. Fernández B, Durán AC, Fernández-Gallego T, Fernández MC, Such M, Arqué JM, Sans-Coma V. Bicuspid aortic valves with different spatial orientations of the leaflets are distinct etiological entities. *J Am Coll Cardiol*. 2009;54:2312–2318.

24. Feiner L, Webber AL, Brown CB, Lu MM, Jia L, Feinstein P, Mombaerts P, Epstein JA, Raper JA. Targeted disruption of semaphorin 3C leads to persistent truncus arteriosus and aortic arch interruption. *Dev Camb Engl*. 2001;128:3061–3070.

25. Hinton RB, Lincoln J, Deutsch GH, Osinska H, Manning PB, Benson DW, Yutzey KE. Extracellular matrix remodeling and organization in developing and diseased aortic valves. *Circ Res*. 2006;98:1431–1438.

26. McCulley DJ, Kang J-O, Martin JF, Black BL. BMP4 is required in the anterior heart field and its derivatives for endocardial cushion remodeling, outflow tract septation, and semilunar valve development. *Dev Dyn Off Publ Am Assoc Anat*. 2008;237:3200–3209.

27. Kodo K, Nishizawa T, Furutani M, Arai S, Yamamura E, Joo K, Takahashi T, Matsuoka R, Yamagishi H. GATA6 mutations cause human cardiac outflow tract defects by disrupting semaphorin-plexin signaling. *Proc Natl Acad Sci U S A*. 2009;106:13933–13938.

28. de Lange FJ, Moorman AFM, Anderson RH, Männer J, Soufan AT, de Gier-de Vries C, Schneider MD, Webb S, van den Hoff MJB, Christoffels VM. Lineage and morphogenetic analysis of the cardiac valves. *Circ Res*. 2004;95:645–654.

29. Kirby ML, Gale TF, Stewart DE. Neural crest cells contribute to normal aorticopulmonary septation. *Science*. 1983;220:1059–1061.

30. Jain R, Engleka KA, Rentschler SL, Manderfield LJ, Li L, Yuan L, Epstein JA. Cardiac neural crest orchestrates remodeling and functional maturation of mouse semilunar valves. *J Clin Invest*. 2011;121:422–430.

31. Xie L, Hoffmann AD, Burnicka-Turek O, Friedland-Little JM, Zhang K, Moskowitz IP. Tbx5-Hedgehog Molecular Networks Are Essential in the Second Heart Field for Atrial Septation. *Dev Cell*. 2012;23:280–291.

32. Brewer A, Nemer G, Gove C, Rawlins F, Nemer M, Patient R, Pizzey J. Widespread expression of an extended peptide sequence of GATA-6 during murine embryogenesis and non-equivalence of RNA and protein expression domains. *Mech Dev*. 2002;119:S121–S129.

33. Gago-Díaz M, Brion M, Gallego P, Calvo F, Robledo-Carmona J, Saura D, Sánchez V, Bermejo J, Sevilla T, Newton-Cheh C, Carracedo Á, Muehlschlegel JD, García-

Dorado D, Body SC, Evangelista A. The genetic component of bicuspid aortic valve and aortic dilation. An exome-wide association study. *J Mol Cell Cardiol*. 2017;102:3–9.

34. Kent KC, Crenshaw ML, Goh DLM, Dietz HC. Genotype-phenotype correlation in patients with bicuspid aortic valve and aneurysm. *J Thorac Cardiovasc Surg*. 2013;146:158–165.e1.

35. Lin X, Huo Z, Liu X, Zhang Y, Li L, Zhao H, Yan B, Liu Y, Yang Y, Chen Y-H. A novel GATA6 mutation in patients with tetralogy of Fallot or atrial septal defect. *J Hum Genet*. 2010;55:662–667.

36. Bui PH, Dorrani N, Wong D, Perens G, Dipple KM, Quintero-Rivera F. First report of a de novo 18q11.2 microdeletion including GATA6 associated with complex congenital heart disease and renal abnormalities. *Am J Med Genet A*. 2013;161A:1773–1778.

37. Lepore JJ, Mericko PA, Cheng L, Lu MM, Morrisey EE, Parmacek MS. GATA-6 regulates semaphorin 3C and is required in cardiac neural crest for cardiovascular morphogenesis. *J Clin Invest*. 2006;116:929–939.

38. van Berlo JH, Elrod JW, van den Hoogenhof MMG, York AJ, Aronow BJ, Duncan SA, Molkentin JD. The transcription factor GATA-6 regulates pathological cardiac hypertrophy. *Circ Res*. 2010;107:1032–1040.

39. Shen F, Li J, Cai W, Zhu G, Gu W, Jia L, Xu B. GATA6 predicts prognosis and hepatic metastasis of colorectal cancer. *Oncol Rep*. 2013;30:1355–1361.

40. Cheng K-S, Liao Y-C, Chen M-Y, Kuan T-C, Hong Y-H, Ko L, Hsieh W-Y, Wu C-L, Chen M-R, Lin C-S. Circulating matrix metalloproteinase-2 and -9 enzyme activities in the children with ventricular septal defect. *Int J Biol Sci*. 2013;9:557–563.

41. Clark TG, Conway SJ, Scott IC, Labosky PA, Winnier G, Bundy J, Hogan BL, Greenspan DS. The mammalian Tolloid-like 1 gene, Tll1, is necessary for normal septation and positioning of the heart. *Dev Camb Engl*. 1999;126:2631–2642.

42. Mo F-E, Lau LF. The matricellular protein CCN1 is essential for cardiac development. *Circ Res*. 2006;99:961–969.

43. Monsonego-Ornan E, Kosonovsky J, Bar A, Roth L, Fraggi-Rankis V, Simsa S, Kohl A, Sela-Donenfeld D. Matrix metalloproteinase 9/gelatinase B is required for neural crest cell migration. *Dev Biol*. 2012;364:162–177.

44. Dietz HC, Cutting GR, Pyeritz RE, Maslen CL, Sakai LY, Corson GM, Puffenberger EG, Hamosh A, Nanthakumar EJ, Curristin SM. Marfan syndrome caused by a recurrent de novo missense mutation in the fibrillin gene. *Nature*. 1991;352:337–339.

45. Lee TC, Zhao YD, Courtman DW, Stewart DJ. Abnormal Aortic Valve Development in Mice Lacking Endothelial Nitric Oxide Synthase. *Circulation*. 2000;101:2345–2348.

46. Aicher D, Kunihara T, Issa OA, Brittner B, Gräber S, Schäfers H-J. Valve Configuration Determines Long-Term Results After Repair of the Bicuspid Aortic ValveClinical Perspective. *Circulation*. 2011;123:178–185.

Figure 2.1

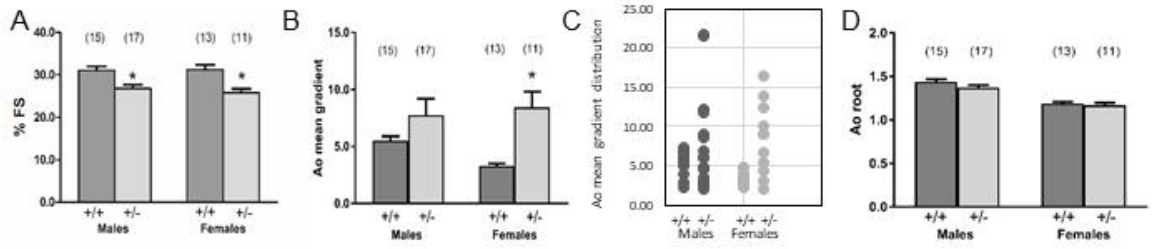

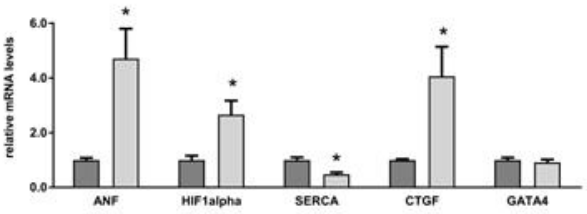

F BAV incidence in *Gata6*$^{+/-}$ mice

	Genotype	Total mice	Mice with BAV	Incidence (%)	p-value
Male	*Gata6+/+*	40	0	0	p<0.0001
	Gata6+/-	57	32	56	
Female	*Gata6+/+*	27	0	0	p=0.0043
	Gata6+/-	26	7	27	

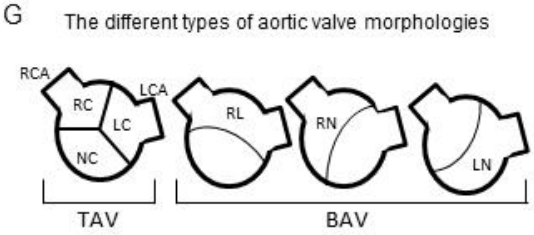

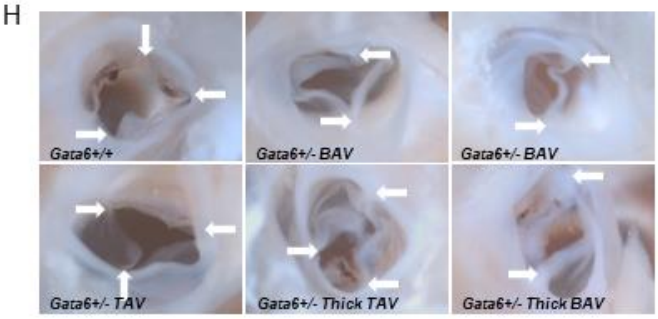

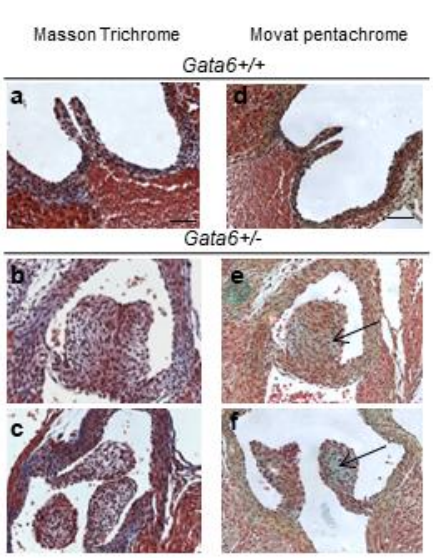

Figure 2.1: Cardiac dysfunction in *Gata6*$^{+/-}$ mice. Echocardiography analysis of *Gata6*$^{+/+}$ and *Gata6*$^{+/–}$ mice at 150-220 days of age (*n* = 15–17 per male group and n=11-13 per female group) showing **A)** decreased Fractional shortening (FS) in *Gata6*$^{+/-}$ groups, **B and C)** increased Aortic mean gradient (AoMG), **D)** no changes in Aortic root area when compared to control littermates. Two groups are shown in **A-D**: group1: *Gata6*$^{+/+}$, group 2: *Gata6*$^{+/-}$. **B)** t-test shows significant difference between female *Gata6*$^{+/+}$ and *Gata6*$^{+/-}$ ($p<0.05$). **C)** The scattered plot shows the distribution of aortic mean gradient in both groups, with normal (2-7) and above normal (>7) aortic mean gradient shown in group 2. Fisher test was performed to assess the prevalence of elevated Ao gradient: Males: *Gata6*$^{+/-}$ 6 out of 17 ($p=0.01918$) and Females: *Gata6*$^{+/-}$ 5 out of 11 ($p=0.01087$). **(E)** Enhanced expression of stress and remodeling markers in *Gata6*$^{+/–}$ ventricles as revealed by qRT-PCR of same mice (*n* = 5–8 per group) (corrected to RPS16). **(F)** BAV incidence in *Gata6*$^{+/-}$ mice. **(G)** The different types of aortic valve morphologies. TAV: Tricuspid Aortic Valve. BAV: Bicuspid Aortic Valve. RL: Right-left. RN: Right-noncoronary. LN: Left-noncoronary. LCA: left coronary artery. RCA: right coronary artery. **(H)** Anatomical analysis of *Gata6*$^{+/–}$ mice revealing the presence of TAV and BAV with multiple presentations (thick and thin valves). **(I)** Trichrome staining of P0 valves from frontal heart sections showing thick aortic valves in *Gata6*$^{+/-}$ when compared to *Gata6*$^{+/+}$ littermates. Movat pentachrome staining showing abnormal ECM in P0 *Gata6*$^{+/-}$ Ao valves marked by increased blue staining within the leaflets of the Ao valves. Scale bar: 400μm. Values are mean + SEM .*$P < 0.05$.

Figure 2.2

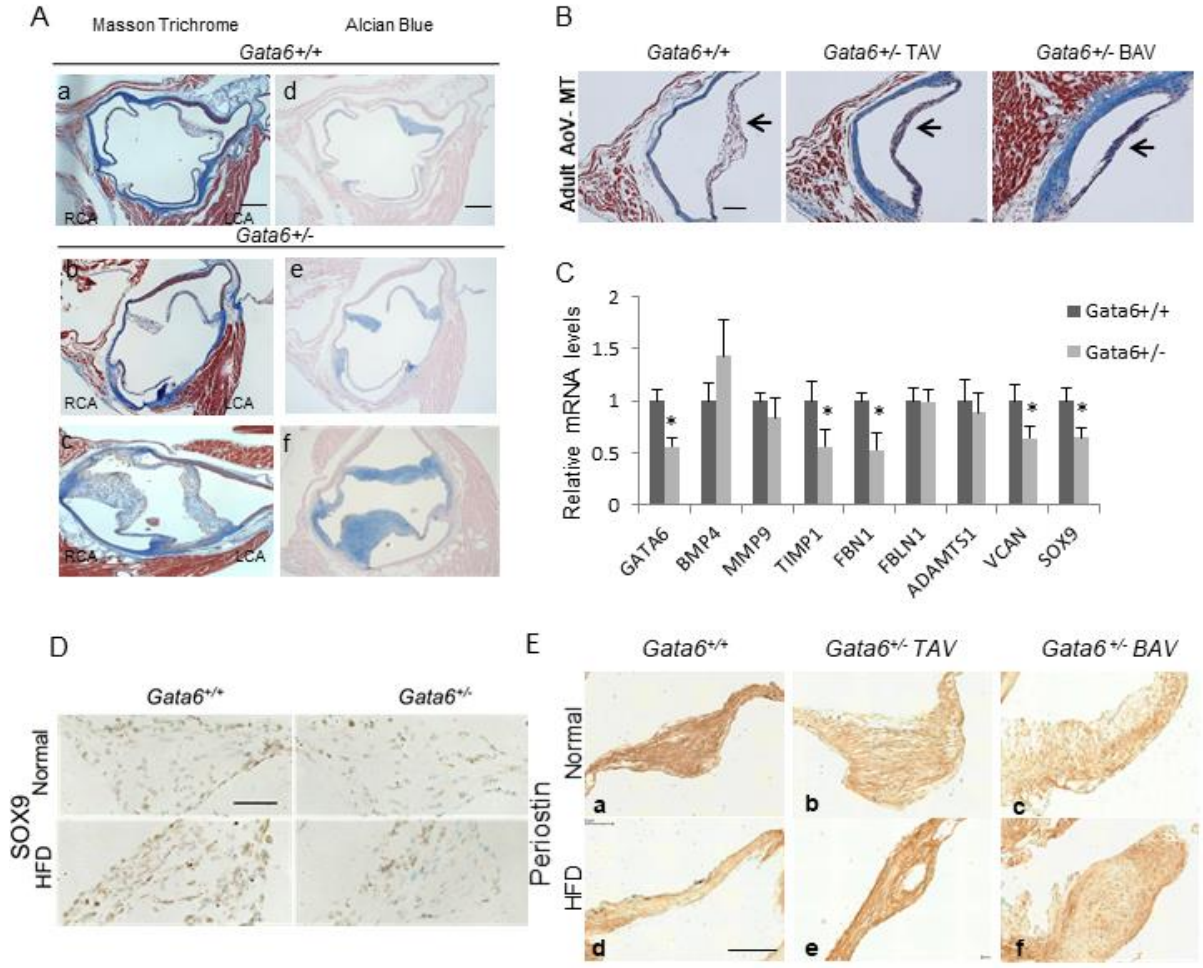
A
Masson Trichrome
Alcian Blue
Gata6+/+
Gata6+/-
RCA
LCA
B
Gata6+/+
Gata6+/- TAV
Gata6+/- BAV
Adult AoV- MT
C
Relative mRNA levels
Gata6+/+
Gata6+/-
GATA6
BMP4
MMP9
TIMP1
FBN1
FBLN1
ADAMTS1
VCAN
SOX9
D
Gata6+/+
Gata6+/-
SOX9
Normal
HFD
E
Gata6+/+
Gata6+/- TAV
Gata6+/- BAV
Periostin
Normal
HFD

Figure 2.2: Analysis of valve structure and gene expression (A) Masson Trichrome staining of transverse sections of adult aortic valve showing the presence of 2 instead of 3 aortic leaflets in *Gata6*$^{+/-}$ mice along with the presence of the RL-type BAV (left panel). Alcian blue staining of adult aortic valves transverse sections showing abnormal glycosaminoglycan composition (increased blue staining) within the aortic leaflets of *Gata6*$^{+/-}$ when compared to control mice (right panel). Scale bars: 200 μm. **(B)** Masson Trichrome stain showing total collagen (blue) content in bicuspid and tricuspid leaflets of *Gata6*$^{+/-}$ compared to their wildtype littermates. Scale bar: 100 μm. **(C)** qRT-PCR on RNA extracted from dissected adult aortic valves showing altered expression of important ECM components. (corrected to RPS16). Values are mean + SEM .*$P < 0.05$. **(D and E)** Sox9 and Periostin staining of adult Ao valves from mice on normal diet and from mice that were fed with a high fat diet for 4 months. HFD: high fat diet. (n=4-7 in each group) Scale bar: **(D)** 50μm, **(E)** 100μm.

Figure 2.3

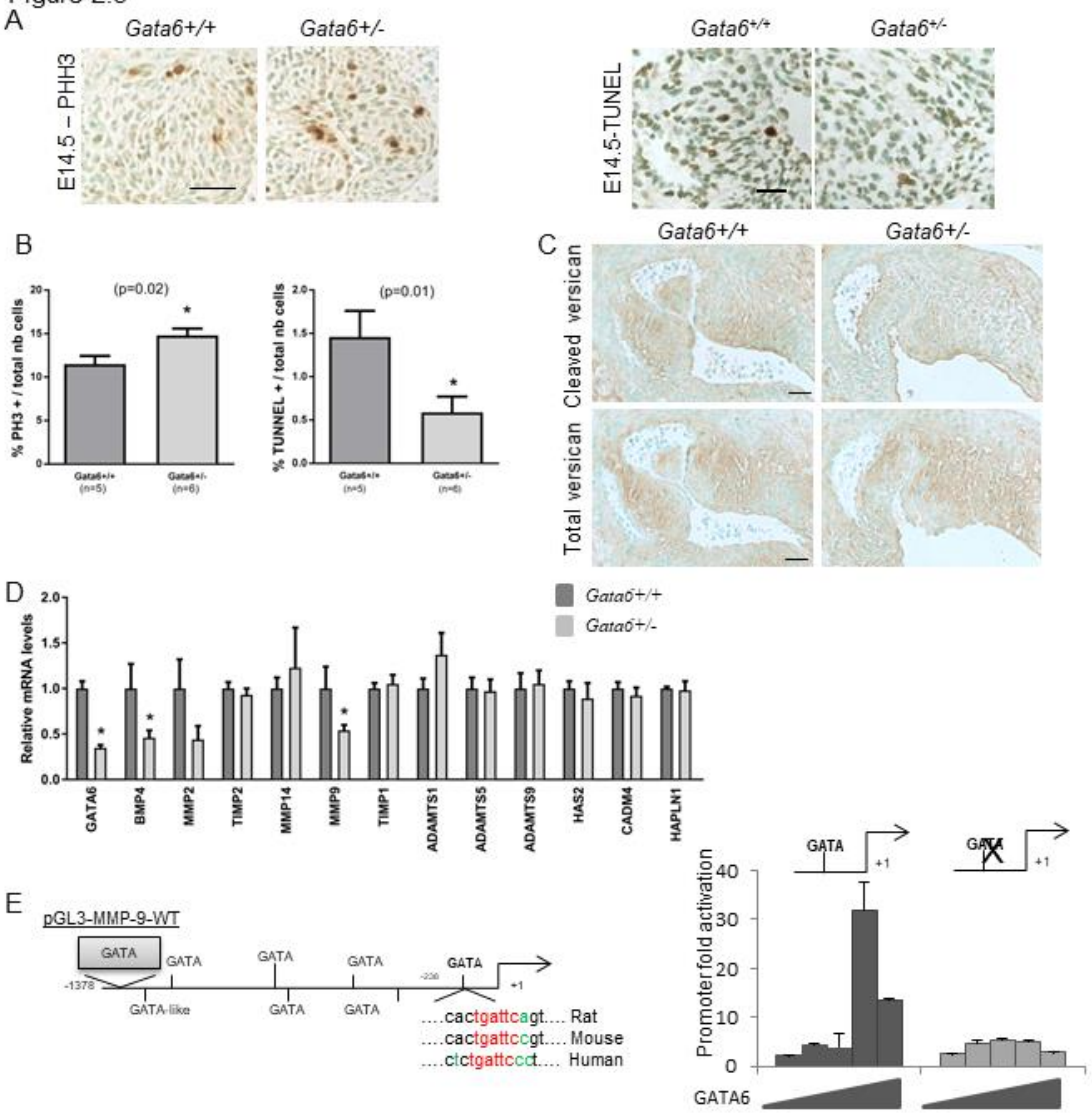
A
Gata6+/+
Gata6+/-
E14.5 – PHH3
Gata6+/+
Gata6+/-
E14.5-TUNEL
B
(p=0.02)
% PH3 + / total nb cells
(p=0.01)
% TUNNEL + / total nb cells
C
Gata6+/+
Gata6+/-
Cleaved versican
Total versican
D
Gata6+/+
Gata6+/-
Relative mRNA levels
GATA6
BMP4
MMP2
TIMP2
MMP14
MMP9
TIMP1
ADAMTS1
ADAMTS5
ADAMTS9
HAS2
CADM4
HAPLN1
E
pGL3-MMP-9-WT
GATA
GATA-like
....cactgattcagt.... Rat
....cactgattccgt.... Mouse
....ctctgattccct.... Human
Promoter fold activation
GATA6

Figure 2.3: Dysregulation of matrix remodeling in *Gata6*$^{+/-}$ mice. (A) Representative images of Phosphohistone H3 and TUNEL positive sections of aortic valve from *Gata6*$^{+/-}$ E14.5 embryos (transverse sections). Scale bar: 40μm. **(B)** Quantification graphs of Phosphohistone H3 and TUNEL positive cells showing the increased cell proliferation and decreased cell death in aortic valves of *Gata6*$^{+/-}$ mice. **(C)** Staining for total and cleaved versican reveals decreased presence of cleaved versican (Neo-VCAN) within the ECM of Ao valves in *Gata6*$^{+/-}$ BAV mice when compared to control group. (n=5-6 in each group). Scale bar: 40μm. **(D)** qRT-PCR on RNA extracted from E11.5 hearts showing altered expression of important septation regulators and ECM components; note the significant decrease in the expression of matrix metalloprotease 9 (MMP9), BMP4 and GATA6 (corrected to RPS16, n=5-8 per group). **(E)** Schematic representation of GATA sites on the MMP9 promoter. pGL3-MMP9-One GATA site is a 5' deletion leaving only one GATA site and p-GL3-MMP9-No GATA site promoter has a mutation in this site. Increasing amounts of GATA6 expression vector are transiently cotransfected with the indicated luciferase reporters in NIH3T3 cells (25, 50, 100, 250 and 500 ng of expression vector). Relative luciferase activities are represented as fold changes. The data is a representative of 3 independent experiments done in duplicates. Values are $*P < 0.05$.

Figure 2.4

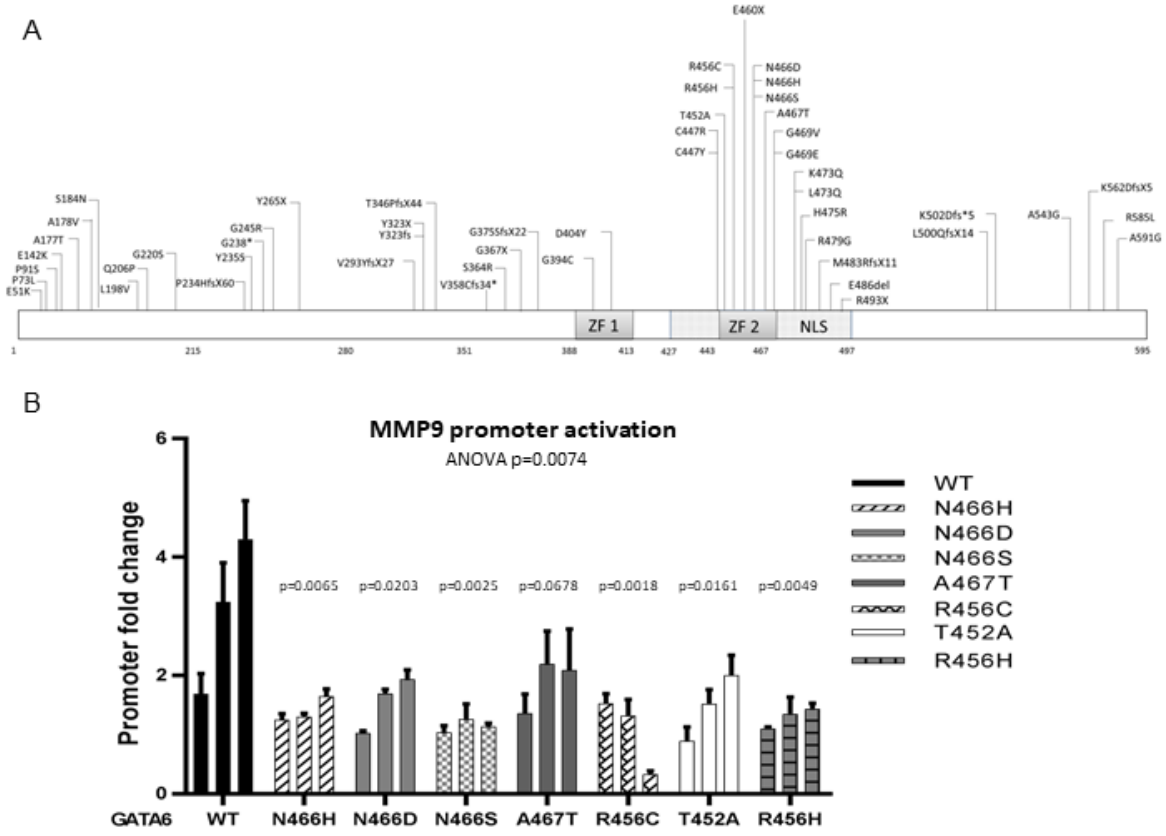
A
E460X
R456C
N466D
N466H
R456H
N466S
T452A
A467T
C447R
G469V
C447Y
G469E
K473Q
L473Q
H475R
R479G
M483RfsX11
E486del
R493X
S184N
A178V
A177T
E142K
P91S
P73L
E51K
G220S
Q206P
L198V
P234HfsX60
Y265X
G245R
G238*
Y235S
T346PfsX44
Y323X
Y323fs
V293YfsX27
G375SfsX22
G367X
S364R
V358Cfs34*
D404Y
G394C
K502Dfs*5
L500QfsX14
A543G
K562DfsX5
R585L
A591G
ZF 1
ZF 2
NLS
1
215
280
351
388
413
427
443
467
497
595
B
MMP9 promoter activation
ANOVA p=0.0074
Promoter fold change
6
4
2
0
p=0.0065
p=0.0203
p=0.0025
p=0.0678
p=0.0018
p=0.0161
p=0.0049
WT
N466H
N466D
N466S
A467T
R456C
T452A
R456H
GATA6
WT
N466H
N466D
N466S
A467T
R456C
T452A
R456H

Figure 2.4: Effect of *GATA6* human mutations on transcriptional activity (A) Schematic representation of reported human *GATA6* mutations. **(B)** Transcriptional activity of WT and mutant GATA6 proteins on full length MMP9 promoter. Transient cotransfection was carried out in NIH3T3 cells using 70, 125 and 500 ng of GATA6 expression vector. Relative luciferase activities are represented as fold changes vs empty vector control. The data are the mean ± SEM of 3 independent experiments done in duplicates. Note that all mutants had significantly lower activity vs WT GATA6. Statistical analysis was done by one-way ANOVA followed by Dunnett's multiple comparison post-hoc analysis.

Figure 2.5

A

Mouse Genotype	Total mice	Mice with BAV	BAV incidence (%)	p-value
Gata6+/+	49	0	0	
Gata6+/-	83	39	47	p<0.0001
Cre-G6Wt/Fl	27	0	0	
Tie2cre+G6Wt/Fl	10	0	0	
Wnt1cre+G6Wt/Fl	13	0	0	
Isl1cre+G6Wt/Fl	9	4	44	p=0.0021

B

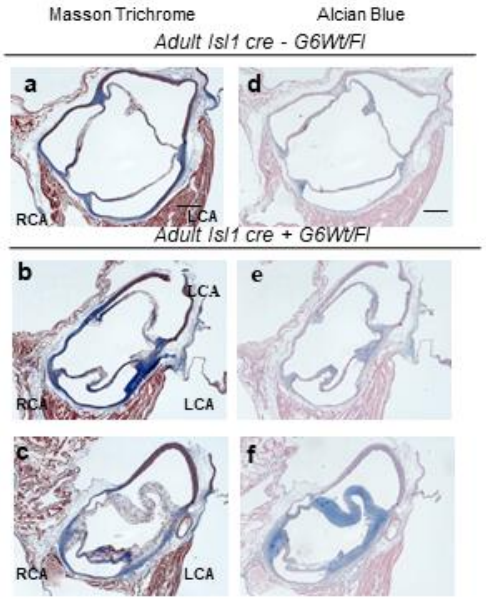

C

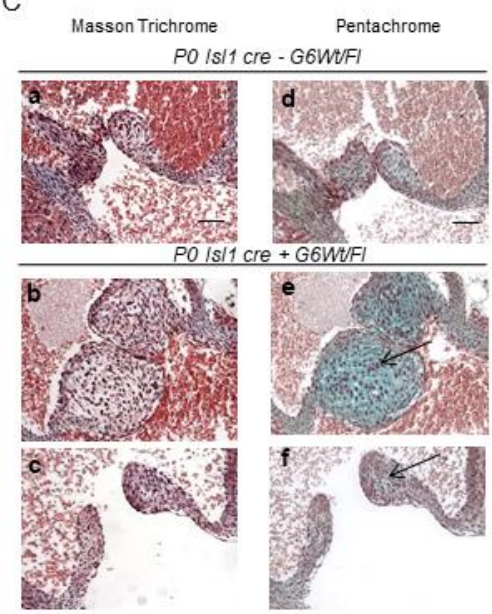

Figure 2.5: *Isl1cre*$^{+}$ *G6*$^{Wt/Fl}$ mice recapitulate the phenotype of *Gata6*$^{+/-}$ (A) Percentage of BAV in the different mouse lines. The incidence in *Gata6*$^{+/-}$ was compared to *Gata6*$^{+/+}$ littermates; *Isl1cre+Gata6*$^{Wt/Fl}$ was compared to *cre-Gata6*$^{Wt/Fl}$. **(B)** Trichrome and Alcian Blue staining of transverse sections of adult aortic valve from *Isl1cre-Gata6*$^{Wt/Fl}$ *and Isl1cre+Gata6*$^{Wt/Fl}$ showing the presence of RL type BAV and increased deposition of glycosaminoglycan within the leaflets of the aortic valve, recapitulating the phenotype observed in *Gata6*$^{+/–}$ mice. Scale bar: 200μm. **(C)** Trichrome staining of P0 valves from frontal heart sections showing thick aortic valves in *Isl1cre+Gata6*$^{Wt/Fl}$ when compared to *Isl1cre-Gata6*$^{Wt/Fl}$ littermates. Movat pentachrome staining showing abnormal ECM in P0 *Isl1cre+Gata6*$^{Wt/Fl}$ Ao valves marked by increased blue staining within the leaflets of the Ao valves (n=6-9 per group). Scale bar: 400μm.

Figure 2.6

A

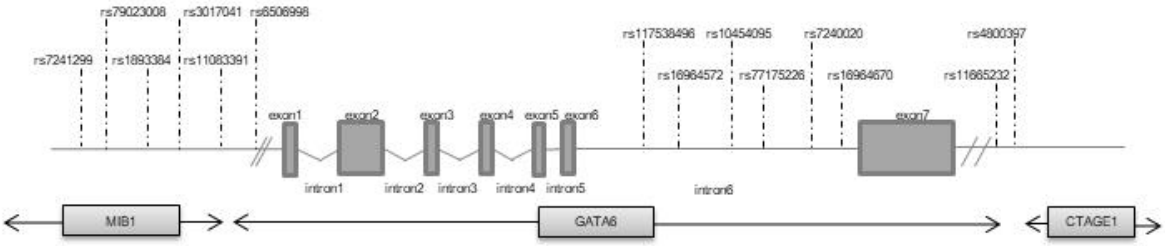

B

Nb	SNP ID	Odds Ratio (OR)	P-value
1	*rs7241299*	1.478	0.00283
2	*rs79023008*	1.492	0.00236
3	*rs1893384*	1.314	0.00095
4	*rs3017041*	1.271	0.00366
5	*rs11083391*	1.457	0.00401
6	*rs6506998*	0.720	0.00683
7	*rs117538496*	0.786	0.273
8	rs16964572	0.563	0.142
9	rs10454095	0.967	0.685
10	rs67205814	1.062	0.598
11	rs7240020	1.025	0.762
12	rs16964670	1.036	0.759
13	rs11665232	1.256	0.00323
14	rs4800397	0.793	0.00404

C

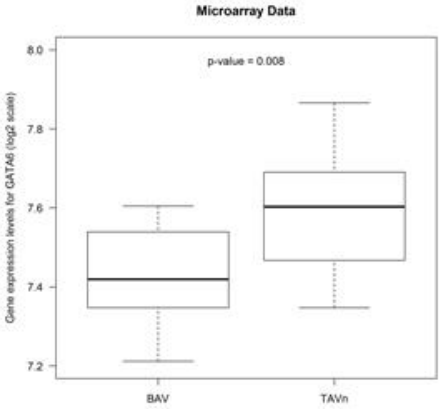

D

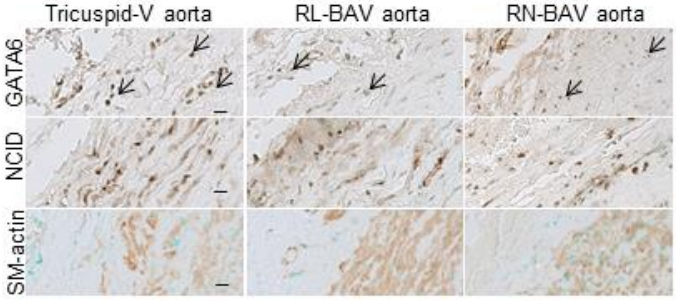

E

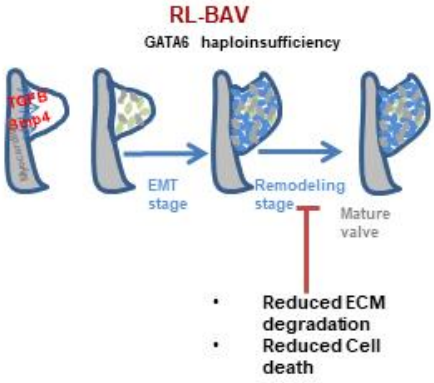

Figure 2.6: GATA6 expression and variants in human BAV. (A and B) Genotyping of 452 BAV cases from the Framingham GWAS study (with 1849 controls) revealed several SNPs in and around *GATA6* (chromosome 18). Schematic representation of the identified SNPs on *GATA6* is shown. **(C)** Microarray analysis of human aortic valve samples. Boxplot of gene expression levels in human aortic valves for GATA6 according to the two groups of aortic valves (calcified BAV and non-calcified TAV controls). The y-axis presents the mRNA expression levels for GATA6 on a log 2 scale. Gene expression was obtained from 12 aortic valves in each group and measured with the HumanHT-12 v4 Expression BeadChip. Values are mean +/- SEM.*$P < 0.05$. **(D)** Immunohistochemical staining of GATA6, NCID, and Smooth muscle actin on samples of dilated aortas from patients with normal TAV (nTAV), RL- and RN- type BAVs showing markedly lower expression of GATA6 in tissues from RL-BAV patients. The data are representative of n=6 for each group. Scale bar: 20 μm. **(E)** Representative summary model of BAV etiology in *Gata6*$^{+/-}$ mice.

Supplementary Figure 2.1

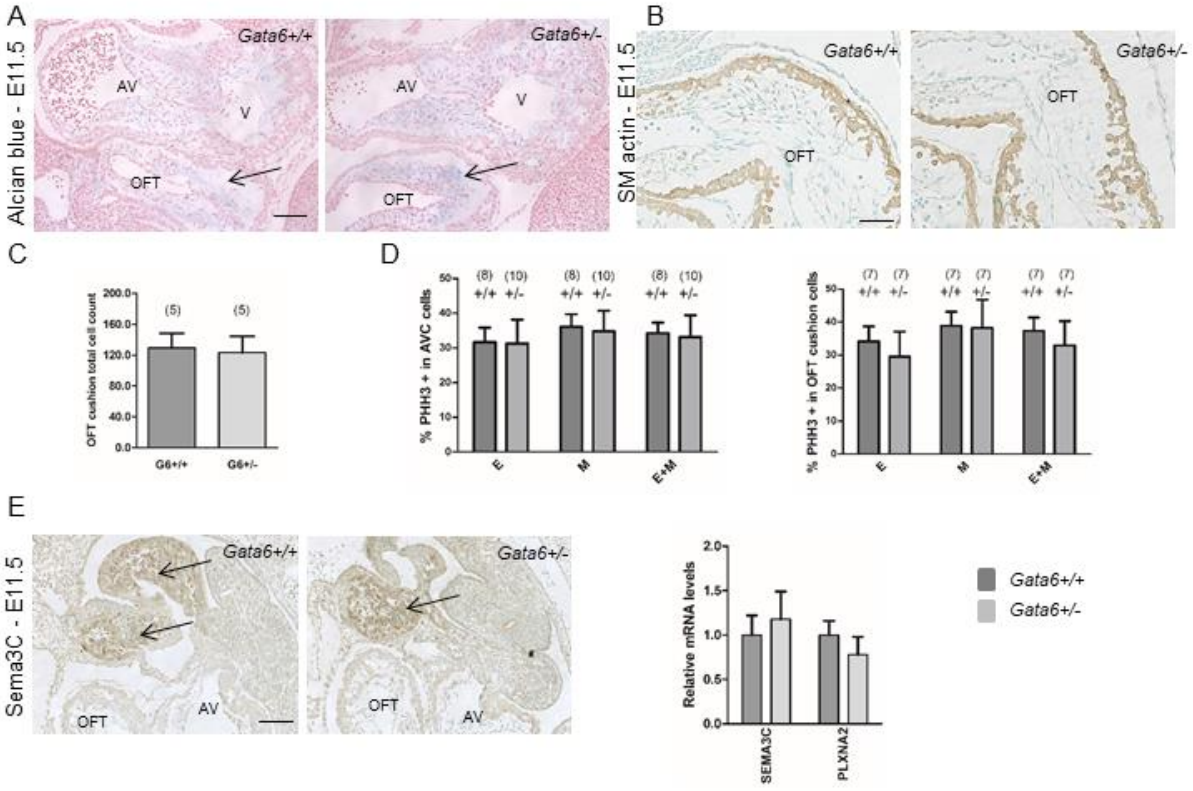

Supplementary Figure 2.1: Normal EMT in E11-11.5 *Gata6*$^{+/-}$ OFT. (A and C) Alcian blue staining was used to visualize acid glycosaminoglycans, such as hyularonic acid, within the outflow tract (OFT) cushion. Note the more intense staining in *Gata6*$^{+/-}$ tissues. Sagittal sections of E11-11.5 embryos (n=7) showing no change in total cell count between *Gata6*$^{+/-}$ and *Gata6*$^{+/+}$. OFT: outflow tract cushion. AV: atrioventricular cushion. V: ventricle. Scale bar: A: 100μm **(B)** Smooth muscle alpha actin staining. Scale bar: 100μm. **(D)** Quantification of Phosphohistone H3 positive cells within the OFT and AV cushions at E11-11.5. E: endothelial. M: mesenchymal. **(E)** No alteration in semaphorine 3C (Sema3C) immunostaining was observed in sagittal heart sections between the groups and no changes in transcript levels as assessed by qRT-PCR (normalized to RPS16, n=5-8 per group). Scale bar: 100μm.Values are mean + SEM.*$P < 0.05$.

Supplementary Figure 2.2: Details of the workflow of human GWAS analysis

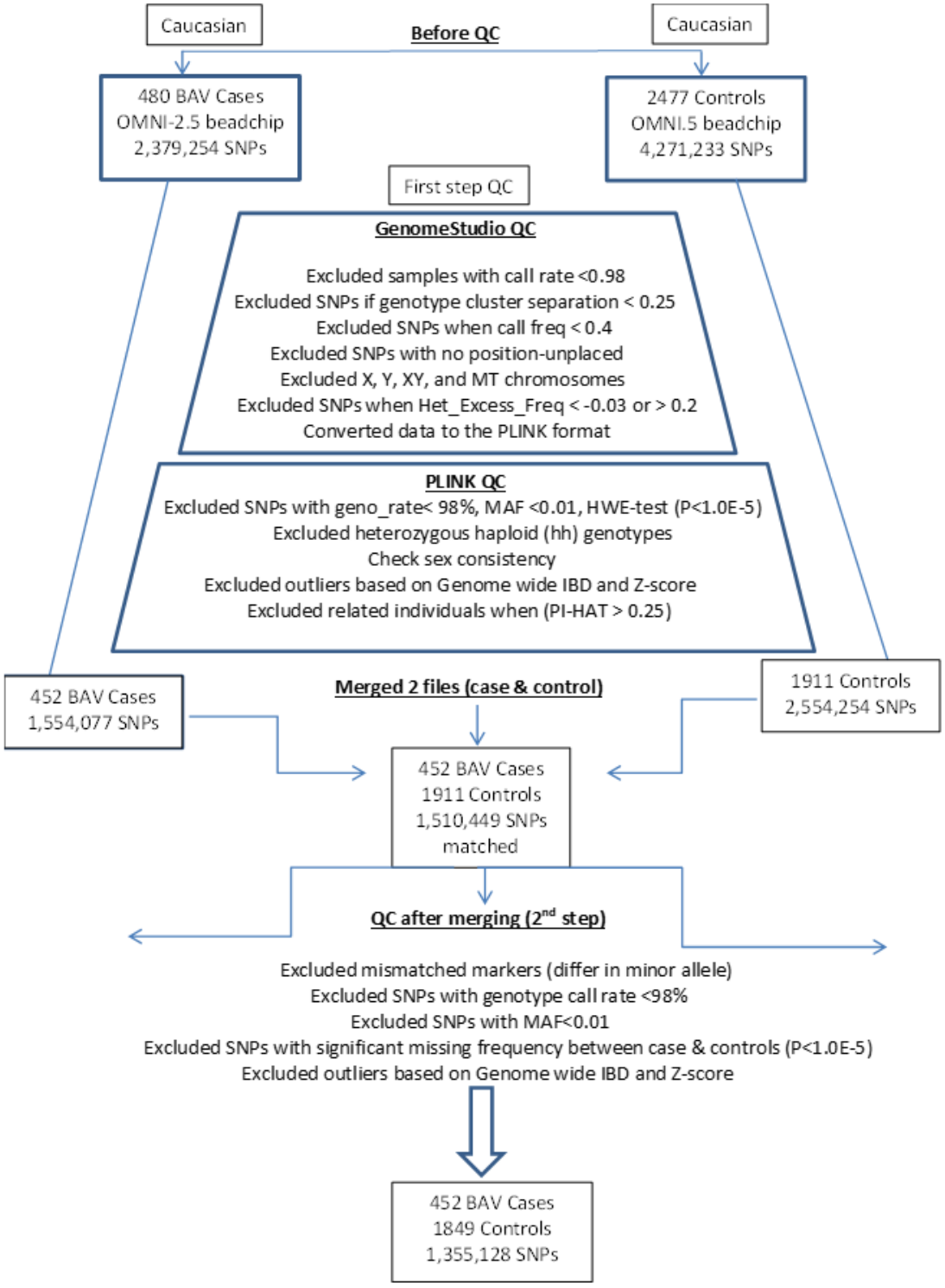

Supplementary Figure 2.3

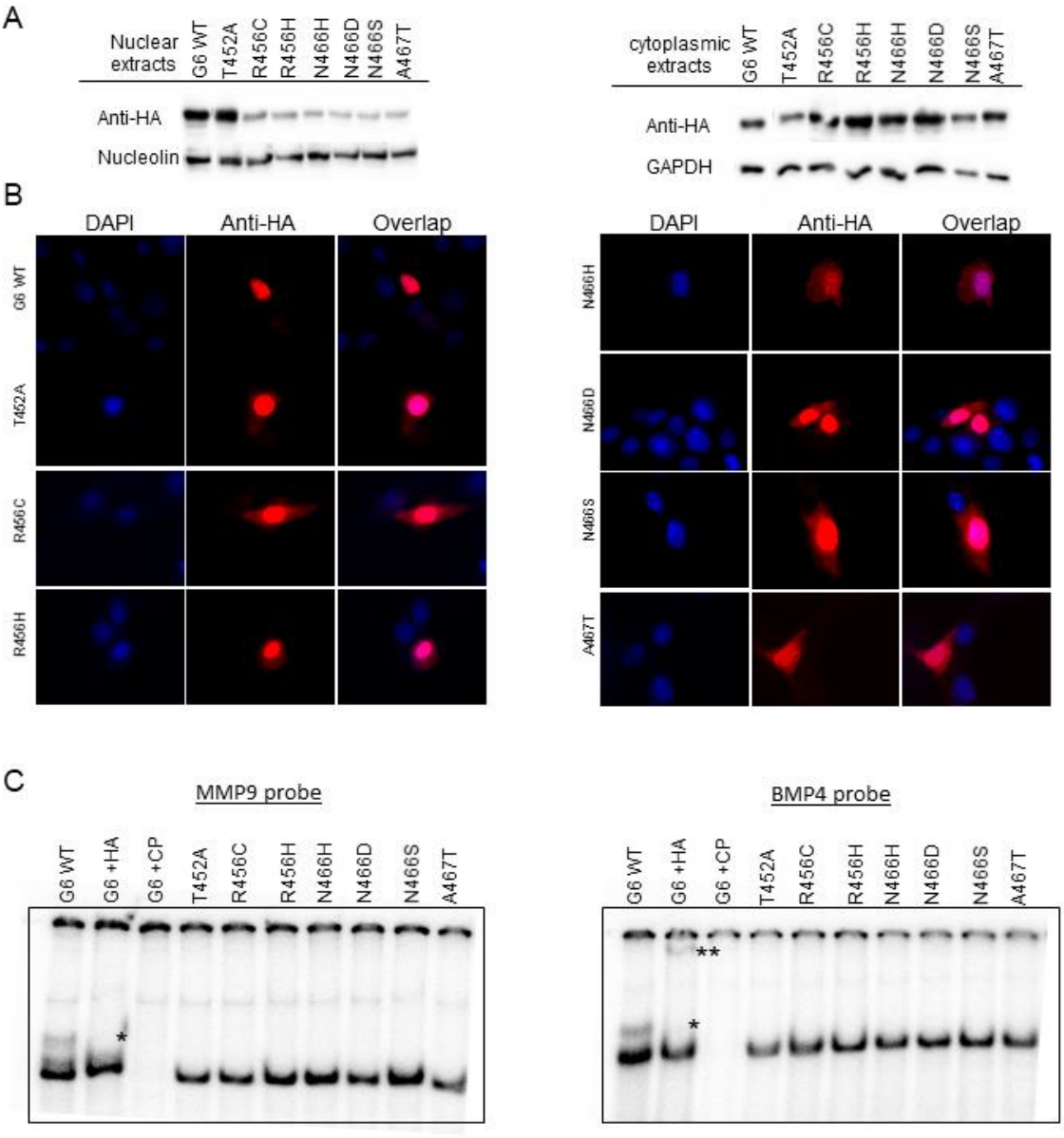

Supplementary Figure 2.3: Biochemical characterization of GATA6 human mutations (A). Western blot analysis of transfected, HA-tagged WT and mutant GATA6 using the HA-antibody. The left panel shows the expression of recombinant HA-GATA6 WT and mutants in nuclear extracts of AD293 cells. The right panel shows the expression in cytoplasmic extracts of the same cells. **(B)** Immunofluorescence localization of GATA6 WT and mutants expressed in AD293 cells using the HA-antibody. Note the complete nuclear localization of GATA6 WT, the mostly cytoplasmic localization of N466H and the nuclear and cytoplasmic distribution of the remaining mutants. **(C)** Electrophoretic mobility shift assays performed using nuclear extracts from AD293 cells overexpression WT and mutant GATA6. The exogenous binding is indicated by an asterisk (*). Supershift/blocking was done with anti-HA antibody and is indicated by a double asterisk (**).

Supplementary Table 2.1: Cardiac Phenotypes associated with the examined GATA6 human mutations.

Mutation	Phenotype	Pubmed ID
T452A	ASD	22158542
R456C	Congenital diaphragmatic hernia with Tetralogy of Fallot (TOF) TOF TA, perimembranous VSD	24385578 22158542 22158542
R456H	PDA, VSD, hypoplastic left pulmonary artery	22158542
N466H	PTA	19666519
N466D	PDA	22158542
N466S	ASD, PS, PDA	23639568
A467T	ASD, PS	22158542

Supplementary Table 2.2a: Demographic population and clinical variables

Variable	Case (n=452)	Control (n=1834)
Male gender – n (%)	336 (74%)	836 (46%)
Age – mean ± SD	54 ± 11	60 ± 12
BMI (kg/m²) - mean ± SD	28 ± 5	25 ± 4
Diabetes	88 (19%)	16 (0.87%)
Smoking	10 (2%)	1402 (76%)
Hypertension	281 (62%)	456 (25%)
Hyperlipidemia	266 (58%)	993 (54%)
Aortic Stenosis	190 (42%)	0
Thoracic Aortic Aneurysm	180 (40%)	0
Coronary artery disease (CAD)	81 (18%)	0
Surgery (valve replacement)	334 (74%)	0

Supplementary Table 2.2b: Human GWAS analysis: Base pairs (BP) and location of each of the reported SNPs

CHR	SNP-rs	BP	A1	A2	MAF	OR	L95	U95	P
18	rs7241299	19,292,517	G	A	0.087	1.478	1.144	1.909	0.00283
18	rs79023008	19,323,399	C	T	0.087	1.492	1.153	1.931	0.00236
18	rs1893384	19,351,344	A	C	0.305	1.314	1.118	1.545	0.00095
18	rs3017041	19,355,507	G	A	0.309	1.271	1.081	1.495	0.00366
18	rs11083391	19,447,927	G	A	0.089	1.457	1.128	1.884	0.00401
18	rs6506998	19,710,668	C	A	0.136	0.720	0.568	0.914	0.00683
18	rs117538496	19,763,287	C	T	0.036	0.786	0.512	1.209	0.273
18	rs16964572	19,765,739	C	T	0.015	0.563	0.261	1.212	0.142
18	rs10454095	19,777,440	T	C	0.356	0.967	0.824	1.136	0.685
18	rs67205814	19,778,036	T	C	0.127	1.062	0.849	1.328	0.598
18	rs7240020	19,778,928	C	T	0.378	1.025	0.874	1.203	0.762
18	rs16964670	19,780,216	A	G	0.135	1.036	0.826	1.301	0.759
18	rs11665232	19,914,353	G	T	0.436	1.256	1.079	1.462	0.00323
18	rs4800397	19,947,663	C	A	0.408	0.793	0.677	0.929	0.00404

* Base pairs (BP) and location of each SNP is reported based on hg19 and Chrch37 assembly

Supplementary Table 2.2b: Measured SNPs in the *GATA6* coding region, and eight SNPs within 500kbp of the coding region that had a P value <0.005, after covariate adjustment for gender and eight PCA covariates. Coordinates are for GRCh37/hg19. The GATA6 genic region is chr18:19,749,404-19,782,491.

Supplementary Table 2.3: Clinical characteristics of patients used in the microarray study according to the two groups of aortic valve in the microarray study

Characteristics	Bicuspid (n = 12)	Tricuspid (n = 12)	P value*
Age (years)	62.3 ± 6.9	58.5 ± 5.5	0.146
Gender (% male)	100	100	NA
Weight (kg)	81.7 ± 18.4	84.8 ± 13.8	0.637
Body surface area (m^2)	1.9 ± 0.2	2.0 ± 0.2	0.334
Waist circumference (cm)	98.7 ± 12.5 [2]	103.3 ± 11.4 [9]	0.578
Body mass index (kg/m^2)	28.2 ± 5.5	27.7 ± 3.7	0.781
Aortic valve area (cm^2)	1.4 ± 0.32	NA	NA
Indexed aortic valve area (cm^2/m^2)	0.7 ± 0.2	NA	NA
Mean gradient (mm Hg)	14.4 ± 5.4	NA	NA
History of CAD	2 [6]	2 [6]	1
Hypertension	6	3	0.400
Dyslipidemia	9	8	1

*T-test and Fisher's exact test were used as appropriate.

Supplementary Table 2.3: Clinical characteristics of the patients according to the two groups of aortic valves in the microarray study. The number of missing values is shown in squared brackets. CAD: coronary artery disease. Continuous variables are expressed as mean ± SD. Dichotomous variables are expressed as percentage (n). CAD was defined as patients presenting a history of coronary artery bypass grafting, myocardial infarction, documented myocardial ischemia or coronary artery stenosis (>50%) on coronary angiography. The mean transvalvular gradient was calculated using the modified Bernoulli equation and the aortic valve area with the continuity equation, both based on Doppler transthoracic echocardiographic measurements. Hypertension was defined as blood pressure above 140/90 mmHg or the use of anti-hypertensive medication. Hypercholesterolemia was defined as total plasma cholesterol levels > 6.2 mmol/l or the use of cholesterol-lowering medication.

Supplementary Table 2.4: Demographic information of patients from whom aortic tissue samples were derived

		Age	Sex	HTN	AI	Smoking	DM	Dysl.	CAD	Stroke	FHx of AoD	FHx of AoVD	AoD	AoVD	AS
Tricuspid-V patients	Patient 1	59	M	0	1	0	0	0	0	0	0	1	1	1	0
	Patient 2	82	F	1	0	1	0	1	1	0	0	0	1	1	1
	Patient 3	76	F	1	1	1	0	0	1	1	0	0	1	1	0
	Patient 4	64	M	0	1	0	0	0	0	0	0	0	1	1	0
	Patient 5	83	F	1	1	0	1	1	0	0	0	0	1	1	0
	Patient 6	71	M	1	1	1	0	1	0	0	0	0	1	1	0
RL-BAV patients	Patient 7	65	M	1	1	0	0	1	0	0	0	0	1	1	0
	Patient 8	58	M	1	1	1	0	1	0	0	0	0	1	1	0
	Patient 9	53	M	1	1	1	0	1	1	0	0	0	1	1	1
	Patient 10	35	M	1	1	1	0	0	0	0	0	0	1	1	0
	Patient 11	57	M	0	1	0	0	1	0	0	0	0	1	1	0
	Patient 12	55	M	0	-	0	0	0	0	0	0	0	1	0	
RN-BAV patients	Patient 13	72	M	0	0	1	1	1	1	0	0	0	1	1	1
	Patient 14	66	M	0	1	0	0	0	0	0	0	0	1	1	1
	Patient 15	50	M	1	1	0	0	1	0	0	0	0	1	1	0
	Patient 16	72	M	0	0	1	0	1	1	0	0	0	1	1	1
	Patient 17	34	M	0	0	0	0	0	0	0	0	0	1	1	1
	Patient 18	62	M	1	1	1	1	1	1	0	0	0	1	1	0

Supplementary Table 2.4: Demographic information of patients from whom aortic tissues were derived. HTN: hypertension; AI: aortic insufficiency; DM: Diabetes Mellitus; Dysl.: Dyslipidemia; CAD: Coronary artery disease; FHx of AoD: Family history of aortic disease; FHx of AoVD: family history of aortic valve disease; AoD: aortic disease; AoVD: aortic valves disease; AS: aortic stenosis.

3. Chapter II: GATA6 regulates structure and function of the cardiac Sinoatrial Node

Lara Gharibeh, Abir Yamak, Aizhu Lu, Simon Thibault, Mathieu Joyal, Hiba Komati, Wenbin Liang, Céline Fiset, Mona Nemer*

1- From the Molecular Genetics and Cardiac Regeneration Laboratory, Department of Biochemistry, Microbiology, and Immunology, University of Ottawa, Ottawa, Ontario, Canada (L.G., A.Y., M.J., H.K., M.N.).
2- From the Research Center, Montreal Heart Institute, Montreal, Quebec, Canada; Faculty of Pharmacy, Université de Montréal, Montreal, Quebec, Canada (S.T., C.F.)
3- From the Cardiovascular Electrophysiology Laboratory, University of Ottawa Heart Institute University of Ottawa, Ontario, Canada (A.L., W.L.)

*Corresponding author:
Dr. Mona Nemer
University of Ottawa
451 smyth road, Room 4522
Ottawa, Ontario K1H 8M5
Tel: 613 562 5800 ext.3995
Email: mona.nemer@uottawa.ca

3.1. Statement of the manuscript

The manuscript ***"GATA6 regulates structure and function of the cardiac Sinoatrial Node"*** is being finalized and will be submitted to *Circulation Cardiovascular genetics* journal.

3.2. Contribution statement

In this chapter, I performed and contributed to the analysis of most of the experiments except for: qRT-PCR analysis on dissected SAN/RA in Figure 3.1D was done by ST and CF. Immunohistochemistry in Figure 3.3 was done by AY. The 3D reconstruction in Figure 3.4B was performed by MJ. ECG analysis and on going ex-vivo experiment (not shown in manuscript) were done by AL and WL. LG, MN, HK and AY interpreted and analyzed results. LG and MN wrote the manuscript.

3.3. Acknowledgements

The authors are grateful to Megan Fortier, Janie Beauregard and and Nathalie Ethier for technical support, Hélène Touchette for secretarial help and members of the Nemer Lab for discussions and helpful suggestions. The authors thank Dr. Sharon Prince for sharing the TBX3-Luc reporter construct. The authors acknowledge the invaluable support of the uOttawa histology and animal physiology cores.

3.4. Funding sources

This work was funded by a Canadian Institute of Health Research (CIHR-IRSC:0077282) grant to MN and a Natural Sciences and Engineering Research Council of Canada (NSERC) grant (RGPIN-2017-05353) to CF. LG holds the M. E. Abbott Scholarship from the Bicuspid Aortic Foundation and a graduate excellence scholarship from the University of Ottawa.

3.5. Disclosure

None

3.6. Abstract

Background: Cardiac rhythm abnormalities are major causes of mortality and morbidity worldwide from fetal to adult life. They can be due to inherited mutations affecting regulators of the cardiac electrical impulse or can develop in response to electrolyte imbalance. The mechanisms leading to cardiac conduction system (CCS) pathophysiology remain incompletely understood. Human genetic studies as well as analysis of genetically engineered mice have contributed to the identification of some CCS regulators such as NKX2.5 and TBX5. Atrioventricular (AV) conduction defects have been shown to result from mutations in these genes. The GATA family of transcription factors has also been reported to play a role in the regulation of CCS genes such as gap junctions and ion channels. Human mutations in these factors are formed in individuals with Atrial Fibrillation (AF).

Methods and Results: we report that GATA6 is highly expressed in the sinoatrial node (SAN) and that *Gata6* haploinsufficiency (*Gata6*$^{+/-}$) in mice results in prolonged PR and QT intervals with some mice showing premature atrial contraction (PAC). *Gata6*$^{+/-}$ mice have hypoplastic SAN marked by reduction in HCN4+ and TBX3+ cells conduction cells. In vivo and in vitro assays revealed a role for GATA6 as a regulator of CCS genes including TBX3. Conditional deletion of *Gata6* from ISL1+ myocytes, TIE2+ endothelial or WNT1+ neural crest cells, interferes with proper SAN formation and normal cardiac electrophysiology.

Conclusions: Together, the data indicate that GATA6 is required in multiple cell types for proper SAN formation and that GATA6 is a regulator of the cardiac pacemaker.

Key words: GATA proteins - Sinoatrial node - cardiac conduction system – Atrial fibrillation

3.7. Introduction

The cardiac conduction system (CCS) consists of muscle cells and conducting fibers that insure the initiation of the impulse and its propagation throughout the heart. The CCS is composed of 1) the sinoatrial node (SAN, pacemaker of the heart) that generates the electrical impulse, and 2) the atrioventricular node (AVN), the His or atrioventricular bundle (AV bundle) and the Purkinje fibers that ensures the propagation of the signal to the ventricular myocytes[1]. Little is known regarding the cellular origins of the CCS components. It is thought that the SAN is mainly composed of cells which have a secondary heart field origin and derive from ISL1 (ISL LIM Homeobox 1) and TBX18 (T-box transcription factor (TF) 18)- expressing cells [2]. The AVN and His bundle on the other hand are thought to segregate from precursors of the working myocardium and are positive for TBX2 [3].

Abnormalities affecting the generation or propagation of the electrical signal can lead to fatal arrhythmias ─ irregular heart beat. Impaired impulse generation in the SAN leads for example to sick sinus syndrome (SSS) manifesting in sinus pause/arrest or bradycardia─ slow heart rate [4]. On the other hand, a partial or complete block of the signal conduction to the AVN or Purkenje fibers would result in atrioventricular block [4]. Atrial Fibrillation (AF), a condition involving a rapid and irregular cardiac rhythm, is the most common type of arrhythmias affecting 2.7 million Americans according to the report of the American Heart association [5]. Its frequency increases with aging and it occurs in isolation or in association with other complications such as dementia, stroke and heart failure [6,7]. Several factors have been known to potentially play a role in its initiation and maintenance such as alterations in atrial electrophysiology, calcium handling abnormalities, genetic factors, and contractile and structural remodeling involving fibrosis and connective tissue deposition, that increase with

aging. Elucidation of the genetic basis of AF revealed an important contribution of cardiac TFs. Mutations in the GATA family of TFs (*GATA4/5/6*), the Tbox factor *TBX5* and the homeodomain TF *NKX2.5* have been reported in many cases with familial form of AF. Six *GATA4* and seven *GATA5* mutations, all of which were associated with loss-of-function effects, were reported in patients with familial AF from cohorts of European and Chinese descents [8]. On the other hand, gain and loss of function mutations in *GATA6* have been reported in familial cases of AF from different descents [9–12].

A role for GATA6 in CCS was suggested by the finding that an enhancer region upstream of the *Gata6* promoter is specifically active in the atrioventricular (AV) conduction system [15]. GATA6 contribution to AV development and function is also supported by analysis of a mouse model with a myocardial-specific deletion of the carboxyl zinc finger domain of *Gata6* [15]. In this model, a truncated GATA6 protein containing the N-terminal activation domain and zinc finger is produced with the ability to interact with important cardiogenic cofactors including other GATA factors and regulators such as TBXs and NKX2.5. Therefore, the phenotype observed may reflect a direct role of GATA6 or may be the consequence of the truncated GATA6 protein interference with other CCS regulators.

To determine whether GATA6 is a CCS regulator, we analyzed mice haploinsufficient for *Gata6.* We found that loss of one *Gata6* allele leads to electrophysiological alterations and increased susceptibility to develop arrhythmias. Furthermore, hypocellularity and reduction in HCN4+/TBX3+ cells (conduction cells) marked the SAN of *Gata6*$^{+/-}$ mice. Cell specific deletion of *Gata6* revealed its requirement in different SAN forming cell types suggestive of an important role in the cellular cross-talk required for proper SAN formation.

3.8. Methods

***Animals* and *Histology*.** Mouse handling and experimentation were done in accordance with institutional guidelines and were approved by the Animal Care committee of the University of Ottawa. *Gata6* heterozygous (*Gata6*$^{+/-}$, C57BL/6) mice were previously described [16]. Cell-specific knockouts mice were oftained by crossing the *Gata6*$^{Fl/Fl}$ line with the respective *cre* lines. Embryos and adult heart tissues were fixed with 4% paraformaldehyde in PBS, paraffin embedded, sectioned at 4-μm intervals, and processed. Masson Trichrome staining was performed by the histology service of the University of Ottawa. For RNA analysis of dissected SAN and right atria, all experiments were performed in accordance with the guidelines of the Canadian Council on Animal Care and the *Guide of the Care and Use of Laboratory Animals* published by the US National Institutes of Health (NIH Publication No. 85-23, revised 1996). Experiments were also approved by the Montreal Heart Institute Animal Care Committee (approval reference number 2015-80-03).

Electrophysiology. Surface ECG recording was done using EMKA technologies platform. PR interval, QRS duration, QT Interval, RR Interval were analyzed using the IOX 2.4.2.6 software and reported. The QT intervals were corrected (QTc) for the heart rate using the standard formula for mice ($QTc=QT/(RR/100)^{1/2}$) [19].

Telemetry analysis (Arrythmias). Implantable radio frequency transmitter (Data Services International, DSI's PhysioTel® ETA-F10) with subcutaneous (SC) leads was placed subcutaneously along the lateral flank to acquire data. The negative lead was fed SC to the right pectoral muscle and the positive lead was fed SC to the left caudal rib region. Precision and proper placement of the ECG leads were crucial to allow recording of the ECG waveforms over a long period of time and with low signal-to-noise tracings. Data was

acquired 20 seconds from every 1 hour for 72 hours. Analysis was perfomed using Ponemah Physiology Platform Software (Version 5.2 SP7, DSI).

***3D reconstruction*.** Serial sections for the SAN from E14.5 embryos were used for the reconstruction using the Free-D software (version 1.14) according to the developer's instructions [19]. Sections were registered before the SAN tracing for each of the serial sections so that the tracing does not interfere with the alignment. Following the SAN tracing, images were stacked to obtain the 3D reconstructions.

Immunohistochemistry. Immunohistochemical stainings were performed as previously described [20]. Briefly, following blocking for an hour with 5% BSA, sections were incubated with the primary antibody overnight at 4°C. After rinsing with PBS, the secondary antibody was applied for 45 min before switching to the streptavidin-HRP conjugated antibody for 30min. The GATA6 and TBX5 antibodies [21,22] were used at a dilution of 1/2000 and 1/2500 respectively. GATA4 (C20) goat polyclonal IgG and TBX3 E-20 antibodies were purchased from Santa Cruz (SC-1237X; dilution 1/600 and SC-31656; dilution 1/750). The HCN4 antibody was purchased from Alomone (APC-052, dilution 1/1000) and the Anti-phospho-Histone H3 (Ser10) antibody from Millipore (06-570, dilution 1/750). The ANF antibody was used at 1/1000 and purchased from Peninsula (T-4014; RGG-9103). The following antibodies were purchased from ABCAM: NKX2.5 (ab35842; dilution 1/100), ISL1 (ab20670; 1/500), TIE2 (ab24859; 1/500), PITX2 (ab192495; 1/750), TBX18 (ab86332; 1/500), WNT1 (ab85060; 1/60). The biotinylated anti-Goat IgG was from Vector Laboratories (BA5000). The anti-Rabbit and anti-Mouse antibodies were from Jackson (Cederlane) (711-065-152 and 715-065-151 respectively). Streptavidin-HRP conjugate was from Perkin Elmer (NEL 750000 1EA).

***RNA analysis*.** C57BL/6, 2-3 months old male mice were anaesthetized by inhalation of isoflurane 2% and killed by cervical dislocation. Sinoatrial nodes (SAN) were isolated under microscope then the right atrium was collected from the same heart [18]. A single right atrium was used for each sample while 4 SAN were pooled to achieve sufficient mRNA concentration. Total mRNA was isolated using TriReagent® (ThermoFisher) and treated with a purification kit (Nucleospin RNA, Machery-Nagel). RNA concentrations were determined with a NanoDrop spectrophotometric analysis (NanoDrop 2000, ThermoFisher). cDNA was synthesized using High Capacity cDNA Reverse Transcription Kit (Applied BioSystems).

Quantitative real-time PCR. **Figure 3.1 D:** qRT-PCR was performed with SYBR Select Master Mix (Applied Biosystems) in a StepOnePlus system (Applied Biosystems). cDNA was amplified by a 40 cycles protocol followed by a melting curve. Each cycle contains a step of denaturation (95°C, 15s), annealing (55°C, 10s) and elongation (60°C, 60s). Data were analyzed in duplicates with the $2^{-\Delta\Delta Ct}$ method. Gene expression was normalized to reference genes HPRT1 and SDHA. **Figure 3.4 A:** Total RNA was isolated from snap-frozen hearts with TRIzol reagent (Life technologies, 15596018) using FastPrep beads (MP-Bio, 6913-100); cDNAs were generated using the Omniscript RT kit (Qiagen, 205113). Oligonucleotide sequences are available on request.

Luciferase assay. Transfections were carried out as previously described [23]. Appropriate amounts of empty DNA vector were added to maintain a constant total amount of DNA. TBX3-Luc reporter construct was a kind gift from Dr. Sharon Prince and was previously described [24].

Statistics. For electrocardiogram analysis, values are presented as standard error of the mean (SEM). Statistical analysis for qRT-PCR was performed with Origin8.0 software (OriginLab, MA). *F*-Test for equality of variance followed by unpaired Student's *t*-test were used to compared data sets. Primer sequences are available upon request. *P* values were generated using Student's 2-tailed *t* test with P values < 0.05 considered as an index of statistical significance.

3.9. Results

3.9.1. Loss of one allele of *Gata6* in mice results in ECG alterations and hypoplastic SAN.

Surface electrocardiogram (ECG) was performed on *Gata6*$^{+/-}$ and control littermates to assess whether these mice display any CCS defects. The ECG profiling showed significant increases in both PR and QT intervals in *Gata6*$^{+/-}$ group indicative of problems in heart depolarization/ repolarization (**Figure 3.1 A and C**). Arrhythmias analysis using DSI/Ponemah platform revealed the occurrence of premature atrial contractions (PAC) in 3 out of 9 *Gata6*$^{+/-}$ hearts (33%); those have been shown to lead to AF when occurring in the atrial vulnerable period [25] (**Figure 3.1 B**). GATA6 expression starts on during gastrulation and persists throughout embryogenesis and adulthood. Whithin the cardiovascular system, GATA6 is expressed in atrial and ventricular myocytes, in some endothelial cells as well as smooth muscle cells forming the outflow tract and neural crest cells [26,27]. GATA6 was also shown to be present in the proximal CCS (AV node, His bundle and Purkinje fibers) but its contribution to the SAN was never assessed [15]. We examined expression of GATA6 in the SAN and right atria. qRT-PCR performed on dissected SAN from control mice revealed the presence of GATA6 and GATA4 in cells of the sinoatrial node (**Figure 3.1 D**). Immunohistochemistry (IHC) staining showed that GATA6 is expressed throughout the heart and confirmed its presence in HCN4 and GATA4 positive cells composing the SAN as early as E14.5 (**Figure 3.1 E**).

Gain and loss of function mutations in *GATA6* are associated with outflow tract defects or CCS abnormalities, such as familial AF [9,12] (**Figure 3.2 A**). Most of the reported mutations linked to familial AF are located within the regulatory C- and N-terminal regions

of the protein- region important for protein-protein interactions. Dilation of right and left atria as well as impaired ventricular function have been shown to be common in patients with chronic AF [28]. Examination of *Gata6*$^{+/-}$ P0 hearts shows that these mice present reduced left ventricular function (data not shown) with some showing enlarged right atria and/or right ventricle (**Figure 3.2 B**). Masson trichrome staining performed on P0 *Gata6*$^{+/-}$ revealed a hypoplastic SAN with fewer myocytes as compared to control littermates (**Figure 3.2 C**). Expression pattern of key regulators of CCS formation was also assessed at this stage. TBX3 is expressed mainly in the SAN and is considered one of the major regulators of the SAN genetic program. It prevents atrialization by repressing the expression of myocardial genes including *Cx43*, *Cx40*, *Nppa/b* and *Scn5a*. Conversely, in the adjacent atrial myocardium, NKX2.5 represses *Hcn4* and *Tbx3* and ectopic expression of TBX3 and HCN4 is found in the heart tube of *Nkx2.5* deficient mice [32]. In this line, expression of NKX2.5 in the right atria was downregulated in *Gata6*$^{+/-}$ when compared to *Gata6*$^{+/+}$ whereas expression of TBX3 was found to be increased in the AV node, bundle of His and SAN, with fewer cells expressing it in the latter (**Figure 3.3 A and B**). Decreased ANF expression in the atria and increased expression in the SAN was evident in *Gata6*$^{+/-}$ P0 mice, indicative of genetic reprogramming (**Figure 3.3 A**). Expression of TBX5 was also shown to be upregulated in the SAN of *Gata6*$^{+/-}$ when compared to control littermates (**Figure 3.3 A**).

3.9.2. Reduced *Hcn4*+ and *Tbx3*+ cells in the SAN of *Gata6*$^{+/-}$.

Since *Gata6*$^{+/-}$ mice showed obvious conduction defects with surface ECG and a hypocellular SAN, we sought to further explore the underlying pathways leading to the conduction abnormalities in these mice. Quantitative and qualitative analysis of several regulators of the CCS was performed by examining early stages of embryonic SAN

development (E11.5 and 14.5). Consistent with the presence of a dysregulated CCS program on E11.5 heart embryos revealed, qRT-PCR analysis revealed decreased conduction channels expression (KIR3.1 and CX43), and decreased expression of the stress marker ANF, shown to be regulated by GATA6[31] (Figure 3.4 A). Staining for HCN4 and TBX3 in E14.5 emrbyos revealed a decreased number of *Hcn4*+ and *Tbx3*+ cells in the SAN, indicative of fewer conduction cells in *Gata6*$^{+/-}$ (**Figure 3.4 C**). As expected, staining for GATA6 was decreased in these mice. Expression of GATA4 and TBX5 was also downregulated in SAN composing cells (**Figure 3.4 C**). To quantitatively assess the size of the SAN in *Gata6*$^{+/-}$, a three-dimensional (3D) reconstruction of the SAN was employed, which revealed significantly smaller SAN in *Gata6*$^{+/-}$ (**Figure 3.4 B**).

Previous studies have shown that TBX3 directly binds and modulates the *Gata6* promoter [32]. We checked whether GATA6 can in turn activate the *TBX3* promoter. In silico analysis of the *TBX3* promoter revealed the presence of 3 putative GATA binding sites. Cotransfection in NIH3T3 cells of GATA6 expressing vector and *TBX3* luciferase construct showed a significant dose dependent GATA6 activation of the *TBX3* promoter which was consistently shown to be higher than achieved over the ANF promoter (**Figure 3.4 E**). These results indicate that GATA6 directly regulate a key CCS gene.

3.9.3. Cellular basis of GATA6 role in SAN formation.

The SAN is a unique structure within the heart that plays the crucial role of initiating its pacemaking activity. It is thought to comprise a variety of cell types regrouping pacemaking (myocardial derived, mainly *ISL1*+ cells) and non-pacemaking cells (**Figure 3.5 A**). Non-pacemaking cells include endothelial and fibroblast cells in addition to transitional cells whose phenotype varies depending on their position within the SAN: the closer they are to

the atria, the more these myocytes resemble the atrial myocytes and lose their pacemaking-like cells phenotype [33]. Immunohistochemical staining of E12.5 *Gata6*$^{+/-}$ and *Gata6*$^{+/+}$ embryos revealed decreased expressions of ISL1 and WNT1 in *Gata6*$^{+/-}$ SAN. Expression of TBX18, an important marker of the SAN program, was also decreased. On the other hand, increased expression of TIE2 and PITX2 marked the SAN of *Gata6*$^{+/-}$ mice (**Figure 3.5 B**). These observations are suggestive of important genetic and cellular reprogramming in *Gata6*$^{+/-}$ SAN.

We used mouse genetics to test which cell type is the responsible for the SAN phenotype in *Gata6*$^{+/-}$ mice. *Gata6* was deleted from endothelial and conduction cells by crossing *Gata6*$^{Fl/Fl}$ mice with *Tie2cre* and *Isl1cre* mice respectively. Deletion of *Gata6* from neural crest cells (NCCs) was also performed using *Wnt1cre* since a contribution of NCC to the CCS has been suggested [34]. Analysis of embryos from timed matings suggested high perinatal lethality when both *Gata6* alleles were conditionally deleted from *Tie2+* and *Isl1+* cells with decreased viability evident as early as E14.5 (**Figure 3.5 C**). However, mice in which both Gata6 alleles were deleted from NCCs survived to birth, but none were found at weaning (**Figure 3.5 C** and data not shown).

Examination of the homozygous embryos from the different lines at E14.5 revealed smaller embryos with multiple defects including growth retardation and abnormal vascularization (in *Isl1cre+G6*$^{Fl/Fl}$ and *Tie2cre+G6*$^{Fl/Fl}$) (**Figure 3.6 A**). Histological analysis of *Wnt1cre+G6*$^{Fl/Fl}$ and *Tie2cre+G6*$^{Fl/Fl}$ embryos revealed a smaller hypocellular SAN, recapitulating the phenotype observed in the *Gata6*$^{+/-}$ model. The SAN of both lines revealed a significant decrease in GATA6 expression along with a decreased presence of HCN4 and TBX3 expressing cells (**Figure 3.6 B**). Similar analysis of *Isl1cre+G6*$^{Fl/Fl}$ embryos was not possible due to the severity of the phenotype.

Since deletion of a single *Gata6* allele from any cell type did not compromise survival, we examined adult hearts from all the lines generated. Masson Trichrome staining revealed an enlarged right ventricle in all the conditionally deleted models; in addition, thickening of the left ventricular wall and abnormal cardiomyocytes in the apex region was found in *Wnt1cre+G6*$^{Wt/Fl}$ mice, suggestive of abnormal heart innervation (**Figure 3.7 A**). Surface ECG showed distinct alterations in the various lines which recapitulated some of those present in *Gata6*$^{+/-}$ mice: *Tie2cre+G6*$^{Wt/Fl}$ mice displayed prolonged QT interval, whereas *Isl1cre+G6*$^{Wt/Fl}$ showed prolonged PR and QRS intervals (**Figure 3.7 B**). *Wnt1cre+G6*$^{Wt/Fl}$ showed a larger R amplitude which is indicative of left ventricular hypertrophy (**Figure 3.7 A and B**). Close examination of E14.5 embryos revealed a dysregulated expression of GATA6, HCN4 and TBX3 in most cases (**Figure 3.7 C**). Taken together, these results suggest that GATA6 is required in various SAN cell types and plays cell autonomous as well as non-cell autonomous functions in SAN development.

3.10. Discussion

The proper contraction of the heart and its relaxation are highly controlled processes orchestrated by the slow and fast conducting structures: the distal and proximal CCS. The proximal components of the CCS comprise the SAN and the AVN while distal ones regroup the His bundle, bundle branches and the Purkinje fibers. Our knowledge on the different regulators of the CCS came largely from studies of knockout and transgenic models as well as from human genetic studies including genome-wide association studies and exon-sequencing. However, despite the remarkable progress that have been made in the past few years, the cellular origins and gene regulatory networks contributing to the specification and development of each of these structures remain to date incompletely understood. Whithin the heart, the SAN develops in the sinus venosus (SV) bordering the right atria whereas the atrioventricular node forms within the atrioventricular cushion and is mostly derived from first heart field cells of the primary heart tube. The atrioventricular bundle on the other hand is located at the top of the interventricular septum and is known to derive from progenitor cells at the border between the first and second heart fields [35]. Lineage tracing analysis have shown a major contribution of ISL1+ progenitor cells to the SAN and SV [36]. As mentioned earlier, the mature SAN is composed of myocardial pacemaker cells (ISL1+), packed in clusters, and surrounded by fibroblasts, transitional and endothelial cells, all lying within a well structured extracellular matrix [33]. Here we show that removal of two copies of *Gata6* from *Isl1+* (SHF) or *Tie2+* (endothelial) cells lead to embryonic lethality with incomplete formation of the SAN, whereas, removal of one copy leads to smaller SAN with dysregulated expression of SAN key regulators (**Tables 3.1 and 3.2**). Taken together, these results reveal an important role for SHF-myocytes and endothelial GATA6 in SAN

formation. To undertand the role that GATA6 play in the formation of the CCS, it is important to understand its role in each of the cell types that form the SAN. It has been shown that in endothelial cells, GATA6 can promote their angiogenic function and survival and can induce endothelial adhesion molecules such as the endothelial vascular adhesion molecule 1 (VCAM1) [37,38]. Its role in SHF-derived myocytes hasn't been explored until recently by our group where we showed its importance in valve morphogenesis and remodeling (**Chapter I**).

Within the heart, NCCs are shown to mainly mark the valves, truncus arteriosus and the proximal conduction system [34]. No direct contribution to the distal CCS has been explored. Their contribution to the CCS was first revealed in chicks where ablation of NCCs resulted in failure of compaction and electrical insulation of the His bundles [39]. GATA6 plays an important in NCCs migration- a critical step in cardiogenesis- via regulation of semaphorin 3C (SEMA3C) expression, a guiding molecule important for neuronal and vascular patterning. NCC-inactivation of GATA6 leads to perinatal mortality mainly due to OFT defects [27]. Human mutations in *GATA6* also cause OFT defects and when tested, the mutants proteins failed to transactivate *Sema3C* and its receptor plexin A2 (*PlnxA2*) [40]. Our results reveal that NCC-inactivation of *Gata6* using *Wnt1-cre* leads to defective SAN formation (**Figure 3.6 B**). However, lineage tracing analysis for *Wnt1* expression using the *R26R* reporter does not show labeling within the SAN [34]. Our findings suggest that NCC-*Gata6* might be indirectly involved in regulating SAN formation.

In vitro studies have shown that within the heart, migrating NCCs can differentiate into different cell types including fibroblasts, smooth muscle cells, pigment cells, chondrocytes, as well as sensory and autonomic neurons [41]. In fact, NCCs has the ability to differentiate into neurons and participate in the formation of the cardiac autonomic

innervation system [42]. Briefly, the heart primarily receives sympathetic innervation at around E14 from the sympathetic ganglia. The sympathetic nerves act then on the SAN and on the myocardium, via secretion of noradrenaline, to increase the rate and the contractility of the heart. On the other hand, parasympathetic nerves from the hindbrain, responding to acetylcholine, maintain the baseline rate of the heart by also acting on the SAN, counteracting the effect of the sympathetic system. Tachycardia or bradycardia (elevated or suppressed heart rate) can result from any imbalance in the opposing components of the nervous system. In the case of *Gata6*$^{+/-}$ mice, disrupted innervation of the heart might underlie the conduction phenotype: these abnormalities can be due to either a disruption in NCC migration or differentiation or due to defective axonal extension. It has been shown that sympathetic axons follow veins to reach and innervate the ventricular myocardium and the SAN, unlike other known cases where they follow arteries [43]. Decreased heart innervation is also reported to be the result of endothelin 1 (*Edn1*) ablation from vascular endothelial cells. EDN1 is known for its role in guiding the sympathetic axons to the heart and its removal from endothelial cell lineage using *Tie2-cre* leads to defects mostly evident in the venous trajectory leading to the SAN [43]. Interestingly, GATA6 have been shown to induce *Edn1* expression in vascular smooth muscle cells in response to inflammatory stimuli and to regulate its promoter in a dose dependent manner when forcely expressed [44]. Interestingly, qRT-PCR analysis shows a downregulation of EDN1 in *Gata6*$^{+/-}$ mice as early as E11.5. These findings, taken together with our results, suggest that expression of GATA6 within the neural crest and endothelial cells can be controlling cardiac/SAN innervation, via regulation of EDN1 expression, herein leading to defective SAN formation and embryonic lethality. Our study reveals a novel role for GATA6 in the formation of the distal conduction system.

3.11. References

1. Park DS, Fishman GI. The cardiac conduction system. *Circulation*. 2011;123:904–915.

2. Liang X, Wang G, Lin L, Lowe J, Zhang Q, Bu L, Chen Y, Chen J, Sun Y, Evans SM. HCN4 dynamically marks the first heart field and conduction system precursors. *Circ Res*. 2013;113:399–407.

3. Aanhaanen WTJ, Brons JF, Domínguez JN, Rana MS, Norden J, Airik R, Wakker V, de Gier-de Vries C, Brown NA, Kispert A, Moorman AFM, Christoffels VM. The Tbx2+ primary myocardium of the atrioventricular canal forms the atrioventricular node and the base of the left ventricle. *Circ Res*. 2009;104:1267–1274.

4. Milanesi R, Bucchi A, Baruscotti M. The genetic basis for inherited forms of sinoatrial dysfunction and atrioventricular node dysfunction. *J Interv Card Electrophysiol Int J Arrhythm Pacing*. 2015;43:121–134.

5. January CT, Wann LS, Alpert JS, Calkins H, Cigarroa JE, Cleveland JC, Conti JB, Ellinor PT, Ezekowitz MD, Field ME, Murray KT, Sacco RL, Stevenson WG, Tchou PJ, Tracy CM, Yancy CW, American College of Cardiology/American Heart Association Task Force on Practice Guidelines. 2014 AHA/ACC/HRS guideline for the management of patients with atrial fibrillation: a report of the American College of Cardiology/American Heart Association Task Force on Practice Guidelines and the Heart Rhythm Society. *J Am Coll Cardiol*. 2014;64:e1-76.

6. Lloyd-Jones DM, Wang TJ, Leip EP, Larson MG, Levy D, Vasan RS, D'Agostino RB, Massaro JM, Beiser A, Wolf PA, Benjamin EJ. Lifetime risk for development of atrial fibrillation: the Framingham Heart Study. *Circulation*. 2004;110:1042–1046.

7. Ott A, Breteler MM, de Bruyne MC, van Harskamp F, Grobbee DE, Hofman A. Atrial fibrillation and dementia in a population-based study. The Rotterdam Study. *Stroke*. 1997;28:316–321.

8. Mahida S. Transcription factors and atrial fibrillation. *Cardiovasc Res*. 2014;101:194–202.

9. Li J, Liu W-D, Yang Z-L, Yang Y-Q. Novel GATA6 loss-of-function mutation responsible for familial atrial fibrillation. *Int J Mol Med*. 2012;30:783–790.

10. Yang Y-Q, Li L, Wang J, Zhang X-L, Li R-G, Xu Y-J, Tan H-W, Wang X-H, Jiang J-Q, Fang W-Y, Liu X. GATA6 loss-of-function mutation in atrial fibrillation. *Eur J Med Genet*. 2012;55:520–526.

11. Yang Y-Q, Wang X-H, Tan H-W, Jiang W-F, Fang W-Y, Liu X. Prevalence and spectrum of GATA6 mutations associated with familial atrial fibrillation. *Int J Cardiol*. 2012;155:494–496.

12. Tucker NR, Mahida S, Ye J, Abraham EJ, Mina JA, Parsons VA, McLellan MA, Shea MA, Hanley A, Benjamin EJ, Milan DJ, Lin H, Ellinor PT. Gain-of-function mutations in GATA6 lead to atrial fibrillation. *Heart Rhythm*. 2017;14:284–291.

13. Adamo RF, Guay CL, Edwards AV, Wessels A, Burch JBE. GATA-6 gene enhancer contains nested regulatory modules for primary myocardium and the embedded nascent atrioventricular conduction system. *Anat Rec A Discov Mol Cell Evol Biol*. 2004;280:1062–1071.

14. Davis DL, Edwards AV, Juraszek AL, Phelps A, Wessels A, Burch JB. A GATA-6 gene heart-region-specific enhancer provides a novel means to mark and probe a discrete component of the mouse cardiac conduction system. *Mech Dev*. 2001;108:105–119.

15. Liu F, Lu MM, Patel NN, Schillinger KJ, Wang T, Patel VV. GATA-Binding Factor 6 Contributes to Atrioventricular Node Development and Function. *Circ Cardiovasc Genet*. 2015;8:284–293.

16. Laforest B, Nemer M. GATA5 interacts with GATA4 and GATA6 in outflow tract development. *Dev Biol*. 2011;358:368–378.

17. Mitchell GF, Jeron A, Koren G. Measurement of heart rate and Q-T interval in the conscious mouse. *Am J Physiol*. 1998;274:H747-751.

18. El Khoury N, Mathieu S, Marger L, Ross J, El Gebeily G, Ethier N, Fiset C. Upregulation of the hyperpolarization-activated current increases pacemaker activity of the sinoatrial node and heart rate during pregnancy in mice. *Circulation*. 2013;127:2009–2020.

19. Andrey P, Maurin Y. Free-D: an integrated environment for three-dimensional reconstruction from serial sections. *J Neurosci Methods*. 2005;145:233–244.

20. Laforest B, Andelfinger G, Nemer M. Loss of Gata5 in mice leads to bicuspid aortic valve. *J Clin Invest*. 2011;121:2876–2887.

21. Nemer G, Nemer M. Transcriptional activation of BMP-4 and regulation of mammalian organogenesis by GATA-4 and -6. *Dev Biol*. 2003;254:131–148.

22. Georges R, Nemer G, Morin M, Lefebvre C, Nemer M. Distinct Expression and Function of Alternatively Spliced Tbx5 Isoforms in Cell Growth and Differentiation. *Mol Cell Biol*. 2008;28:4052–4067.

23. Nemer G, Nemer M. Cooperative interaction between GATA5 and NF-ATc regulates endothelial-endocardial differentiation of cardiogenic cells. *Dev Camb Engl*. 2002;129:4045–4055.

24. Mowla S, Pinnock R, Leaner VD, Goding CR, Prince S. PMA-induced up-regulation of TBX3 is mediated by AP-1 and contributes to breast cancer cell migration. *Biochem J*. 2011;433:145–153.

25. Jensen TJ, Haarbo J, Pehrson SM, Thomsen B. Impact of premature atrial contractions in atrial fibrillation. *Pacing Clin Electrophysiol PACE*. 2004;27:447–452.

26. van Berlo JH, Elrod JW, van den Hoogenhof MMG, York AJ, Aronow BJ, Duncan SA, Molkentin JD. The transcription factor GATA-6 regulates pathological cardiac hypertrophy. *Circ Res*. 2010;107:1032–1040.

27. Lepore JJ, Mericko PA, Cheng L, Lu MM, Morrisey EE, Parmacek MS. GATA-6 regulates semaphorin 3C and is required in cardiac neural crest for cardiovascular morphogenesis. *J Clin Invest*. 2006;116:929–939.

28. Xiao HB, Rizvi SAH, McCrea D, Kaufman B. The association of chronic atrial fibrillation with right atrial dilatation and left ventricular dysfunction in the elderly. *Med Sci Monit Int Med J Exp Clin Res*. 2004;10:CR516-520.

29. Mommersteeg MTM, Hoogaars WMH, Prall OWJ, de Gier-de Vries C, Wiese C, Clout DEW, Papaioannou VE, Brown NA, Harvey RP, Moorman AFM, Christoffels VM. Molecular pathway for the localized formation of the sinoatrial node. *Circ Res*. 2007;100:354–362.

30. van Weerd JH, Christoffels VM. The formation and function of the cardiac conduction system. *Dev Camb Engl*. 2016;143:197–210.

31. Charron F, Paradis P, Bronchain O, Nemer G, Nemer M. Cooperative interaction between GATA-4 and GATA-6 regulates myocardial gene expression. *Mol Cell Biol*. 1999;19:4355–4365.

32. Lu R, Yang A, Jin Y. Dual functions of T-box 3 (Tbx3) in the control of self-renewal and extraembryonic endoderm differentiation in mouse embryonic stem cells. *J Biol Chem*. 2011;286:8425–8436.

33. Liang X, Evans SM, Sun Y. Development of the cardiac pacemaker. *Cell Mol Life Sci CMLS*. 2017;74:1247–1259.

34. Nakamura T, Colbert MC, Robbins J. Neural crest cells retain multipotential characteristics in the developing valves and label the cardiac conduction system. *Circ Res*. 2006;98:1547–1554.

35. Mohan R, Boukens BJ, Christoffels VM. Lineages of the Cardiac Conduction System. *J Cardiovasc Dev Dis*. 2017;4:5.

36. Mommersteeg MTM, Domínguez JN, Wiese C, Norden J, de Gier-de Vries C, Burch JBE, Kispert A, Brown NA, Moorman AFM, Christoffels VM. The sinus venosus

progenitors separate and diversify from the first and second heart fields early in development. *Cardiovasc Res*. 2010;87:92–101.

37. Froese N, Kattih B, Breitbart A, Grund A, Geffers R, Molkentin JD, Kispert A, Wollert KC, Drexler H, Heineke J. GATA6 promotes angiogenic function and survival in endothelial cells by suppression of autocrine transforming growth factor beta/activin receptor-like kinase 5 signaling. *J Biol Chem*. 2011;286:5680–5690.

38. Umetani M, Mataki C, Minegishi N, Yamamoto M, Hamakubo T, Kodama T. Function of GATA transcription factors in induction of endothelial vascular cell adhesion molecule-1 by tumor necrosis factor-alpha. *Arterioscler Thromb Vasc Biol*. 2001;21:917–922.

39. Gurjarpadhye A, Hewett KW, Justus C, Wen X, Stadt H, Kirby ML, Sedmera D, Gourdie RG. Cardiac neural crest ablation inhibits compaction and electrical function of conduction system bundles. *Am J Physiol Heart Circ Physiol*. 2007;292:H1291-1300.

40. Kodo K, Nishizawa T, Furutani M, Arai S, Yamamura E, Joo K, Takahashi T, Matsuoka R, Yamagishi H. GATA6 mutations cause human cardiac outflow tract defects by disrupting semaphorin-plexin signaling. *Proc Natl Acad Sci U S A*. 2009;106:13933–13938.

41. Sieber-Blum M. Cardiac neural crest stem cells. *Anat Rec A Discov Mol Cell Evol Biol*. 2004;276:34–42.

42. Hasan W. Autonomic cardiac innervation: development and adult plasticity. *Organogenesis*. 2013;9:176–193.

43. Manousiouthakis E, Mendez M, Garner MC, Exertier P, Makita T. Venous endothelin guides sympathetic innervation of the developing mouse heart. *Nat Commun*. 2014;5:3918.

44. Lepore JJ, Cappola TP, Mericko PA, Morrisey EE, Parmacek MS. GATA-6 regulates genes promoting synthetic functions in vascular smooth muscle cells. *Arterioscler Thromb Vasc Biol*. 2005;25:309–314.

Figure 3.1

A

		Age (days)	RR	HR	PR	P duration	QRS	AMP of R	ST LEVEL	ST ELEVATION	QT	QTC F	FC
Avg	Gata6$^{+/+}$ (n=14)	116.29	131.50	461.76	40.14	10.85	10.21	0.69	0.01 *	0.04 *	38.40 *	75.53 *	0.46
	Gata6$^{+/-}$ (n=15)	114.20	142.35	430.80	45.08 *	11.75	10.61	0.64	-0.02 *	0.00 *	43.55 *	83.46 *	0.43
SEM	Gata6$^{+/+}$	4.61	3.90	13.18	1.06	0.76	0.39	0.05	0.01	0.01	1.65	3.00	0.01
	Gata6$^{+/-}$	5.73	5.42	16.37	1.03	1.07	0.25	0.05	0.01	0.01	1.36	1.93	0.02

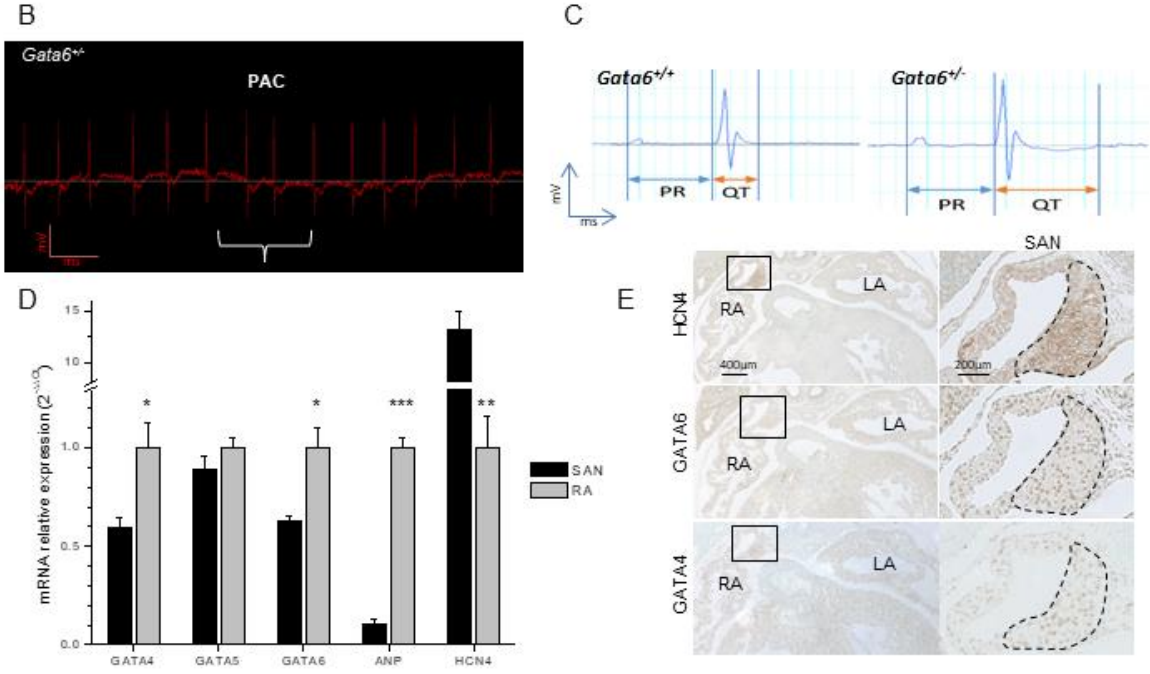

Figure 3.1: *Gata6*$^{+/-}$ display ECG abnormalities. (A) Electrocardiogram profile showing the different interval measurements for *Gata6*$^{+/+}$ and *Gata6*$^{+/-}$ mice. HR: heart rate. Fc: cardiac frequency. Values are mean + SEM.*$P < 0.05$. **(B)** Representation of PAC resulting from the arrhythmias analysis performed on adult *Gata6*$^{+/+}$ and *Gata6*$^{+/-}$ mice. PAC: premature atrial contraction. **(C)** Representative ECG showing prolonged QT in *Gata6*$^{+/-}$ mice. ECG: electrocardiogram. **(D)** Relative mRNA expression of GATA4, GATA5, GATA6, ANP and HCN4 genes in SAN (n=5) and in RA (n=5). Results are normalized to the expression of the housekeeping genes GAPDH and SDHA of the same sample. All samples were analyzed in duplicates with the $2^{-\Delta\Delta Ct}$ method (Data are presented as mean ± SEM) (* P<0.05, ** P<0.01 and *** P<0.001). **(E)** Immunohistochemistry staining for HCN4, GATA6 and GATA4 in the SAN of E14.5 *Gata6*$^{+/+}$ control embryos. The micrographs are representative of similar findings in 4-5 embryos for each genotype. RA: right atria. SAN: sinoatrial node. LA: left atria. Scale bar: 400μm. 200μm.

Figure 3.2

A

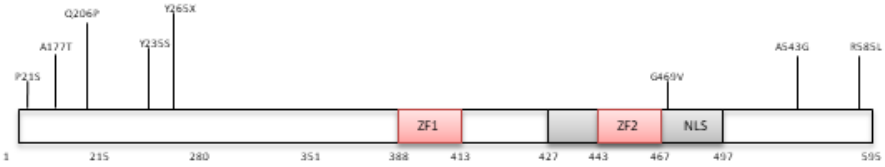

Mutation	Biochemistry	PubmedID
P21S	Increased transcriptional activity on NPPA, NPPB and α -MHC promoters	27756709
A177T	Increased transcriptional activity on NPPA, NPPB and α -MHC promoters	27756709
Q206P	Not tested	22257684
Y235S	Decreased transcriptional activity on ANP and CX40 promoters	22750565
Y265X	Not tested	22257684
G469V	Decreased transcriptional activity on ANP promoter	22824924
A543G	Increased transcriptional activity on NPPA, NPPB and α -MHC promoters	27756709
R585L	Increased transcriptional activity on NPPA, NPPB and α -MHC promoters	27756709

B

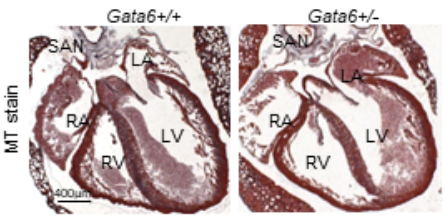

C

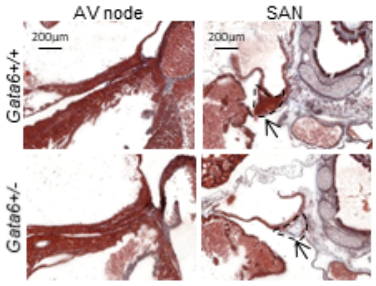

Figure 3.2 : Hypoplastic SAN in *Gata6*$^{+/-}$ mice. (A) List of GATA6 human mutations associated with Atrial Fibrillation. ZF1: zinc finger 1. ZF2: zinc finger 2. NLS: nuclear localization signal. **(B)** Masson Trichrome staining showing enlarged right atria and ventricle in *Gata6*$^{+/-}$ newborn mice. Scale bar: 400µm. **(C)** Masson Trichrome staining on newborn *Gata6*$^{+/+}$ and *Gata6*$^{+/-}$ showing hypolastic SAN in *Gata6*$^{+/-}$ mice (n=5-9). Arrows are pointing to the SAN. AV node: atrioventricular node. SAN: sinoatrial node. RA: right atria. LA: left atria. RV: right ventricle. LV: left ventricle. Scale bar: 200µm.

Figure 3.3

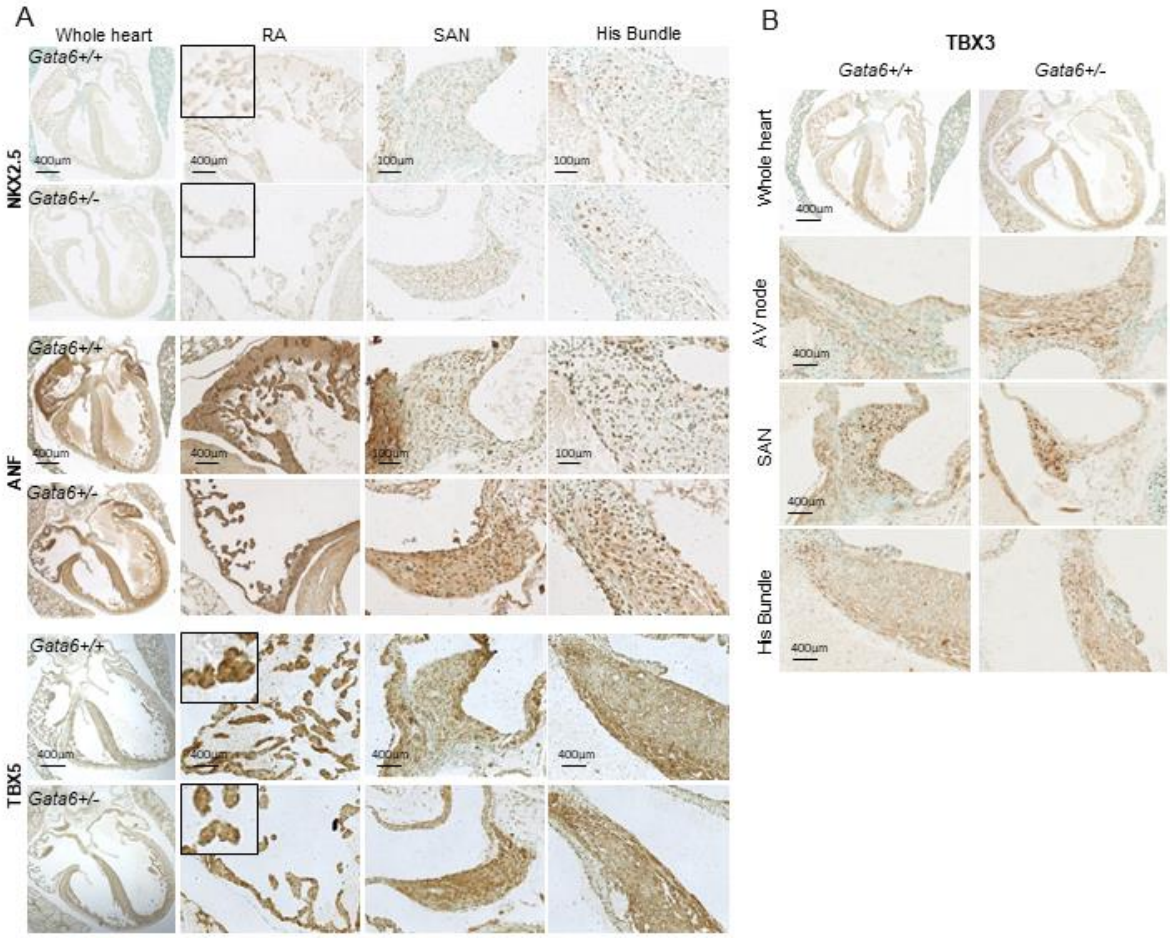
A
Whole heart
RA
SAN
His Bundle
NKX2.5
ANF
TBX5
Gata6+/+
Gata6+/-
400µm
100µm
B
TBX3
Gata6+/+
Gata6+/-
Whole heart
AV node
SAN
His Bundle
400µm

Figure 3.3: Dysregulation of CCS regulators in *Gata6*$^{+/-}$ SAN. Immunohistochemistry in the SAN, RA, AV node and His bundle of *Gata6*$^{+/+}$ and *Gata6*$^{+/-}$ mice showing dysregulated expression of **(A)** NKX2.5**,** ANF,TBX5 and **(B)** TBX3 (n=5-9). SAN: sinoatrial node. AV node: atrioventricular node. RA: right atria. Scale bar: 400μm. 100μm.

Figure 3.4

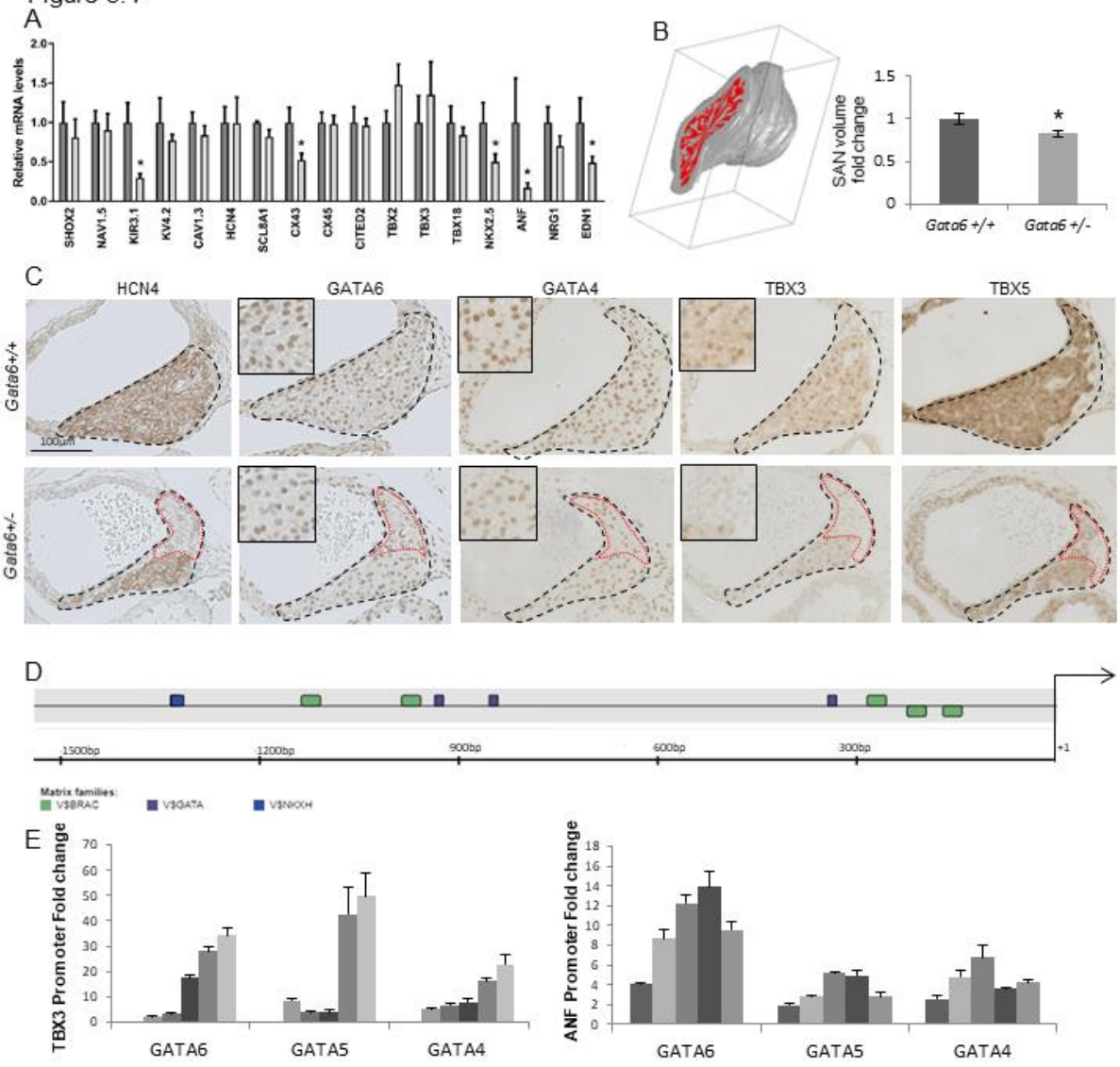
A
Relative mRNA levels
SHOX2
NAV1.5
KIR3.1
KV4.2
CAV1.3
HCN4
SCL8A1
CX43
CX45
CITED2
TBX2
TBX3
TBX18
NKX2.5
ANF
NRG1
EDN1
B
SAN volume fold change
Gata6 +/+
Gata6 +/-
C
HCN4
GATA6
GATA4
TBX3
TBX5
Gata6+/+
Gata6+/-
100um
D
1500bp
1200bp
900bp
600bp
300bp
+1
Matrix families:
V$BRAC
V$GATA
V$NKXH
E
TBX3 Promoter Fold change
GATA6
GATA5
GATA4
ANF Promoter Fold change
GATA6
GATA5
GATA4

Figure 3.4: Reduced Hcn4+ and Tbx3+ cells in the SAN of *Gata6*$^{+/-}$ (A) qRT-PCR on RNA extracted from E11.5 hearts showing altered expression of important conduction system regulators; note the significant decrease in the expression of KIR3.1, NKX2.5, CX43, ANF and EDN1(corrected to RPS16, n=5-8 per group). **(B)** 3D reconstruction of the sinoatrial node (SAN) from E14.5 embryos showing smaller SAN in *Gata6*$^{+/-}$ mice (n=3-9). **(C)** Immunohistochemistry staining on SAN from E14.5 *Gata6*$^{+/+}$ and *Gata6*$^{+/-}$ embryos showing expression of HCN4, GATA6**,** GATA4, TBX3**,** and TBX5. Note the decreased expression of GATA6, GATA4 and TBX5, and the lack of HCN4+ and TBX3+ cells in SAN of *Gata6*$^{+/-}$ mice. The micrographs are representative of similar findings in 4-5 embryos for each genotype. Scale bar: 100μm. **(D)** Schematic representation of TBX3 promoter showing the different GATA, T-box and Nkx-binding sites. **(E)** Increasing amounts of GATA4/5/6 expression vectors are transiently cotransfected with the luciferase reporter under the control of the TBX3 and ANF promoters in NIH3T3 cells (25, 50, 100, 250 and 500 ng of expression vector). Relative luciferase activities are represented as fold changes. The data are a representative of 3 independent experiments done in duplicates. Values are mean + SEM.

Figure 3.5

A

B

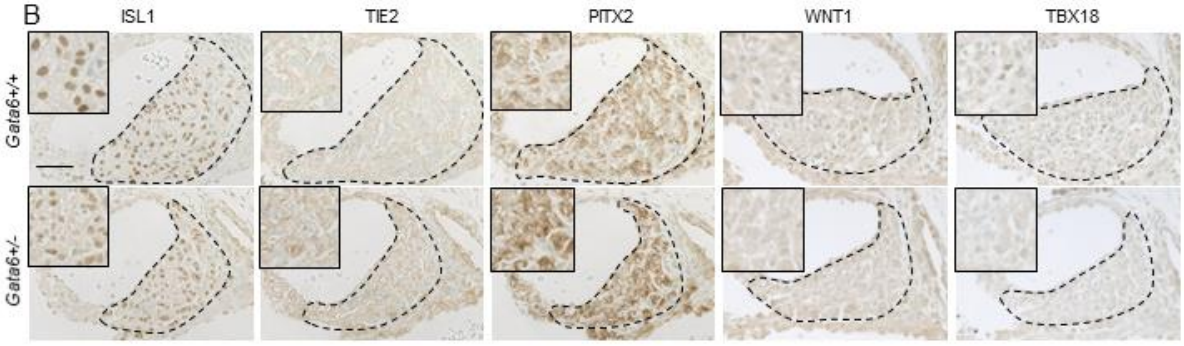

C

	Age	Nb genotyped	Cre-G6WtFl	Cre+G6WtFl	Cre-G6FlFl	Cre+G6FlFl
Tie2	P0	12	6 (50%)	6 (50%)	0	0
	E14.5	22	3 (14%)	13 (59%)	4 (18%)	2 (9%)
Wnt1	P0	16	3 (19%)	3 (10%)	6 (37%)	4 (25%)
	E14.5	34	15 (44%)	5 (15%)	5 (15%)	9 (26%)
Isl1	P0	18	4 (22%)	10 (56%)	4 (22%)	0
	E14.5	12	3 (25%)	4 (33%)	3 (25%)	2 (17%)

Figure 3.5 : Cellular basis of GATA6 role in SAN formation. (A) Schematic figure representing the different cell types contributing to the formation of the SAN. ECM: extracellular matrix. (B) Immunohistochemistry staining for ISL1, TIE2, PITX2, WNT1 and TBX18 in the SAN of E12.5 embryos control and *Gata6*$^{+/-}$ mice. The micrographs are representative of similar findings in 4-5 embryos for each genotype. Scale bar: 50 μm. (C) Frequency of genotypes obtained from generating *Tie2cre*, *Wnt1cre* and *Isl1cre* conditional knockout mice. Embryonic and perinatal lethality of *cre+ G6*$^{Fl/Fl}$ is demonstrated by the reduced frequencies of those embryos at various developmental stages.

Figure 3.6

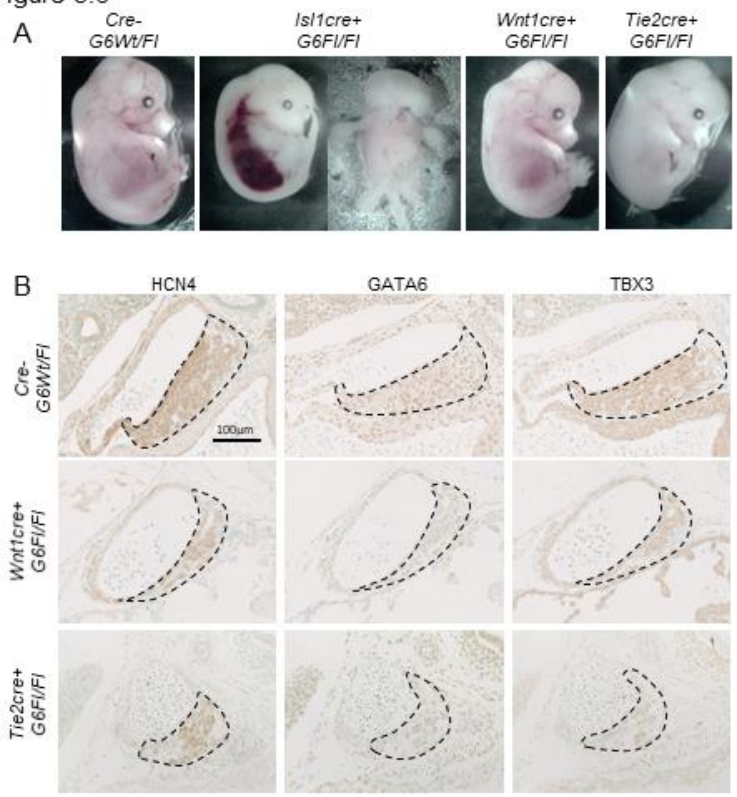
A
Cre-
G6Wt/Fl
Isl1cre+
G6Fl/Fl
Wnt1cre+
G6Fl/Fl
Tie2cre+
G6Fl/Fl
B
HCN4
GATA6
TBX3
Cre-
G6Wt/Fl
100um
Wnt1cre+
G6Fl/Fl
Tie2cre+
G6Fl/Fl

Figure 3.6: Multiple defects in homozygous conditionally deleted *Gata6* embryos. (A) Representation of E14.5 *Gata6* homozygous embryos resulting from *Tie2cre*, *Wnt1cre* and *Isl1cre* conditional knockout mice. (B) Immunohistochemistry staining for HCN4, GATA6, and TBX3 in the SAN of E14.5 embryos control and *cre+Gata6*$^{Fl/Fl}$ mice. The micrographs are representative of similar findings in 4-5 embryos for each genotype. Scale bar: 100 μm.

Figure 3.7

A

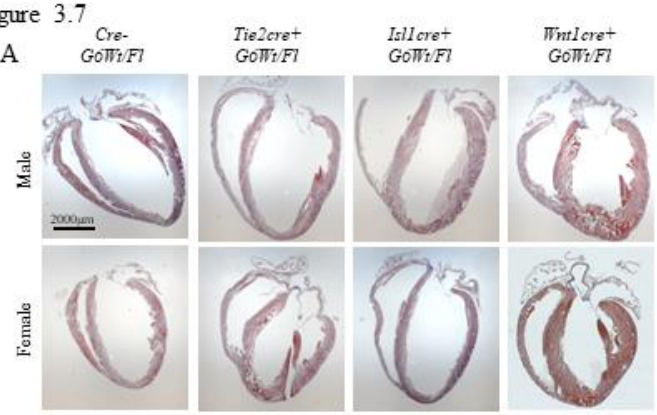

B

		Age (days)	RR	HR	PR	P duration	QRS	AMP of R	ST LEVEL	ST ELEVATION	QT	QTC F	CF
Cre-	$G6^{Wt/Fl}$	73.74	123.23	489.65	36.23	9.40	10.10	0.71	0.01	0.03	36.65	73.67	0.49
SEM	n=19	2.66	2.01	7.96	0.55	0.64	0.31	0.06	0.00	0.01	0.83	1.51	0.01
Tie2cre+	$G6^{Wt/Fl}$	91.50	119.35	507.43	36.40	7.44	10.28	0.78	0.00	0.01	39.68	80.63*	0.51
SEM	n=8	2.83	4.29	17.68	0.92	0.56	0.20	0.06	0.01	0.01	1.43	2.56	0.02
Isl1cre+	$G6^{Wt/Fl}$	61.11	127.08	474.31	38.20*	11.96*	9.03*	0.54	-0.01	-0.01*	36.71	73.13	0.47
SEM	n=9	1.23	2.95	10.59	0.58	0.65	0.31	0.04	0.01	0.01	1.86	3.84	0.01
Wnt1cre+	$G6^{Wt/Fl}$	65.92	123.76	486.21	37.72	9.99	9.74	0.89*	0.01	0.04	36.44	73.16	0.49
SEM	n=12	1.18	1.94	7.54	0.71	0.72	0.21	0.05	0.01	0.01	2.20	4.44	0.01

C

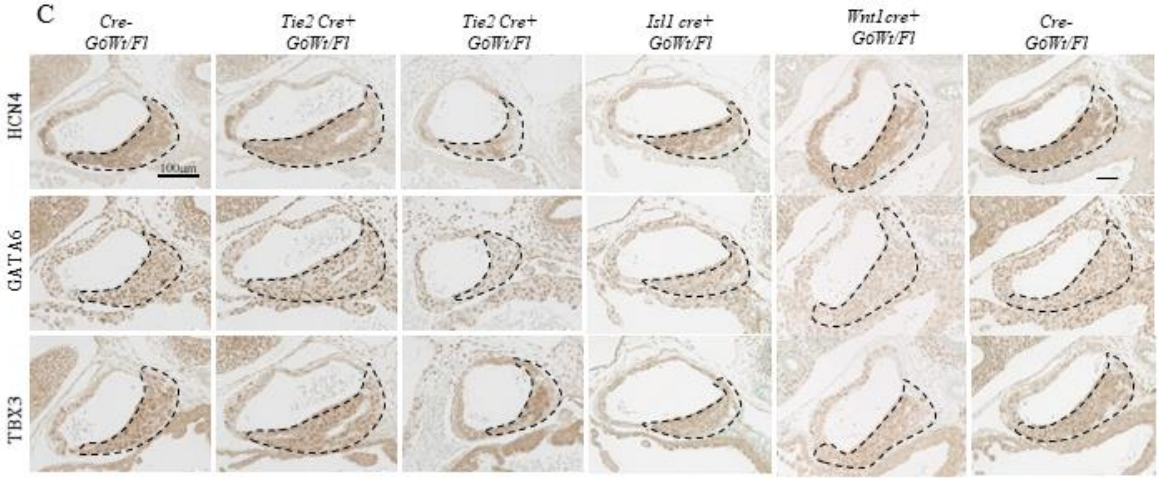

Figure 3.7: Conduction defects in heterozygous conditionally deleted *Gata6* embryos. (A) Masson trichrome staining on adult heart from *Tie2cre+*, *Wnt1cre+* and *Isl1cre+* $G6^{Wt/Fl}$ mice. Scale bar: 2000 μm. **(B)** Electrocardiogram profile showing the different interval measurements for each of the conditional knockout mice. HR: heart rate. Fc: cardiac frequency. Values are mean + SEM.*$P < 0.05$. **(C)** Immunohistochemistry staining for HCN4, GATA6, and TBX3 in the SAN of E14.5 embryos control and *cre+Gata6*$^{Fl/Fl}$ mice.The micrographs are representative of similar findings in 4-5 embryos for each genotype. Scale bar: 100 μm.

Table 3.1: Summary of conduction defects

Genotype	n	Defects
$Gata6^{+/+}$	33	None
$Gata6^{+/-}$	15	Prolonged PR and QT intervals, ST elevation
$Tie2cre^{+}$ $G6^{Wt/Fl}$	8	Prolonged QT interval
$Wnt1cre^{+}$ $G6^{Wt/Fl}$	12	Increased amplitude or R
Isl1cre+ $G6^{Wt/Fl}$	9	Prolonged PR interval and P duration, ST elevation, decreased QRS interval

* Electrophysiological defects assessed at 60-115 days

Table 3.2: Frequency of smaller SAN

Genotype	Percentage
Control	None (0/9)
$Gata6^{+/-}$	100% (6/6)
$Tie2cre^{+}$ $G6^{Wt/Fl}$	50% (4/8)
$Tie2cre^{+}$ $G6^{Fl/Fl}$	100% (2/2)
$Wnt1cre^{+}$ $G6^{Wt/Fl}$	40% (2/5)
$Wnt1cre^{+}$ $G6^{Fl/Fl}$	83% (5/6)
Isl1cre+ $G6^{Wt/Fl}$	67% (2/3)
$Isl11cre^{+}$ $G6^{Fl/Fl}$	ND

* SAN structure assessed at E14.5

4. Chapter III. GATA6 haploinsufficiency results in heart and limb abnormalities

Lara Gharibeh, Wael Maharsy, Mathieu Joyal, Abir Yamak, Mona Nemer

1- From the Molecular Genetics and Cardiac Regeneration Laboratory, Department of Biochemistry, Microbiology, and Immunology, University of Ottawa, Ottawa, Ontario, Canada (L.G., W.M., M.J., A.Y., M.N.)

*Corresponding author:
Dr. Mona Nemer
University of Ottawa
451 smyth road, Room 4522
Ottawa, Ontario K1H 8M5
Tel: 613 562 5800 ext.3995
Email: mona.nemer@uottawa.ca

4.1. Statement of the manuscript

The manuscript ***"Gata6 haploinsufficiency results in heart and limb abnormlaties"*** is in final stages of preparation.

4.2. Contribution statement

In this chapter, I performed the *in vivo* and *in vitro* work and contributed to almost all the analysis. Immunohistochemistry of Figure 4.2A was performed by AY. qRT-PCR analysis in Figure 4.4D was done by MJ. LG and MN wrote the manuscript. LG, WM and MN interpreted all experiments and edited the manuscript.

4.3. Acknowledgment

The authors are grateful to Megan Fortier and Janie Beauregard for technical support, Hélène Touchette for secretarial help and members of the Nemer Lab for discussions and helpful suggestions. The authors thank Dr. Sergio Jimenez for sharing the SOX9-Luc reporter construct. The authors acknowledge the invaluable support of the uOttawa histology and animal physiology cores.

4.4. Sources of funding

This work was funded by a CIHR foundation scheme grant (CIHR-IRSC: 0077282) to MN. LG holds the M. E. Abbott Scholarship from the Bicuspid Aortic Foundation and a graduate excellence scholarship from the University of Ottawa.

4.5. Disclosure

None

4.6. Abstract

Introduction: CHDs as well as limb defects often occur simultaneously in many types of neonatal syndromes, such is the case of Elis-Van Creveld, Bardet-Biedl and Holt Oram (HOS) syndromes. HOS for example is a CHD characterized by abnormalities of the upper limbs and heart, caused by mutations in *TBX5* gene. Genetic causes that explain the appearance of these phenotypes simultaneously remain poorly understood. Mutations in all 3 cardiac GATA factors, *GATA4*, *5* and *6* have been also linked to various human CHD. In mice, *Gata4* and *Gata6* haploinsufficiency (*Gata6*$^{+/-}$) as well as homozygous deletion of *Gata5* result in CHD. Homozygous conditional deletion of *Gata6* from the limb bud using *Prx1-cre* was shown to result in pre-axial polydactyly.

Methods and results: Here we show that *Gata6*$^{+/-}$ mice develop pre-axial polydactyly (extra digit near the toe) and/or SD (fusion of digits) of the lower limbs. We show that GATA6 lead to polydactyly via induction of mesenchymal cell proliferation by dysregulation of SOX9 and SHH signaling and to SD via disrupted interdigital cell death. Therefore, we suggest a potential common role for GATA6 in regulating, in a dosage sensitive manner, multiple processes governing heart and limb morphogenesis, including cell proliferation and ECM remodeling and maturation as well as cell death induction.

Conclusion: Together, the data helps in including *GATA6* in the list of genes whose mutations are potentially associated with combined heart and limb abnormalities.

Keywords: GATA6 - SOX9 – Polydactyly – Syndactyly - heart-limb defects

4.7. Introduction

Cell death is a mechanism by which highly organized cells, forming complex tissues, activate an intracellular death program as a mechanism of auto-regulation. This process is critical for normal organism development and is considered a vital component of various processes including normal cell turnover, embryonic development, and normal development and function of the immune system. It usually balances cell division by preventing tissues from over growing and becoming abnormal specifically in the ones where the number of cells should be reduced at a specific developmental stage [1]. In some cases, cells die when the structure they formed is no longer needed; such is the case of valve cushions during valvulogenesis and valve remodeling. After EMT and cushion formation, the thick cushions undergo extensive compaction (ECM degradation and cell death) which leads to reduction in cell number and attenuation of the cushions into trilaminar organized thin leaflets [2]. In other cases, cell death serves in defining the digits in the developing limb bud during mouse embryogenesis. The limb bud appears first to have a spadelike structure which then starts to transform into individual digits that only separate as the cells between them die [1]. Throughout the past years, studies have identified most of the genes that control the killing process of programmed cell death, which acts via various pathways.

Digit patterning is a complex process requiring orchestrated signals involved in the regulation of cell proliferation, differentiation, and death, along the different limb axes: the anteroposterior (A-P), the proximo-distal (P-D) and the dorsal ventral (D-V) axes (**Figure 4.1 A**). The A-P axis is determined by diffusion of a secreted protein, SHH, from the zone of polarizing activity (ZPA) located at the posterior pole, whose role is to dictate to the limb bud mesenchymal cells their A-P fate. Experimental evidence has shown that mesenchymal

cells previously expressing SHH as part of the ZPA, contribute to the formation of posterior digits 3 to 5, whereas cells exposed for a long time to SHH signaling, contribute to digit 2 and partly digit 3 [3]. The thumb (the most anterior digit) does not require SHH signaling but rather depends on expression of the Sal-like 4 (SALL4), T-box 5 (TBX5) and HOX transcriptional regulators [1].The P-D axis gives rise to the different compartments of the limb and is characterized by the presence of the AER in the distal zone. Cells of the AER mainly produce members of the fibroblast growth factors (FGFs) ensuring the specification of this axis at early stages. Studies have shown that in the limb bud, retinoic acid induces proximal cell identity whereas the AER-FGFs induce distal cell identity [4]. This process is known as the two-signal model. The regulated spatiotemporal expression and the cross talk between signals important in the specification of both axes are crucial factors to ensure proper limb bud outgrowth, digit determination and chondrogenic differentiation (reviewed in [1]). The dorsal (knuckles, nails) and ventral (pads, soles) polarity of the limb bud is determined by the ectodermal layer surrounding it with WNT-7a being the most important molecule required for its specification [5] (**Figure 4.1 A**).

Limb and musculoskeletal defects are abnormalities of the upper and/or the lower limbs that occur during pregnancy and result from failure of proper formation of either the whole limb, or part of it. In 2007, epidemiological studies show that the incidence of congenital limb defects (CLD) varies from 3.5/10,000 to 2.27/1000 births depending on the country [6,7]. These defects range from severe forms such as absence of part or the entire limb, to more subtle defects such as polydactyly, defined as presence of extra digits, and syndactyly (SD), which is a fusion between two or more digits. Accounting for 1/2000 births, SD is considered one of the most common CLD [8]. It is found to affect males twice as much

as females and to involve feet more frequently than hands [9]. The spectrum of SD defects ranges from a simple interdigital skin webbing to complete bone fusion. SD can be presented as sporadic, or inherited autosomal dominant/recessive, or X-linked diseases [10]. Genetic evidence resulting from human and mice knockout studies contributed to date to our understanding of SD and identified (TFs) (*Hox11/12/13, Sp6*), matrix proteins (*Lama5, Itga3/6, Adamts5/9/20*) and signaling molecules (*Sostdc1, Sfrp2, Ptch1*) as contributors to the SD phenotype (reviewed in **Tables 4.1 and 4.2**). However, there are still large gaps in *our* knowledge of SD that need to be addressed. GATA6 is a ZF TF whose role in the heart has been extensively studied. A recent report revealed its involvement in limb bud formation and determination of the A-P axis [11]. Here we show that *Gata6* haploinsufficiency leads to preaxial polysyndactyly (PPSD) - additional digit towards digit 1 and is fused to it - only in hindlimbs of *Gata6* heterozygous mice. Our results confirm a role for GATA6 in the regulation of cell proliferation via controlling the expression of the secreted protein SHH and the TF sex-determining SOX9, which underlie the polydactyly phenotype in *Gata6*$^{+/-}$ mice. On the other hand, abnormal interdigital cell death (ICD) as well as dysregulated SOX9/WNT/β-CATENIN/FGF signaling is leading to SD in *Gata6*$^{+/-}$ hindlimbs. Together, our results indicate that GATA6 is a crucial regulator of limb bud morphogenesis and digit patterning.

4.8. Materials and Methods

***Animals* and *Histology*.** Mouse handling and experimentation were performed in accordance with institutional guidelines. All protocols were approved by the institutional Animal Care committee of the University of Ottawa. *Gata6* heterozygous (*Gata6*$^{+/-}$, C57/B6) mice were previously described [12]. Staged mouse embryos tissues were fixed with 4% paraformaldehyde in PBS, paraffin embedded, sectioned at 4-μm intervals, and processed.

Immunohistochemistry. Immunohistochemical studies were performed as described previously [13]. Briefly, sections were blocked with 5% BSA for an hour and incubated in the primary antibody overnight at 4°C. After rinsing with PBS, the sections were incubated with the secondary antibody for 45 min followed by the streptavidin-HRP conjugated antibody for 30min. The GATA6 antibody [14] was used at a dilution of 1/1000. Goat polyclonal IgG GATA4 (C20) antibody was purchased from SANTA CRUZ (SC-1237X; dilution 1/600). The Anti-phospho-Histone H3 (Ser10) antibody was from MILLIPORE (06-570, dilution 1/750). SOX9 and cleaved VCAN antibodies were purchased from ABCAM (ab3697; dilution 1/100 and ab177480, dilution 1/250). The biotinylated anti-Goat IgG and anti-Rabbit antibodies were from Vector Laboratories (BA5000) and Jackson (Cederlane) (711-065-152) respectively. Streptavidin-HRP conjugate was from Perkin Elmer (NEL 750000 1EA).

Skeletal preparation. De-skinned newborns were stained with 0.015% Alizarin Red in 70% ethanol and 13% glacial acetic acid for 3 days, cleared in 0.5% KOH overnight and stored in glycerin.

X rays. Images were acquired by the cardiac imaging department at the University of Ottawa Heart Institute using the DRX Carestream Revolution Mobile X-ray system. Images were

taken on a 24x30cm Ciesium Scintillator digital detector using technical factors of apx. 55 kVp at 0.6 mAs.

***RNA analysis*.** Total RNA was isolated from snap-frozen right and left limb buds of E11.5 embryos with TRIzol reagent (Life technologies, 15596018) using FastPrep beads (MP-Bio, 6913-100); cDNAs were generated using the Omniscript RT kit (Qiagen, 205113). Droplet digital PCR was carried out on the QX200 Biorad Droplet Digital PCR system using cDNA from embryonic limb and using sequence specific primers as indicated and according to manufacturer's protocol. Oligonucleotide sequences are available on request.

Luciferase assay. Transfections were carried out as previously described [15]. The total amount of DNA was maintained constant by adding the appropriate amount of empty DNA vector. Full length SOX9-Luc reporter construct was a kind gift from Dr. Sergio Jimenez and was previously described [16].

Electrophoretic mobility shift assays. Nuclear extracts from AD293 cell line overexpressing GATA6 WT protein were used. The DNA binding activity of GATA6 protein was assessed using nuclear extracts and GATA site from the SOX9 promoter as described previously [14].

TUNEL. Apoptag kit was used according to the manufacturer's instructions to end label Terminal deoxynucleotidyl transferase-mediated dUTP (TUNEL) (Intergen, Purchase, NY, USA).

***Statistics*.** For gene expression analysis, values are presented as means + standard error of the mean (SEM). *P* values were generated using Student's 2-tailed *t* test. *P* values < 0.05 were considered as an index of statistical significance.

4.9. Results

4.9.1. *Gata6* haploinsufficient mice display limb abnormalities.

Examination of *Gata6*$^{+/-}$ forelimbs and hindlimbs revealed that 29% of *Gata6*$^{+/-}$ (30 out of 103 *Gata6*$^{+/-}$) have limb abnormalities, more specifically PPSD in their hindlimbs, with no abnormalities observed in their forelimbs: 1) pre-axial polydactyly presented as an extra digit located near the thumb, and 2) SD presented as fusion of the first 2 digits (**Table 4.3 and Figure 4.1 B**). The PPSD in most of the cases occurred unilaterally (right 23/30 or left 2/30 and 5/30 bilateral). Multiple presentations of limb abnormalities were observed in *Gata6*$^{+/-}$ ranging from partial to complete PPSD (**Figure 4.1 B**). Xray imaging also revealed variations in the polydactyly phenotype, where in some cases the digits were completely separate or shared the same metatarsal bones (*bones* between the ankle and toes) but had different phalanges (**Figure 4.1A, B and C**). Alizarin red bone staining protocol was performed on P0 *Gata6*$^{+/+}$ and *Gata6*$^{+/-}$ to visualize limb deformities right after birth which showed polydactyly and digit fusion in the anterior region of the feet in *Gata6*$^{+/-}$ mice (**Figure 4.1 D**). Little is known about the role of GATA6 in skeletal muscle and limb formation. Therefore, the expression of GATA6 as well as the expression of GATA4 in forelimbs and hindlimbs of control mice at E11.5 and E13.5 was assessed by immunohistochemistry (IHC) staining. At E13.5, very low expression levels of GATA4 and GATA6 (interdigital region) were detected in the control forelimbs (**Figure 4.2 A**). While extremely low levels of GATA4 were detected in the hindlimb, a significant expression of GATA6 highlighted the anterior region of the hindlimb with lower expression in the posterior part (**Figure 4.2 A**). Expression levels of GATA6 were also assessed in E11.5 control limb buds, comparing left and right hindlimbs (LH and RH), using digital PCR.

Results showed that GATA6 levels in the RH are significantly lower than those in the LH, mimicking the expression levels of the paired like homeodomain 2 (PITX2), a marker of L-R asymmetry with a left predominance (**Figure 4.2 B**) [17].

4.9.2. *Gata6* haploinsufficiency leads to Polydactyly.

Genetic evidence from mouse and human studies has contributed to date to our understanding of polydactyly and showed that polydactyly is often a result of single mutations. These studies revealed that polydactyly is mainly the result of defective anterior-posterior (A-P) axis patterning of the developing limb and can occur as an isolated malformation or as part of a more complex syndrome. Therefore, we checked, using qRT-PCR, the expression of key regulators of limb development as well as the expression of genes that have been linked to polydactyly (**Figure 4.2 C and 4.3 A**). Kozhemyakina *et al.* reported in 2014 that homozygous specific deletion of *Gata6* from the limb bud results in pre-axial polydactyly [11] further supporting our own observation on *Gata6*$^{+/-}$ mice. They suggested that SHH signaling played a key role in the mechanism of the observed polydactyly. In fact, the secreted molecule SHH, a marker of the posterior region of the limb, is known for its role in digit patterning and cell proliferation [18–20]. Therefore, expression of its receptor patched 1 (PTCH1) as well as its downstream targets GLI family zinc finger 1 and 3 (GLI1/GLI3) and zinc finger of the cerebellum 3 (ZIC3) was evaluated. Whereas no changes in expression of GLI1 and GLI3 (**Figure 4.2C and 4.3A**) occurred, expression of PTCH1was increased in hindlimbs of *Gata6*$^{+/-}$ when compared to *Gata6*$^{+/+}$ littermates (**Figure 4.3 B**). Our results, in addition to the previous findings by Kozhemyakina *et al*. 2014, support a dysregulated SHH signaling which is affecting the A-P axis patterning and leading to polydactyly in *Gata6*$^{+/-}$ mice.

Sex determining region-Y (SOX9) is a TF known to be expressed in committed chondroprogenitor cells and differentiated chondrocytes during limb development. These cells undergo mesenchymal condensation, a critical step in defining the shape, size and number of the primordia of the skeletal elements [21]. *Sox9* haploinsufficiency leads to defective mesenchymal condensations and to premature skeletal mineralization [22]. On the other hand, misexpression of *Sox9* from the limb bud mesenchyme triggers the formation of ectopic mesenchymal condensations resulting in hindlimb polydactyly [23]. qRT-PCR performed on E11.5 limbs from *Gata6*$^{+/+}$ and *Gata6*$^{+/-}$ showed a significant downregulation of SOX9 in both the RH and LH (**Figure 4.3 A**). Interestingly, GATA6 has been shown to play a role in chondrogenesis since abundant levels of GATA6 were detected in pre-cartilaginous condensations (PCCs), in both the axial and appendicular skeleton of mouse embryos, and in committed primary chondrocyte precursors [24].

Given the important role of SOX9 during skeletal patterning and its abnormal expression in *Gata6*$^{+/-}$ mice, we decided to examine whether SOX9 is a direct target of GATA6 during limb morphogenesis. IHC staining in E14.5 embryos revealed a dysregulated protein expression of SOX9 in cells of the digital limb (**Figure 4.3 C**). To test whether GATA6 is able to transcriptionally regulate expression of *SOX9*, analysis of *SOX9* promoter region was done revealing the presence of two main GATA binding sites along with 5 GATA-like sites in its upstream region. NIH3T3 cells transfected with increasing concentration of human GATA6, along with SOX9 luciferase-fused promoter, showed that GATA6 can significantly activate the *SOX9* promoter in a dose dependent manner (**Figure 4.3 D and E**). GATA6 was also tested for its ability to bind SOX9-GATA consensus site using electrophoretic mobility-shift assay. We show, using a radiolabeled probe (32P) harboring a GATA element from the *SOX9* promoter, that GATA6 is able to bind to this

consensus region on the *SOX9* promoter and that this binding is completely abolished when competitor unlabeled oligonucleotides are added at 100-fold excess (**Figure 4.3 E**). Our results imply that GATA6 plays an important role during limb formation and digit determination processes.

4.9.3. *Gata6* haploinsufficiency leads to Syndactyly.

During limb development, ICD occurs at the level of the mesenchyme situated between the forming digits (the condensed cartilage), starting from the distal region underlying the AER. This process is critical to assure a proper digit separation and occurs between E13 and E14.5 in mice. It has been shown that dying cells are mainly detected in the ventral side of interdigital regions despite the fact that more digit separation occurs on the dorsal side, in addition to a dominance of ICD in the anterior region when compared to the posterior one [25]. Reduced or absent ICD results in evident soft tissue remaining between digits therefore resulting in SD. Complete simple SD is observed when signals promoting cell death are missing whereas those inducing growth remain active. On the other hand, partial SD results from reduced cell death with no change in interdigital tissue growth [26]. To determine whether excessive proliferation might be contributing to the SD phenotype in *Gata6*$^{+/-}$ mice, sections from E14.5 limb embryos were stained for Phosphohistone H3 (PH3) antibody. Total number of cells in the big toe (digit 1) and in the middle toe (digit 3) - including the interdigital regions nearby- was counted as well as the number of PH3+ cells. Results showed no difference in proliferation between *Gata6*$^{+/+}$ and *Gata6*$^{+/-}$ groups (both subgroups: with and without SD) (**Figure 4.4 A**). The percentage of TUNEL positive cells over the total number of cells in digits 1 and 3 was also evaluated in E14.5 limbs to check if a dysregulated cell death mechanism is contributing to the SD phenotype. While no changes

were obvious in *Gata6*$^{+/-}$ with normal limbs, we observed a significant reduction in the percentage of dead cells in *Gata6*$^{+/-}$ with PPSD when compared to control groups (**Figure 4.4 B**). In addition to cell death, web regression requires the degradation of the ECM, rich in hyaluronan, fibronectin, proteoglycans, and collagenase which has a major role in its regression. ADAMTs, important proteases composing the ECM, are able to cleave the proteoglycan VCAN, generating a specific C-term neo-epitope (DPEAAE) that can be detected by IHC [27]. Staining for cleaved VCAN revealed a marked reduction in its expression in the interdigital region with tissue persistent SD, whereas it was normally present in the interdigital webs of control mice (**Figure 4.4 C**).

The major regulators of distal and proximal ICD include members of the fibroblast growth family (FGF4, FGF8 and FGFR2), msh homeobox members (MSX1and 2), the retinoic acid and the WNT/β-CATENIN signaling [26]. Members of the bone morphogenetic program (BMP4, BMP7 and BMPR1A) play an important role in cell death during limb development since inhibition of the BMP signaling results in tissue SD and polydactyly [28]. qRT-PCR analysis performed on right and left limbs from *Gata6*$^{+/+}$ and *Gata6*$^{+/-}$ did not reveal any changes in expression of BMP4, BMP7 as well as MSX1 however expressions of β-catenin, FGF4 and Laminin 5 (LAMA5) were upregulated in both the left and right hindlimbs (**Figure 4.3 A and 4.4 D**). Interestingly, overexpression of FGF4 or β-CATENIN in the limb bud of transgenic mice lead to SD due to reduced ICD [29,30]. Taken together, these results suggest that the SD phenotype observed in *Gata6*$^{+/-}$ mice is due to a reduction in the ICD process along with a dysregulation of important ICD regulators, therefore contributing to the persistence of soft tissue in the anterior region of the hindlimb.

4.10. Discussion

During limb bud outgrowth and specification, disrupted signaling affecting any of the axes can result in limb and digit anomalies. Conditional deletion of *Gata6* from the limb bud results in the perturbation of the A-P axis and pre-axial polydactyly due to dysregulated expression of SHH [11]. The downregulation of SHH in the *Prx1-cre*-mediated homozygous *Gata6* inactivation rescues the digit phenotype. However, the limitation of this study resides in their use of *Prx1-cre* for the conditional inactivation of *Gata6*: *Prx1-cre* is not expressed in the entire hindlimb bud, therefore leading to a hypomorph mutation in the hindlimb and a complete inactivation in the forelimb. In this study, we show that *Gata6* haploinsufficiency leads to PPSD. Our results are consistent with the previously reported role for GATA6 as an upstream regulator of SHH [11]. In addition, we report a role for GATA6 in regulating the expression of SOX9 within the limb bud. We suggest that GATA6 works upstream of SHH and SOX9, inhibiting SHH expression in the anterior region whereas promoting expression of SOX9 (**Figure 4.5**). In the case of *Gata6* haploinsufficiency, SHH inhibition is removed, and expression of SOX9 is downregulated, therefore maintaining mesenchymal cell proliferation active. On the other hand, SOX9 is known to inhibit the WNT/β-CATENIN signaling. Hence, increased expression of β-CATENIN resulting from the dysregulated expression of SOX9 in *Gata6*$^{+/-}$ mice leads, along with the dysregulated expression of SHH, to the formation of preaxial-polydactyly. SD in *Gata6*$^{+/-}$ mice, on the other hand, results mainly from the deficiency in the ICD, as was shown by TUNEL and VCAN downregulation, which only affects the anterior region of the limb, where GATA6 is predominantly expressed.

It is known that during early embryonic stages, and under the control of different signaling pathways, the mesoderm gives rise to the different cardiac and muscle cell lineages. During this process, any defects in cell migration, proliferation, and differentiation processes, affecting common or overlapping signaling pathways can lead to abnormal organ development. Congenital heart abnormalities and limb malformations are found to occur simultaneously in many types of neonatal syndromes such as EIis-van Creveld syndrome (EVC), Holt-Oram syndrome (HOS) [31] and Timothy syndrome. EVC syndrome for example is an autosomal recessive skeletal dysplasia characterized by the presence of retarded growth and short stature in addition to polydactyly and heart defects mainly ASD occurring in 60% of patients with EVC [32,33]. On the other hand, SD is observed in patients with Timothy syndrome, a condition affecting the heart conduction system- long QT interval [34]. The genetic causes underlying the appearance of these heart and limb phenotypes together remain to date poorly understood.

Limb defects are also found to occur in combination with abnormalities other than CHDs. Acro-renal syndrome refers to a combined occurrence of limb and congenital renal defects. It is a rare disease with only 20 cases reported in the literature with patients displaying a variety of limb and kidney phenotypes [35]. Acro-renal defects can also occur in combination with eye anomalies resulting in the so-called Acro-renal-ocular syndrome (AROS) with patients displaying thumb hypoplasia (underdeveloped thumb), abnormal anatomic location of one or both of the kidneys, and optical canal defects [36]. On the other hand, disorders of the vascular system can also occur in combination with limb abnormalities; such is the case of Parkes Weber syndrome (PWS), characterized by capillary

malformations and overgrowth of bone and soft tissue of one leg, making it longer and larger than the other one [37].

Organs of the human body have different composition and exert specific physiological functions and some share common cellular composition. The knowledge whether the same cell type plays same roles in different tissues is still limited, but studies have shown that common genes are expressed within these tissues. These genes could be controlling either similar pathways or different ones within these tissues. Given this, mutations in these genes could lead to phenotypes affecting both organs. GATA6 is expressed within the heart, pancreas, kidneys, liver, lungs, and ovaries as well as in the central nervous system, and is found to play crucial roles in directing their development and function [38–43]. We previously reported that *Gata6* haploinsufficiency leads to congenital heart abnormalities: RL-BAV with 47% penetrance characterized by a fusion of the heart aortic valve leaflets leading to two asymmetric leaflets instead of three symmetrical ones (**Chapter I**). Interestingly, here we show that in addition to the heart phenotype, these mice have PPSD with 29% partial penetrance. In some instances, both phenotypes occurred simultaneously in the same *Gata6*$^{+/-}$ mouse whereas in others they were observed independently. The incomplete penetrance of BAV and polydactyly observed in *Gata6*$^{+/-}$ are suggestive of a dosage sensitive response for GATA6 in different cell types/structures. Together, these findings support a role for *GATA6* as a candidate heart and limb malformations causing gene, similar to the role of *TBX5* in HOS. Further studies still need to be done to explore defects in other organs of *Gata6*$^{+/-}$ mice, where GATA6 is also found to be highly expressed.

4.11. References

1. Zeller R, López-Ríos J, Zuniga A. Vertebrate limb bud development: moving towards integrative analysis of organogenesis. *Nat Rev Genet*. 2009;10:845–858.

2. Butcher JT, Markwald RR. Valvulogenesis: the moving target. *Philos Trans R Soc Lond B Biol Sci*. 2007;362:1489–1503.

3. Suzuki T. How is digit identity determined during limb development? *Dev Growth Differ*. 2013;55:130–138.

4. Mercader N, Leonardo E, Piedra ME, Martínez-A C, Ros MA, Torres M. Opposing RA and FGF signals control proximodistal vertebrate limb development through regulation of Meis genes. *Dev Camb Engl*. 2000;127:3961–3970.

5. Dealy CN, Roth A, Ferrari D, Brown AM, Kosher RA. Wnt-5a and Wnt-7a are expressed in the developing chick limb bud in a manner suggesting roles in pattern formation along the proximodistal and dorsoventral axes. *Mech Dev*. 1993;43:175–186.

6. Irvine B, Luo W, León JA. Congenital Anomalies in Canada 2013: A Perinatal Health Surveillance Report by the Public Health Agency of Canada's Canadian Perinatal Surveillance System. *Health Promot Chronic Dis Prev Can Res Policy Pract*. 2015;35:21–22.

7. Jaruratanasirikul S, Tangtrakulwanich B, Rachatawiriyakul P, Sriplung H, Limpitikul W, Dissaneevate P, Khunnarakpong N, Tantichantakarun P. Prevalence of congenital limb defects: Data from birth defects registries in three provinces in Southern Thailand. *Congenit Anom*. 2016;56:203–208.

8. Schwabe GC, Mundlos S. Genetics of congenital hand anomalies. *Handchir Mikrochir Plast Chir*. 2004;36:85–97.

9. Castilla EE, Paz JE, Orioli-Parreiras IM. Syndactyly: frequency of specific types. *Am J Med Genet*. 1980;5:357–364.

10. Malik S. Syndactyly: phenotypes, genetics and current classification. *Eur J Hum Genet*. 2012;20:817–824.

11. Kozhemyakina E, Ionescu A, Lassar AB. GATA6 Is a Crucial Regulator of Shh in the Limb Bud. *PLoS Genet*. 2014;10.

12. Laforest B, Nemer M. GATA5 interacts with GATA4 and GATA6 in outflow tract development. *Dev Biol*. 2011;358:368–378.

13. Laforest B, Andelfinger G, Nemer M. Loss of Gata5 in mice leads to bicuspid aortic valve. *J Clin Invest*. 2011;121:2876–2887.

14. Nemer G, Nemer M. Transcriptional activation of BMP-4 and regulation of mammalian organogenesis by GATA-4 and -6. *Dev Biol*. 2003;254:131–148.

15. Nemer G, Nemer M. Cooperative interaction between GATA5 and NF-ATc regulates endothelial-endocardial differentiation of cardiogenic cells. *Dev Camb Engl*. 2002;129:4045–4055.

16. Piera-Velazquez S, Hawkins DF, Whitecavage MK, Colter DC, Stokes DG, Jimenez SA. Regulation of the human SOX9 promoter by Sp1 and CREB. *Exp Cell Res*. 2007;313:1069–1079.

17. Ryan AK, Blumberg B, Rodriguez-Esteban C, Yonei-Tamura S, Tamura K, Tsukui T, de la Peña J, Sabbagh W, Greenwald J, Choe S, Norris DP, Robertson EJ, Evans RM, Rosenfeld MG, Belmonte JCI. Pitx2 determines left–right asymmetry of internal organs in vertebrates. *Nature*. 1998;394:545–551.

18. Chiang C, Litingtung Y, Harris MP, Simandl BK, Li Y, Beachy PA, Fallon JF. Manifestation of the limb prepattern: limb development in the absence of sonic hedgehog function. *Dev Biol*. 2001;236:421–435.

19. Kraus P, Fraidenraich D, Loomis CA. Some distal limb structures develop in mice lacking Sonic hedgehog signaling. *Mech Dev*. 2001;100:45–58.

20. Zhu J, Nakamura E, Nguyen M-T, Bao X, Akiyama H, Mackem S. Uncoupling Sonic hedgehog control of pattern and expansion of the developing limb bud. *Dev Cell*. 2008;14:624–632.

21. Akiyama H, Kim J-E, Nakashima K, Balmes G, Iwai N, Deng JM, Zhang Z, Martin JF, Behringer RR, Nakamura T, de Crombrugghe B. Osteo-chondroprogenitor cells are derived from Sox9 expressing precursors. *Proc Natl Acad Sci U S A*. 2005;102:14665–14670.

22. Bi W, Huang W, Whitworth DJ, Deng JM, Zhang Z, Behringer RR, de Crombrugghe B. Haploinsufficiency of Sox9 results in defective cartilage primordia and premature skeletal mineralization. *Proc Natl Acad Sci U S A*. 2001;98:6698–6703.

23. Akiyama H, Stadler HS, Martin JF, Ishii TM, Beachy PA, Nakamura T, de Crombrugghe B. Misexpression of Sox9 in mouse limb bud mesenchyme induces polydactyly and rescues hypodactyly mice. *Matrix Biol J Int Soc Matrix Biol*. 2007;26:224–233.

24. Alexandrovich A, Qureishi A, Coudert AE, Zhang L, Grigoriadis AE, Shah AM, Brewer AC, Pizzey JA. A role for GATA-6 in vertebrate chondrogenesis. *Dev Biol*. 2008;314:457–470.

25. Salas-Vidal E, Valencia C, Covarrubias L. Differential tissue growth and patterns of cell death in mouse limb autopod morphogenesis. *Dev Dyn Off Publ Am Assoc Anat*. 2001;220:295–306.

26. Hernández-Martínez R, Covarrubias L. Interdigital cell death function and regulation: new insights on an old programmed cell death model. *Dev Growth Differ*. 2011;53:245–258.

27. Sandy JD, Westling J, Kenagy RD, Iruela-Arispe ML, Verscharen C, Rodriguez-Mazaneque JC, Zimmermann DR, Lemire JM, Fischer JW, Wight TN, Clowes AW. Versican V1 proteolysis in human aorta in vivo occurs at the Glu441-Ala442 bond, a site that is cleaved by recombinant ADAMTS-1 and ADAMTS-4. *J Biol Chem*. 2001;276:13372–13378.

28. Guha U, Gomes WA, Kobayashi T, Pestell RG, Kessler JA. In vivo evidence that BMP signaling is necessary for apoptosis in the mouse limb. *Dev Biol*. 2002;249:108–120.

29. Lu P, Minowada G, Martin GR. Increasing Fgf4 expression in the mouse limb bud causes polysyndactyly and rescues the skeletal defects that result from loss of Fgf8 function. *Dev Camb Engl*. 2006;133:33–42.

30. Villacorte M, Suzuki K, Hayashi K, de Sousa Lopes SC, Haraguchi R, Taketo MM, Nakagata N, Yamada G. Antagonistic crosstalk of Wnt/beta-catenin/Bmp signaling within the Apical Ectodermal Ridge (AER) regulates interdigit formation. *Biochem Biophys Res Commun*. 2010;391:1653–1657.

31. Basson CT, Bachinsky DR, Lin RC, Levi T, Elkins JA, Soults J, Grayzel D, Kroumpouzou E, Traill TA, Leblanc-Straceski J, Renault B, Kucherlapati R, Seidman JG, Seidman CE. Mutations in human TBX5 [corrected] cause limb and cardiac malformation in Holt-Oram syndrome. *Nat Genet*. 1997;15:30–35.

32. Huber C, Cormier-Daire V. Ciliary disorder of the skeleton. *Am J Med Genet C Semin Med Genet*. 2012;160C:165–174.

33. Kamal R, Dahiya P, Kaur S, Bhardwaj R, Chaudhary K. Ellis-van Creveld syndrome: A rare clinical entity. *J Oral Maxillofac Pathol JOMFP*. 2013;17:132–135.

34. Lo-A-Njoe SM, Wilde AA, Erven L van, Blom NA. Syndactyly and long QT syndrome (CaV1.2 missense mutation G406R) is associated with hypertrophic cardiomyopathy. *Heart Rhythm*. 2005;2:1365–1368.

35. Natarajan G, Jeyachandran D, Subramaniyan B, Thanigachalam D, Rajagopalan A. Congenital anomalies of kidney and hand: a review. *Clin Kidney J*. 2013;6:144–149.

36. Halal F, Homsy M, Perreault G. Acro-renal-ocular syndrome: autosomal dominant thumb hypoplasia, renal ectopia, and eye defect. *Am J Med Genet*. 1984;17:753–762.

37. Revencu N, Boon LM, Mulliken JB, Enjolras O, Cordisco MR, Burrows PE, Clapuyt P, Hammer F, Dubois J, Baselga E, Brancati F, Carder R, Quintal JMC, Dallapiccola B, Fischer G, Frieden IJ, Garzon M, Harper J, Johnson-Patel J, Labrèze C, Martorell L, Paltiel HJ, Pohl A, Prendiville J, Quere I, Siegel DH, Valente EM, Van Hagen A,

Van Hest L, Vaux KK, Vicente A, Weibel L, Chitayat D, Vikkula M. Parkes Weber syndrome, vein of Galen aneurysmal malformation, and other fast-flow vascular anomalies are caused by RASA1 mutations. *Hum Mutat*. 2008;29:959–965.

38. Cai KQ, Caslini C, Capo-chichi CD, Slater C, Smith ER, Wu H, Klein-Szanto AJ, Godwin AK, Xu X-X. Loss of GATA4 and GATA6 Expression Specifies Ovarian Cancer Histological Subtypes and Precedes Neoplastic Transformation of Ovarian Surface Epithelia. *PLoS ONE*. 2009;4.

39. Decker K, Goldman DC, Grasch CL, Sussel L. Gata6 is an important regulator of mouse pancreas development. *Dev Biol*. 2006;298:415–429.

40. Kamnasaran D, Guha A. Expression of GATA6 in the human and mouse central nervous system. *Brain Res Dev Brain Res*. 2005;160:90–95.

41. Viger RS, Guittot SM, Anttonen M, Wilson DB, Heikinheimo M. Role of the GATA Family of Transcription Factors in Endocrine Development, Function, and Disease. *Mol Endocrinol*. 2008;22:781–798.

42. Yang H, Lu MM, Zhang L, Whitsett JA, Morrisey EE. GATA6 regulates differentiation of distal lung epithelium. *Dev Camb Engl*. 2002;129:2233–2246.

43. Zhao R, Watt AJ, Li J, Luebke-Wheeler J, Morrisey EE, Duncan SA. GATA6 is essential for embryonic development of the liver but dispensable for early heart formation. *Mol Cell Biol*. 2005;25:2622–2631.

Table 4.1: Mouse models of hindlimb and forelimb syndactyly and polysyndactyly

Gene	Genotype	Phenotype of Hindlimb	Phenotype of Forelimb	Pubmed ID
SP6	$Sp6^{-/-}$	Syndactyly of digits III and IV	Syndactyly of digit II and III or II, III, IV	18297738
HOXD13	Spdh/Spdh		Preaxial/postaxial/central Polysyndactyly	11850178
	$Hoxd13^{+21Ala}$, Spdh/Spdh		Postaxial Polysyndactyly	19075394
HOX11,12,13	Del/Del	Polysyndactyly	Polysyndactyly	8900279
ADAMTS9	Prx1-Cre; $Adamts9^{del/flox}$	Syndactyly	Syndactyly	24753090
MEGF7	$Megf7^{-/-}$	Polysyndactyly	Polysyndactyly	16207730
LAMA5	$Lama5^{-/-}$	Syndactyly	Syndactyly	9852162
NID1, NID2	$Nid1^{-/-}$ $Nid2^{-/-}$	Syndactyly	Syndactyly	17023412
ADAMTS5	$Adamts5^{-/-}$;bt/bt	Syndactyly		19922873
PTCH1	$Ptch1DL/Ptch1^{null}$	Preaxial Polysyndactyly	Preaxial Polysyndactyly	23897749
WDR35	$Wdr35^{yet/yet}$	Postaxial Polysyndactyly	Postaxial Polysyndactyly	21473986
SFPR2	$Sfpr2^{-/-}$	Preaxial Polysyndactyly	Preaxial Polysyndactyly	18729207
SOSTDC1	$Sostdc1^{-/-}$		Preaxial Polysyndactyly	23994639

Table 4.2: Human mutations causing polysyndactyly

Gene	Syndrome	Cardiac defect	Pubmed ID
BBS20	Bardet-Biedl Syndrome	NS	26763875
EVC	Ellis van-Creveld Syndrome	Hypoplastic left heart with mitral valve stenosis, aortic valve astresia, , left ventricule outflow track obstruction, ventricular septal defect	23220543
EVC2	Ellis-van Creveld syndrome	NS	21815252
GLI3	preaxial-postaxial Polysyndactyly complex	NS	25267529
	Complex digital anomalies	NS	21320477
	Accrocallosal syndrome	NS	23633388
	Non-syndromic digital anomalies	NS	21320477
HOXD13	Non-syndromic Polysyndactyly	NS	26581570
NEK1	Short rib-polydactyly syndrome type III (Verma-Naumoff)	NS	22795106
	Short rib-polydactyly syndrome type II (Majewski)	NS	22482978
RAB23	Carpenter syndrome	Enlarged heart, septal defects, patent ductus arteriosus	25168863
WDPCP	Orofaciodigital syndrome	coarctation of the aorta	25427950
ZRS	Non-syndromic Polysyndactyly	NS	22786669
	Townes-Brocks syndrome	Atrial septal defect, patent ductus arteriosus	22903933

NS: non specified

Table 4.3: Limb phenotype in *Gata6*$^{+/-}$ mice (n=215)

	***Gata6*$^{+/+}$**	***Gata6*$^{+/-}$**
Expected mendelian ratio (%)	50	50
Observed ratio (%)	52.1	47.9
Normal Forelimbs (n)	112	103
Forelimbs with polydactyly/syndactyly (n)	0	0
% of Forelimbs polydactyly/polysyndactyly		**0%**
Normal Hindlimbs (n)	112	73/103
Hindlimbs with polydactyly/ synpolydactyly (n):	0	30/103
RH only		23/30
LH only		2/30
RH and LH		5/30
% of Hindlimbs polydactyly/polysyndactyly		**29%**

n= number of mice

Figure 4.1

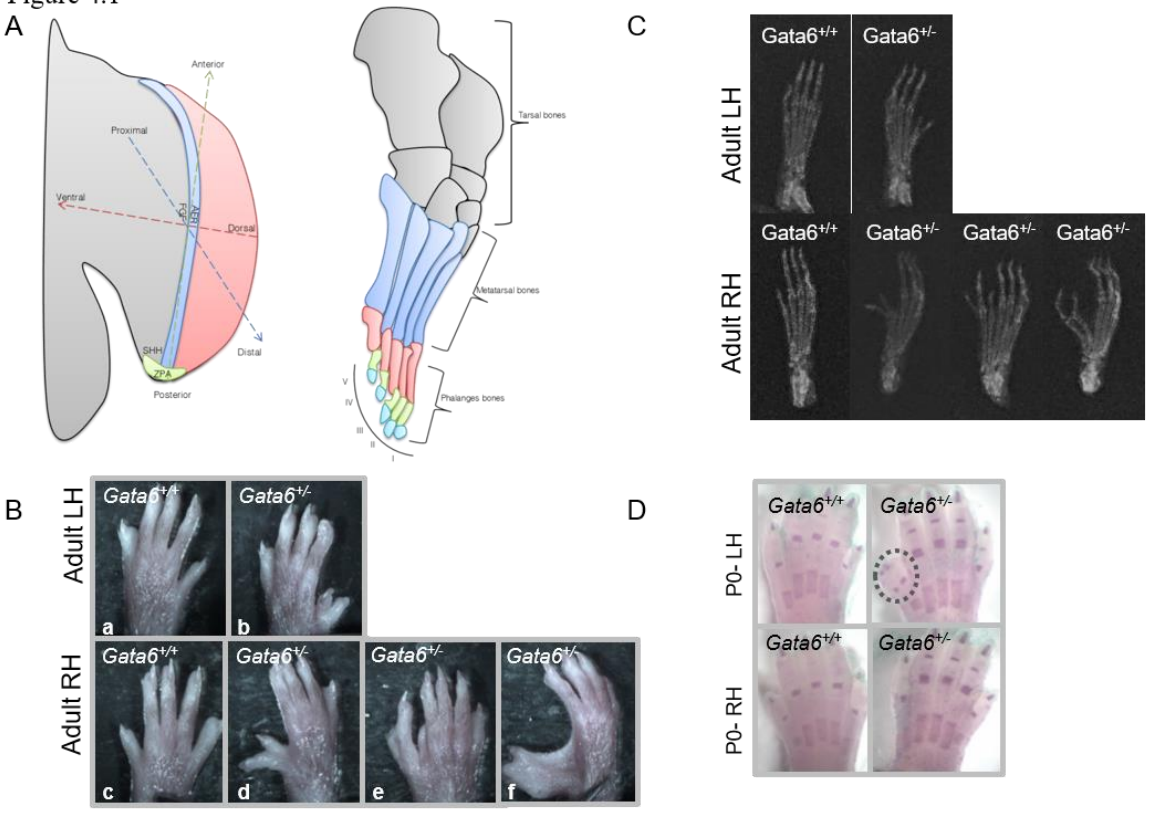
A
Anterior
Proximal
Ventral
Dorsal
Distal
Posterior
SHH
ZPA
Tarsal bones
Metatarsal bones
Phalanges bones
C
Adult LH
Adult RH
Gata6+/+
Gata6+/-
B
Adult LH
Adult RH
a
b
c
d
e
f
D
P0- LH
P0- RH

Figure 4.1: *Gata6* haploinsufficiency results in hindlimb abnormalities. (A) Representation of the different axes forming the limb bud as well as the different bones forming the hindlimb (foot). **(B and C)** Multiple representations of hindlimb abnormalities in *Gata6*$^{+/-}$ showing left and right polysyndactyly (Xray images shown in pannel B). **(D)** Alizarin red staining of the hindlimbs of P0 *Gata6*$^{+/-}$ mice showing preaxial polysyndactyly which was not present in *Gata6*$^{+/+}$ littermates. RH: right hindlimb. LH: left hindlimb.

Figure 4.2

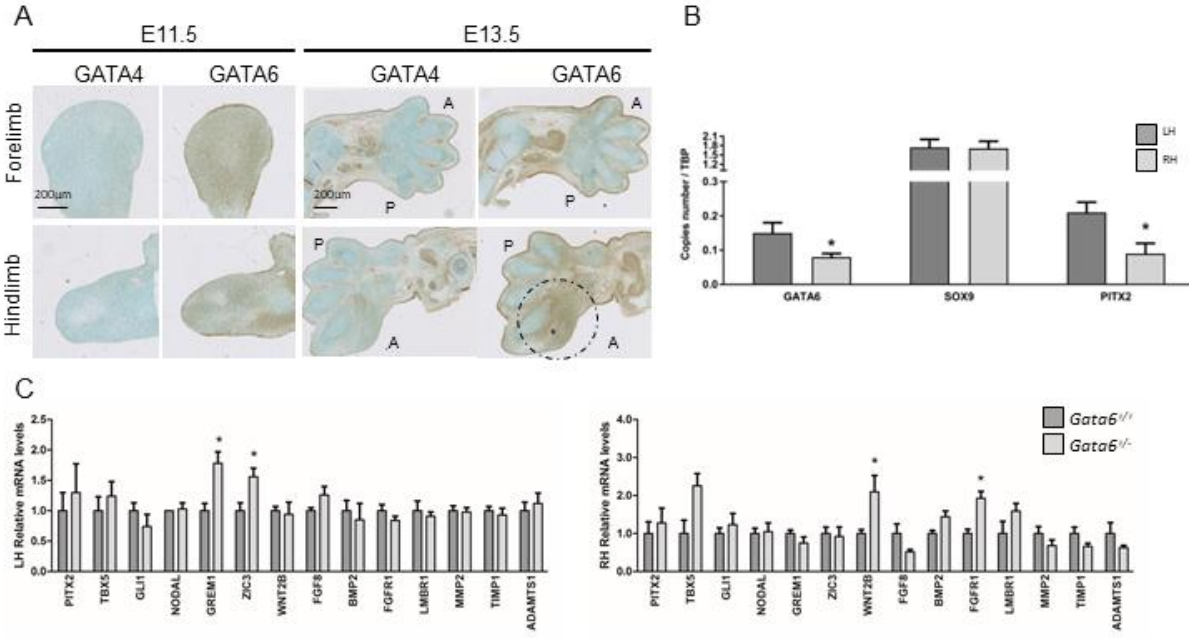
A
E11.5
E13.5
GATA4
GATA6
GATA4
GATA6
Forelimb
Hindlimb
200µm
200µm
A
P
B
LH
RH
Copies number / TBP
GATA6
SOX9
PITX2
C
LH Relative mRNA levels
RH Relative mRNA levels
Gata6+/+
Gata6+/-
PITX2
TBX5
GLI1
NODAL
GREM1
ZIC3
WNT2B
FGF8
BMP2
FGFR1
LMBR1
MMP2
TIMP1
ADAMTS1

Figure 4.2: Expression levels of limb regulators. (A) Immnohistochemistry staining of GATA4 and GATA6 in E11.5 and E13.5 wildtype forelimbs and hindlimbs showing increased expression of GATA6 in the anterior region of the hindlimbs. RH: right hindlimb. LH: left hindlimb. A: anterior. P: posterior. Scale bar: 200µm. **(B)** Expression levels of GATA6, SOX9 and PITX2 assessed by digital PCR in right and left hindlimbs from E11.5 *Gata6*$^{+/+}$ mice. **(C**) Differential expression of regulators of limb development in right and left hindlimbs from E11.5 *Gata6*$^{+/+}$ and *Gata6*$^{+/-}$ embryos. Values are mean + SEM.*$P < 0.05$.

Figure 4.3

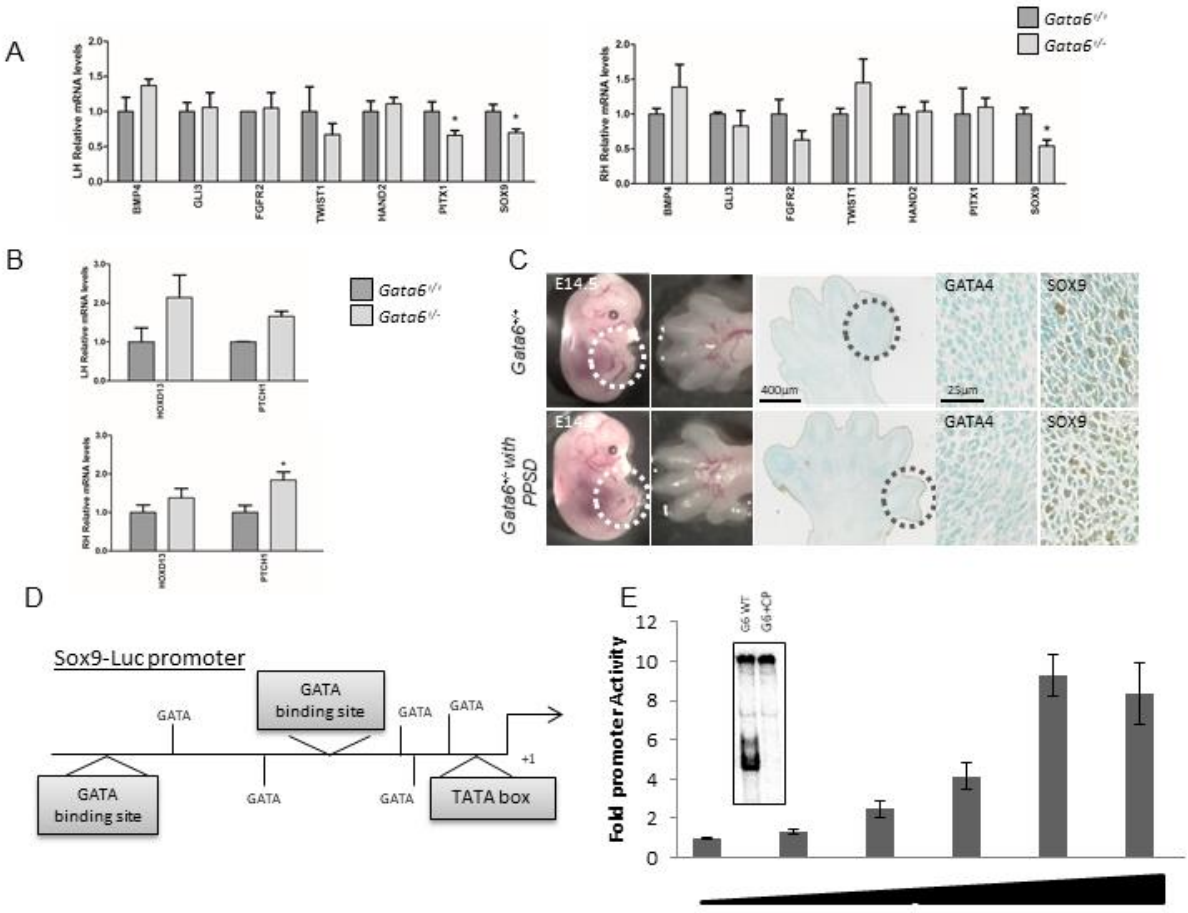
A
LH Relative mRNA levels
RH Relative mRNA levels
BMP4
GLI3
FGFR2
TWIST1
HAND2
PITX1
SOX9
Gata6+/+
Gata6+/-
B
HOXD13
PTCH1
C
E14.5
Gata6+/+
Gata6+/- with PPSD
400um
25um
GATA4
SOX9
D
Sox9-Luc promoter
GATA
GATA binding site
TATA box
+1
E
Fold promoter Activity
G6 WT
G6-ICP

Figure 4.3: GATA6 is an upstream regulator of SOX9. (A and B) Expression of genes linked to polydactyly was assayed by qRT-PCR in right and left hindlimbs from E11.5 *Gata6*$^{+/+}$ and *Gata6*$^{+/-}$ mice E11.5 embryos (n = 3–7 per group). Values are mean + SEM.*P < 0.05. **(C**) Polydactyly representation in E14.5 Gata6$^{+/-}$ hindlimb**.** Immunohistochemistry of GATA4 and SOX9 showing a dysregulated expression of SOX9 in the anterior region of the hindlimb in *Gata6*$^{+/-}$ with polysyndactyly when compared to control littermates (right hindlimb). PPSD: polysyndactyly. Scale bar: 400μm, 25 μm. **(D)** Schematic representation of GATA and GATA-like binding sites on SOX9 full length promoter sequence. **(E)** Transcriptional activity of GATA6 proteins on SOX9-Luc promoter (Ctrl, 25, 70, 125, 250, 500ng). Relative luciferase activities are represented as fold changes. The data are a representative of 3 independent experiments done in duplicates +/- standard error. WT: wildtype control. **DNA binding properties of GATA6**. Electrophoretic mobility shift assay was performed using nuclear extracts from AD293 cells overexpressing GATA6. Results show a strong binding of GATA6 to GATA consensus region from the SOX9 promoter and that this binding is abolished when competitor (CP) unlabeled oligonucleotides are added at 100-fold excess.

Figure 4.4

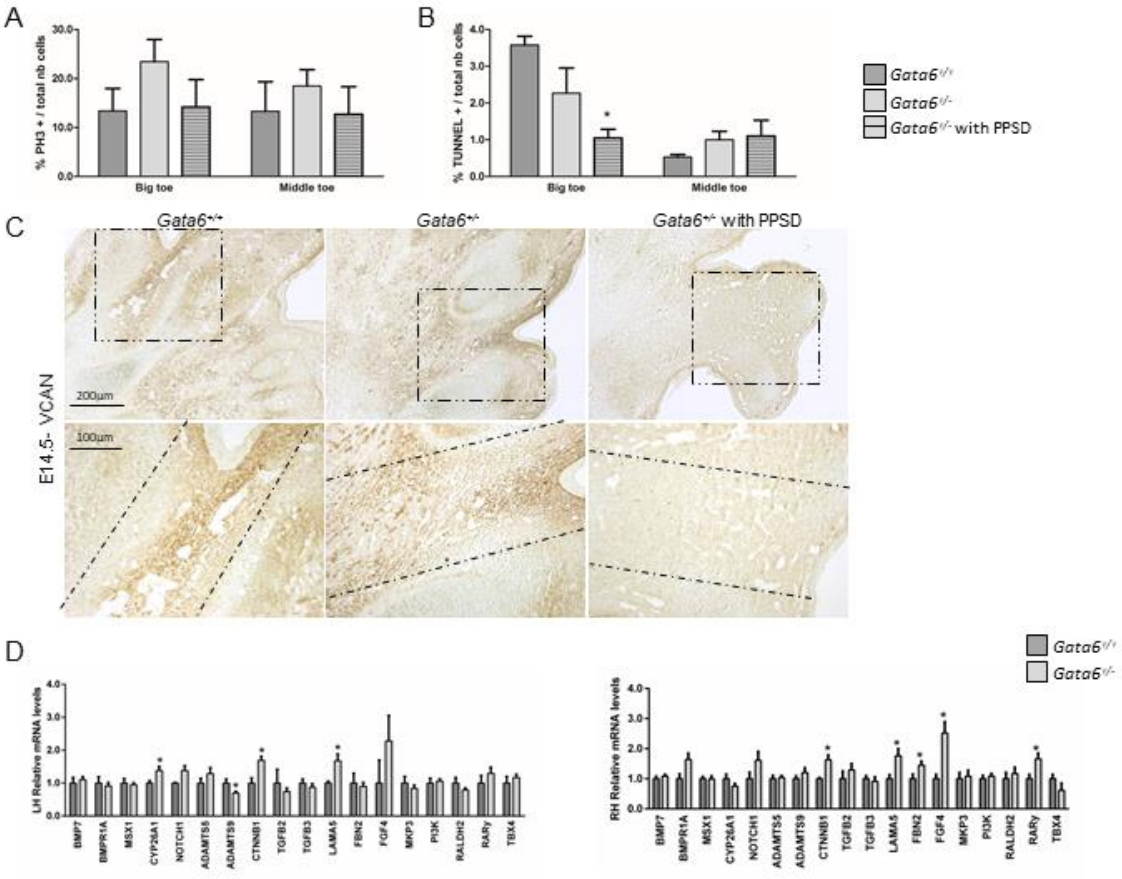
A
% PH3 + / total nb cells
Big toe
Middle toe
B
% TUNNEL + / total nb cells
Big toe
Middle toe
Gata6+/+
Gata6+/-
Gata6+/- with PPSD
C
Gata6+/+
Gata6+/-
Gata6+/- with PPSD
E14.5- VCAN
200µm
100µm
D
Gata6+/+
Gata6+/-
LH Relative mRNA levels
RH Relative mRNA levels
BMP7
BMPR1A
MSX1
CYP26A1
NOTCH1
ADAMTS5
ADAMTS9
CTNNB1
TGFB2
TGFB3
LAMA5
FBN2
FGF4
MKP3
PI3K
RALDH2
RARγ
TBX4

Figure 4.4: Significant cell death deficiency in *Gata6*$^{+/-}$ mice with syndactyly. (A) Counting of phosphohistone (PH3) positive cells within hindlimbs from E14.5 *Gata6*+/- and *Gata6*+/+ did not show differences among groups (*Gata6*$^{+/+}$, normal *Gata6*$^{+/-}$ and *Gata6*$^{+/-}$ with SD, n=4-7). **(B)** TUNEL assay perfomed on hindlimbs from E14.5 embryos sections showing a significant decrease in the TUNEL positive cells in the big toe of *Gata6*$^{+/-}$ with SD when compared to other littermates (*Gata6*$^{+/+}$ and normal *Gata6*$^{+/-}$, n=4-7). Values are mean + SEM.*$P < 0.05$. RH: right hindlimb. LH: left hindlimb. **(C)** Immunohistochemistry of Versican showing a reduction in its expression in the anterior region of *Gata6*$^{+/-}$ with polysyndactyly when compared to control littermates (right hindlimb). PPSD: polysyndactyly. Scale bar: 200μm, 100 μm. **(D)** Expression of genes linked to SD was assayed by qRT-PCR in right and left hindlimbs from E11.5 *Gata6*$^{+/+}$ and *Gata6*$^{+/-}$ mice E11.5 embryos. (n = 3–7 per group).

Figure 4.5

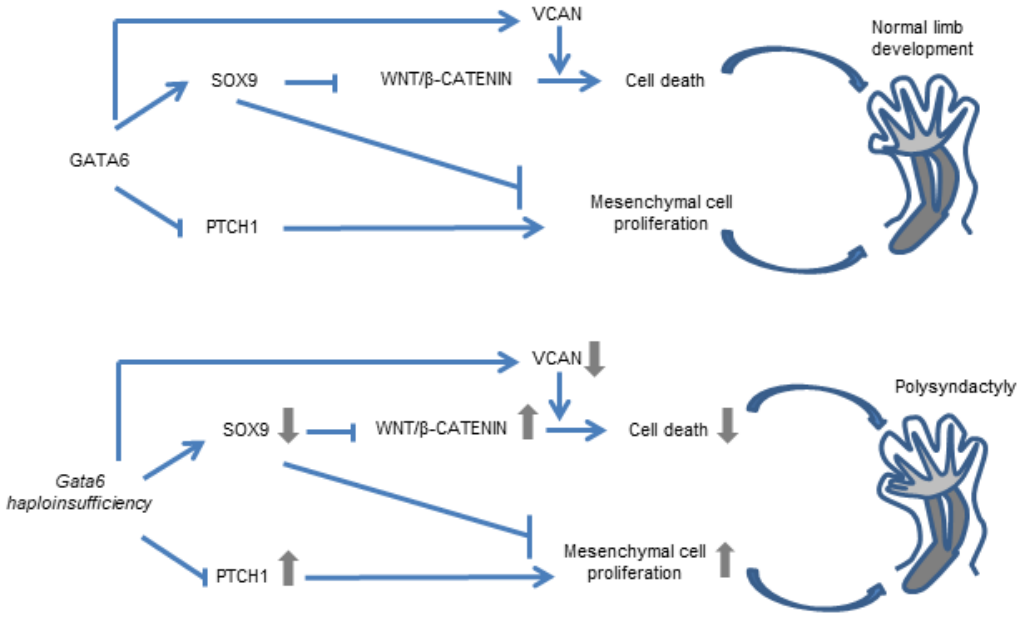
VCAN
Normal limb development
SOX9
WNT/β-CATENIN
Cell death
GATA6
PTCH1
Mesenchymal cell proliferation
VCAN
Polysyndactyly
SOX9
WNT/β-CATENIN
Cell death
Gata6 haploinsufficiency
PTCH1
Mesenchymal cell proliferation

Figure 4.5: Representative summary model of poly-syndactyly formation in *Gata6*$^{+/-}$ mice hindlimbs. GATA6, mainly expressed in the anterior region of the hindlimb bud and regulates the expression of SHH and SOX9. In the case of *Gata6* haploinsufficiency, SOX9 downregulation along with SHH upregulation lead to Preaxial Polydactyly due to absence of cell proliferation inhibitory signals. In its turn, SOX9 downregulation derepresses Wnt/β catenin signaling. Thus, as a consequence, the hindlimb of these animals display decreased interdigital cell death (as was also shown by TUNEL and decresed expression of VCAN) leading to SD.

5. General Discussion

GATA6, a member of the GATA family of transcription (TFs), is one of the most important and therefore intensely studied cardiac TFs. Mutations of *GATA6* in human lead to a variety of cardiac phenotypes ranging from structural to conduction defects. GATA6 spatiotemporal expression in different cell types and compartments of the heart suggests a specialized function in heart morphogenesis that was not fully understood. In this thesis, we demonstrate that GATA6 is required for proper aortic valve formation. We report that loss of one *Gata6* allele from all cells or from *Isl1*-positive cells leads to RL-type bicuspid aortic valve (BAV), the most common cardiac birth defect in human. At the molecular level, the defect is due to disruption of valve remodeling and extracellular matrix (ECM) composition. This is the first study that reports the requirement of GATA6 in secondary heart field (SHF) cells for proper aortic valvulogenesis. Moreover, we demonstrate that GATA6 is required for cardiac conduction system (CCS) formation. GATA6 is important not only for the development of the proximal conduction system, but also controls the proper formation of the sinoatrial node (SAN) via a cross-talk mechanism among different SAN cells. Lastly, we report that removal of one copy of *Gata6* also results in lower limb polysyndactyly, which suggests that *GATA6*, similar to *TBX5* in HOS, is a potential heart-limb defect causing gene.

5.1. GATA6 role in matrix regulation and remodeling

During embryogenesis, the ECM regulates individual structures of the heart during their development, remodeling, and maturation. ECM is involved in cell-cell signaling, and the regulation of cell proliferation, differentiation, and migration. Tight spatiotemporal regulation of ECM components is essential to ensure proper formation of different structures. Perturbation in gene expression of these matrix regulators, will lead to prenatal lethality or to

CHDs such as septal defects (ASD and VSD), valve and arch defects (PTA, PDA) as well as complex syndromes like TOF. Mice lacking hyaluronen, versican, collagens, proteases, or other ECM components, have a variety of cardiac and vascular phenotypes [1]. Human mutations in important TFs regulating heart morphogenesis, such as *GATA6*, have been shown to lead to these phenotypes [2,3]. Mutations in *GATA6* have been reported in patients with PTA, ASD, VSD, PDA and TOF as well as in patients with atrial fibrillation (AF) [2,4]. In mice, deletion of *Gata6* using *Sm22-cre* or *Wnt1-cre* leads to OFT defects, hence, pointing to a crucial role for GATA6 in OFT septation [5]. GATA6 is also shown to play a role in vasculature formation by promoting vascular smooth muscle cell (VSMC) contractile phenotype and inhibiting their proliferation. Microarray screening in VSMC revealed GATA6 regulation of multiple genes involved in cell-cell signaling and cell-matrix interactions, as well as regulation of angiotensin receptor 1 (*AT1a*) and endothelin (*ET1*), whose expressions correlated with GATA6 expression changes [6]. Together with our findings, these data suggest that GATA6 might be involved in ECM regulation and remodeling processes.

Early evidence for a function of GATA6 in the regulation of ECM components came from studies performed on cancer invasion and metastasis. Cancerous cells are known to detach from the area where they are initially formed, to travel through the blood or lymphatic system, and form new tumors in new areas of the body. This breakage cannot be achieved without involvement of ECM components, which loosen the structure by breaking cell-to-cell contact, allowing migration of cells to the new site. Knockdown of GATA6 in established colorectal cancer cell lines decreases the ability of these cells to invade and migrate; unlike its overexpression, which enhances their migration and invasion [7]. On the

other hand, GATA4 or GATA6 silencing in ovarian granulosa alters the expression of important ECM components and affects the ECM structure. This effect was found to be more pronounced when both *Gata4* and *Gata6* are knocked out. A role for both GATA6 and GATA4 is suggested in the build-up of the extracellular components required during this process [8].

Beyond cancer, a role for GATA6 in airway remodeling was reported in a murine model of chronic asthma. This remodeling was shown to occur via regulation of calveolin1 (*CAV1*), a scaffolding protein important in the regulation of airway epithelial integrity, inflammation and fibrosis, and known to alter ECM proteins expression [9,10]. Expression of GATA6 in this model was shown to be elevated, whereas expression of CAV1 was inversely correlated. Silencing of GATA6 resulted in reduction of inflammatory cell accumulation, and inhibition of expression of *Mmp9* and *2*, as well as a disintegrin and metalloproteinase 8 (*Adam8*) and *Adam33*, which are all important in remodeling [9]. Taken together, these studies support a role of GATA6 in ECM regulation and remodeling of structures beyond the heart.

The heart responds to stress and altered conditions via extensive remodeling, which includes functional (contractility, electrophysiology) or structural (fibrosis, hypertrophy) changes. A compensatory and beneficial remodeling response is initially mounted to optimize the heart pumping function but might progress into a pathologic, detrimental state later on (*e.g.* arrhythmias, heart failure). Our results reveal a role for GATA6 in early valvulogenesis via regulation of expression of ECM components (*Mmp9* and *Vcan*). GATA6 is able to bind to the *Mmp9* promoter and to activate it in a dose dependent manner. During valve remodeling, expression of MMPs should be induced, allowing the degradation of ECM and the formation of mature leaflets. Here we showed that *Gata6* haploinsufficiency disrupts

proper valve remodeling and ECM degradation, leading to abnormal OFT cushion septation and thus BAV. It is well established that BAV is a risk factor for calcific AoV disease, which includes dysregulation of the valvular ECM [11]. Whether GATA6 plays a direct role in ECM remodeling and valve calcification will need to be addressed.

Atrial fibrillation (AF) is associated with ECM remodeling, involving atrial fibrosis and atrial dilatation. Changes in expression of collagens (COL I and III) and disturbed MMP/TIMP ratios have been implicated in this process [12]. Mutations in *GATA6* have been reported in patients with AF [4]. Our results reveal an important contribution of GATA6 to SAN formation, as shown by altered expression of CCS regulators and abnormal electrical signals when one copy of *Gata6* was removed. Dysregulated matrix composition of *Gata6*$^{+/-}$ SAN may be contributing, along with other factors, to the abnormal phenotype. Some *Gata6*$^{+/-}$ mice revealed signs of PAC, which have been shown to lead to AF [13]. Whether these mice are naturally susceptible to develop late onset AF or whether GATA6 indeed plays a role in atrial and SAN remodeling, should be further explored.

Finally, the formation of digits within the limb also requires the degradation of the interdigital matrix, which is regulated by several proteases. Failure of ECM degradation results in syndactyly. Our results reveal that GATA6 participates in matrix remodeling during development and organogenesis, not only in the heart, but also in digits determination. In our model, *Gata6* haploinsufficiency leads to abnormal matrix regression and results in pre-axial syndactyly, therefore revealing a new role of GATA6 in limb matrix regulation. These findings are suggestive of a putative common role for GATA6 in regulating heart and limb formation. Increasing our knowledge of ECM regulators is very valuable in elucidating the mechanisms involved in the pathogenesis of heart diseases.

5.2. Importance of animal model of human disease

Despite the outstanding progress of recent years, our understanding of the mechanisms underlying the etiology of diseases and their progression remain poorly elucidated. The importance of deciphering the pathways leading to disease will help in the development of new therapeutic approaches. In the last decade or two, animal models have been indispensable in contributing to understanding human disease and in advancing therapies. The availability of a well-defined genetic system has opened the possibility of generation of transgenic and gene knockout animals. These models have helped in our understanding of how diseases progress and have helped in confirming the role of modifier genes that were reported by genome-wide or candidate gene approaches.

5.2.1. Identification of modifier genes

Cardiovascular and neuromuscular diseases are among the leading causes of morbidity and mortality worldwide. Genetic diagnosis testing when available, points to the primary mutation, associated with the phenotype. However, individuals with the same genetic mutation might display different phenotypes, hence the complexity of these diseases. Differences in phenotypes may be due to either genetic or environmental changes. Modifier genes can alter the disease outcome and are identified using candidate gene and genomic approaches. Animal models have helped tremendously in the identification of these modifiers, with some having successfully translated to treat human diseases.

Inherited neuromuscular diseases (NMDs) cause muscle weakness, chronic disability, and premature death, and are known to affect approximately 1/3000 people worldwide [14]. Many genetic modifiers in NMDs have been identified using different genetic approaches. The candidate gene approach helped, for example, in identifying modifier genes for different

types of NMDs, including chondrolectin for spinal muscular atrophy (SMA), ciliary neurotrophic factor (CNTF) for amyotrophic lateral sclerosis (ALS), and osteopontin for Duchenne Muscular Dystrophy (DMD) [15–17]. Identification of modifiers in human NMDs was also performed using genome-wide approaches, where quantitative trait locus (QTL) mapping or genome-wide association studies (GWAS) were employed. However, some disadvantages arise from using GWAS: besides the large sample size required and the high burden of multiple testing, the identification of modifiers using GWAS is often biased. Using animal models offers advantages in the identification of modifier genes since the variability arising from the environmental differences can be reduced (*i.e.* housing, diet). However, some caveats still remain. Namely, the modifier pathway might not translate to human, which is considered a major limitation of the animal models [18]. It is important to note that mouse models of ALS with different background strains yet carrying the same superoxide dismutase 1 (SOD1) mutation, display different phenotypes, which is suggestive of a role of genetic modifiers [19].

Genetic modifiers have also been reported to be major contributors of CHD in people with Down Syndrome (DS), for example. Only half the people with trisomy for human chromosome 21 (*HSA21*) display CHDs. In people with DS displaying AVSD, sequencing of cysteine rich with EGF like domains 1 (*CRELD1),* a gene associated with AVSD in people with or without DS, and *HEY2*, a gene when mutated in mouse leads to septal defects, was performed. Mice with mutant forms of either *Creld1* or *Hey2* were crossed with the *Ts65Dn*, a mouse model of DS, and resulting mice showed increased frequency of CHD. These results reveal that, when inherited together, these modifiers interact with trisomic genes and further affect heart development [20]. The availability of these mouse models has helped to further our

understanding of how these modifiers affect the disease, which would not have been possible with human studies alone.

Exploration of genetic variation in mice has also helped in yielding novel insights into human disease mechanisms, such as dilated cardiomyopathy and heart failure. A link between cardiac troponin I interacting kinase (*Tnni3k*) and acceleration of disease progression in the calsequestrin (*Csq*) heart failure model was revealed. The use of the *Csq* transgenic mouse model, where the major calcium binding protein of the sarcoplasmic reticulum is overexpressed in different mouse genetic backgrounds, revealed variations in the disease progression depending on the background which correlated with expression levels of TNNI3K: higher expression of TNNI3K worsened the phenotype. The overexpression of human *TNNI3K* alone does not exhibit any heart phenotype, however, the double transgenics *Tnni3k*/*Csq* mice display reduced survival rate and impaired systolic function. Heart failure induced by constriction of the transverse aorta (pressure-overload model) revealed increased expression of TNNI3K with exacerbation of the cardiac dysfunction. Taken all together, these results confirm that *TNNI3k* is a strong modifier of murine heart failure development [21]. While further work will be required to confirm that TNNI3K can also modulate the progression of the disease in human, without these animal models, comparisons eliminating environmental changes and TNNI3K transcript level correlations with disease progression would not have been possible.

The finding that the severity of the phenotype can be controlled by changes of gene expression is very beneficial and helps in revealing new pathways involved in disease pathogenesis. To date, no direct disease causing *GATA6* human mutation have been reported in patients with BAV, suggesting that more screening on large cohorts should be performed

to unravel potential disease-causing mutations. However, Lin *et al.* reported in 2010 a mutation in *GATA6* (S184N) in a patient with ASD. Interestingly, one of the parents was a carrier of the mutation and had BAV [22]. Taken together, these results and our findings suggest that *GATA6* may be a modifier gene, either enhancing or suppressing the outcome of a primary disease-causing mutation. Further knowledge of the exact genetic changes that are mediating the presence of the phenotype would improve genetic testing, prognosis and help in treatment of individuals with differential genetic compositions.

5.2.2. Pathophysiology

Complications resulting from cardiac and vascular pathologies are very difficult to prevent and are controlled by many genetic and environmental factors. The development of animal models of cardiovascular diseases has helped in gaining more insights into the disease pathophysiology and progression and was an essential tool in development of techniques for disease prediction and complications prevention. The most common models of cardiovascular diseases include, among others, models to study heart failure, atherothrombotic diseases, and valve diseases.

Studies on heart failure are mainly performed in small (mice, rats) and large animal models (rabbits, dogs, pigs), mimicking as close as possible the conditions found in human. The myocardial damage is often induced by surgery (ligation of left coronary artery [23]), pharmaceutical (treatment with isoproterenol, a beta-one adrenergic receptor agonist [24]) or electrical (generation of burns in exposed hearts [25]) interventions. Temporary occlusion of the artery is also used and reproduces human ischemia/reperfusion injury, permitting visual monitoring of the reperfusion and analysis of the infarct size [26]. The availability of the different models and the capacity to perform different types of interventions has extensively

helped in our understanding of myocardial damage and heart failure, in addition to testing new preventive drugs.

Atherosclerosis is a multifactorial disease characterized by the formation of lesions. Genetically modified models of atherosclerosis are generated by alteration of lipoprotein metabolism, in addition to dietary changes. The most widely used models currently are the low-density lipoprotein receptor-deficient mice (*Ldlr*$^{-/-}$ mice) and apolipoprotein E-deficient mice (*ApoE*$^{-/-}$ mice), a hypercholesterolemia and hyperlipidemia models, respectively [27]. In these models, addition of risk factors such as diabetes and hypertension are known to exacerbate lesion formation. These models have helped in the identification of atherosclerosis modifying genes and in deciphering the mechanisms and different cell-types involved in atherogenesis. In addition to that, they were used to dissect the effect of drugs on atherogenesis (effect of Simvastatin when tested on both *Ldlr*$^{-/-}$ and *ApoE*$^{-/-}$ mice [28]) as well in assessing new therapies to prevent the progression of lesions [27].

The previously described models (*Ldlr*$^{-/-}$ and *ApoE*$^{-/-}$) have been also used in studying valvular heart diseases, with the aortic valve being the most frequently affected. The response of the cardiac valve to injury or age-related degeneration is mainly translated by a disorganized ECM structure, remodeling, and in some cases calcification, all together leading to valvular dysfunction. These models have been shown to develop aortic valve calcification when mice are subjected to a high fat/high cholesterol diet, constituting great tools to study valve disease progression [29,30]. The presence of BAV is also associated with increased risk of calcific AoV disease as well as aortic aneurisms [31]. Mutations in *NOTCH1* and *GATA5* have been shown to cause BAV and calcific AoV disease in human [32,33]. Mice, heterozygote for *Notch1* or deficient for *Gata5*, display partially penetrant RN-

type BAV, with the later having reduced expression of NOS3 and NOTCH signaling [34,35]. These mice offer the opportunity to study the development of BAV-associated complication, aortic valve calcification and ascending aortic aneurysms, which can be induced by high fat/high cholesterol diet and stress-induced pressure overload via angiotensin II treatments [36].

Here we show that *Gata6*$^{+/-}$ mouse model, with partially penetrant RL-type BAV (approximately 50%), is a novel tool to study the most common type of BAV in human. With the availability of both BAV models in our laboratory (RN and RL), we will be able to further uncover the underlying pathways leading to the different types of BAV and help in our understanding of disease progression. In human, RL-type BAVs have been shown to be associated with elevated wall shear stress in the ascending aorta and more common calcium deposition in the aortic valves when compared to RN-type BAV [37,38].

5.3. Cellular basis of cardiac defects: cell autonomous and cell-cell communication roles of GATA6

As stated in the thesis general **Introduction**, many cell types contribute to the proper formation of the different heart structures, including myocardial, endocardial, and neural crest cells. Their migration, proliferation, and differentiation are orchestrated by tight expression of regulatory genes. These genes are known to exert their role either in a cell autonomous manner, or via a paracrine effect, inducing changes in nearby cells. The exact outcome of gene activation is strongly dependent on the gene dosage and the cellular context.

Cysteine rich transmembrane BMP regulator 1 (CRIM1) is a type-I transmembrane protein broadly expressed during embryonic development. It has been shown to play

essential autocrine as well as paracrine roles in heart development. In mice, *Crim1* loss-of-function results in epicardial defects, VSD, and hypoplastic myocardium of the ventricles. A cell autonomous role of CRIM1 in fate specification of cells derived from the epicardium is suggested: cells residing in the myocardium and lacking *Crim1* are shown to proliferate less and to give rise to a reduced number of cardiac fibroblasts. On the other hand, epicardial loss of *Crim1* is shown to influence the compact myocardial development, revealing its paracrine effect [39].

However, some genes are shown to have only a paracrine effect. Such is the case of *TBX1*, which has been strongly associated as a major contributor to Di-George syndrome. This syndrome is caused by heterozygous deletion of a region of chromosome 22q11.2 (containing *TBX1*), and is characterized by CHDs, in addition to their immunodeficient phenotype. Defective neural crest-derived structures are thought to be the underlying cause of the different anomalies. However, TBX1 is expressed in the pharyngeal endoderm but not in neural crest cells, revealing that TBX1 is able to influence indirectly NCC migration and maturation [40,41]. Another example is endothelin (EDN1), a guiding molecule secreted by endothelial cells, which plays a role in guiding the migration of NCC into the heart to participate in its innervation. Endothelial-specific deletion of *Edn1* using *Tie2-cre* leads to defective NCC migration and decreased heart innervation, supporting a paracrine role for EDN1 in the regulation of NCC [42].

On the other hand, other genes are found to play more of a cell autonomous role within the heart and vasculature; such is the case of *NOTCH1*. Loss of global *Notch1* is known to result in early embryonic lethality. Mutant embryos lacking endothelial *Notch1* die early on, recapitulating the phenotypes of the total knock out model, and revealing an

essential cell-autonomous role of NOTCH1 signaling during vascular development in the endothelium [43]. More recently, a role for SHF-NOTCH1 has been reported in ascending aortic aneurysms (AscAA), a complication mainly associated with BAV. *Notch1* haploinsufficiency was shown to exacerbate AscAA and this phenotype was recapitulated when heterozygous deletion of *Notch1* was performed in the SHF lineage [44]. These results further reveal that the same gene might be playing different roles in different cell types, in a cell-autonomous manner.

We have previously shown that GATA5 is important during valvulogenesis, and that loss of *Gata5* in mice lead to RN-type BAV. Conditional deletion of *Gata5* from endocardial cells is sufficient to recapitulate the same percentage of BAV as in *Gata5*$^{-/-}$, confirming an endocardial-specific role for GATA5 during valve formation. We report in this thesis, a cell-autonomous role of GATA6 during valve formation. Heterozygous deletion of *Gata6* from SHF lineage ─ but not from endothelial or NCC ─ was able to recapitulate the RL-BAV phenotype, with similar penetrance (around 50%) to that found in the global heterozygous model. These results highlight a crucial role for SHF-GATA6 in regulation of aortic valve development. On the other hand, our results also reveal a cell-cell communication role of GATA6 during SAN formation. Homozygous deletion of *Gata6* from each of endothelial cells, SHF cells and NCC lead to embryonic or postnatal lethality, with an abnormal SAN formation recapitulating the phenotype of *Gata6*$^{+/-}$. Heterozygous deletion of *Gata6* from each of these cell types leads to a variety of electrophysiological defects, along with SAN abnormalities, but not as severe as in the case of homozygous deletions. Taken together, these results reveal a cell-cell communication role of GATA6 in facilitating the cross talk among different cells contributing to the proper formation of the SAN.

5.4. Conclusion and future perspectives

Congenital and cardiovascular diseases are the leading cause of mortality in the general population, with CHDs accounting for 1-2% of live births. Disruption of any of the signals ensuring proper cell proliferation, migration and differentiation will lead to defective heart formation. Using *in vivo* and *in vitro* approaches, we examined in the current study the different defects associated with heterozygous *Gata6* loss of function and determined the underlying mechanisms leading to the different cardiac and non-cardiac phenotypes.

We revealed that half of the mice that are heterozygote for *Gata6* have RL-type BAV. Patients with BAV can be asymptomatic or can have many BAV-associated complications such as aortic root dilation, aortic aneurysm and dissection, as well as valve calcification and endocarditis, with RL-BAVs being more prone to calcification than other BAV types [37]. With the availability of both mice models (*Gata6*$^{+/-}$ and *Gata5*$^{-/-}$) corresponding to both types of human BAVs (RL- and RN-types), it would be interesting to study aortic valve disease progression. After these mice are subjected to high fat/high cholesterol (HF/HC) diet for a period of minimum 4 months, valve calcification can be monitored to see whether these mice are more susceptible to valve calcification than their counter littermates. Replicating the calcification found in human BAV patients will allow a better understanding of the remodeling events in the diseased valves, and will show whether differences exist between RL and RN valves, rendering one more susceptible to calcification than the other. This will open the door for potential targeted therapy.

Furthermore, since BAVs are associated with aortic root dilation and aortic aneurysms/dissection, it is possible that the genetic mutation leading to the formation of the BAV might also be the underlying cause leading to aorthopathy in BAV patients. Therefore,

ascending and descending aortas from these models will be assessed, at both baseline and in response to stress using angiotensin II (Ang II) or isoproterenol infusion ─ both known to induce pressure overload ─ to determine whether any dilation or aneurysms are present. Understanding the ECM composition and the elastic property of the aorta from both models will help in determining the cause of rupture in cases of stress. Conditional knockout of *Gata6* and *Gata5* from different cell types contributing to aortic formation will help reveal the exact role that GATA6 and GATA5 play in each of the cell types. These findings will potentially help in determining whether the presence of BAV in these models affects aortopathy progression. In addition, it will contribute in the potential discovery of biomarkers, which will help identify individuals that require close cardiovascular monitoring and be predictive of aortic complications, thereby decreasing unnecessary aortic aneurysm repair surgeries.

In some cardiovascular diseases, disruptive mutations in genes involved in proper cardiac formation are the underlying causes of disease manifestation, whereas in others, while the manifestation of the phenotype is clear, no disease-causing mutation is anywhere to be found. Therefore, epigenetic modifications (methylation, phosphorylation, acetylation, glycosylation, etc.) might be the likely perpetrators in such cases. DNA methylations are able to decrease the accessibility of chromatin, inhibiting the binding of transcription factors to the DNA, therefore leading to silencing of the gene. Following nicotinic stimulation of acetylcholine in experimental animals, a downregulation of TBX5 and GATA4 in differentiating embryonic bodies and in hearts of offspring as well as promoter hypermethylation were observed. This also resulted in inhibition of myocardial differentiation [45,46].

Histones modifications are also linked to the function of the cardiovascular system. The proximal promoter of the nitric oxide (eNOS) gene was found to be highly regulated by changes in its dynamic signature (enriched with different histone modifications: H2A, H3K4me2, H3K4me3, H3K9Ac, and the H4K12Ac,). Deficiency in the H3K36me3 was shown to result in embryonic lethality due to vascular remodeling defects, suggesting a role for this methyltransferase in vascular development [47].

Finally, non-coding RNAs (Nc-RNAs) are known to influence gene expression whether at the transcriptional or the translational levels, in response to or during cell differentiation. In the cardiovascular system, miRNAs are the best studied Nc-RNAs acting as activator/repressors via targeting the promoter region of the gene. Such is the case of miR-499, miR-208a, and miR-208b, present in the myosin gene and responsible for cardiomyocytes contraction [48].

The absence of direct *GATA6* BAV-causing mutation in the population that we explored could suggest the presence of some epigenetic modifications that might be influencing the expression of GATA6 in patients with BAV. Further studies should be conducted to 1) determine DNA methylation state in patients with BAV compared to healthy controls, and 2) unravel Nc-RNAs that might be affecting GATA6 expression in these patients. Uncovering new epigenetic variants associated with BAV would be possible using epigenome-wide association studies (EWAS) that rely on microarrays capable of measuring DNA methylation [49].

Taken together, the findings reported in this thesis reveal that *GATA6* is a major regulator of human heart development and screening for mutations in *GATA6* in patients with

CHD (more specifically BAV, AF and CHD-associated aortopathies) will have a high clinical relevance. Phenotype variability and incomplete penetrance are common in CHDs, supporting the existence of genetic modifiers. Therefore, the use of next-generation technologies such as whole exome and whole genome sequencing should be considered to help determine gene mutations and modifiers, opening the possibility of development of new therapeutic approaches.

5.5. References

1. Lockhart M, Wirrig E, Phelps A, Wessels A. Extracellular Matrix and Heart Development. *Birt Defects Res A Clin Mol Teratol*. 2011;91:535–550.

2. Kodo K, Nishizawa T, Furutani M, Arai S, Yamamura E, Joo K, Takahashi T, Matsuoka R, Yamagishi H. GATA6 mutations cause human cardiac outflow tract defects by disrupting semaphorin-plexin signaling. *Proc Natl Acad Sci U S A*. 2009;106:13933–13938.

3. Wang J, Luo X-J, Xin Y-F, Liu Y, Liu Z-M, Wang Q, Li R-G, Fang W-Y, Wang X-Z, Yang Y-Q. Novel GATA6 mutations associated with congenital ventricular septal defect or tetralogy of fallot. *DNA Cell Biol*. 2012;31:1610–1617.

4. Li J, Liu W-D, Yang Z-L, Yang Y-Q. Novel GATA6 loss-of-function mutation responsible for familial atrial fibrillation. *Int J Mol Med*. 2012;30:783–790.

5. Lepore JJ, Mericko PA, Cheng L, Lu MM, Morrisey EE, Parmacek MS. GATA-6 regulates semaphorin 3C and is required in cardiac neural crest for cardiovascular morphogenesis. *J Clin Invest*. 2006;116:929–939.

6. Lepore JJ, Cappola TP, Mericko PA, Morrisey EE, Parmacek MS. GATA-6 regulates genes promoting synthetic functions in vascular smooth muscle cells. *Arterioscler Thromb Vasc Biol*. 2005;25:309–314.

7. Shen F, Li J, Cai W, Zhu G, Gu W, Jia L, Xu B. GATA6 predicts prognosis and hepatic metastasis of colorectal cancer. *Oncol Rep*. 2013;30:1355–1361.

8. Bennett J, Baumgarten SC, Stocco C. GATA4 and GATA6 silencing in ovarian granulosa cells affects levels of mRNAs involved in steroidogenesis, extracellular structure organization, IGF-I activity, and apoptosis. *Endocrinology*. 2013;154:4845–4858.

9. Fang P, Shi H-Y, Wu X-M, Zhang Y-H, Zhong Y-J, Deng W-J, Zhang Y-P, Xie M. Targeted inhibition of GATA-6 attenuates airway inflammation and remodeling by regulating caveolin-1 through TLR2/MyD88/NF-κB in murine model of asthma. *Mol Immunol*. 2016;75:144–150.

10. Thompson C, Rahim S, Arnold J, Hielscher A. Loss of caveolin-1 alters extracellular matrix protein expression and ductal architecture in murine mammary glands. *PLOS ONE*. 2017;12:e0172067.

11. Merryman WD, Schoen FJ. Mechanisms of Calcification in Aortic Valve Disease: Role of Mechanokinetics and Mechanodynamics. *Curr Cardiol Rep*. 2013;15:355.

12. Polyakova V, Miyagawa S, Szalay Z, Risteli J, Kostin S. Atrial extracellular matrix remodelling in patients with atrial fibrillation. *J Cell Mol Med*. 2008;12:189–208.

13. Jensen TJ, Haarbo J, Pehrson SM, Thomsen B. Impact of premature atrial contractions in atrial fibrillation. *Pacing Clin Electrophysiol PACE*. 2004;27:447–452.

14. Emery AE. Population frequencies of inherited neuromuscular diseases--a world survey. *Neuromuscul Disord NMD*. 1991;1:19–29.

15. Giess R, Holtmann B, Braga M, Grimm T, Müller-Myhsok B, Toyka KV, Sendtner M. Early onset of severe familial amyotrophic lateral sclerosis with a SOD-1 mutation: potential impact of CNTF as a candidate modifier gene. *Am J Hum Genet*. 2002;70:1277–1286.

16. Pegoraro E, Hoffman EP, Piva L, Gavassini BF, Cagnin S, Ermani M, Bello L, Soraru G, Pacchioni B, Bonifati MD, Lanfranchi G, Angelini C, Kesari A, Lee I, Gordish-Dressman H, Devaney JM, McDonald CM, Cooperative International Neuromuscular Research Group. SPP1 genotype is a determinant of disease severity in Duchenne muscular dystrophy. *Neurology*. 2011;76:219–226.

17. Sleigh JN, Barreiro-Iglesias A, Oliver PL, Biba A, Becker T, Davies KE, Becker CG, Talbot K. Chondrolectin affects cell survival and neuronal outgrowth in in vitro and in vivo models of spinal muscular atrophy. *Hum Mol Genet*. 2014;23:855–869.

18. Lamar K-M, McNally EM. Genetic Modifiers for Neuromuscular Diseases. *J Neuromuscul Dis*. 2014;1:3–13.

19. Nardo G, Iennaco R, Fusi N, Heath PR, Marino M, Trolese MC, Ferraiuolo L, Lawrence N, Shaw PJ, Bendotti C. Transcriptomic indices of fast and slow disease progression in two mouse models of amyotrophic lateral sclerosis. *Brain J Neurol*. 2013;136:3305–3332.

20. Li H, Cherry S, Klinedinst D, DeLeon V, Redig J, Reshey B, Chin MT, Sherman SL, Maslen CL, Reeves RH. Genetic Modifiers Predisposing to Congenital Heart Disease in the Sensitized Down Syndrome Population. *Circ Cardiovasc Genet*. 2012;5:301–308.

21. Wheeler FC, Tang H, Marks OA, Hadnott TN, Chu P-L, Mao L, Rockman HA, Marchuk DA. Tnni3k Modifies Disease Progression in Murine Models of Cardiomyopathy. *PLoS Genet* [Internet]. 2009 [cited 2017 Nov 16];5. Available from: https://www.ncbi.nlm.nih.gov/pmc/articles/PMC2731170/

22. Lin X, Huo Z, Liu X, Zhang Y, Li L, Zhao H, Yan B, Liu Y, Yang Y, Chen Y-H. A novel GATA6 mutation in patients with tetralogy of Fallot or atrial septal defect. *J Hum Genet*. 2010;55:662–667.

23. Pfeffer MA, Pfeffer JM, Fishbein MC, Fletcher PJ, Spadaro J, Kloner RA, Braunwald E. Myocardial infarct size and ventricular function in rats. *Circ Res*. 1979;44:503–512.

24. Zbinden G, Bagdon RE. Isoproterenol-induced heart necrosis, an experimental model for the study of angina pectoris and myocardial infarct. *Rev Can Biol*. 1963;22:257–263.

25. Adler N, Camin LL, Shulkin P. Rat model for acute myocardial infarction: application to technetium-labeled glucoheptonate, tetracycline, and polyphosphate. *J Nucl Med Off Publ Soc Nucl Med*. 1976;17:203–207.

26. Michael LH, Entman ML, Hartley CJ, Youker KA, Zhu J, Hall SR, Hawkins HK, Berens K, Ballantyne CM. Myocardial ischemia and reperfusion: a murine model. *Am J Physiol*. 1995;269:H2147-2154.

27. Zaragoza C, Gomez-Guerrero C, Martin-Ventura JL, Blanco-Colio L, Lavin B, Mallavia B, Tarin C, Mas S, Ortiz A, Egido J. Animal Models of Cardiovascular Diseases [Internet]. BioMed Res. Int. 2011 [cited 2017 Nov 17];Available from: https://www.hindawi.com/journals/bmri/2011/497841/

28. Wang YX, Martin-McNulty B, Huw LY, da Cunha V, Post J, Hinchman J, Vergona R, Sullivan ME, Dole W, Kauser K. Anti-atherosclerotic effect of simvastatin depends on the presence of apolipoprotein E. *Atherosclerosis*. 2002;162:23–31.

29. Donnelly KB. Cardiac Valvular Pathology: Comparative Pathology and Animal Models of Acquired Cardiac Valvular Diseases. *Toxicol Pathol*. 2008;36:204–217.

30. Weiss RM, Ohashi M, Miller JD, Young SG, Heistad DD. Calcific aortic valve stenosis in old hypercholesterolemic mice. *Circulation*. 2006;114:2065–2069.

31. Hoffman JIE, Kaplan S. The incidence of congenital heart disease. *J Am Coll Cardiol*. 2002;39:1890–1900.

32. Bonachea EM, Chang S-W, Zender G, LaHaye S, Fitzgerald-Butt S, McBride KL, Garg V. Rare GATA5 sequence variants identified in individuals with bicuspid aortic valve. *Pediatr Res*. 2014;76:211–216.

33. Garg V, Muth AN, Ransom JF, Schluterman MK, Barnes R, King IN, Grossfeld PD, Srivastava D. Mutations in NOTCH1 cause aortic valve disease. *Nature*. 2005;437:270–274.

34. Laforest B, Andelfinger G, Nemer M. Loss of Gata5 in mice leads to bicuspid aortic valve. *J Clin Invest*. 2011;121:2876–2887.

35. Nigam V, Srivastava D. Notch1 represses osteogenic pathways in aortic valve cells. *J Mol Cell Cardiol*. 2009;47:828–834.

36. Crowley SD, Gurley SB, Herrera MJ, Ruiz P, Griffiths R, Kumar AP, Kim H-S, Smithies O, Le TH, Coffman TM. Angiotensin II causes hypertension and cardiac hypertrophy through its receptors in the kidney. *Proc Natl Acad Sci*. 2006;103:17985–17990.

37. Lee M, Sung J, Cho SJ, Choi SH, Cho SW, Oh JK, Park S-J, Kim D-K. Aortic dilatation and calcification in asymptomatic patients with bicuspid aortic valve: analysis in a Korean health screening population. *Int J Cardiovasc Imaging*. 2013;29:553–560.

38. Mahadevia R, Barker AJ, Schnell S, Entezari P, Kansal P, Fedak PWM, Malaisrie SC, McCarthy P, Collins J, Carr J, Markl M. Bicuspid aortic cusp fusion morphology alters aortic three-dimensional outflow patterns, wall shear stress, and expression of aortopathy. *Circulation*. 2014;129:673–682.

39. Iyer S, Chou FY, Wang R, Chiu HS, Raju VKS, Little MH, Thomas WG, Piper M, Pennisi DJ. Crim1 has cell-autonomous and paracrine roles during embryonic heart development. *Sci Rep* [Internet]. 2016 [cited 2017 Nov 20];6. Available from: https://www.ncbi.nlm.nih.gov/pmc/articles/PMC4731764/

40. Sander TL, Klinkner DB, Tomita-Mitchell A, Mitchell ME. Molecular and Cellular Basis of Congenital Heart Disease. *Pediatr Clin North Am*. 2006;53:989–1009.

41. Yutzey KE. DiGeorge syndrome, Tbx1, and retinoic acid signaling come full circle. *Circ Res*. 2010;106:630–632.

42. Manousiouthakis E, Mendez M, Garner MC, Exertier P, Makita T. Venous endothelin guides sympathetic innervation of the developing mouse heart. *Nat Commun*. 2014;5:3918.

43. Limbourg FP, Takeshita K, Radtke F, Bronson RT, Chin MT, Liao JK. Essential Role of Endothelial Notch1 in Angiogenesis. *Circulation*. 2005;111:1826–1832.

44. Koenig SN, LaHaye S, Feller JD, Rowland P, Hor KN, Trask AJ, Janssen PM, Radtke F, Lilly B, Garg V. Notch1 haploinsufficiency causes ascending aortic aneurysms in mice. *JCI Insight*. 2017;2.

45. Jiang X-Y, Feng Y-L, Ye L-T, Li X-H, Feng J, Zhang M-Z, Shelat HS, Wassler M, Li Y, Geng Y-J, Yu X-Y. Inhibition of Gata4 and Tbx5 by Nicotine-Mediated DNA Methylation in Myocardial Differentiation. *Stem Cell Rep*. 2017;8:290–304.

46. van der Harst P, de Windt LJ, Chambers JC. Translational Perspective on Epigenetics in Cardiovascular Disease. *J Am Coll Cardiol*. 2017;70:590–606.

47. Yan MS, Marsden PA. Epigenetics in the Vascular Endothelium: Looking From a Different Perspective in the Epigenomics Era. *Arterioscler Thromb Vasc Biol*. 2015;35:2297–2306.

48. Beermann J, Piccoli M-T, Viereck J, Thum T. Non-coding RNAs in Development and Disease: Background, Mechanisms, and Therapeutic Approaches. *Physiol Rev*. 2016;96:1297–1325.

49. Zhong J, Agha G, Baccarelli AA. The Role of DNA Methylation in Cardiovascular Risk and Disease: Methodological Aspects, Study Design, and Data Analysis for Epidemiological Studies. *Circ Res*. 2016;118:119–131.

6. Appendix

6.1. Review paper

Title*: The hereditary basis of bicuspid aortic valve disease: a role for screening?*

Publication copyrights from Dove Medical Press Ltd:

Confirmation Number: 11696132
Order Date: 01/30/2018

If you paid by credit card, your order will be finalized and your card will be charged within 24 hours. If you choose to be invoiced, you can change or cancel your order until the invoice is generated.

Payment Information

Lara Gharibeh
gharibeh.lara@gmail.com

Payment Method: n/a

Order Details

Advances in Genomics and Genetics

Order detail ID:	70977907
Order License Id:	4278971008393
ISSN:	1179-9870
Publication Type:	Journal
Volume:	
Issue:	
Start page:	
Publisher:	Dove Medical Press Ltd

Permission Status: **Granted**

Permission type: Republish or display content
Type of use: Republish in a thesis/dissertation

View details

Note: This item will be invoiced or charged separately through CCC's **RightsLink** service. More info **$ 0.00**

Total order items: 1

This is not an invoice.

Order Total: 0.00 USD

Advances in Genomics and Genetics

Dovepress
open access to scientific and medical research

Open Access Full Text Article

REVIEW

The hereditary basis of bicuspid aortic valve disease: a role for screening?

This article was published in the following Dove Press journal:
Advances in Genomics and Genetics
23 December 2014
Number of times this article has been viewed

Lara Gharibeh
Mona Nemer

Molecular Genetics and Cardiac Regeneration Laboratory, Department of Biochemistry, Microbiology and Immunology, University of Ottawa, Ottawa, ON, Canada

Abstract: Over the past years, human and molecular genetic studies have provided new understanding of valve development and the molecular pathogenesis of bicuspid aortic valve (BAV) disease. BAV is an autosomal dominant disease with incomplete penetrance and is found to affect 1%–2% of the population. It can occur in isolation or coexists with other congenital heart diseases such as ventricular septal defect and tetralogy of fallot. BAV is a risk factor for premature cardiovascular disease and can lead to severe complications affecting the aorta and the valves. To date, *NOTCH1* and *GATA5* are the only genes linked to human BAV, and the genetic basis for most BAVs remains unidentified. Large-scale screening as well as whole exome sequencing studies hold promise for uncovering BAV-causing genes. Similarly, molecular analysis of valve development in animal models is needed for better insight of normal and pathologic valve formation. Together, these approaches will undoubtedly accelerate discovery of disease-causing genes opening the way for early diagnosis of BAV and prevention of valve degeneration and cardiovascular complications.

Keywords: congenital heart disease, valvulogenesis, genetic screening

General overview

The formation of the heart is a very complex process that begins at early stages of fetal development and is orchestrated by complex regulatory networks ensuring the formation of a fully mature four-chambered heart. The mammalian heart contains three layers: an inner endothelial cell lining called the endocardium, surrounded by a muscular component forming the majority of the heart called the myocardium, and an outer protective layer that envelops the myocardium called the pericardium. The unidirectional flow of blood into the whole body is ensured by the presence of thin structures, composed of leaflets opening and closing with each heart contraction. The valve leaflets originate from mesenchymal outgrowths known as the cardiac cushions. These cardiac cushions result from the transformation of endothelial cells into mesenchymal cells through a process called EMT (epithelial to mesenchymal transformation), where endothelial cells invade the cardiac jelly separating the outer myocardium from the inner endothelium, at the base of the outflow tract (OFT). The cushions containing mesenchymal-derived cells then elongate and undergo extensive remodeling to gradually mature and form thin leaflets known as valves. Mature valves are composed of a highly organized extracellular matrix (ECM) consisting of three distinct layers made of collagens (fibrosa), proteoglycans (spongiosa), and elastin (ventricularis).[1,2] The heart valves comprise the semilunar valves (aortic and pulmonary valves), controlling the systemic flow of blood; and the atrioventricular valves

Correspondence: Mona Nemer
Molecular Genetics and Cardiac Regeneration Laboratory, Department of Biochemistry, Microbiology and Immunology, Room 246, University of Ottawa, 550 Cumberland, Ottawa, ON, Canada K1N 6N5
Tel +1 613 562 5270
Fax +1 613 562 5271
Email mona.nemer@uottawa.ca

(mitral and tricuspid valves), controlling the flow of blood between the heart compartments. The semilunar valves arise from two types of cushions: the conotruncal and the intercalated cushions situated at the OFT. The mature aortic valve (AoV) is composed of three symmetrical leaflets (also called tricuspid aortic valve [TAV]): the right and left leaflets originate from the conotruncal cushions, and the posterior aortic leaflet is formed from the right-posterior intercalated cushion, adjacent to the conotruncal cushion.[3–5] The proper formation of the heart valves ensures the unidirectional flow of blood into the systemic circulation.

Semilunar valve malformations are very common and affect 2%–3% of the population causing a variety of valvular complications including valve stenosis and/or regurgitation.[6] There are two types of valve diseases: 1) congenital valve diseases that are present at birth such as bicuspid aortic valve (BAV), mitral valve prolapse, and tricuspid atresia and 2) acquired valve diseases that develop later in life such as valve calcification and dysfunction.[7] BAV is the most common congenital abnormality affecting 1%–2% of the population with a higher (3:1) male prevalence.[8] It results in the presence of two asymmetrical cusps or leaflets instead of three symmetrical ones with the presence or absence of a raphe (connecting ridge) on the larger leaflet marking the failure of separation between leaflets (Figure 1). Familial clustering studies have shown that BAV is a heritable trait with a prevalence of 9% among first-degree relatives and up to 24% in families where more than one member is affected. BAV follows an autosomal dominant mode of inheritance with incomplete penetrance suggestive of gene–gene and gene–environment interactions.[9–11] Leaflets orientation varies widely among BAV patients resulting in different types of BAVs classified according to the leaflets position relative to the right and left coronary arteries (Figure 1). The most frequent type in human is the RL-type BAV resulting from fusion of the right and left coronary cusps and representing 59% of all BAV cases. The RN-type results from fusion of the right and noncoronary cusps and is less frequent accounting for 37% of BAV cases.[12] A less common type, the LN BAV, results from a failure of separation between the left and noncoronary leaflets. Recent studies on animal models suggest that RL- and RN-type BAVs have distinct etiologies: RL-type BAV results from defective septation during valvulogenesis, while RN BAVs are caused by a defect in the formation of the OFT cushions.[13] Despite its importance, the underlying pathways leading to the different types of BAV remain undetermined.

BAV is a risk factor for premature valvulo-vascular disease

BAV occurs in isolation or coexists with other congenital heart diseases such as coarctation of the aorta, interruption of the aortic arch, and ventricular septal defects. Individuals with BAV are often asymptomatic but are at an increased risk of several life threatening events ranging from aortic stenosis and regurgitation, aneurisms, and dilation and rupture of the aorta to infective endocarditis.[12,14] So it is clear that BAV is a

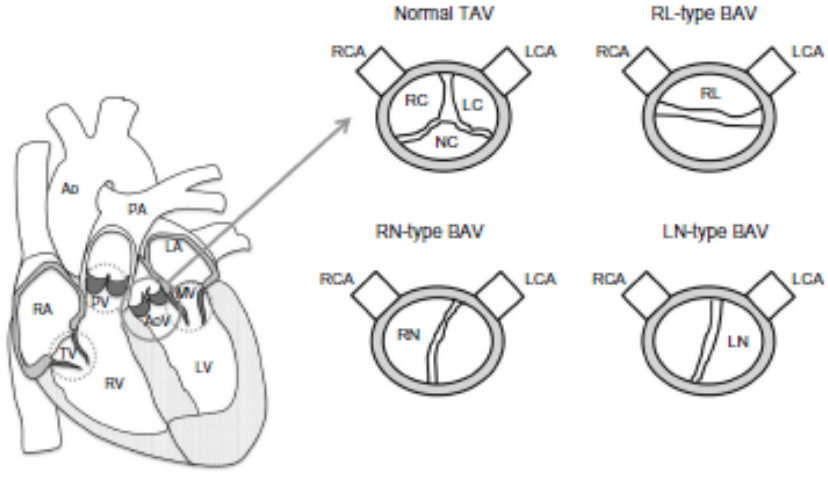

Figure 1 Representation of a normal TAV and different types of BAV.
Abbreviations: Ao, aorta; AoV, aortic valve; BAV, bicuspid aortic valve; LA, left atria; LC, left coronary; LCA, left coronary artery; LN, left-noncoronary; LV, left ventricle; MV, mitral valves; NC, noncoronary; PA, pulmonary artery; PV, pulmonary valves; RA, right atria; RC, right coronary; RCA, right coronary artery; RL, right-left; RN, right-noncoronary; RV, right ventricle; TAV, tricuspid aortic valve; TV, tricuspid valves.

risk factor for many valvulo-vascular complications. Increased shear stress (effect of blood velocity and viscosity) is thought to play a crucial role in the pathogenesis of BAV-associated disease. The presence of BAV might be associated with pressure overload that could in part be due to the presence of malfunctioning valves; both conditions are risk factors for aortic dissection and rupture.[15] The most common phenotypic pattern in BAV disease is mid ascending aortic dilatation and is correlated with older age, whereas the other pattern, aortic root dilatation, is more associated with younger age and male sex.[16] The normal aortic wall consists of an internal intimal endothelial layer (intima), a medial layer (media) composed of smooth muscle cells with an ECM (rich in elastic and collagen fibers), and a covering protective layer rich in collagen fibers called the adventia.[17] BAV patients tend to develop aortic dilation, which is thought to be due to a disruption of the ECM by itself, caused by the lack of Fibrillin-1 and the presence of a cystic medial necrosis. Fibrillin-1 is a glycoprotein that ensures the strong interaction between vascular smooth muscle cells and elastin and collagen-rich matrix as well as maintaining the structural integrity of the aortic wall.[18] Studies have shown that regardless of the AoV function, BAV patients have a defect in the structure of the aortic wall that will eventually result in aortic disease.[19] BAV was found to be a pathological event since it was associated with accelerated degeneration of the medial layer of the aorta.[20] In the aorta of BAV patients, less elastic tissue loss and fragmentation, and less changes in the intimal layer were observed when compared to aortas from TAV patients.[21] Examination of specimens taken from BAV patients with aortic dissection showed a thinner medial layer due to elastic fiber necrosis (less vascular smooth muscle cells) leaving a greater distance between elastin fibers in those patients, which was not the case in TAV patients.[22] On the other hand, an elevation of matrix metalloproteinases, endogenous enzymes that degrade matrix components, has been reported to play an important role in the formation of aortic aneurysm in the aorta of patients with BAVs.[20] Beyond cardiovascular diseases, an increased risk of development of intracranial aneurysms was also found to correlate with the presence of BAV in a study done by Schievink et al. The study was done on a small population (61 BAV patients), so additional investigations are required before drawing any conclusions.[23] Together, these data raise the possibility that other subclinical genetic abnormalities in vascular endothelial or smooth muscle cells coexist with BAV and contribute to aortic disease. The development of animal models where BAV and TAV are present on a similar genetic background will help answer this important question.

With regard to the AoVs and their function, BAV is found to lead to severe valvular complications at late onset. The valve's ECM is regulated by valve interstitial cells (VICs) that are fibroblast like and quiescent in normal conditions. Changes in the hemodynamic environment are controlled by valve endothelial cells, which form a protective layer around the leaflets and communicate with the VICs through different molecular signals. In the presence of BAV, disruption of normal valve morphogenesis is accompanied by changes in the ECM composition, endothelial cell disruption, and VIC activation, eventually causing valvular dysfunction and calcification.[2,24] Valve disease is most commonly diagnosed as regurgitation, a leaking of the AoV that causes blood to flow in the reverse direction, or stenosis, a disease of the AoV in which the opening of the valves is narrowed. Both disease presentations are caused by disruptions in the structure and function of the valves. A study of 542 surgical BAV patients showed that 75% of the BAV cases had aortic stenosis; the same study showed that only 13% had aortic regurgitation. In fact, the regurgitation group had a higher rate of annular dilatation and a higher male to female ratio when compared to the stenosis group that had a higher prevalence of aortic calcification.[25] Studies have also shown that the presentation of valve disease varies among different BAV subtypes. RL-type BAVs are found to have more severe stenosis when compared to RN-type BAVs that develop more severe regurgitation.[26] In congenital bicuspid valve stenosis, aortic stenosis, which is secondary to the BAV, is found to lead to the development of calcification, occurring usually within the cusp's spongiosa.[27] This calcification in BAVs is due to the presence of an abnormal distribution of stress across the cusps in the deformed valves, leading to calcification earlier than in the case of TAV.[28] It can also be the result of mechanical disruptions (elastin and collagen fragments) that lead to the formation of nucleation sites for calcification.[29] In the case of calcified aortic valve disease, activation of the VICs is found to lead to the expression of bone development genes such as osteopontin, Runx2, and osteocalcin.[30] Once the valves are calcified, a surgical intervention is recommended in the case of severe valve dysfunction or the presence of comorbidities, which could further affect cardiac function and lead ultimately to heart failure.

Genetic basis of BAV: what we know from human and animal models

Even though the heritability of BAV is well documented, BAV causing genes remain largely unknown. Recent studies suggest that BAV is a complex process that can be caused by several genes, each with a distinct mode of inheritance, which

might explain why identifying the genetics of BAV through classical human genetic studies has been challenging.[10] To date, mutations in only two genes in human, *NOTCH1* (member of the Notch signaling pathway) and *GATA5* (member of the GATA family of transcription factors), were found to be linked to BAV. Based on DNA-sequencing of all coding exons and adjacent splice consensus sequences of the *NOTCH1* gene, missense mutations (p.T596M and p.P1797H) leading to amino acid substitution in a well-conserved region in *NOTCH1* were identified in patients with sporadic BAV, which were absent in 327 healthy individuals.[31] In another study, two novel mutations, p.P284L and p.Y1619X, a missense and a nonsense mutation, were found in the *NOTCH1* gene in two unrelated Italian families where the mutations segregated with the disease in both families.[32] Garg et al also identified two mutations in *NOTCH1*: the first mutation (p.R1108X) in a European-American five generation family showed linkage for BAV to a single locus on chromosome 9q34-35, whereas the second mutation (p.H1505del) cosegregated with the disease in three affected family members.[33] Consistent with a role for the BMP signaling in AoV formation, mutations in *SMAD6*, a component of the BMP intracellular signal transduction pathway, were reported in two out of 24 BAV patients with aortic stenosis and coarctation. Whether the mutations are causally linked with BAV remains uncertain since inactivation of *SMAD6* in mice did not cause BAV; instead, hyperplastic thickening of the valves and aortic ossification were observed.[34]

In order to further understand the complex process of valve morphogenesis, animal models lacking important regulators of valve formation were generated. Inactivation of key players during this process led to a wide variety of valvular malformations including BAV. One of the first models of BAV was reported in mice lacking NOS3 (endothelial nitric oxide synthase) where BAV was reported in five out of 12 mature NOS3-deficient mice (41.6%), all sharing the RN type with no BAV observed in any of the 26 wild-type littermates.[35] Another study by Bosse et al supports the important role of NOS3 in AoV formation by regulating NOTCH1 signaling and AoV disease prognosis. *NOS3–/– NOTCH1+/–* mice display 100% penetrance of BAV compared to the partial penetrance in the *NOS3–/–* (26%) and in the *NOTCH1+/–* (8%) single knockouts.[36] These results confirm a crucial role for the Notch pathway in AoV development and suggest that any deficiency in one or more of its key regulators could lead to valve defects including BAV.

In 2011, our group reported that targeted deletion of *GATA5* in mice leads to partially penetrant BAV (26%). GATA5, a member of the GATA family of transcription factors crucial for heart morphogenesis, is restricted to endocardial cells during early embryonic development. Whether GATA5 is deleted in all cells or only in endocardial cells, partial penetrance of RN-type BAV is consistently observed. Mechanistically, GATA5 was found to regulate important pathways associated with endocardial cushion differentiation such as NOS3, NOTCH, BMP4, and TBX20.[37] *GATA5* mutations were later reported in several patients with BAV. A genetic analysis in 100 BAV cases identified four rare nonsynonymous *GATA5* variants (Gln3Arg, Ser19Trp, Tyr142His, and Gly166Ser) in GATA5 transactivational domain, pointing out a possible role for GATA5 in the pathogenesis of BAV. These mutations were in highly conserved and functional regions, which would affect protein function.[38] In another study, 78 BAV patients were analyzed using Sanger sequencing to screen for these *GATA5* variants. Two rare nonsynonymous heterozygote mutations, p.Gln3Arg and p.Leu233Pro, with a frequency of 2.6% (2/78), were found in patients with aortic coarctation and RN- or RL-type BAV.[39]

Even though no human mutations linked to BAV in genes other than *NOTCH1* and *GATA5* were reported, potential candidate genes that could underlie the formation of BAV were discovered by examination of the AoVs of genetically engineered mice. Activin type I receptor (ALK2) is expressed in endocardial cells, and its role in endothelial EMT in the atrioventricular cushions is well established.[40] Deletion of ALK2 from the cushion mesenchyme after EMT using *GATA5*-Cre results in AoV defect (BAV) and development of aortic insufficiency and/or stenosis in some of the mutant mice. These results indicate an important role of ALK2 in AoV development and suggest that its absence can lead to AoV diseases.[41] No human mutations in *HOXA1* gene are observed in BAV patients, but its inactivation in mice was found to result in 24% penetrance of BAV, among other cardiac malformations. *HOXA1* null mice show defects such as interrupted aortic arch, tetralogy of fallot, and abnormal subclavian artery, pointing to an important role of HOXA1 in patterning of the OFT of the heart.[42] On the other hand, studies done on *NKX2-5* heterozygous mice showed an increased frequency of 8.2% of stenotic BAV with three out of 35 *NKX2-5* heterozygous mutant mice showing an increase in the aortic blood flow velocity and BAV with mild thickening upon autopsy. The presence of BAV in these mice was dependent on the genetic background confirming the presence of genetic modifiers as suggested in human genetic studies.[43]

All the mice models of BAV mentioned above displayed the RN-type BAV. A study by Sans-Coma et al in 1995

reported the first RL BAV model in inbred Syrian hamsters. In all, 16 out of 29 embryos had a fusion between the left and right cushions resulting in two abnormal valve cushions (a ventral and a dorsal).[44] To date, no genetically modified mouse model of RL BAV, the most common type of BAV observed in human, has been reported.

Given the lack of identification of BAV causative genes, studies have aimed at determining genetic loci associated with familial BAV. Early studies have identified genomic regions 17q29.3 (*KCJN2* gene) and 9q34.3 (*NOTCH1*) to be responsible for BAV in a small proportion of cases. A mutation in *KCJN2* gene, encoding the inward-rectifying potassium current, KIR2.1, was reported in patients with Anderson syndrome having sex-specific cardiac (BAV) and skeletal muscle phenotypes.[32,45] Genome-wide scan studies have identified three chromosomal regions, 18q, 5q, and 13q, associated with BAV, but the genes therein remain to be identified.[46] BAV is also manifested in some human syndromes such as Loeys–Dietz and Marfan. Loeys–Dietz syndrome is caused by a defect in the TGFB signaling pathway (mutations in *TGFBR1* [TGFB receptor 1] and *TGFBR2*) and is characterized by the presence of congenital heart disease and mental retardation among other abnormalities. Marfan syndrome is a connective tissue disorder characterized by cardiovascular, skeletal, and ocular manifestations. It is caused by a defect in the fibrillin-1 (*FBN1*) gene (essential for the formation of elastic fibers found in connective tissues) localized on chromosome 15q21.1 and is inherited in an autosomal dominant manner.[47,48] Mutations in *HOXA1* gene were also found in Bosley-Salih-Alorainy as well as in Athabaskan brainstem dysgenesis syndromes, which are characterized by a wide range of heart defects including ventricular septal defects, tetralogy of fallot, and BAV.[49] A high prevalence of BAV is also observed in patients with Turner syndrome, caused by a deletion of the short arm of the X chromosome. This suggests that abnormal AoV and aortic arch development can also be caused by haploinsufficiency in Xp gene (Table 1).[50]

Is it important to screen?

Asymptomatic individuals with BAV may go undetected for a lifetime and many will be disease free. However, a significant proportion will develop cardiovascular events that could be life threatening, requiring surgical intervention in some cases. A recent study showed that 25% of BAV subjects had to undergo premature valvular or aortic surgeries.[51] Whether the BAV is the direct cause of aortic events or whether subtle defects in vascular cells – caused by the same genetic alterations – are responsible for BAV-associated cardiovascular complications remain to be determined. Be it as it may, BAV is a cardiovascular risk factor as also evidenced in the ASTRONOMER study.[52] It is now well established that early detection of affected individuals allows for better

Table 1 Genes associated with human and animal (mouse) BAV phenotypes

Genes	Human valve phenotype	Animal model valve phenotype (mouse)	Reference
Transcription factors			
NKX2.5	Not reported	Partial penetrance of BAV (8.2%) with aortic aneurism	43
HOXA1	Not reported	Partial penetrance of BAV (24%)	42
GATA5	BAV with aortic stenosis and regurgitation	Partial penetrance of BAV (30%)	32,37–39
Enzymes			
NOS3	Not reported	Partial penetrance of BAV (41.6%)	35
Channels			
KCNJ2	BAV with coarctation of aorta	Not reported	45
Ligands			
NOTCH1	BAV with aortic aneurism, calcification (5%)	Partial penetrance of BAV	31–33,35
Receptors			
TGFBR2	BAV with aortic aneurism	Not reported	32
ALK2	Not reported	BAV with aortic insufficiency and/or stenosis	41
Chromosomal regions			
Loci 5q-gene unknown	Partial penetrance of BAV		46
Loci 5q-gene unknown	Partial penetrance of BAV		46
Loci 5q-gene unknown	Partial penetrance of BAV		46
Xp gene	BAV		50
Signal transducer			
SMAD6	BAV with mild aortic stenosis BAV with mild aortic stenosis and coarctation of the aorta	Not reported	34

Abbreviation: BAV, bicuspid aortic valve.

monitoring and preventative care. Echocardiography and magnetic resonance imaging have been reliable techniques so far to detect BAVs and dilated aortas, but the infrastructure and cost of these tests make them impractical for large-scale population screening. Moreover, valvular problems and dilated aortas caused by BAV are not detected at childhood, and the late identification of BAV often occurs when AoV disease has become irreversible.

Given the established familial contribution to BAV, the use of next-generation technologies such as whole exome sequencing (WES) and whole genome sequencing should be considered. Given the high cost of whole genome sequencing, WES is currently a more viable approach to determine the protein-coding sequence variations. In previous studies, WES has proven to be useful in revealing genetic variants in individuals affected with rare forms of heart diseases such as BAG3 gene in familial dilated cardiomyopathy.[53] Other genes causing severe hypercholesterolemia (ABCG) and familial combined hypolipidemia (ANGPTL3) could not have been identified without the availability of this technique.[54,55] In a not so distant future, WES and eventually WEG might well become routine techniques for sequencing due to accelerated developments that are resulting in rapid drop in cost. Investments in those technologies will accelerate discovery of BAV causing genes, ultimately enhancing patient management and treatment.[56] Recent studies have shown that WES is useful for disease diagnosis, which informs patient treatment. Since most BAVs diagnosed to date usually have a familial history, it is important to screen first-degree relatives of a patient with BAV. WES has helped in the diagnosis of Crohn's disease due to a mutation in the X-linked inhibitor of apoptosis gene in a 15-month old boy. The patient successfully underwent a hematopoietic progenitor cell transplant.[57] Discovery of BAV causing genes will also help develop genotype–phenotype correlations and open the way to personalized treatment. For example, knowledge of which BAV genotype might be predictive of valvulo-vascular complications will decrease unnecessary interventions such as unnecessary aortic aneurism repair surgeries while pointing to individuals who require closer cardiovascular monitoring. Therefore, it is important to accelerate the search for new causative genes that will allow for genetic screening as well as a better understanding of the molecular basis of BAV formation and degeneration. This holds great promise for secondary prevention and might open new therapeutic avenues.

Acknowledgment

Work in our lab is supported by the Canadian Institutes of Health Research, the Heart and Stroke Foundation of Canada, and the McCain Foundation.

Disclosure

The authors report no conflicts of interest in this work.

References

1. Tam PP, Parameswaran M, Kinder SJ, Weinberger RP. The allocation of epiblast cells to the embryonic heart and other mesodermal lineages: the role of ingression and tissue movement during gastrulation. *Development*. 1997;124(9):1631–1642.
2. Hinton RB Jr, Lincoln J, Deutsch GH, et al. Extracellular matrix remodeling and organization in developing and diseased aortic valves. *Circ Res*. 2006;98(11):1431–1438.
3. Restivo A, Piacentini G, Placidi S, Saffirio C, Marino B. Cardiac outflow tract: a review of some embryogenetic aspects of the conotruncal region of the heart. *Anat Rec A Discov Mol Cell Evol Biol*. 2006;288(9):936–943.
4. Okamoto N, Akimoto N, Hidaka N, Shoji S, Sumida H. Formal genesis of the outflow tracts of the heart revisited: previous works in the light of recent observations. *Congenit Anom (Kyoto)*. 2010;50(3):141–158.
5. Anderson RH, Webb S, Brown NA, Lamers W, Moorman A. Development of the heart: (2) septation of the atriums and ventricles. *Heart*. 2003;89(8):949–958.
6. Brickner ME, Hillis LD, Lange RA. Congenital heart disease in adults. First of two parts. *N Engl J Med*. 2000;342(5):334–342.
7. LaHaye S, Lincoln J, Garg V. Genetics of valvular heart disease. *Curr Cardiol Rep*. 2014;16(6):487.
8. Ward C. Clinical significance of the bicuspid aortic valve. *Heart*. 2000;83(1):81–85.
9. Padang R, Bannon PG, Jeremy R, Semsarian C, Richmond DR, Vallely M. The genetic and molecular basis of bicuspid aortic valve associated thoracic aortopathy: a link to phenotype heterogeneity. *Ann Cardiothorac Surg*. 2013;2(1):83–91.
10. Cripe L, Andelfinger G, Martin LJ, Shooner K, Benson DW. Bicuspid aortic valve is heritable. *J Am Coll Cardiol*. 2004;44(1):138–143.
11. Siu SC, Silversides CK. Bicuspid aortic valve disease. *J Am Coll Cardiol*. 2010;55(25):2789–2800.
12. Friedman T, Mani A, Elefteriades JA. Bicuspid aortic valve: clinical approach and scientific review of a common clinical entity. *Expert Rev Cardiovasc Ther*. 2008;6(2):235–248.
13. Fernández B, Durán AC, Fernández-Gallego T, et al. Bicuspid aortic valves with different spatial orientations of the leaflets are distinct etiological entities. *J Am Coll Cardiol*. 2009;54(24):2312–2318.
14. Yuan S, Jing H. The bicuspid aortic valve and related disorders review article. *Sao Paulo Med J*. 2010;128(5):296–301.
15. Homme JL, Aubry M-C, Edwards WD, et al. Surgical pathology of the ascending aorta: a clinicopathologic study of 513 cases. *Am J Surg Pathol*. 2006;30(9):1159–1168.
16. Della Corte A, Bancone C, Quarto C, et al. Predictors of ascending aortic dilatation with bicuspid aortic valve: a wide spectrum of disease expression. *Eur J Cardiothorac Surg*. 2007;31(3):397–404; discussion 404–405.
17. Choudhury N, Bouchot O, Rouleau L, et al. Local mechanical and structural properties of healthy and diseased human ascending aorta tissue. *Cardiovasc Pathol*. 2009;18(2):83–91.
18. Aboulhosn J, Child JS. Left ventricular outflow obstruction: subaortic stenosis, bicuspid aortic valve, supravalvar aortic stenosis, and coarctation of the aorta. *Circulation*. 2006;114(22):2412–2422.
19. Hahn RT, Roman MJ, Mogtader AH, Devereux RB. Association of aortic dilation with regurgitant, stenotic and functionally normal bicuspid aortic valves. *J Am Coll Cardiol*. 1992;19(2):283–288.
20. Fedak PW, de Sa MP, Verma S, et al. Vascular matrix remodeling in patients with bicuspid aortic valve malformations: implications for aortic dilatation. *J Thorac Cardiovasc Surg*. 2003;126(3):797–806.
21. Collins MJ, Dev V, Strauss BH, Fedak PW, Butany J. Variation of the histopathological features of patients with ascending aortic aneurysms: a study of 111 surgically excised cases. *J Clin Pathol*. 2008;61(4):519–523.
22. Bauer M, Pasic M, Meyer R, et al. Morphometric analysis of aortic media in patients with bicuspid and tricuspid aortic valve. *Ann Thorac Surg*. 2002;74(1):58–62.

23. Schievink WI, Raissi SS, Maya MM, Velebir A. Screening for intracranial aneurysms in patients with bicuspid aortic valve. *Neurology*. 2010; 74(18):1430–1433.
24. Tao G, Kotick JD, Lincoln J. Heart valve development, maintenance, and disease: the role of endothelial cells. *Curr Top Dev Biol*. 2012;100: 203–232.
25. Sabet HY, Edwards WD, Tazelaar HD, Daly RC. Congenitally bicuspid aortic valves: a surgical pathology study of 542 cases (1991 through 1996) and a literature review of 2,715 additional cases. *Mayo Clin Proc*. 1999;74(1):14–26.
26. Sonoda M, Takenaka K, Uno K, Ebihara A, Nagai R. A larger aortic annulus causes aortic regurgitation and a smaller aortic annulus causes aortic stenosis in bicuspid aortic valve. *Echocardiography*. 2008;25(3): 242–248.
27. Isner JM, Chokshi SK, DeFranco A, Braimen J, Slovenkai GA. Contrasting histoarchitecture of calcified leaflets from stenotic bicuspid versus stenotic tricuspid aortic valves. *J Am Coll Cardiol*. 1990;15(5):1104–1108.
28. Ladich E, Nakano M, Carter-Monroe N, Virmani R. Pathology of calcific aortic stenosis. *Future Cardiol*. 2011;7(5):629–642.
29. Bailey MT, Pillarisetti S, Xiao H, Vyavahare NR. Role of elastin in pathologic calcification of xenograft heart valves. *J Biomed Mater Res A*. 2003;66(1):93–102.
30. Rajamannan NM, Evans FJ, Aikawa E, et al. Calcific aortic valve disease: not simply a degenerative process: a review and agenda for research from the National Heart and Lung and Blood Institute Aortic Stenosis Working Group. Executive summary: calcific aortic valve disease-2011 update. *Circulation*. 2011;124(16):1783–1791.
31. Mohamed SA, Aherrahrou Z, Liptau H, et al. Novel missense mutations (p.T596M and p.P1797H) in NOTCH1 in patients with bicuspid aortic valve. *Biochem Biophys Res Commun*. 2006;345(4):1460–1465.
32. Foffa I, Ait Ali L, Panesi P, et al. Sequencing of NOTCH1, GATA5, TGFBR1 and TGFBR2 genes in familial cases of bicuspid aortic valve. *BMC Med Genet*. 2013;14:44.
33. Garg V, Muth AN, Ransom JF, et al. Mutations in NOTCH1 cause aortic valve disease. *Nature*. 2005;437(7056):270–274.
34. Tan HL, Glen E, Töpf A, et al. Nonsynonymous variants in the SMAD6 gene predispose to congenital cardiovascular malformation. *Hum Mutat*. 2012;33(4):720–727.
35. Lee TC, Zhao YD, Courtman DW, Stewart DJ. Abnormal aortic valve development in mice lacking endothelial nitric oxide synthase. *Circulation*. 2000;101(20):2345–2348.
36. Bosse K, Hans CP, Zhao N, et al. Endothelial nitric oxide synthase regulates Notch1 in aortic valve disease. Endothelial nitric oxide signaling regulates Notch1 in aortic valve disease. *J Mol Cell Cardiol*. 2013;60:27–35.
37. Laforest B, Andelfinger G, Nemer M. Loss of Gata5 in mice leads to bicuspid aortic valve. *J Clin Invest*. 2011;121(7):2876–2887.
38. Padang R, Bagnall RD, Richmond DR, Bannon PG, Semsarian C. Rare non-synonymous variations in the transcriptional activation domains of GATA5 in bicuspid aortic valve disease. *J Mol Cell Cardiol*. 2012; 53(2):277–281.
39. Bonachea EM, Chang SW, Zender G, et al. Rare GATA5 sequence variants identified in individuals with bicuspid aortic valve. *Pediatr Res*. 2014;76(2):211–216.
40. Wang J, Sridurongrit S, Dudas M, et al. Atrioventricular cushion transformation is mediated by ALK2 in the developing mouse heart. *Dev Biol*. 2005;286(1):299–310.
41. Thomas PS, Sridurongrit S, Ruiz-Lozano P, Kaartinen V. Deficient signaling via Alk2 (Acvr1) leads to bicuspid aortic valve development. *PLoS One*. 2012;7(4):e35539.
42. Makki N, Capecchi MR. Cardiovascular defects in a mouse model of HOXA1 syndrome. *Hum Mol Genet*. 2012;21(1):26–31.
43. Biben C, Weber R, Kesteven S, et al. Cardiac septal and valvular dysmorphogenesis in mice heterozygous for mutations in the homeobox gene *Nkx2-5*. *Circ Res*. 2000;87(10):888–895.
44. Sans-Coma V, Fernández B, Durán AC, et al. Fusion of valve cushions as a key factor in the formation of congenital bicuspid aortic valves in Syrian Hamsters. *Anat Rec*. 1996;244(4):490–498.
45. Andelfinger G, Tapper AR, Welch RC, Vanoye CG, George AL Jr, Benson DW. *KCNJ2* mutation results in Andersen syndrome with sex-specific cardiac and skeletal muscle phenotypes. *Am J Hum Genet*. 2002;71(3):663–668.
46. Martin LJ, Ramachandran V, Cripe LH, et al. Evidence in favor of linkage to human chromosomal regions 18q, 5q and 13q for bicuspid aortic valve and associated cardiovascular malformations. *Hum Genet*. 2007;121(2):275–284.
47. Loeys BL, Chen J, Neptune ER, et al. A syndrome of altered cardiovascular, craniofacial, neurocognitive and skeletal development caused by mutations in TGFBR1 or TGFBR2. *Nat Genet*. 2005;37(3):275–281.
48. Dietz HC, Cutting GR, Pyeritz RE, et al. Marfan syndrome caused by a recurrent de novo missense mutation in the fibrillin gene. *Nature*. 1991;352(6333):337–339.
49. Tischfield MA, Bosley TM, Salih MA, et al. Homozygous HOXA1 mutations disrupt human brainstream, inner ear, cardiovascular and cognitive development. *Nat Genet*. 2005;37(10):1035–1037.
50. Bondy C, Bakalov VK, Cheng C, Olivieri L, Rosing DR, Arai AE. Bicuspid aortic valve and aortic coarctation are linked to deletion of the X chromosome short arm in Turner syndrome. *J Med Genet*. 2013; 50(10):662–665.
51. Michelena HI, Desjardins VA, Avierinos JF, et al. Natural history of asymptomatic patients with normally functioning or minimally dysfunctional bicuspid aortic valve in the community. *Circulation*. 2008;117(21):2776–2784.
52. Chan KL, Teo K, Dumesnil JG, Ni A, Tam J, ASTRONOMER Investigators. Effect of Lipid lowering with rosuvastatin on progression of aortic stenosis: results of the aortic stenosis progression observation: measuring effects of rosuvastatin (ASTRONOMER) trial. *Circulation*. 2010;121(2):306–314.
53. Norton N, Li D, Rieder MJ, et al. Genome-wide studies of copy number variation and exome sequencing identify rare variants in BAG3 as a cause of dilated cardiomyopathy. *Am J Hum Genet*. 2011;88: 273–282.
54. Musunuru K, Pirruccello JP, Do R, et al. Exome sequencing, ANGPTL3 mutations, and familial combined hypolipidemia. *N Engl J Med*. 2010;363:2220–2227.
55. Rios J, Stein E, Shendure J, Hobbs HH, Cohen JC. Identification by whole genome resequencing of gene defect responsible for severe hypercholesterolemia. *Hum Mol Genet*. 2011;19:4313–4318.
56. Rabbani B, Tekin M, Mahdieh N. The promise of whole-exome sequencing in medical genetics. *J Hum Genet*. 2014;59(1):5–15.
57. Worthey EA, Mayer AN, Syverson GD, et al. Making a definitive diagnosis: successful clinical application of whole exome sequencing in a child with intractable inflammatory bowel disease. *Genet Med*. 2011;13:255–262.

6.2. Editorial

Title: *Guiding cardiac conduction with GATA.*

Publication copyrights from Circulation: Cardiovascular Genetics:

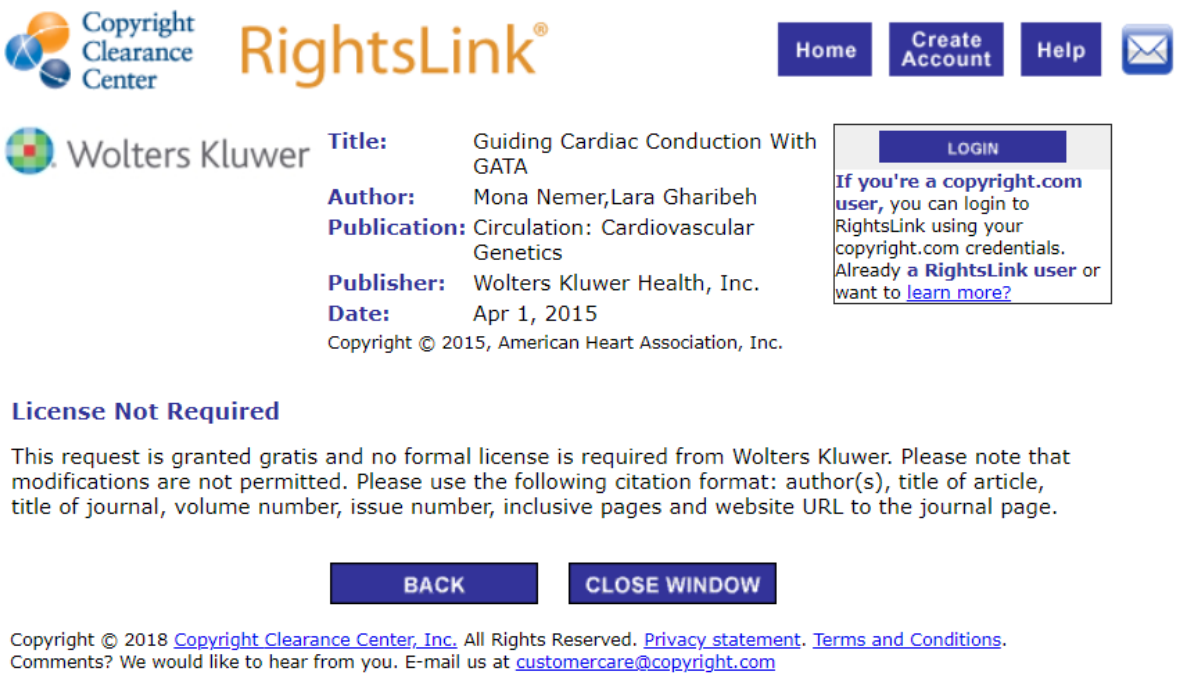

Copyright Clearance Center RightsLink®

Home | Create Account | Help

Wolters Kluwer

Title: Guiding Cardiac Conduction With GATA
Author: Mona Nemer,Lara Gharibeh
Publication: Circulation: Cardiovascular Genetics
Publisher: Wolters Kluwer Health, Inc.
Date: Apr 1, 2015
Copyright © 2015, American Heart Association, Inc.

LOGIN

If you're a copyright.com user, you can login to RightsLink using your copyright.com credentials. Already **a RightsLink user** or want to learn more?

License Not Required

This request is granted gratis and no formal license is required from Wolters Kluwer. Please note that modifications are not permitted. Please use the following citation format: author(s), title of article, title of journal, volume number, issue number, inclusive pages and website URL to the journal page.

BACK | CLOSE WINDOW

Copyright © 2018 Copyright Clearance Center, Inc. All Rights Reserved. Privacy statement. Terms and Conditions.
Comments? We would like to hear from you. E-mail us at customercare@copyright.com

Editorial

Guiding Cardiac Conduction With GATA

Mona Nemer, PhD; Lara Gharibeh, MS

Despite remarkable progress in the past few years, the gene regulatory networks underlying formation and function of the cardiac conduction system (CCS) remain incompletely understood. Transcription factors such as NXK2.5 and TBX2/3/5 that control various aspects of heart development have emerged as key regulators of cardiac conduction gene expression and function. By showing alterations in the structure of the atrioventricular node (AVN) and the electrophysiological parameters of mice harboring a mutated GATA-binding factor 6 (GATA6) protein, Liu et al[1] add a new player to the growing list of transcription factors involved in cardiac rhythm regulation. This finding provides insight that will help advance efforts to elucidate the pathogenesis of cardiac rhythm disturbances.

Article see p 284

In human, cardiac rhythm disturbances are a major cause of mortality and morbidity from fetal to adult life. They can develop in response to numerous conditions, such as electrolyte imbalance, cardiovascular disease including ischemia and pressure overload, structural heart malformations, or as undesirable drug side effects. Arrhythmias and conduction defects can also be because of inherited mutations in genes that affect generation or propagation of the electric impulse of the heart, as exemplified by the long QT Syndrome. How these genetic or acquired factors influence cardiac rhythm is not yet fully understood. In the past years, great strides were achieved for treatment of these important disorders from drug and ablation therapy to implantable devices. However, all treatments have significant short falls and none is curative. A better understanding of the molecular mechanism underlying normal development of the CCS will help unravel the pathogenesis of rhythm disturbances and the development of effective therapies.

Proper heart contraction and relaxation processes are controlled by the CCS, a specialized component of the heart responsible for initiating and orchestrating the propagation of the electric signal required for optimal blood delivery into the circulation. The CCS is composed of slow and fast conducting structures forming the proximal and distal CCS. The pacemaker sinoatrial node and the AVN compose the proximal component of the CCS while the interatrial conduction tracts the His bundle, bundle branches, and Purkinje fibers make up the distal component. Small perturbations in any of the CCS components can lead to drastic outcomes ranging from heart arrhythmias, heart block to sudden death. Understanding the mechanisms of CCS pathophysiology is, therefore, critical.

Our knowledge of CCS development has come largely from studies of transgenic and conditional knockout mouse model, which helped to identify developmental regulators of various CCS components. Human genetic studies, including more recent genome-wide association studies and exon sequencing of candidate genes have also contributed to identifying genes and genetic loci associated with rhythm disturbances. The emerging genetic circuits involved in the formation and function of the pacemaker node include several transcription factors that play crucial roles in many other aspects of heart development. They include *NKX2.5* as well as *TBX5*, the gene mutated in Holt–Oram syndrome.[2] These same genes also contribute to AVN formation as first suggested by the discovery that familial mutations in *NKX2.5* and *TBX5* transcription factors are associated with atrioventricular conduction defects.[3,4] Mouse models with haploinsufficiency in either factor replicate the human phenotypes: NKX2.5 haploinsufficiency results in defective central and peripheral conduction systems along with absence of the AVN subdomain.[5] Similarly, TBX5 haploinsufficiency results in PR interval prolongation[6] (the period between the onset of atrial depolarization and the beginning of ventricular depolarization) along with defective patterning of the right and left bundle branches.[7] The role of other Tbox proteins TBX2/3 as well as NOTCH signaling in AVN formation and specification have also been documented.[2]

Evidence for an important role for the GATA family of zinc finger proteins, and more specifically the cardiac subfamily GATA4, 5, and 6 has been accumulating. First, all the 3 proteins are expressed in cardiomyocytes and cardiac structures and cell types that are important for conduction, including atrioventricular canal myocardium, cardiac neural crest, and cardiac fibroblasts. Therein, GATA proteins regulate many conduction relevant genes, such as those for gap junction and ion channels. They also physically and functionally interact with NKX2.5 and TBX2/3/5 to modulate their activity on target genes; as such they act as genetic modifiers of arrhythmia causing genes. Interestingly, mutations in all the 3 proteins have been reported in association with human atrial fibrillation.[8–10] The most extensively studied GATA factor in relation to cardiac conduction is GATA4 which was shown to activate Cx30.2,[11] as well as Cx40, and several atrioventricular canal enhancers.[12,13] Consistent with this, mice heterozygote for Gata4 were reported to have shorter PR.[11]

From the Molecular Genetics and Cardiac Regeneration Laboratory, Department of Biochemistry, Microbiology, and Immunology, University of Ottawa, Ottawa, Ontario, Canada.

Correspondence to Mona Nemer, PhD, Molecular Genetics and Cardiac Regeneration Laboratory, Department of Biochemistry, Microbiology, and Immunology, University of Ottawa, 550 Cumberland, Room 246, Ottawa, ON K1N 6N5, Canada. E-mail mona.nemer@uottawa.ca

(*Circ Cardiovasc Genet.* 2015;8:247-249.
DOI: 10.1161/CIRCGENETICS.115.001039.)

Circ Cardiovasc Genet is available at http://circgenetics.ahajournals.org
DOI: 10.1161/CIRCGENETICS.115.001039

No studies, to date, have directly linked GATA6 with regulation of the CCS but previous studies showed that an enhancer region upstream of the GATA6 promoter is specifically active in the Atrioventricular conduction structure.[14] GATA6 was also shown to activate the NCX1 and Kv4.2 promoters.[13,15] Localized on chromosome 18 in human and in mice, GATA6 is expressed in myocardial, neural crest, and endocardial cells as well as in vascular smooth muscle cells.[16] Consistent with an important role for GATA6 in heart morphogenesis and outflow tract development, many mutations in the human gene were reported in association with a large spectrum of congenital heart diseases, including atrial and ventricular septal defects, Tetralogy of Fallot and Patent Ductus Arteriosus.

In this issue of *Circulation Cardiovascular Genetics*, Liu et al[1] report that in addition to its crucial role in heart morphogenesis, intact GATA6 is required for normal development and functional maintenance of the AVN. GATA6 was found to be abundantly expressed in the proximal CCS at E12.5 to E16.5 and its expression overlapped with TBX3, a marker of the atrioventricular conduction system, and with the transcriptional repressor ID2. To determine if GATA6 contributes to CCS, a mouse model with myocardial-specific deletion of the carboxyl zinc finger domain of *Gata6* under the control of the myosin light chain 2v (*MLC2v*) promoter, was generated resulting in truncation of GATA6 in the ventricular myocardium, right ventricular outflow tract, and atrioventricular annulus. ECG analysis performed in young animals revealed prolonged PR intervals and AVN defects in these mutant mice. The myocardial-specific mutation of GATA6 led to defects affecting only the proximal atrioventricular conduction but not the infranodal CCS; these defects included AVN hypoplasia, probably because of reduced cell-cycle exit of TBX3+ myocytes in the atrioventricular myocardium and defective myocyte differentiation. Myocardial-specific deletion of the carboxyl zinc finger domain of *Gata6* was also shown to lead to downregulation of the transcriptional repressor ID2 in the proximal CCS of mutant embryos, as well as in the AVN and lower nodal region of adult mutant hearts. Transfection experiments confirmed that the *Id2* promoter is directly activated by GATA6.

This work provides, for the first time, experimental evidence linking GATA6 to AVN formation and function and represents an important contribution to our evolving understanding of CCS in development and disease.

Although the work clearly shows that intact GATA6 is essential for proper AVN development, many questions about the cellular and molecular mechanisms underlying this effect remain to be answered. A role for GATA6 in the AVN is in line with its involvement in atrioventricular canal development as demonstrated by the use of the same floxed allele to delete myocardial *Gata6* more broadly using NKX2.5-cre mice.[17] This led mostly to ventricular septal defect, whereas mice with MLC2v-cre–mediated deletion did not apparently have any such structural cardiac defects. Given that NKX2.5 is expressed in the proximal CCS, this raises interesting questions about temporal as well as spatial GATA6 function. The exact cell type(s) contributing to GATA6-dependent AVN defects will likely need to be directly addressed through additional cell-specific deletion of Gata6 including in CCS cells.

Equally intriguing is the absence of rhythm disturbances in Gata6 heterozygote animals.[11] Whether this reflects dosage sensitivity or whether truncation versus loss of GATA6 leads to differing phenotypes will need to be ascertained. Such possibility might be of great relevance for understanding the effect of different *GATA6* genotypes on their associated phenotypes.

Finally, the mechanisms by which loss of the C-terminal half of GATA6 alters AVN size and gene expression requires further investigation. The remaining truncated GATA6 protein contains functional domains, including the N-terminal activation domain and the N-zinc finger. By analogy to GATA4, such protein would have a nuclear localization, maintain the ability to interact with critical cardiogenic cofactors, including BAF60c[18] and other GATA proteins[19] or GATA regulators such as FOG 2.[20] This, in turn, will affect the activity of such important AVN regulators as NKX2.5 and TBXs. Thus, the observed mouse phenotype may reflect the combined role of GATA6 and that of other transcription factors in CCS cells. Similar manipulations using another available Gata6 floxed allele[11] would help to clarify the exact role of GATA6 in cardiac conduction.

Notwithstanding these mechanistic considerations, the finding that intact GATA6 is required for proper AVN function represents an important contribution to understanding the intricate regulation of the cardiac pacemaker. Prolonged PR intervals may indicate first degree heart block and are an undesirable side effect of several widely used drugs including calcium channel and β-blockers. Prolonged PR interval doubles the risk of atrial fibrillation and triples the risk of needing a pacemaker device according to the Framingham Heart Study.[21] The identification of a new regulator of the PR interval has potential applications in many sectors including pharmacogenetics where much work is still needed.

Sources of Funding

Work in our laboratory is supported by the Canadian Institutes of Health Research, the Heart and Stroke Foundation of Canada, and the McCain Foundation.

Disclosures

None.

References

1. Liu F, Lu MM, Patel NN, Schillinger KJ, Wang T, Patel VV. GATA-binding factor 6 contributes to AV node development and function. *Circ Cardiovasc Genet*. 2015;8:284–293.doi: 10.1161/CIRCGENETICS.113.000587.
2. Munshi NV. Gene regulatory networks in cardiac conduction system development. *Circ Res*. 2012;110:1525–1537. doi: 10.1161/CIRCRESAHA.111.260026.
3. Schott JJ, Benson DW, Basson CT, Pease W, Silberbach GM, Moak JP, et al. Congenital heart disease caused by mutations in the transcription factor NKX2-5. *Science*. 1998;281:108–111.
4. Basson CT, Bachinsky DR, Lin RC, Levi T, Elkins JA, Soults J, et al. Mutations in human TBX5 [corrected] cause limb and cardiac malformation in Holt-Oram syndrome. *Nat Genet*. 1997;15:30–35. doi: 10.1038/ng0197-30.
5. Jay PY, Harris BS, Maguire CT, Buerger A, Wakimoto H, Tanaka M, et al. Nkx2-5 mutation causes anatomic hypoplasia of the cardiac conduction system. *J Clin Invest*. 2004;113:1130–1137. doi: 10.1172/JCI19846.
6. Bruneau BG, Nemer G, Schmitt JP, Charron F, Robitaille L, Caron S, et al. A murine model of Holt-Oram syndrome defines roles of the T-box transcription factor Tbx5 in cardiogenesis and disease. *Cell*. 2001;106:709–721.

7. Moskowitz IP, Pizard A, Patel VV, Bruneau BG, Kim JB, Kupershmidt S, et al. The T-Box transcription factor Tbx5 is required for the patterning and maturation of the murine cardiac conduction system. *Development*. 2004;131:4107–4116. doi: 10.1242/dev.01265.
8. Posch MG, Gramlich M, Sunde M, Schmitt KR, Lee SH, Richter S, et al. A gain-of-function TBX20 mutation causes congenital atrial septal defects, patent foramen ovale and cardiac valve defects. *J Med Genet*. 2010;47:230–235. doi: 10.1136/jmg.2009.069997.
9. Yang YQ, Li L, Wang J, Zhang XL, Li RG, Xu YJ, et al. GATA6 loss-of-function mutation in atrial fibrillation. *Eur J Med Genet*. 2012;55:520–526. doi: 10.1016/j.ejmg.2012.06.007.
10. Wang XH, Huang CX, Wang Q, Li RG, Xu YJ, Liu X, et al. A novel GATA5 loss-of-function mutation underlies lone atrial fibrillation. *Int J Mol Med*. 2013;31:43–50. doi: 10.3892/ijmm.2012.1189.
11. Munshi NV, McAnally J, Bezprozvannaya S, Berry JM, Richardson JA, Hill JA, et al. Cx30.2 enhancer analysis identifies Gata4 as a novel regulator of atrioventricular delay. *Development*. 2009;136:2665–2674. doi: 10.1242/dev.038562.
12. Stefanovic S, Barnett P, van Duijvenboden K, Weber D, Gessler M, Christoffels VM. GATA-dependent regulatory switches establish atrioventricular canal specificity during heart development. *Nat Commun*. 2014;5:3680. doi: 10.1038/ncomms4680.
13. Koban MU, Brugh SA, Riordon DR, Dellow KA, Yang HT, Tweedie D, et al. A distant upstream region of the rat multipartite Na(+)-Ca(2+) exchanger NCX1 gene promoter is sufficient to confer cardiac-specific expression. *Mech Dev*. 2001;109:267–279.
14. Davis DL, Edwards AV, Juraszek AL, Phelps A, Wessels A, Burch JB. A GATA-6 gene heart-region-specific enhancer provides a novel means to mark and probe a discrete component of the mouse cardiac conduction system. *Mech Dev*. 2001;108:105–119.
15. Jia Y, Takimoto K. GATA and FOG2 transcription factors differentially regulate the promoter for Kv4.2 K(+) channel gene in cardiac myocytes and PC12 cells. *Cardiovasc Res*. 2003;60:278–287.
16. Nemer G, Nemer M. Transcriptional activation of BMP-4 and regulation of mammalian organogenesis by GATA-4 and -6. *Dev Biol*. 2003;254:131–148.
17. Tian Y, Yuan L, Goss AM, Wang T, Yang J, Lepore JJ, et al. Characterization and *in vivo* pharmacological rescue of a Wnt2-Gata6 pathway required for cardiac inflow tract development. *Dev Cell*. 2010;18:275–287. doi: 10.1016/j.devcel.2010.01.008.
18. Gallagher JM, Komali H, Roy E, Nemer M, Latinkić BV. Dissociation of cardiogenic and postnatal myocardial activities of GATA4. *Mol Cell Biol*. 2012;32:2214–2223. doi: 10.1128/MCB.00218-12.
19. Charron F, Paradis P, Bronchain O, Nemer G, Nemer M. Cooperative interaction between GATA-4 and GATA-6 regulates myocardial gene expression. *Mol Cell Biol*. 1999;19:4355–4365.
20. Zhou B, Ma Q, Kong SW, Hu Y, Campbell PH, McGowan FX, et al. Fog2 is critical for cardiac function and maintenance of coronary vasculature in the adult mouse heart. *J Clin Invest*. 2009;119:1462–1476. doi: 10.1172/JCI38723.
21. Cheng S, Keyes MJ, Larson MG, McCabe EL, Newton-Cheh C, Levy D, et al. Long-term outcomes in individuals with prolonged PR interval or first-degree atrioventricular block. *JAMA*. 2009;301:2571–2577. doi: 10.1001/jama.2009.888.

KEY WORDS: Editorials ■ atrioventricular node ■ congenital heart disease ■ GATA6 protein ■ heart conduction system ■ transcription factors

Circulation
Genomic and Precision Medicine

Guiding Cardiac Conduction With GATA

Mona Nemer and Lara Gharibeh

Circ Cardiovasc Genet. 2015;8:247-249
doi: 10.1161/CIRCGENETICS.115.001039
Circulation: Cardiovascular Genetics is published by the American Heart Association, 7272 Greenville Avenue, Dallas, TX 75231

Print ISSN: 1942-325X. Online ISSN: 1942-3268